ADAPTIVE ARRAY PROCESSING FOR SOURCE LOCATION AND INTERFERENCE CANCELLATION

by

Athanassios N. Manikas

A Thesis Submitted for the Degree of

Doctor of Philoshophy

of the University of London

and

the Diploma of Imperial College

Department of Electrical Engineering,

Imperial College of Science and Technology,

University of London,

SEPTEMBER 1988.

DEDICATED TO

my wife ELENI

ABSTRACT

Superresolution Techniques and related Signal Subspace Algorithms have as their main objective the location of a number of emitting sources using an array of sensors (e.g. antennas). However, these techniques fail if some of the incident signals are correlated, a situation which arises in signal environments where *smart* jamming or multipath propagation is present. Also, signal subspace algorithms need to have a priori knowledge of the number of signals present in order to function properly. The research reported on in this thesis is concerned with the development of new techniques for overcoming the problems just referred to.

Firstly, techniques for modelling the input signals in a general environment have been developed, which take into account both spherical wave propagation as well as the existence of multipath.

Then, a new algorithm called Adaptive Signal Parameter Estimation and Classification Technique (ASPECT) is introduced which, unlike existing Superresolution Techniques, provides correct information concerning:

- the number of signals incident to the array,
- the direction of arrivals (azimuth and elevation angles),
- the relative powers and phases;

even in a correlated (coherent) signal environment. Its operation is based mainly on mapping the array manifold on to an error surface and then searching that surface for the solution.

The algorithm is examined both for plane and spherical wave

propagation, for different levels of noise and for both correlated and uncorrelated sources with widely differing power levels. The results obtained so far indicate that ASPECT correctly detects, resolves and estimates the directions of incident signals and is robust with respect to noise level.

Finally, the ideas of Signal Subspace Algorithms are extended to steered vector array processing in order to provide weight vectors

- for complete interference cancellation
- which do not suffer from power inversion problems
- are susceptible to pointing errors and
- provide deep distinct nulls in the directions of interferences with the ability to resolve two interferences located close together.

Simulation results support the theory, and a small modification of ASPECT makes it appropriate for functioning in steered vector adaptive arrays.

ACKNOWLEDGEMENTS

I would like to express my sincere gratitude to my supervisor Professor L.F. Turner for his guidance and friendship. It has been a privilege to work with him.

I should also like to thank Dr M.P. Ralls, Dr F.G.A. Coupe and Mr J. Allan for many useful discussions during the last two years, and all the research students in the Digital Communication Section for their unfailing friendship and co-operation.

I thank my parents Nikos and Maria and my brother-in-law Dinos Rados for their support and encouragment.

CONTENTS *PAGE*

CONTENTS *PAGE*

LIST OF FIGURES

LIST OF PRINCIPLE SYMBOLS

$\mathbf{R}_{mm}$	Covariance matrix of the directional signals
$\mathbf{R}_{xx}$	Data covariance matrix
$\mathbf{R}_{nn}$	Noise covariance matrix
$\mathbf{S}$	Source Position matrix
$\mathbf{P}$	Projection operator
$\mathbf{Q}$	Complement Projection operator
$\mathbb{E}$	Matrix of eigenvectors
$\mathbf{I}$	Unity Matrix
$\mathbf{K}$	Matrix with columns wavenumber vectors
$\mathbf{G}$	each column of $\mathbf{G}$ has as elements the directional gains of the array elements for a specific direction.
$\underline{S}$	Source Position Vector
$\underline{r}$	Location in a 3-dim space
$\underline{k}$	Wavenumber vector
$\underline{k}_o$	Wavenumber vector which correspond to the steering direction
$\underline{n}(t)$	noise vector
$\underline{m}(t)$	signal vector
$\underline{\alpha}$	Slowness vector
$\mathcal{N}^+$	Set of all positive integers
$\mathcal{R}$	Set of real numbers
N	Number of array elements (sensors)
M	Number of incident signals
D	Number of emitting sources
L	Number of paths from an emmiting source
σ^2	Variance of the noise

$\|\|.\|\|$	Norm of a vector (Euclidean norm)
$E[\![.]\!]$	Expectation operator
eig_i	the i^{th} element of the vector containing the eigenvalues of a matrix
θ	Azimuth angle
ϕ	Elevation angle
R	Range
ξ	Performance criterion
$\underline{\nabla}$	Gradient vector
$\underline{\nabla}^2$	Hessian Matrix
∇	An element of the gradient vector
∇^2	An element of the Hessian Matrix
i	as subscript of $\underline{r}$ (that is $\underline{r}_i$) refers to the i^{th} emitting source
k	as subscript of $\underline{r}$ (that is $\underline{r}_k$) refers to the k^{th} array element
θ	as subscript of the matrices **S**, **G** and **K** means differentiation of each column of those matrices with respect to its azimith angle
ϕ	as subscript of the matrices **S**, **G** and **K** means differentiation of each column of those matrices with respect to its elevation angle

N.B.:

- the term "correlated sources" is considered to mean "fully correlated sources" throughout the thesis;
- the term "elevation angle" is redefined as (90° − elevation) through out the simulation examples presented in the thesis.

CHAPTER 1

INTRODUCTION

By distributing a number of sensors (transducing elements) in a 3-dimensional cartesian space, an array is formed; the region over which the sensors are distributed is called the aperture of the array. The general array processing problem is the obtaining of information about a signal environment from the waveforms received at the array elements (*Figure* 1.1), where the signal environment consists of a number of emitting sources plus noise. These emitting sources, in the case of radar-based systems, are often targets which either reflect transmitted signals (as in active radars) or emit their own signals, (as in passive radar). In situations involving the use of sonar and seismic signals the problems are essentially the same as those encountered in the case of radar.

An important topic in the array processing problem is concerned with interference rejection. Since the emitting sources are distributed in space the array can perform both spatial and temporal filtering in order to optimize the reception of a signal from a desired source (desired signal). This can be achieved by using an array-pattern-forming-network (*Figure* 1.2*a*) so as to place relatively high gain in those

FIGURE – 1.1

ARRAY PROCESSING PROBLEM

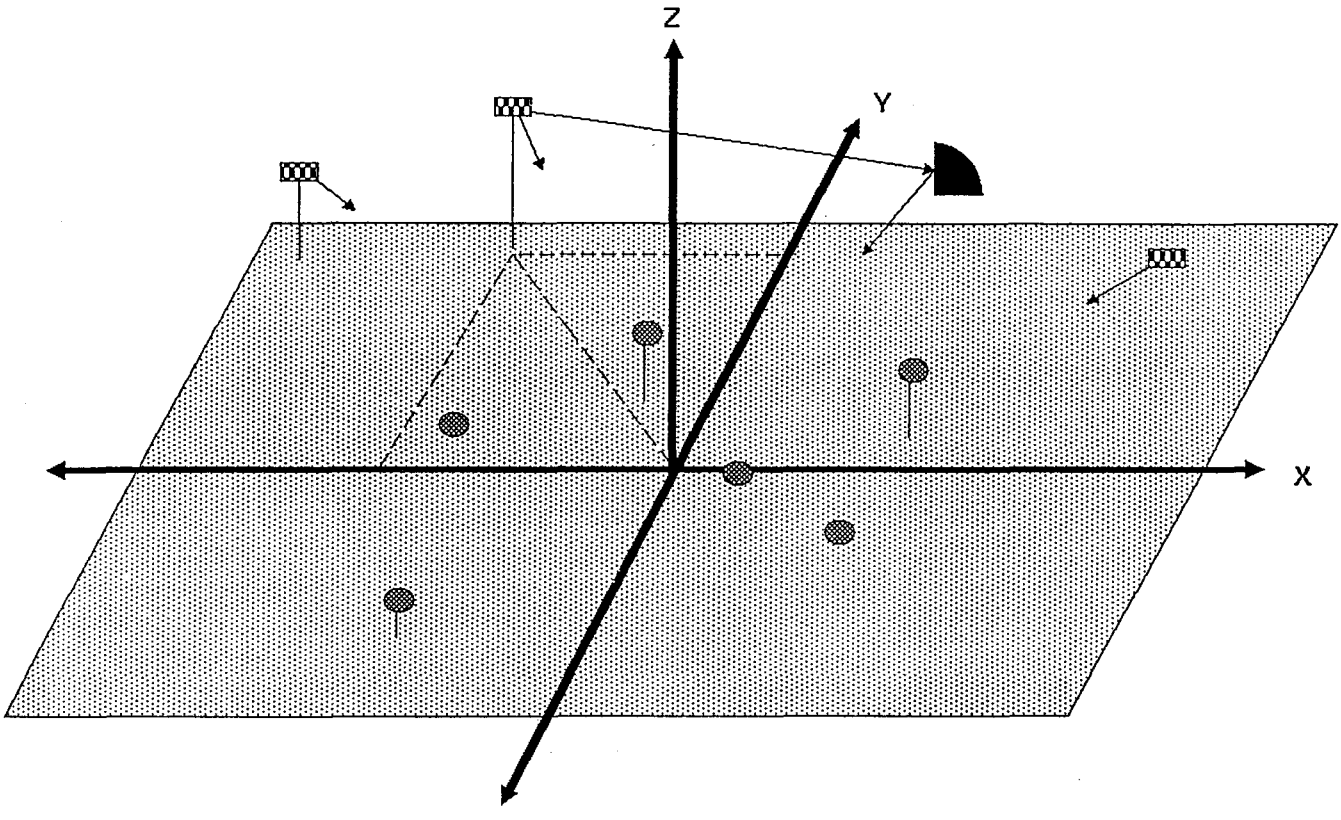

: denotes an array element

: denotes an emitting source

: denotes a reflecting surface

PROBLEM: USING A NUMBER OF SENSORS ESTIMATE SIGNAL ENVIRONMENT IN THE PRESENCE OF NOISE

directions and frequencies which contain the desired signal and at the same time place nulls in the directions and frequencies of the remaining unwanted (interfering) sources.

If the signal environment is known then the pattern-forming network can be fixed and the array response pre-determined. However, in practice the signal environment is often unknown and may vary with time or change its structure (i.e. the turning on and off of certain sources) and thus a very versatile scheme must be used which leads to the concept of adaptive arrays. In adaptive arrays there is an adaptive processor which controls the pattern-forming network according to some performance criterion (*Figure* 1.2*b*).

Another array processing problem is concerned with spatial spectrum estimation and identification. With problems of this type, the array detects the number of directional signals present in the array environment and estimates their parameters; such as location, power, cross correlation etc. Classical spatial spectral estimation techniques are based on the Fourier transform (Conventional Beamformer). The main drawback of the Fourier methods is that they offer limited resolving capabilities. Thus, in the last decade the so called *High Resolution Methods* have been introduced, their main object being to improve the resolving capabilities by using a model for the signals better than that used by Fourier methods. These methods have given fresh impetus to the array processing problem by dealing with the question of the resolution of the arrays in such a way that there is elimination of the effects of *Signal-to-Noise-plus-Interference Ratio* (*SNIR*) on resolution, in contrast to the conventional methods where the resolution is limited by noise.

Recently, the new class of processing techniques called *High Resolution Adaptive Array Processing* [GAB-80], [GAB-86], [GA2-86]

has been created by merging the objectives of both the above mentioned classes. The new class relies heavily on Adaptive Array Techniques, Modern Estimation Theory and Parallel Computer Processing. In general, the aim of *High Resolution Adaptive Array Processing* is to isolate one source and, in addition, to provide estimates of certain other parameters such as the number of interferences present and their directions etc. thus giving solutions to many physical problems arising in radar, sonar, geophysics etc.

The research reported on in this thesis is concerned with some important questions in this general area.

1.1. HISTORICAL PERSPECTIVES

Early work in array processing for interference suppression was carried out at the MIT Lincoln Laboratory in 1963 [ALL-63]. This work was concerned with a non-adaptive interference canceller which could handle one source at a time. The basic idea was to use a main antenna to look at the desired signal and a second antenna to look at the interference and then to subtract the output of the second antenna from the main antenna, with a proper phasing being employed.

Although the term "*adaptive arrays*" was first introduced by Van Atta in 1959, the first papers on adaptive arrays were probably those published in 1964 in a special *IEEE* issue on *Antenna and Propagation* 1964. In 1966 the foundations of array processing and particularly

FIGURE – 1.2

PATTERN FORMING BLOCK DIAGRAM

a)FIXED

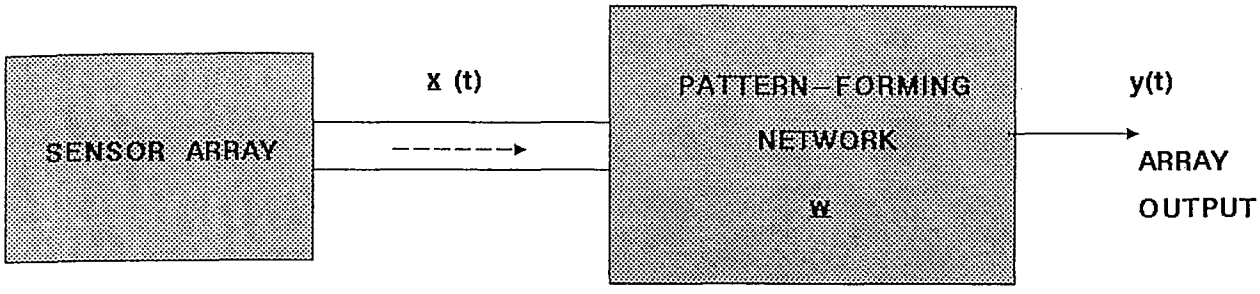

b)ADAPTIVE

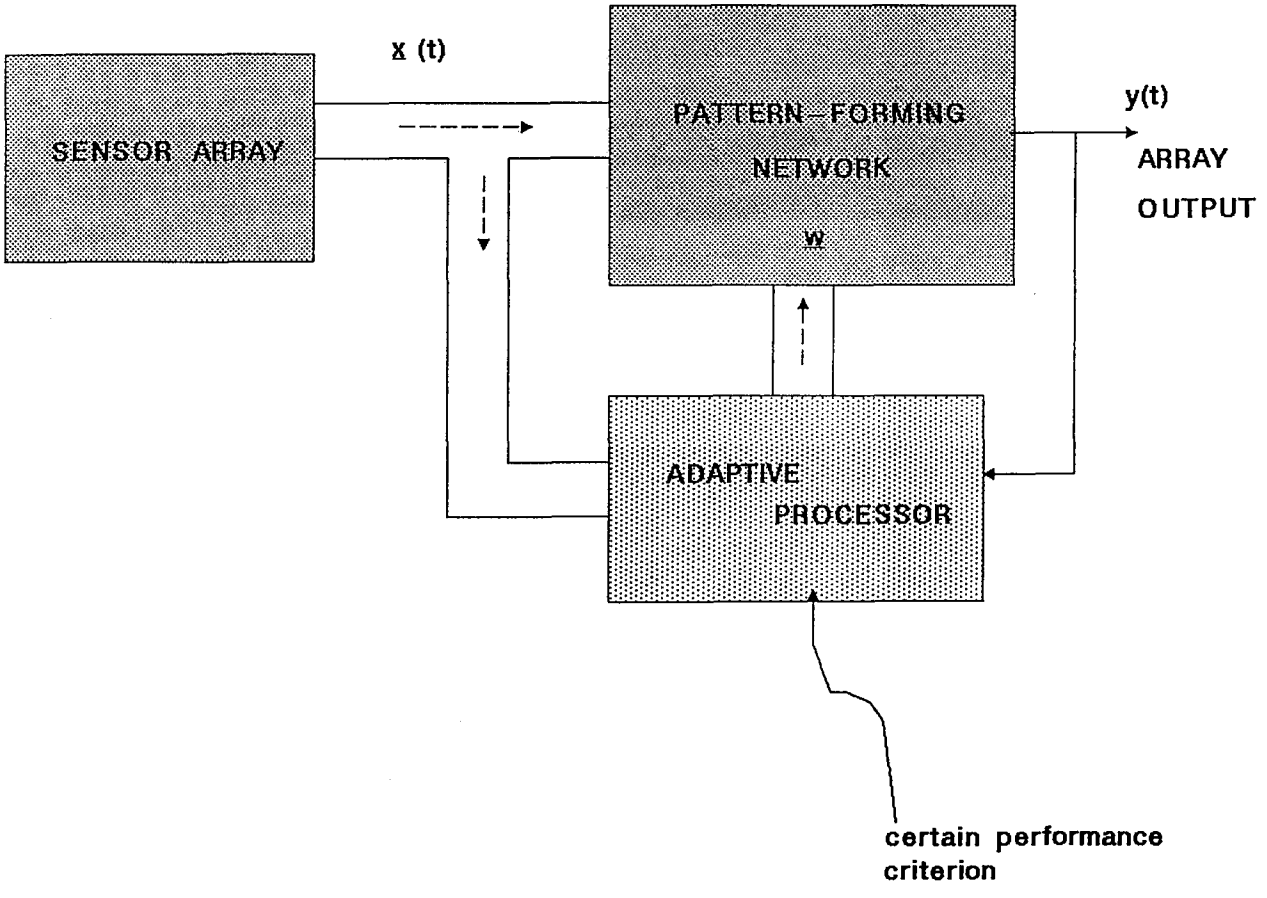

adaptive array processing were established in two papers: by Widrow [WID-66] and Applebaum [APP-66]. The paper by Widrow introduced a new approach for controlling the weights of an adaptive filter and the paper by Applebaum presented a sidelobe canceller capable of handling multiple jamming sources by using the concept of a *correlation feedback loop* (known today as *Applebaum's loop*), for maximizing the signal-to-noise ratio (SNR). Applebaum's sidelobe canceller does, however, need prior knowledge of the signal directions and uses a high gain antenna as the main channel. In general, in adaptive arrays, there is however no need for prior knowledge of the directions of the sources, nor is there a need for use of a high gain antenna. The sidelobe canceller approach is thus not very general.

The first paper on *General Adaptive Arrays* was published the following year (1967) by Widrow et al [WID-67] who applied the ideas contained in his previous paper [WID-66] to develop an adaptive array system. Widrow's work was epoch making and it was based on the minimization of the mean square error between the desired signal and the array output. This approach has come to be known as the Least Mean Square (LMS) algorithm. Applebaum's loop and LMS algorithm have two common points: both use the array covariance matrix in order to derive their adaptive weights and both converge towards the same steady state weight vector which is the WIENER-HOPF solution [HUD-81], [MON-80].

An attractive alternative to the LMS algorithm was introduced in 1974 by Reed, Mallet and Brennan [REE-74] which overcomes the sensitivity of the LMS-type algorithm to eigenvalue spread. The Reed-Mallet-Brennan approach has come to be known as the Sample Matrix Inversion (SMI) algorithm. In the SMI algorithm the optimum weights

are found by estimating the covariance matrix and then solving a linear system of equations. Reference [MAR-86] provides a detailed set-review of references in the area of adaptive arrays.

One of the main problems with conventional adaptive arrays is related to their inability to resolve two sources which are positioned close together. This is illustrated in *Figure* 1.3a, which shows simulation results obtained with a linear array of 5 isotropic uniformly distributed elements. This inability is imposed by the fact that the resolution of adaptive arrays is limited by the SNR. This is demonstrated in *Figure* 1.3*b* in conjunction with *Figure* 1.3*a*., which shows that if SNR is 10dB then the array is unable to resolve the two signals incident from directions 30° and 35° correspondingly (*Figure* 1.3*a*); with a SNR of approximately 30dB (*Figure* 1.3*b*) the two sources of *Figure* 1.3*a* can be resolved. The inability of an array to resolve sources that are close together when noise is present gave rise to a new class of techniques that have been used for the location of emitting sources [MER-81]. These techniques are called *High Resolution* (or *Super-resolution*) techniques (see for instance [SCH-86], [BUR-75], [CAP-69], [JOH-82], [TUF-83], [HUD-85], [WAX-85], [ROY-86]). Two popular methods belonging to this new class are the so called Maximum Likelihood Method (MLM) which is based on the work of Capon [CAP-69] on frequency-wavenumber analysis, and the Maximum Entropy Method (MEM) of Burg [BUR-75]. Capon's method is based on the minimization of the output power subject to the constraint that the inner product of the weight-vector and Source Position Vector is equal to 1. On the other hand, Burg's method is based on an iterative search technique which maximizes the entropy subject to a number of constraints.

Perhaps the most important High Resolution Techniques cur-

FIGURE – 1.3 : ADAPTIVE ARRAY RESOLUTION LIMITATION DUE TO SNR

RELATIVE POWER TABLE :

TOP GRAPH:	BOTTOM GRAPH:
desired signal :1.0	desired signal :1.0
Jammer No.1 (J1):1.0	Jammer No.1 (J1):1.0
Jammer No.2 (J2):1.0	Jammer No.2 (J2):1.0
Noise :0.1	Noise :0.001

a)

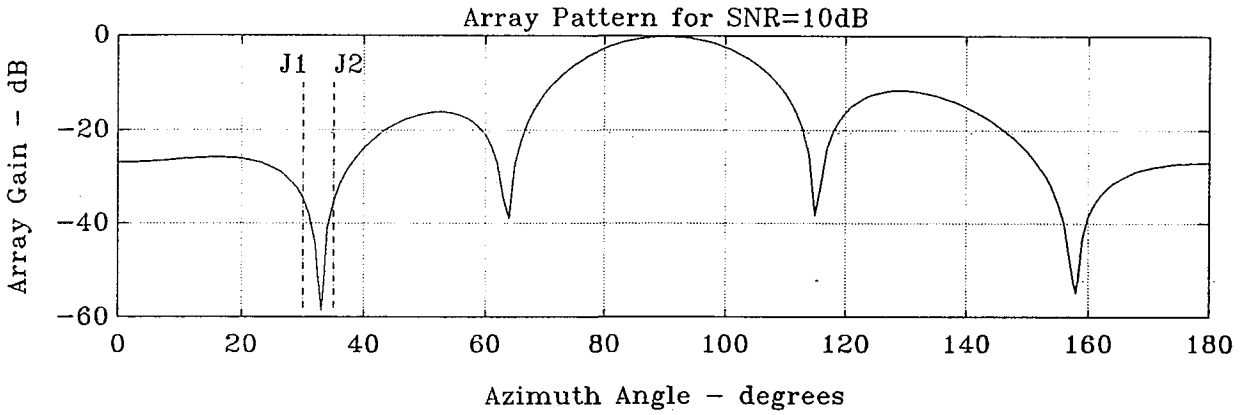

b)

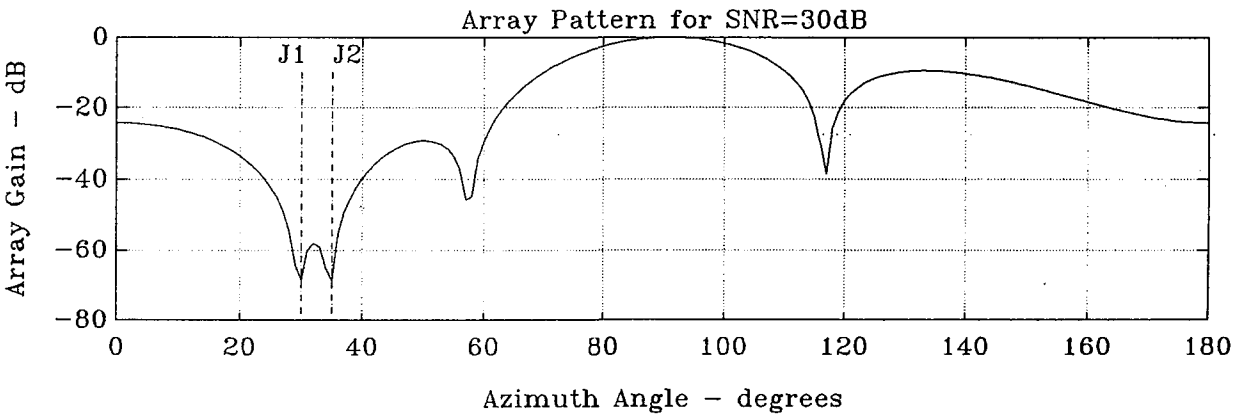

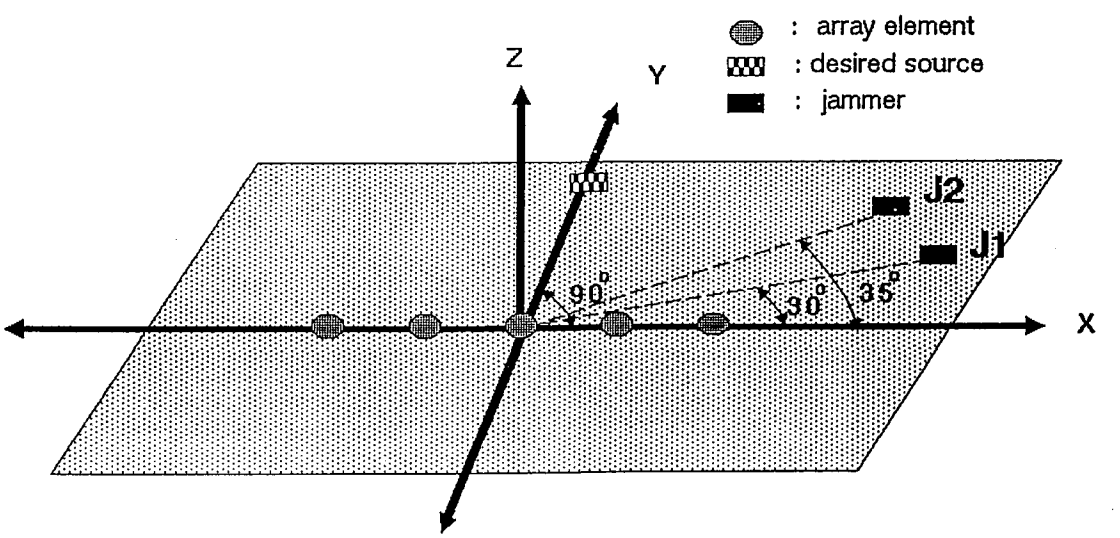

rently being examined are the so called *Signal Subspace* techniques. Aspects relating to techniques of this kind go back to 1795 when Baron de Prony published his work on the fitting of superimposed exponentials to data. The Signal Subspace approach was first introduced formally by Schmidt 1981 [SCH-81] in narrow-band array processing problems and rediscovered independently by Bienvenu and Kopp [BIE-81]. In 1983 Su [SU-83] extended the Schmidt algorithm to the broadband case. Pisarenko [PIS-73] had solved the time series version counterpart problem in a similar way to that of (but earlier than) Schmidt.

The Signal Subspace approach to high resolution involves two main stages of processing. In the first stage a covariance matrix of the data at the sensors of the array is formed and in the second stage an eigenvector decomposition is performed (see for example MUSIC algorithm [SCH-81], [SCH-86]). By the eigenvector decomposition, the observation space is partitioned into two disjoint subspaces:

- the Signal Subspace (SS), with dimension equal to the number of sources, spanned by the Source Position Vectors (SPV);
- the Noise Subspace (NS), with dimension equal to the number of sensors, minus the number of sources.

Thus, every vector belonging to the NS is orthogonal to each SPV. The signal subspace approach offers higher resolving power and less ambiguity than other high resolution methods including the MLM technique of Capon and the MEM method of Burg. This can be seen, for example, in the comparative computer simulation studies carried out by Johnson and Miner [JOH-86] where:

(*i*) the MLM was capable of resolving two sources with 10° separation, provided the SNR was

sufficiently high, but it was unable to do so for sources with 5° separation;

(*ii*) the MEM produced no usable results and

(*iii*) the MUSIC algorithm (a signal subspace technique) produced results in every considered situation.

Thus, signal subspace techniques, which have been used mainly in estimating the directions of emitting sources by employing a spatial array, offer asymptotically "infinite" resolving power capabilities, with limitations imposed only by the limited observation time and the inaccurate modelling of the medium [BIE-85].

Introductory, material for general high resolution estimation can be found in [KAY-88], [MRP-87].

1.2 PROBLEM FORMULATION

From the previous discussion it is obvious that the main interest lies in two problems; these are illustrated briefly in *Figure* 1.4.

The first problem addressed in this thesis is concerned with the source location problem and the use of *Signal Subspace* techniques.

It has been mentioned that high resolution methods and particularly Signal Subspace techniques can handle the source location problem. This is true as long as the present signals are not correlated (coherent). If some of the incident signals are correlated (coherent), then all known existing signal subspace techniques fail. This is a serious limitation since there are many situations in which signal correlation

FIGURE – 1.4

GENERAL PROBLEMS OF MAIN INTEREST
AND GENERAL TECHNIQUES FOR THEIR SOLUTION

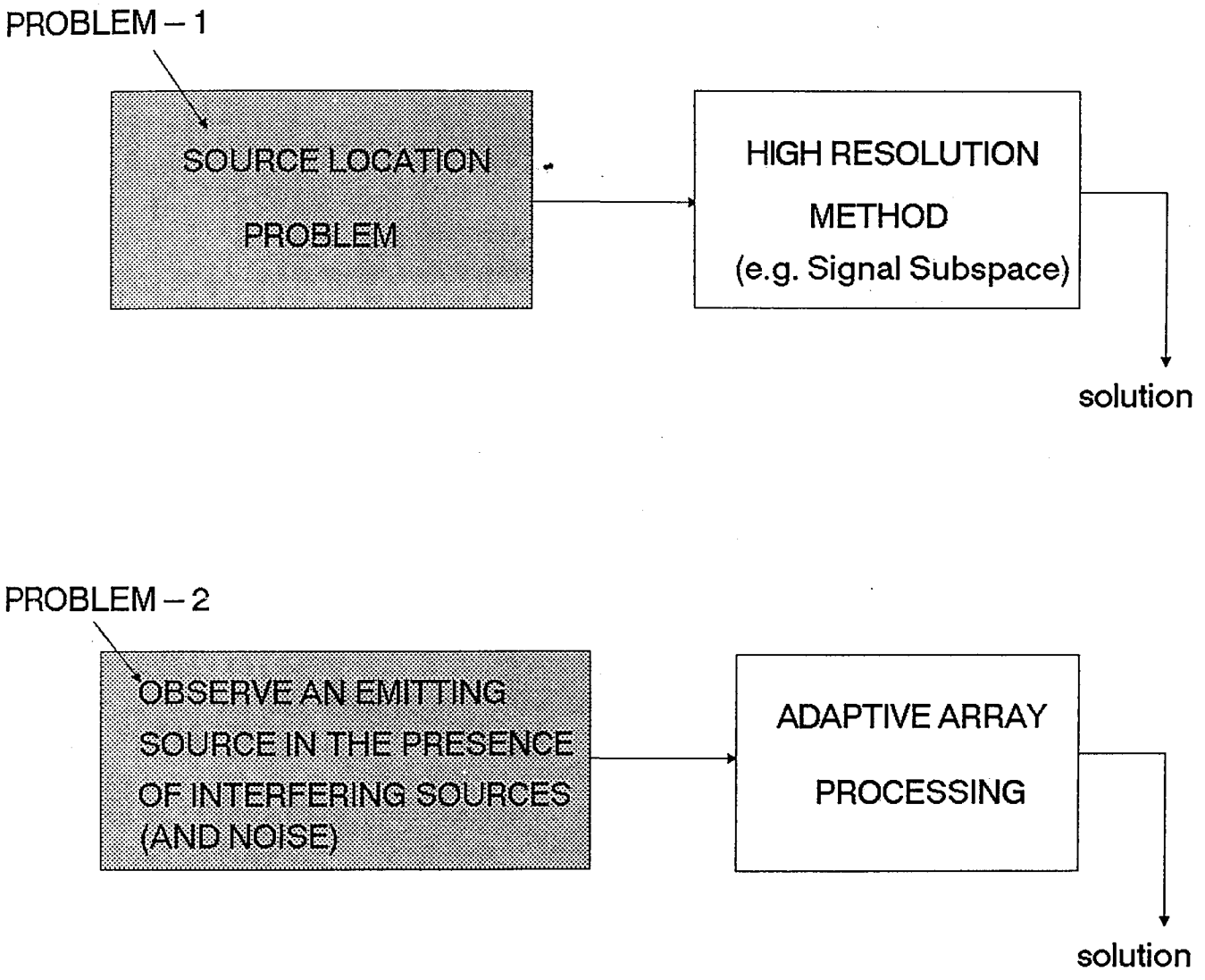

exists. Two common examples are those where *smart* jamming exist and *multipath* propagation is present. The nature of the failure of existing techniques is illustrated in *Figure* 1.5 where a linear array of 5 isotropic elements is considered and three signals, two of which are assumed correlated, are present. *Figure* 1.5, shows that although the Signal Subspace algorithm (MuSIC) correctly indicates the location (direction) of the uncorrelated source, it fails completely to indicate even the existence of the two correlated sources.

In addition to their inability to operate with correlated signals, signal subspace algorithms also require prior knowledge of the number of signals present in order to be able to function correctly.

Thus, at this time much effort is being devoted to the question of handling correlated (multipath) sources. In order to rectify this 'breakdown' of high resolution and particularly signal subspace techniques when signal correlation (or coherence) is involved, a number of new techniques have been developed. The most significant of those new techniques are based on the idea of *subaperture sampling* or *spatial smoothing* discovered originally by Evans, Johnson and Sun [EVA-81] and independently rediscovered and improved by Shan, Wax and Kailath [SHA-85], [SH2-85]. The *Spatial Smoothing* technique is based on defining a number of subarrays and for each subarray the covariance matrix $\mathbf{R}_i$ is formed. Then the average covariance matrix $\widetilde{\mathbf{R}}$ is estimated as follows:

$$\widetilde{\mathbf{R}} = \frac{1}{No.\ of\ subarrays} \cdot \sum_i \mathbf{R}_i \qquad (1.1)$$

After this, the next stage in the process is to use the previously developed MuSIC algorithm [SCH-86] to provide the location of the

FIGURE – 1.5 (ASSUMING SOURCES S1 and S2 ARE FULLY CORRELATED)

	TRUE directions	directions estimated by MUSIC
source No.1 (S1)	(0.0, 30.0)	Failure
source No.2 (S2)	(0.0, 135.0)	Failure
source No.3 (S3)	(0.0, 90.0)	(0.0000, 90.0000)

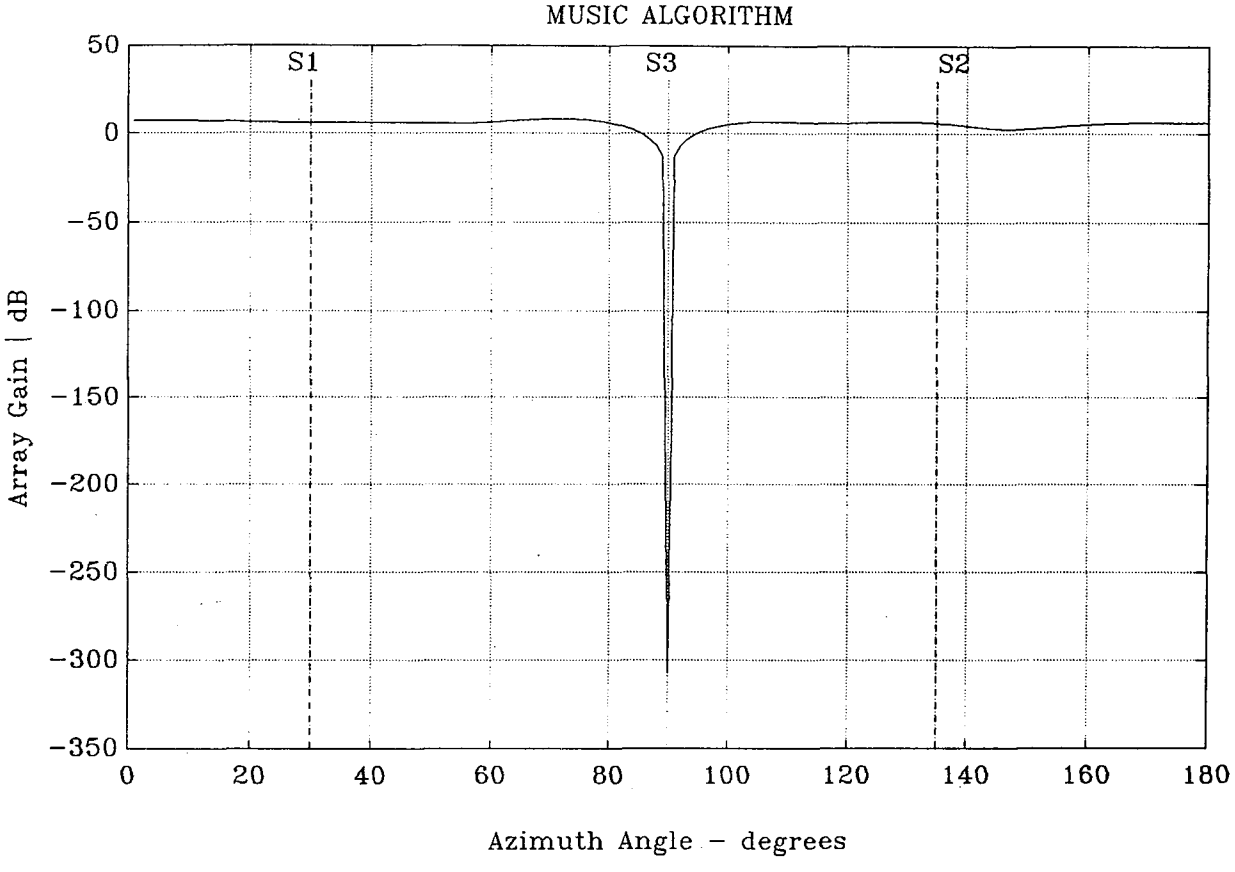

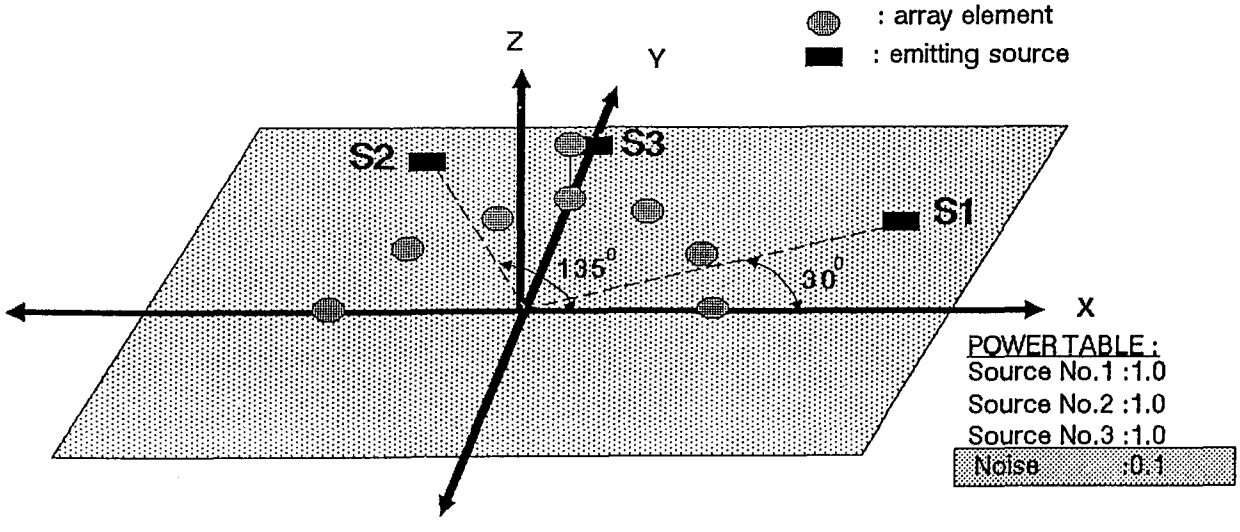

sources. At this time, to the author's knowledge, the Shan, Wax and Kailath technique is the only significant method to have been published which handles correlated sources. However, this method can only be applied to linear arrays with uniformly spaced identical sensors. In addition, it provides a reduction of array aperture which implies a reduction in resolving power. Thus the Shan, Wax and Kailath technique is not very satisfactory.

The research reported on in this thesis (see *Chapter* 3 and 4) is concerned with new techniques which are applicable to general non-linear arrays.

The research aims at the development of new techniques which will have a dual function: to provide satisfactory results for the signal environment where the existing superresolution techniques work and, in addition, to overcome the problems of existing Signal Subspace techniques just referred to above.

The general problem addressed in this thesis is concerned with processing the output of an array of sensors for the general environment in which

- there is an array of sensors with no helpful symmetry to be obtained from the suitable disposition of the sensors.
- the number of sources is a priori unknown (although it is assumed that the number of such sources is less than the number of elements in the array),
- multipath (correlated) propagation may be involved;
- there are unknown noise effects.

The general aims are to process the output of the array in order to estimate parameters such as the number of signal sources, their

locations, their power etc, in the presence of noise.

In *Chapter* 3 the theoretical framework of a newly developed algorithm, called ASPECT, is set out. This algorithm is capable of handling both correlated (coherent) and uncorrelated (uncoherent) sources and is general in that it is applied to a general array geometry (not just to linear array). The results of computer simulations of applications of ASPECT algorithm are given in *Chapter* 4 and the superiority of the results, which confirm the validity and generality of ASPECT algorithm, is discussed.

The second problem addressed in this thesis (Problem 2, *Figure* 1.4) is concerned with observing a so-called "*wanted*" emitting source in the presence of other "unwanted" (interfering) sources and noise. This is a well known problem with a well-known solution, the so-called Wiener-Hopf solution (e.g. see [HUD-81]). If the direction of the desired signal is known, or can be measured, then the problem can be handled by steered vector adaptive arrays. However, steered vector adaptive arrays have a number of drawbacks, depending on the presence or otherwise of the desired signal. Two main drawbacks of the steered vector adaptive array approach are the power inversion problem and the problem due to pointing errors. If the desired signal power at the input of the array increases, this results in a reduction of the desired signal power at the output of the array, which may result in its total cancellation. This is known as the power inversion problem. On the other hand, pointing errors occur when knowledge about the direction of the desired signal is inaccurate. In addition steered vector arrays always allow interference to pass at the output thus contaminating the desired signal. Furthermore, they are incapable of providing information about the directions of the unknown interferences. In *Chapter* 5 a new approach is

adopted in which the concepts of signal subspace methods are extended into conventional steered vector adaptive arrays in order:

- to analyze the behaviour of the array and highlight the above problems; and
- to present a new algorithm capable of isolating a desired signal in the presence of unknown interferences and at the same time provide
  i) complete interference cancellation and
  ii) the interference locations.
  The new algorithm although still susceptible to pointing errors does not suffer from power inversion problems.

The approach is different in important ways from that put forward relatively recently by Citron and Kailath [CIT-84].
Following this a modification of the ASPECT algorithm is presented. By this modification it is then possible to use the so-modified ASPECT algorithm to obtain information relating to the direction of unknown interferences even in correlated situations.

In *Chapter* 6 simulation results of the new algorithms are presented showing that the proposed processor:

- provides the complete cancellation of unknown interferences at the output of the array;
- provides complete information about the location of interfering sources
- does not suffer from power inversion problems;
- offers less susceptibility to pointing errors. In the case of the ASPECT algorithm, the pointing errors are eliminated.

Some conclusions together with suggestions for further work are presented in *Chapter* 7.

In *Chapter* 2, which follows, some essential notation is introduced and the signals forming the input to the adaptive array are formulated.

A general signal model, which takes into account both spherical wave and multipath propagation, is developed and important aspects of the structure of the covariance matrix are discussed. Following this, noise models are formulated and the concepts of the array manifold and array manifold dimensionality are introduced and defined. The material presented in *Chapter* 2 is used extensively in later chapters of the thesis.

CHAPTER 2

FORMULATION OF ARRAY INPUT SIGNALS

In this chapter some basic material relating to array processing is presented. This material is essential for the analysis given in the chapters which follow. The mathematical formulation of the signal environment is defined, from which the signal structure of the array can be determined in terms of the geometrical configuration of the array for both spherical wave and plane wave propagation. Finally, the correlation functions, the noise quantities and the concepts of array manifold and array manifold dimensionality are defined.

2.1 NOTATION : ENVIRONMENT STRUCTURE

In the following, both lower and upper case symbols are used to represent scalars, underlined symbols are used to represent vectors, and **BOLDFACE** symbols are used to represent matrices. The symbols T and H when used as superscripts of vectors or matrices are used to indicate transposition and complex conjugate transposition,respectively.

The subscript k is used to indicate *the k^{th} sensor of the array* and this sensor is considered to be positioned at a specific point, $\underline{r}_k$, in space. The subscript i is used to indicate *the i^{th} source* which is considered to be positioned at a point $\underline{r}_i$ in space. A double subscript is taken to represent the direction from the point specified by the first subscript to the point specified from the second one; for instance the double subscript of $\underline{k}_{ik}$ indicates that the vector $\underline{k}$ has direction from the point $\underline{r}_i$ to the point $\underline{r}_k$.

The signal environment is assumed in general to be composed of both directional and isotropic signal sources (non-directional). The signal of directional sources are represented by:

$$m_i(t) \quad for \quad i \in [1, \ldots, D] \quad and \quad i, D \in \mathcal{N}^+ \tag{2.1}$$

where D is the number of sources. The structure of the signal of a directional source can be considered to involve both amplitude and phase modulation of a carrier. That is, the signal $m_i(t)$ emitting from the i^{th} source can be considered to be:

$$m_i(t) = A_i(t).cos[\, 2\pi f_0 t + \; h_i(t) + a_i \,] \tag{2.2}$$

where A_i(t) and $h_i(t)$ represent slowly varying signals that modulate the amplitude and phase respectively of $m_i(t)$, while the combined isotropic plus thermal noise at each sensor element of the array can be modelled by:

$$n_k(t) = B_k(t).cos[\, 2\pi f_0 t + b_k] \tag{2.3}$$

$k \in [1, \ldots, N]$, $k, N \in \mathcal{N}^+$, N *is the number of sensors*

In *Equations* 2.2 and 2.3 the modulations $A_i(t)$, $h_i(t)$ and $B_k(t)$ are assumed to be zero mean sample functions of independent, ergodic, random processes. Since the noise terms $n_k(t)$ are considered to be bandlimited white noises processes, B_k has a Rayleigh distribution. In addition the independent random variables a_i, b_k are considered uniformly distributed on $(0,2\pi)$ and are included to ensure stationarity.

2.2 SPHERICAL WAVE MODELLING

Consider a source current (a time-varying current or charge) located, as shown in *Figure* 2.1, in a spherical coordinate system, producing an electromagnetic field. It is well known [KRA-81] that the phasor field can be expressed by:

$$\underline{E} = \frac{1}{j\omega\mu\epsilon}\underline{\nabla}\,(\underline{\nabla}\,.\underline{A}\,) \;-\; j\omega\underline{A} \qquad\qquad H = \frac{1}{\mu}(\underline{\nabla}\times\,\underline{A}) \qquad (2.4)$$

where

$\underline{E}$	*is the electric field vector* $\underline{E}=(E_r,E_\theta,E_\phi)$
$\underline{H}$	*is the magnetic field vector* $\underline{H}=(H_r,H_\theta,H_\phi)$
μ,ϵ	*are constants (permeability and permitivity respectively)*

Thus, the electromagnetic field transmitted by a source has six components. Depending on the nature of the source, some of the components may be zero. For example, if the source is a dipole then the

FIGURE – 2.1

GEOMETRY FOR DETERMINING THE RATIATION FIELD AT $\underline{r}_k$
FROM A SOURCE-CURRENT LOCATED AT $\underline{r}_i$

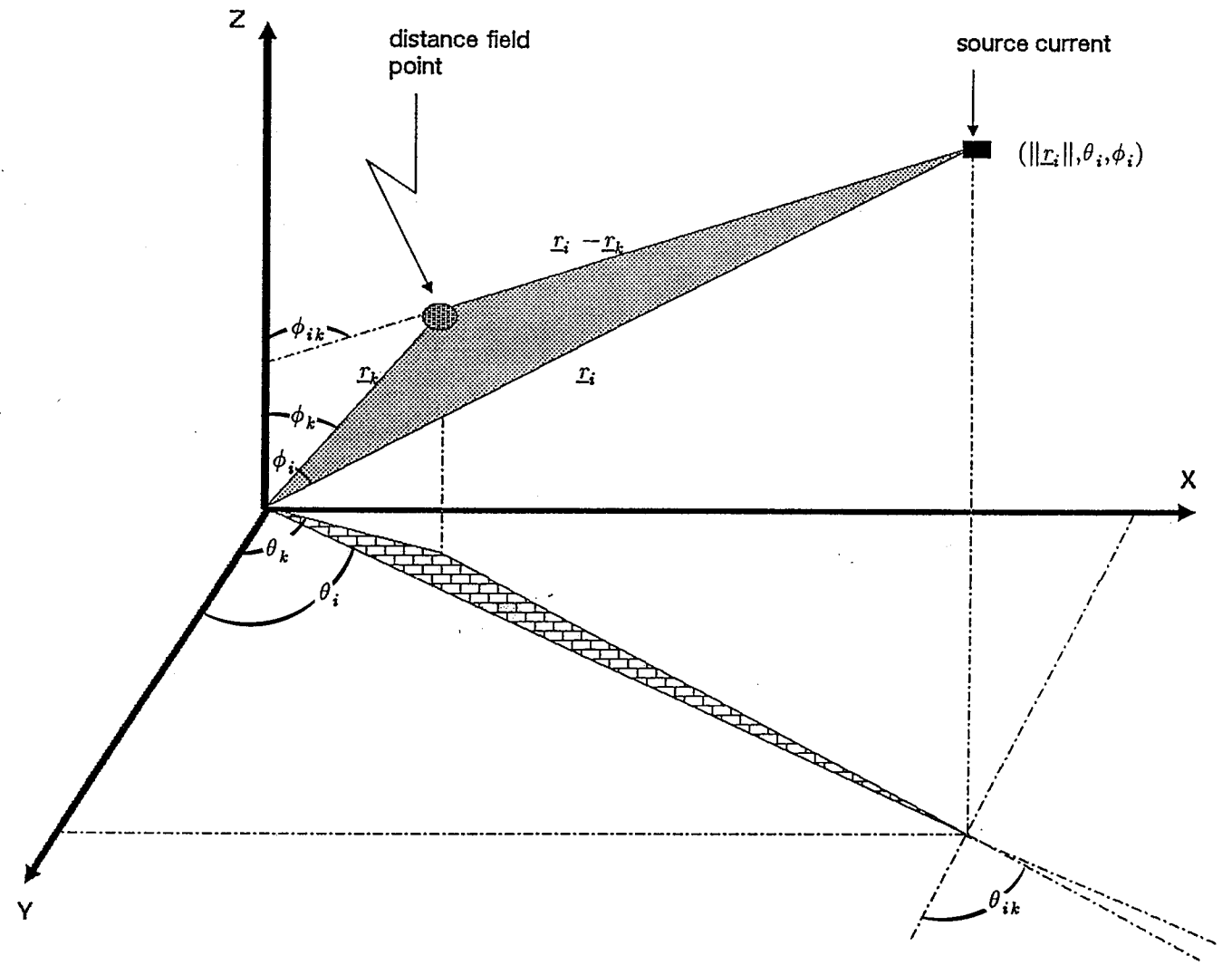

electromagnetic field consists of only three components, E_r,E_θ and H_ϕ. However, the antenna region can be partitioned into two well-known sub-regions [KRA-81], namely the *near* and *far field* zones. Moreover, since the *near field* does not contribute to the time average power flow away from the emitting source it can be ignored. Thus, the only region of interest is *far field* zone. By examining the six components of the electromagnetic waves in the *far field*, it can be shown [NEF-81] that E_r,H_r are both zero. This is true regardless of the nature of the antenna being used.

Thus, the *six* components in the *far field* can be summarized in general terms as follows, for any antenna:

$$\begin{aligned} E_r &= 0 & H_r &= 0 \\ E_\theta &= -j\omega A_\theta & H_\theta &= -\frac{E_\phi}{\eta} \\ E_\phi &= -j\omega A_\phi & H_\phi &= -\frac{E_\theta}{\eta} \end{aligned} \tag{2.5}$$

In the above equations η is a propagation constant and A_θ and A_ϕ will always have the general form [NEF-81]:

$$\begin{aligned} A_\theta &= \frac{\mu}{4\pi} \cdot F_\theta(\theta_{ik},\phi_{ik}) \cdot I_i(t-\frac{||\underline{r}_i-\underline{r}_k||}{c}) \cdot \frac{exp[-j\underline{k}^T(\underline{r}_i-\underline{r}_k)]}{||\underline{r}_i-\underline{r}_k||} \\ A_\phi &= \frac{\mu}{4\pi} \cdot F_\phi(\theta_{ik},\phi_{ik}) \cdot I_i(t-\frac{||\underline{r}_i-\underline{r}_k||}{c}) \cdot \frac{exp[-j\underline{k}^T(\underline{r}_i-\underline{r}_k)]}{||\underline{r}_i-\underline{r}_k||} \end{aligned} \tag{2.6}$$

In *Equation* 2.6 above, $I_i(t)$ represents the excitation current of the transmitting antenna, $\underline{k}$ is the wave-number vector, or spatial frequency, with $\underline{k} = \underline{\alpha}.\omega$ where $\underline{\alpha}$ is the slowness vector which shows the

direction of propagation, c is the velocity of propagation while F_θ,F_ϕ represent functions depending on the type of the transmitting antenna. On the basis of the *Equation* 2.5 it can be seen that only two of the six components are of great significance; namely E_θ and E_ϕ. Therefore, a *point source* located at the $\underline{r}_i$ (i^{th}—source, say) which excites the transmitting antenna with an excitation current $I_i(t)$, produces at a point $\underline{r}_k$ an electric field $\underline{E}=E_\theta.\underline{a}_\theta+E_\phi.\underline{a}_\phi$ whose magnitude expressed in a general form is as follows (regardless of the type of antenna being used):

$$\|\underline{E}\| = F_i(\theta_{ik},\phi_{ik}) \cdot I_i(t-\frac{\|\underline{r}_i-\underline{r}_k\|}{c}) \cdot \frac{exp[-j\underline{k}^T(\underline{r}_i-\underline{r}_k)]}{\|\underline{r}_i-\underline{r}_k\|} \qquad (2.7)$$

where $F_i(\theta_{ik},\phi_{ik})=\frac{-j\omega\mu}{4\pi} \cdot \sqrt{F_\theta(\theta_{ik},\phi_{ik})^2 + F_\phi(\theta_{ik},\phi_{ik})^2}$

Supposing, next, that there is a receiving element at point r_k with directional gain $G_k(\theta_{ik},\phi_{ik})$. Then the received signal due to i^{th}-source will be:

$$x_k = G_k(\theta_{ik},\phi_{ik}).F_i(\theta_{ik},\phi_{ik}) \cdot I_i(t-\frac{\|\underline{r}_i-\underline{r}_k\|}{c}) \cdot \frac{exp[-j\underline{k}^T(\underline{r}_i-\underline{r}_k)]}{\|\underline{r}_i-\underline{r}_k\|} \qquad (2.8)$$

Consider now that the excitation current time function $I_i(t)$ is equal to the baseband modulation function $m_i(t)$ as given by *Equation* 2.2 of the previous section. That is:

$$I_i(t) = m_i(t) \qquad (2.9)$$

Then equation 2.8 can be written as:

$$x_k = m_i(t - \frac{\|\underline{r}_i - \underline{r}_k\|}{c}) \cdot F_i(\theta_{ik},\phi_{ik}) \cdot \frac{G_k(\theta_{ik},\phi_{ik})}{\|\underline{r}_i - \underline{r}_k\|} \cdot exp[-j\underline{k}_{ik}{}^T(\underline{r}_i - \underline{r}_k)] \tag{2.10}$$

In *Equation* 2.10 the subscript ik has been added to the wave-number vector $\underline{k}$ in order to stress the fact that the direction of propagation is

$$from\ point\ \ \underline{r}_i = (\|\underline{r}_i\|,\theta_i,\phi_i)\ \ \ to\ point\ \ \underline{r}_k = (\|\underline{r}_k\|,\theta_k,\phi_k)$$

By shifting the time origin at the centre of the array the function $m(t)$ becomes:

$$m_i(t - \frac{\|\underline{r}_i - \underline{r}_k\|}{c}) = m_i(t + \frac{\|r_i\| - \|\underline{r}_i - \underline{r}_k\|}{c}).exp[\ j.\underline{k}_i{}^T.\underline{r}_i] \tag{2.11}$$

Thus *Equation* 2.10 becomes:

$$x_k = m_i(t - T_{i_{ok}}) \cdot F_i(\theta_{ik},\phi_{ik}) \cdot \frac{G_k(\theta_{ik},\phi_{ik})}{\|\underline{r}_i - \underline{r}_k\|} \cdot exp[j\underline{k}_i{}^T\underline{r}_i - j\,\underline{k}_{ik}^T(\underline{r}_i - \underline{r}_k)] \tag{2.12}$$

$$\text{where } T_{i_{ok}} = -\frac{\|r_i\| - \|\underline{r}_i - \underline{r}_k\|}{c}$$

2.3 REFLECTED SPHERICAL WAVE

Consider that the received signal is a result of a geometrical situation such as that illustrated in *Figure* 2.2. Using the analysis of the previous section it is easy to show that the signal received by an element at point $\underline{r}_k$, is given by:

$$x_{k\text{-}refl} = m_i(t - \frac{\|\underline{r}_i - \underline{r}_{l_i}\| + \|\underline{r}_{l_i} - \underline{r}_k\|}{c}) \cdot F_i(\theta_{il_i}, \phi_{il_i})$$

$$\cdot \frac{G_k(\theta_{l_ik}, \phi_{l_ik}).exp[-j\underline{k}_{il_i}{}^T.(\underline{r}_i - \underline{r}_{l_i})]}{\|\underline{r}_i - \underline{r}_{l_i}\| + \|\underline{r}_{l_i} - \underline{r}_k\|} \cdot exp[-j\underline{k}_{l_ik}{}^T.(\underline{r}_{l_i} - \underline{r}_k)] \tag{2.13}$$

Note that if there is no reflection, then the above equation simplifies to *Equation* 2.12 on the substitution of $\underline{r}_{l_i}$ for either $\underline{r}_k$ or $\underline{r}_i$.
By shifting the time origin at the centre of the array, the *Equation* 2.13 becomes:

$$x_{k\text{-}refl} = m_i(t + \frac{\|\underline{r}_i\| - \|\underline{r}_i - \underline{r}_{l_i}\| - \|\underline{r}_{l_i} - \underline{r}_k\|}{c}) \cdot F_i(\theta_{il_i}, \phi_{il_i}) \cdot$$

$$\cdot \frac{G_k(\theta_{l_ik}, \phi_{l_ik})}{\|\underline{r}_i - \underline{r}_{l_i}\| + \|\underline{r}_{l_i} - \underline{r}_k\|} \cdot exp[-j\underline{k}_{il_i}^T.(\underline{r}_i - \underline{r}_{l_i}) - j\underline{k}_{l_ik}^T.(\underline{r}_{l_i} - \underline{r}_k) + j.\underline{k}_i{}^T.\underline{r}_i] \tag{2.14}$$

However, it is reasonable to express this equation with respect to the baseband signal coming via the direct path, that is with respect to $m_i(t - T_{i_{ok}})$. Then, *Equation* 2.14 implies:

FIGURE—2.2

GEOMETRY FOR DETERMINING THE RATIATION PATTERN
WHEN REFLECTION IS INVOLVED

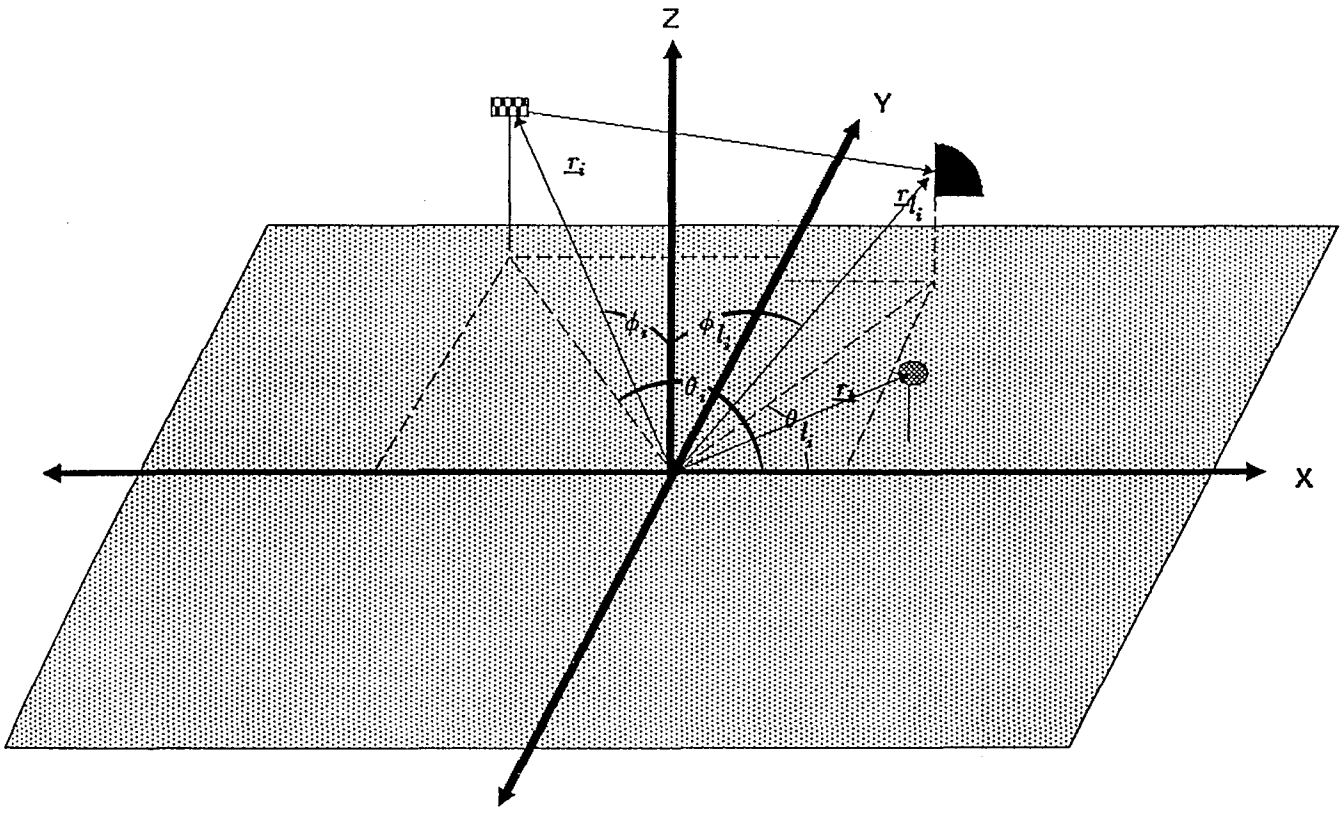

: denotes the k^{th} array element

: denotes the i^{th} emitting source

: denotes a reflecting surface

$$x_{k\text{-}refl} = m_i(t-T_{i_{ok}}).\ F_i(\theta_{il_i},\phi_{il_i}) \cdot \frac{G_k(\theta_{l_ik},\phi_{l_ik})}{\|\underline{r}_i-\underline{r}_{l_i}\|+\|\underline{r}_{l_i}-\underline{r}_k\|}\cdot$$

$$.exp[-j2\underline{k}_{il_i}^T.(\underline{r}_i-\underline{r}_{l_i})-j2\underline{k}_{l_ik}^T.(\underline{r}_{l_i}-\underline{r}_k)].\ exp[j.\underline{k}_i{}^T.\underline{r}_i+j\underline{k}_{ik}^T.(\underline{r}_i-\underline{r}_k)] \tag{2.15}$$

The last equation is the exact equation for a reflected signal, received by the k^{th} element of an array of sensors.

At the receiving elements the function $F_i(\theta_{il_i},\phi_{il_i})$ is constant and it is convenient to omit it. Thus, *Equation* 2.15 becomes

$$x_{k\text{-}refl} = \rho_{il_i}.exp[j.\Delta p_{il_ik}]\ .\ m_i(t-T_{i_{ok}}).$$

$$\frac{G_k(\theta_{l_ik},\phi_{l_ik})}{\|\underline{r}_{l_i}-\underline{r}_k\|}\ .\ exp[j\underline{k}_{l_i}^T.\underline{r}_{l_i}-j\underline{k}_{l_ik}^T.(\underline{r}_{l_i}-\underline{r}_k)] \tag{2.16}$$

where Δp_{il_ik} is the phase difference introduced by the il_ik path while ρ_{il_ik} is the attenuation introduced by il_i part of the il_ik path with:

$$\rho_{il_ik}=\frac{\|\underline{r}_{l_i}-\underline{r}_k\|}{\|\underline{r}_i-\underline{r}_{l_i}\|+\|\underline{r}_{l_i}-\underline{r}_k\|} \tag{2.17}$$

$$\Delta p_{il_ik}=-2\underline{k}_{il_i}^T.(\underline{r}_i-\underline{r}_{l_i})-\underline{k}_{l_ik}^T.(\underline{r}_{l_i}-\underline{r}_k)+\underline{k}_i{}^T.\underline{r}_i+\underline{k}_{ik}^T.(\underline{r}_i-\underline{r}_k)-\underline{k}_{l_ik}^T.\underline{r}_{l_i} \tag{2.18}$$

Now, the subscript *refl* in *Equation* 2.16 can be dropped since that relation is so general as to include *Equation* 2.12 as a special case. This becomes clear by considering $l_i=i$; then $\Delta p_{il_ik}=0$ and $\rho_{il_ik}=1$. Thus, *Equation* 2.16 will be used as the model of incident directional signals for spherical wave propagation.

2.4 SIGNAL STRUCTURE AT THE ARRAY

Consider an array of N sensors (elements) in which each element has known directional characteristics and is located in a known, but arbitrary, position. The array environment is considered to be narrowband. This consideration is not essential but is made to simplify notation and problem formulation. It should be noted that wideband problems can be decomposed into a set of narrowband problems.

Thus, consider that there are D narrowband stationary zero-mean sources whose frequencies of emissions are centred at the frequency ω_0. It is assumed also that there is additive noise present at all N elements and that this noise is assumed to be an unknown, stationary, zero mean random process, which may be correlated from sensor to sensor.

On the basis of the above analysis, the received signal at the k^{th} sensor at the time instant t due to all transmitting sources and noise can be expressed as:

$$x_k(t) = n_k(t) + \sum_{i=1}^{D} \sum_{l=1}^{L_i} \rho_{i l_i} . exp[j.\Delta p_{i l_i k}] \; . \; m_i(t - T_{i_{ok}}) . \frac{G_k(\theta_{l_i k}, \phi_{l_i k})}{\|\underline{r}_{l_i} - \underline{r}_k\|} \; . \; exp[j\underline{k}_{l_i}^T . \underline{r}_{l_i} - j\underline{k}_{l_i k}{}^T . (\underline{r}_{l_i} - \underline{r}_k)] \qquad (2.19)$$

$$with \quad \begin{cases} l_i = i \\ \Delta p_{i l_i k} = 0 \qquad for \;\; all \;\; direct \;\; paths \;\; \forall i[1,..,D] \\ \rho_{i l_i k} = 1 \end{cases}$$

where, in the *Equation* 2.19, L_i represents the number of paths from the i^{th} source to the k^{th} sensor with:

$$\sum_{i=1}^{D} L_i = M < N \tag{2.20}$$

In the *Equation* 2.20 M represents the number of signals incident on the array and M becomes equal to D if each of the signal sources arrives at the array through only one path and, otherwise $D<M$. Thus, the array input signal-vector (N *in dim*) can be expressed in the following compact form:

$$\underline{x}(t) = \sum_{i=1}^{D} \sum_{l=1}^{L_i} \mathbf{D}_{l_i} . \underline{S}_{l_i} + \underline{n}(t) \tag{2.21}$$

where

$$\underline{x}(t) = [\![\ x_1(t),\ x_2\ (t),\ ...,\ x_N(t)\ ]\!]^T$$

$$n(t) = [\![\ n_1(t),\ n_2(t),\ ...,\ n_N(t)\ ]\!]^T$$

$$\mathbf{S} = [\![\underline{S}_{1_1},\ \underline{S}_{1_2},\ ...,\ \underline{S}_{1_{L_1}},\ S_{2_1},\ \underline{S}_{2_2},\ ...,\underline{S}_{D_{L_D}}]\!]$$

$$\underline{S}_{l_i} = \begin{bmatrix} \frac{G_1(\theta_{l_i 1},\phi_{l_i 1})}{\|\underline{r}_{l_i} - \underline{r}_1\|} . exp[j.\underline{k}_{l_i}^T . \underline{r}_{l_i} - j.\underline{k}_{l_i 1}^T . (\underline{r}_{l_i} - \underline{r}_1)] \\ \frac{G_2(\theta_{l_i 2},\phi_{l_i 2})}{\|\underline{r}_{l_i} - \underline{r}_2\|} . exp[j.\underline{k}_{l_i}^T . \underline{r}_{l_i} - j.\underline{k}_{l_i 2}^T . (\underline{r}_{l_i} - \underline{r}_2)] \\ ..... \\ ..... \\ \frac{G_N(\theta_{l_i N},\phi_{l_i N})}{\|\underline{r}_{l_i} - \underline{r}_N\|} . exp[j.\underline{k}_{l_i}^T . \underline{r}_{l_i} - j.\underline{k}_{l_i N}^T . (\underline{r}_{l_i} - \underline{r}_N)] \end{bmatrix}$$

$$\mathbf{D}_{l_i} = diag \begin{bmatrix} \rho_{i l_i 1} . exp[j.\Delta p_{i l_i 1}] \ .\ m_i(t - T_{i_{o1}}) \\ \rho_{i l_i 2} . exp[j.\Delta p_{i l_i 2}] \ .\ m_i(t - T_{i_{o2}}) \\ ..... \\ ..... \\ \rho_{i l_i N} exp[j.\Delta p_{i l_i N}] \ .\ m_i(t - T_{i_{oN}}) \end{bmatrix}$$

If, however, the signals are narrowband, and the time of propagation across the array is sufficiently small then

$$\rho_{il_i1}=\rho_{il_i2}=...=\rho_{il_iN}=\rho_{il_i}$$

and

$$\Delta p_{il_i1}=\Delta p_{il_i2}=....=\Delta p_{il_iN}=\Delta p_{il_i}.$$

This makes the diagonal matrix $\mathbf{D}_{l_i}$ equivalent to a scalar; that is

$$\mathbf{D}_{l_i} = \rho_{il_i}.exp[j.\Delta p_{il_i}] \; . \; m_i(t-T_{io}). \quad (2.22)$$

Thus, *Equation* 2.21 can be expressed in the following convenient form:

$$\underline{x}(t) = \mathbf{S} \; . \; \underline{m}(t) + \underline{n}(t) \quad (2.23)$$

where

$$\underline{m}(t)=[\![m_{1_1}(t),m_{2_1}(t),...,m_{L_1}(t),m_{1_2}(t), \; .... \; , \; m_{L_D}(t)]\!]^T$$

with $m_{l_i}(t) = \rho_{il_i}.exp[j.\Delta p_{il_i}]. \; m_i(t-T_{io})$

N.B.:the subscript $(.)_{1_i}$ *refers to direct path of* i^{th} *source*

Both *Equation* 2.23 and *Equation* 2.21 provide a model of a very general array environment where:

(i) the array is a 3-dimensional non-uniform antenna array;
(ii) spherical wave propagation is considered;
(iii) the range as well as the direction of arrival (azimuth-elevation angles) is involved;
(iv) the reception of signals through multipath environment is taken into account.
(v) additive noise effects are included.

In many applications in practice a simplified model is used by ignoring the range of the source and approximating the spherical wave propagation by plane waves. This simplified model is discussed in the following section.

2.5 PLANE WAVE APPROXIMATION

A significant difference between a plane wave and a spherical wave is that a plane wave suffers no attenuation (in a lossless medium) whereas a spherical wave does because it expands over a larger and larger region as it propagates. This is reflected by the term:

$$\frac{1}{\|\underline{r}_{l_i} - \underline{r}_k\|} \tag{2.24}$$

in *Equation* 2.19. This term is known as the *spherical spreading term*, where, for the direct path, $l_i = i$. If, however, the array is located far from the transmitted sources, or, equivalently, if

$$\|\underline{r}_k\| << \|\underline{r}_{l_i}\| \tag{2.25}$$

then the *spherical spreading term* both for direct and reflected paths remains constant.

In addition, the direction of propagation from point $\underline{r}_{l_i}$ to $\underline{r}_k$ can be considered under the above assumption as being parallel to the

direction of the vector $\underline{r}_{l_i}$ so

$$\underline{k}_{l_i k}^{T}.\underline{r}_{l_i} \quad \Rightarrow \quad \underline{k}_{l_i}^{T}.\underline{r}_{l_i} \qquad \textit{and}$$

$$G_k(\theta_{l_i k},\phi_{l_i k}) \quad \textit{becomes} \quad G_k(\theta_{l_i},\phi_{l_i})$$

On the basis of the above discussion, it can be seen that *Equation* 2.19 can be simplified to the following form:

$$x_k(t) = \sum_{i=1}^{D} \sum_{l=1}^{L_i} \rho_{i l_i}.exp[j.\Delta p_{i l_i}] \; . \; m_i(t). \\ .G_k(\theta_{l_i},\phi_{l_i}) \; . \; exp[-j\,\underline{k}_{l_i}^{T}.\underline{r}_k] + n_k(t) \qquad (2.26)$$

Thus the array input signal-vector (N in dim) can be expressed in a compact form as:

$$\underline{x}(t) = \mathbf{S} \; . \; \underline{m}(t) + \underline{n}(t) \qquad (2.27)$$

where

$$\underline{m}(t)=[\![m_{1_1}(t),m_{2_1}(t),...,m_{L_1}(t),m_{1_2}(t), \; ...., \; m_{L_D}(t)]\!]^T$$

with $m_{l_i}(t) = \rho_{i l_i}.exp[j.\Delta p_{i l_i}].\; m_i(t)$

N.B.: the subscript $(.)_{l_i}$ *refers to direct path of* i^{th} *source*

$$\mathbf{S} \;\; = \;\; [\![\underline{S}_{1_1}, \; \underline{S}_{1_2}, \; ..., \; \underline{S}_{1_{L_1}}, \; S_{2_1}, \; \underline{S}_{2_2}, \; ...,\underline{S}_{D_{L_D}}]\!]$$

$$\underline{S}_{l_i} = \begin{bmatrix} G_1(\theta_{l_i},\phi_{l_i}).exp[-j.\underline{k}_{l_i}^{T}.\underline{r}_1], \\ G_2(\theta_{l_i},\phi_{l_i}).exp[-j.\underline{k}_{l_i}^{T}.\underline{r}_2], \\ \qquad ..... \\ \qquad ..... \\ G_N(\theta_{l_i},\phi_{l_i}).exp[-j.\underline{k}_{l_i}^{T}.\underline{r}_N)] \end{bmatrix}$$

The effects that the medium has had on the amplitude and phase of the received signals, and also the effects that the transfer function of the array elements themselves have had on the received signals are contained within *Equation* 2.27. The modelling represented by *Equation*-2.27, has been used in the study and simulation reported on in this thesis when considering the plane wave situation.

2.6 ARRAY COVARIANCE MATRIX

In this section, attention is focused on the array covariance matrix, a knowledge of which is essential in array processing [BUR-82]. Under the assumption that the signals and noise are zero mean processes, the terms covariance and correlation are equivalent; the zero mean assumption is employed for simplicity. For an array of N elements the $(N \times N)$ data covariance matrix of the array input signals $\underline{x}(t)$ is defined as:

$$\mathbf{R}_{xx} = E[\![\underline{x}(t).\underline{x}(t)^H]\!] \qquad with\ \mathbf{R}_{xx} \in C^{N \times N} \tag{2.28}$$

Using *Equation* 2.27, which assumes plane wave approximation, or *Equation* 2.23 for spherical wave propagation, the data covariance matrix becomes:

$$\mathbf{R}_{xx} = \mathbf{S}.\mathbf{R}_{mm}.\mathbf{S}^H + \mathbf{R}_{nn} \tag{2.29}$$

where

$$\mathbf{R}_{mm} = E[\![\underline{m}(t).\underline{m}(t)^H]\!] \qquad with\ \mathbf{R}_{mm} \in C^{M\times M} \tag{2.30}$$

is the signal covariance matrix

$$\mathbf{R}_{nn} = E[\![\underline{n}(t).\underline{n}(t)^H]\!] \qquad with\ \mathbf{R}_{nn} \in C^{N\times N} \tag{2.31}$$

is the additive noise covariance matrix

In *Equation* 2.29 the noise is assumed uncorrelated from the directional sources. In many cases in practice, the estimated covariance matrix, instead of the ensemble average (given by *Equation* 2.28), is used. In the case in which q observations (snapshots) are available the estimated covariance matrix is given by:

$$\tilde{\mathbf{R}}_{xx} = \frac{1}{q} \cdot \sum_{n=1}^{q} \underline{x}(t_n).\underline{x}(t_n)^H \tag{2.32}$$

On the basis of the above definitions it is apparent that the matrix $\mathbf{R}_{xx}$ contains all the geometrical information about the various sources with respect to some reference point. The influence of the signal environment on the structure [RUH-70] of the matrix is considerable. If, for example, the number of signals, that is, the number of emitting sources, is less than the number of sensors in the array, then the matrix $\mathbf{S}.\mathbf{R}_{mm}.\mathbf{S}^H$ is singular and its rank is equal to the number of emitting sources. If the incident wavefronts are uncorrelated, or partially correlated, then the matrix $\mathbf{R}_{mm}$ is non-singular and has a diagonal form for the uncorrelated only case. However, if $\mathbf{R}_{mm}$ is singular this means that some of, or all of, the incident wavefronts are fully correlated or coherent and, except for the Shan-Wax-Kailath [SHA-85] algorithm

which is restricted to linear arrays, all existing signal locations, resolution and suppression algorithms fail in this situation. *Figure* 2.3 shows the most general structure of the matrix $\mathbf{R}_{mm}$.

2.7 NOISE MODELLING

In the previous section the noise covariance matrix $\mathbf{R}_{nn}$ was defined. Consider that $\mathbf{R}_{nn}$ has the general form

$$\mathbf{R}_{nn}=c.\mathbf{N}_{nn} \tag{2.33}$$

where c is a constant and $\mathbf{N}_{nn}$ is a $N\times N$ symmetric matrix. If the noise is assumed isotropic and thermal noise uncorrelated from sensor to sensor then

$$\mathbf{N}_{nn}=\mathbf{I} \qquad and \qquad c=\sigma^2 \tag{2.34}$$

where σ is the standard deviation of the noise and $\mathbf{I}$ the identity matrix. This is a reasonable model of the noise effects as far as it relates to thermal and isotropic noise.

In the case where there are non-isotropic noise effects and as long as the distribution of the noise is known, that is

$$\mathbf{N}_{nn}=known\ general\ Hermitian\ matrix$$
$$and \qquad c=unknown\ scalar \tag{2.35}$$

then $\mathbf{N}_{nn}$ can be decomposed as follows:

FIGURE – 2.3

GENERAL STRUCTURE OF ARRAY DIRECTIONAL SIGNALS COVARIANCE MATRIX

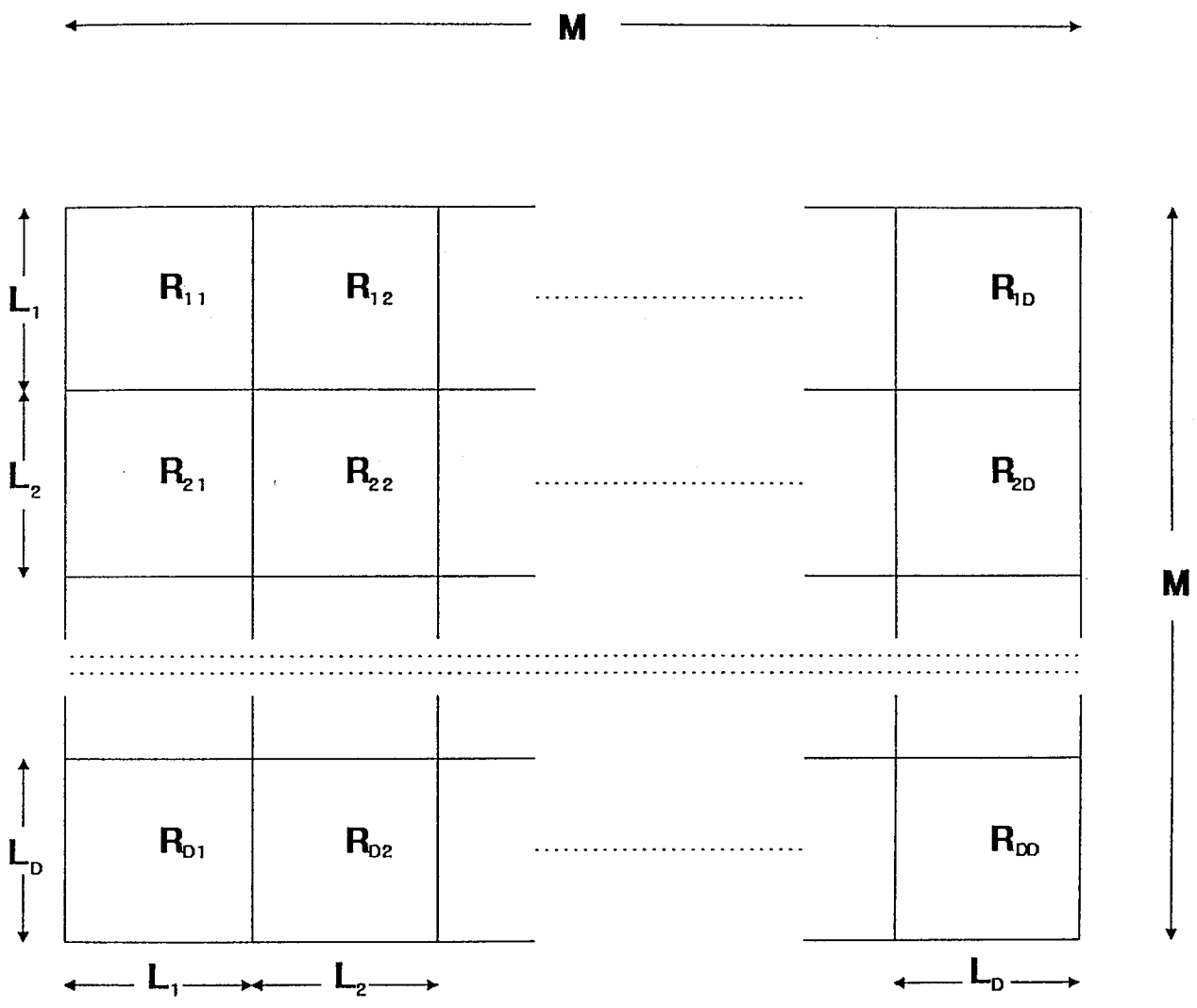

where **D** is the number of sources

L_I is the number of paths for the i – th source

R_{IJ} is the cross correlation between the signals $m_I(t)$ (arriving via L_I paths) and $m_J(t)$ (arriving via L_J paths)

$$\mathbf{N}_{nn} = c.\mathbf{N}_d.\mathbf{N}_d{}^H \tag{2.36}$$

It is apparent then that by preprocessing the data covariance matrix of the previous section (*Equation* 2.28) with a known process $\mathbf{N}_d^{-1}$, the result will be given by:

$$\tilde{\mathbb{R}}_{xx} = \mathbf{N}_d^{-1}.\mathbb{R}_{xx}.\mathbf{N}_d^{-1}{}^H \tag{2.37}$$

where

$$\tilde{\mathbb{R}}_{xx} = \tilde{\mathbf{S}}.\mathbb{R}_{mm}.\tilde{\mathbf{S}}^H + c.\mathbb{I} \tag{2.38}$$

$$\tilde{\mathbf{S}} = \mathbf{N}_d^{-1}.\mathbf{S} \tag{2.39}$$

On the basis of the above discussion it can be said that, by applying the above pre-transformation, any algorithm, which assumes a noise (thermal plus isotropic) which is uncorrelated from sensor to sensor, can be easily extended to the more general noise environment in which there is non-isotropic noise.

Thus, non-isotropic noise effects, which have a *known directionality*, can be handled. A typical non-isotropic noise (for more examples see [HUD-81]) is one which is ellipsoidal in shape, indicating that the noise strength is greater in some directions than others. If the noise is non-isotropic and completely unknown then a very difficult problem exists. In order to handle such a situation the theoretical development of the main process should not be based on any assumption with respect to the noise covariance matrix other than that it is a Hermitian matrix. The assumption of *thermal plus isotropic uncorrelated noise* will be used in this thesis. Questions relating to unknown non-isotropic noise will be left for another time.

2.8 ARRAY MANIFOLD

In this section the array manifold is defined and the array ambiguity problem is considered in conjunction with those array manifold dimensionality concepts which are useful for the remainder of the thesis.

2.8.1 DEFINITION OF ARRAY MANIFOLD.

Consider an array of N sensors and form the Source Position Vector $\underline{S}$ ($\underline{S}_{l_i}$ in *Equation* 2.27 - for plane waves) corresponding to the direction (θ,ϕ), where θ is the azimuth and ϕ the elevation angle. Rewrite $\underline{S}$ as $\underline{S}(\theta,\phi)$. Next, record the continuum of the vector $\underline{S}(\theta,\phi)$ as a function of θ,ϕ. This continuum is a two-dimensional continuum lying in a N dimensional space and is otherwise known as the *array manifold.* In the case of spherical waves mentioned earlier, the Source Position Vector ($\underline{S}_{l_i}$ in *Equation* 2.21) can be represented by $\underline{S}(\|\underline{r}\|,\theta,\phi)$ i.e. it is a function of range, azimuth and elevation, and in such a case the manifold is a 3-dim. continuum in a N dimensional space. This *array manifold* can be calculated and stored for a particular array only from the knowledge of the locations and directional characteristics of array elements. Thus, according to Schmidt [SCH-81] the array manifold completely characterizes any array and provides a representation of the real array into N-dimensional complex space.

2.8.2 ARRAY AMBIGUITIES

Source location ambiguity may arise whenever i) the array manifold repeats itself or ii) a point on the array manifold can be written as a linear combination of some other points. A simple example as a help in visualizing case (ii) is when a ray from the origin intersects the manifold at more than one point. A useful way of measuring the degree of ambiguity is by means of manifold dimensionality [SU-83]. Thus, consider that M is the largest number, such that for every combination of M distinct directions their corresponding Source Position Vector (SPV) can be a base of an M dimensional subspace. Then M is defined as the dimensionality of the array manifold. Once the array manifold, for a particular *visible area*, has been calculated and stored the array manifold dimensionality can be estimated and therefore becomes known for that particular array design. The dimensionality reflects the maximum number of signals which can be uniquely resolved by the array without any ambiguity arising.

It is important to point out that the array does not present the same resolution characteristics in the whole domain of directions.

CHAPTER 3

Adaptive Signal Parameter Estimation and Classification Technique

(ASPECT)

Superresolution Techniques and related Signal Subspace Algorithms provide correct information about the signal environment as long as that environment does not involve any coherent signals. However, the use of these techniques in signal environments where smart jamming or multipath propagation is present results in complete failure. Thus, if we are looking for an algorithm which is able to work in a signal environment with any degree of correlation (coherence), existing superresolution techniques, as well adaptive array systems, are not appropriate. In this chapter the theoretical framework of a new adaptive algorithm called ASPECT (**A**daptive **S**ignal **P**arameter **E**stimation and **C**lassification **T**echnique) is developed. This new algorithm, unlike superresolution techniques, provides correct information concerning:

- the number of signals incident to the array,
- the direction of arrivals (azimuth and elevation angles),
- the relative powers and phases.

The algorithm works independent of whether or not the signal are

correlated and it is not restricted to linear arrays.
The main assumption is that the emitters can be considered as point sources while no assumption is made as to whether the propagated wave is spherical, or if it is a plane wave.

3.1 EIGENSTRUCTURE ANALYSIS

As mentioned in *Chapter* 1, in recent years new array processing techniques known as *high resolution - signal subspace methods* have appeared. These methods are based on the eigenstructure of the sensor covariance matrix [JOH-85], [BIE-83]. They have been used mainly in estimating the direction of sources by employing a spatial array and they involve two main stages: the first stage is to estimate the covariance matrix of the data at the sensors of the array, and the second stage is to perform an eigenstructure analysis ([WLK-66]) of this matrix. As was mentioned in *Chapter* 1, using this information the observation space is partitioned, into the following two disjoint subspaces:

- the *signal subspace* with dimension equal to the number of sources, spanned by the source position vectors which correspond to the directions of incident signals;
- the *noise subspace* which is the complement of the signal subspace with respect to the observation space.

In order to appreciate the problems involved in the use of this decomposition, it is necessary to consider two situations with respect to

signal environment. The first situation involves signal environments where there are not correlated sources present and the second situation is one in which correlated sources exist.

THE ABSENCE OF CORRELATED SIGNALS

In the case of uncorrelated sources the decomposition referred to above can be performed correctly only if the dimensionality of the signal subspace is known. This dimensionality is equal to the number of signals arriving at the array. Thus, any algorithm based on the signal subspace approach assumes that the number of incident signals arriving at the array is known a priori. In practice, this prior information can be provided by a number of algorithms. A conventional approach is the so called *Bartlett-Lawley test* [LAW-56]. This test, however, suffers from the disadvantage of involving subjective decisions. Recently, Wax and Kailath [WAX-84] [WAX-85] have proposed a new method based on information theoretic criteria for model identification. The criteria are *the Akaike* (AIC) and *Minimum-Description-Length* criteria which overcome the need for subjective decisions; Another work of interest in this respect is the criterion proposed by Zhao el al [ZHA-87] called the *Efficient Detection Criterion*, of which the *Minimum-Description-Length* criterion is a special case.

The most representative and powerful technique of the Signal Subspace methods is the so-called MUSIC algorithm. This technique, which was developed at Stanford University [SCH-81], [SCH-86], has become very popular. The power of the MUSIC algorithm can be demonstrated by a simple example, where there is a linear array of five

uniformly distributed sensors, in the presence of three uncorrelated sources with azimuth angles of 30°, 135° and 90° respectively. *Figure* 3.2*a* shows that the directions of the signals are indicated by distinct deep nulls. If now the second source approaches the first, that is, the azimuth angles become 30°, 32° and 90° respectively then the MUSIC still provides results as shown in *Figure* 3.2*b*. In this situation all other previously known algorithms fail. A number of computer simulations were performed in [JOH-86]. These showed that when comparing the performance of *high resolution methods*, under a range of different criteria, the MUSIC algorithm outperformed all other high-resolution methods considered.

Signal-Subspace techniques are based mainly on the concept that the eigenvector decomposition of the covariance matrix provides the basis of the signal subspace while the $rank(\mathbf{R}_{xx}-\sigma^2.\mathbf{I})$ provides the number of incident signals (see *Appendix* 1). When correlated sources are present, however, the approach fails. Neither the decomposition of the covariance matrix nor the $rank(\mathbf{R}_{xx}-\sigma^2.\mathbf{I})$ provide correct information.

THE PRESENCE OF CORRELATED SIGNALS

In order to provide some insights into the problem of handling correlated sources, which according to Schmidt [SCH-81]

> "*... has been the most difficult to treat due to the extreme sensitivity of almost all methods to the high degree of temporal cross correlation (i.e. similarity) between directional signals*".

it is instructive to examine the structure of the matrix $\mathbf{R}_{mm}$, which was

FIGURE – 3.1

MUSIC ALGORITHM FOR THREE UNCORRELATED SOURCES

DIRECTIONS FOR THE TOP GRAPH:

source No.1 : 90 – degrees

source No.1 : 30 – degrees

source No.1 : 135 – degrees

DIRECTIONS FOR THE BOTTOM GRAPH:

source No.1 : 90 – degrees

source No.1 : 30 – degrees

source No.1 : 32 – degrees

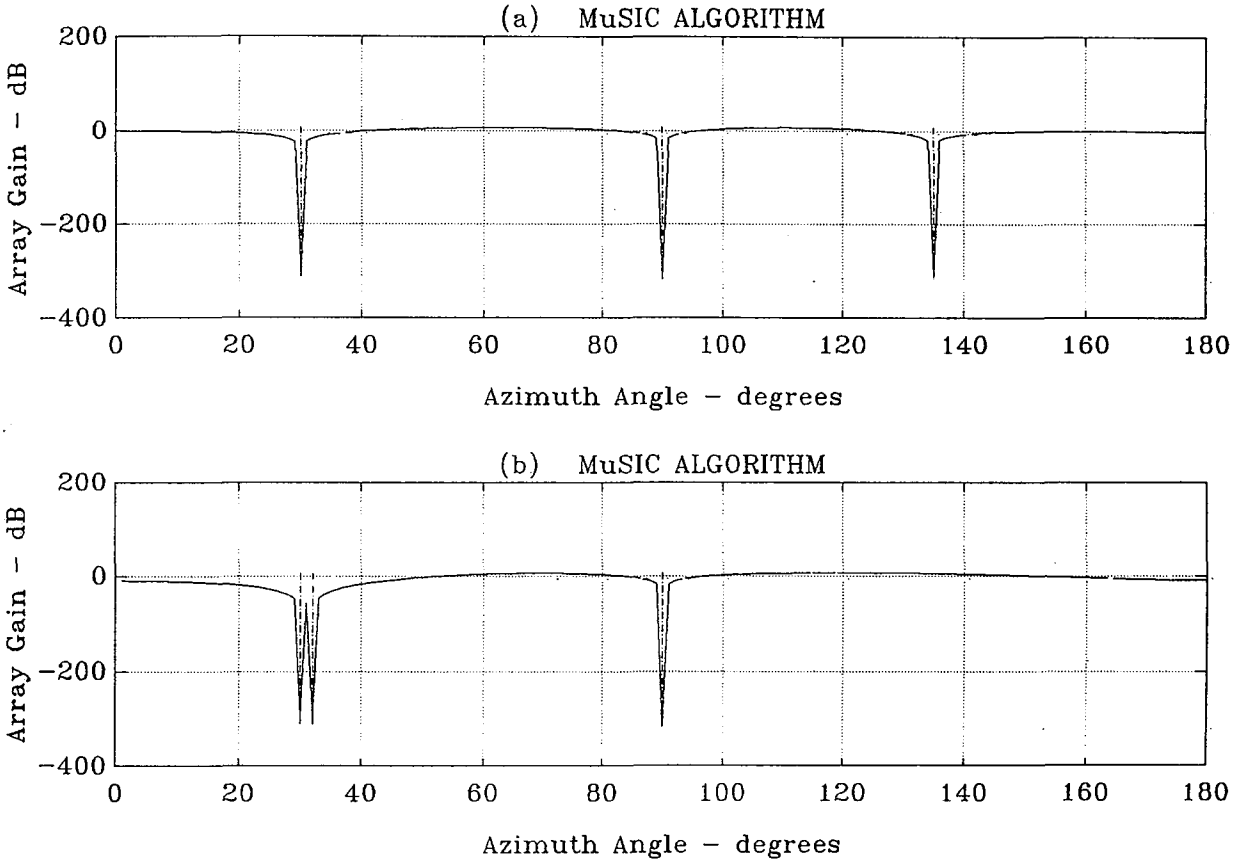

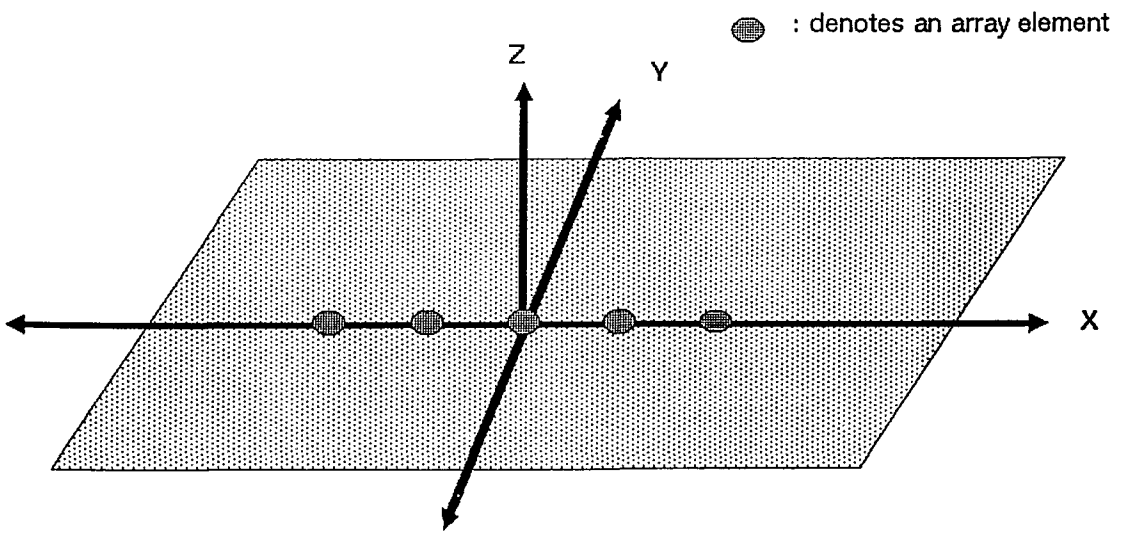

defined in *Section* 2.6. If we restrict ourselves to the assumption that the signals present at the array environment come via only one path then each '*square block*' on the matrix $\mathbf{R}_{mm}$ in *Figure* 2.3 has dimension 1×1, which means that these '*squares blocks*' are scalars. If, however, for some of the incident signals multipath propagation is involved, then one or more of those 'squares' takes the form of a singular matrix rather than a scalar, and the methods referred to and discussed above fail to operate. As a result of the signals correlation, the matrix $\mathbf{R}_{mm}$ also becomes a singular matrix with rank:

$$1 \leq rank(\mathbf{R}_{mm}) \leq M \qquad (3.2)$$

$$(with \quad rank(\mathbf{R}_{mm}) = D = M \ when \ \mathbf{R}_{mm} \ is \ non\text{-}singular)$$

In such a case any signal subspace algorithm (e.g. the MUSIC algorithm [SCH-86]), which has to work in an environment which results in a matrix $\mathbf{R}_{mm}$ with rank different from the number of incident signals M, breaks down. The reason for this is that the eigenvectors of the covariance matrix which belong to the noise subspace are not orthogonal to signal subspace. In other words, the space which is considered as the signal subspace by these algorithms is not the true signal subspace, although the algorithms "think" that it is. The worst case is, however, when $rank(\mathbf{R}_{mm})=1$, which occurs when there is one source coming via many paths, or when there are many sources, all of which are correlated. The above mentioned problem is illustrated in *Figure* 3.3 for a linear array of seven isotropic elements and for three sources located at 30°,90° and 135°, where the three sources are correlated.

It is important to note also that in a situation such as that

FIGURE – 3.2 (MUSIC ALGORITHM FOR THREE FULLY CORRELATED SOURCES)

	TRUE directions	directions estimated by MUSIC
source No.1(S1)	(0.0, 30.0)	failure
source No.2(S2)	(0.0, 90.0)	failure
source No.3(S3)	(0.0, 135.0)	failure

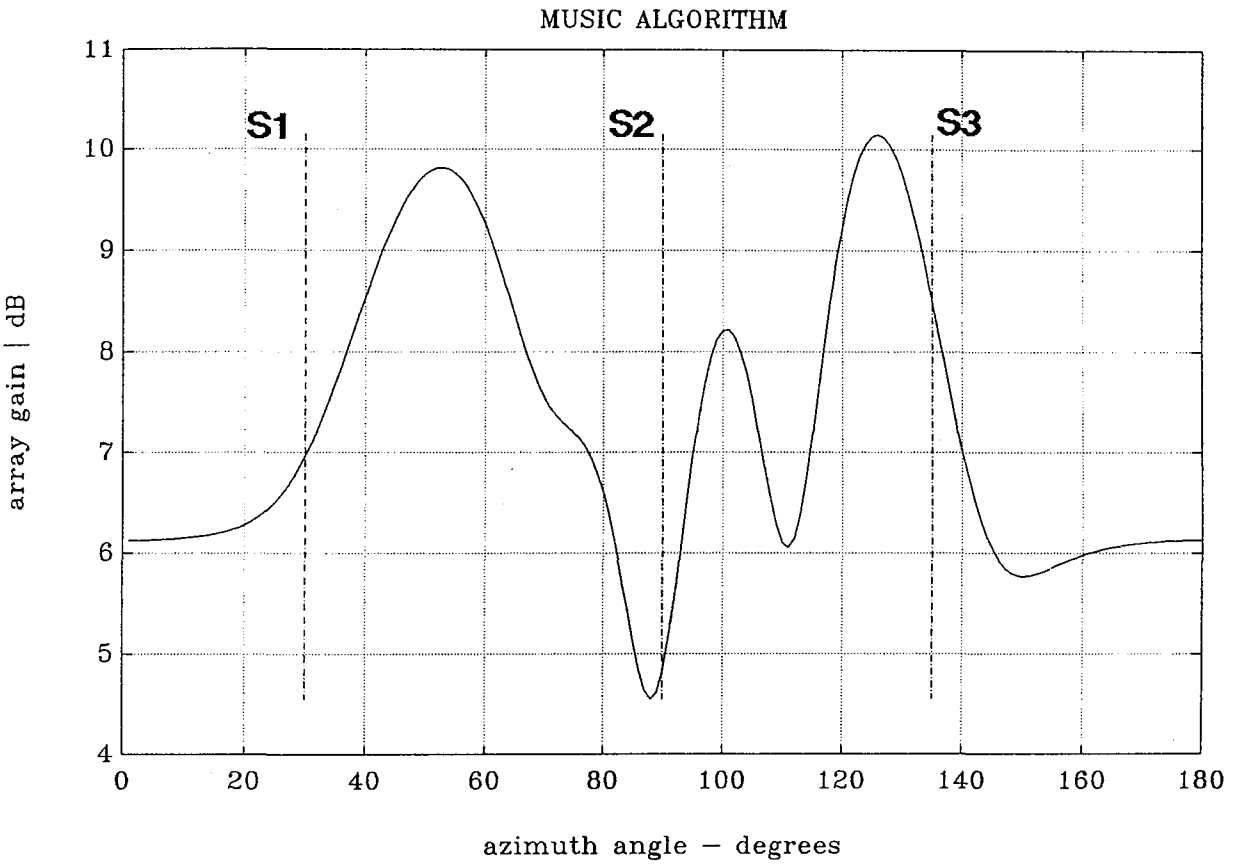

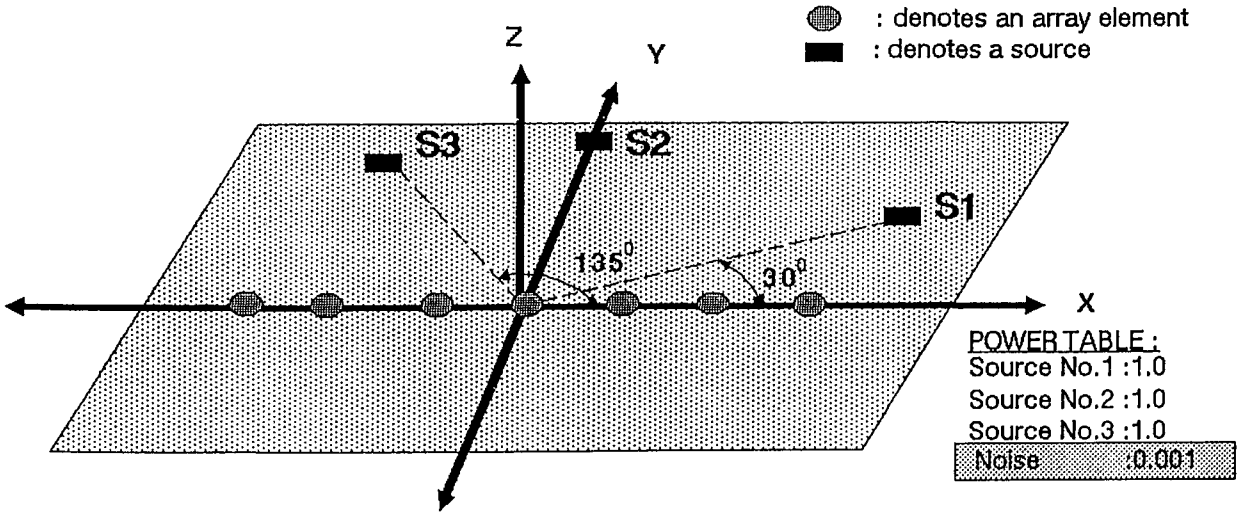

illustrated in *Figure* 3.2, even the AIC and the Bartlett test will fail to provide the correct number of signals present. The reason is that they try to find the rank of the data covariance matrix by setting a threshold to its eigenvalues. However, in the correlated situation this rank does not correspond to the number of signals, as it is obvious from the previous discussion.

Recently attempts have been made (see for example [FED-86], [SHH-87], [DI-85], [SHA-85], [CAD-87] etc) to overcome these difficulties and the most promising approach appears to be that of Shan, Wax and Kailath [SHA-85], [SH2-85] which uses the concept of spatial smoothing, or sub-aperture sampling, in order to restore the rank of the covariance matrix so that it is equal the number of signals. The method defines a number of subsets (sub-arrays) and for each subset a data covariance matrix $\mathbf{R}_i$ is formed. Then, the average covariance matrix $\widetilde{\mathbf{R}}$ is estimated as follows:

$$\widetilde{\mathbf{R}}=\frac{1}{No.of\ subarrays}\cdot\sum_i \mathbf{R}_i \tag{3.3}$$

After this the MuSIC can then be used to provide the locations of the sources. This method of approach is at this time very popular and a considerable amount of research effort is being done on the *spatial smoothing* technique [CLE-85], [ATT-87], [WIL-87], [MAD-87], [WIL-88]. This technique does however suffer from two main disadvantages. The first one is that it reduces the effective aperture of the array and the second that the method can only be applied to linear sensors arrays with uniformly-spaced identical sensors.

3.2 THEORETICAL BASE

In this thesis a totally new alternative approach to that of Shan-Kailath is that provided in the form of the ASPECT algorithm. This algorithm measures up to the requirements contained in the general statement of Schmidt

> *"The proper perspective is that the general multiple emitter case includes the multipath as a special case."*

ASPECT will be shown to provide a solution in the general case in which the '*squares blocks*' of matrix $\mathbf{R}_{mm}$ in *Figure* 2.3 are matrices of any dimension. One Lemma and three Theorems will now be developed and they will be used as a theoretical basis of the ASPECT algorithm, which is to be presented later in this chapter. In addition a second Lemma, Lemma-2, will be presented without proof.

LEMMA 1.: *Let* $\mathbb{F}$ *be any set of* N*-dimensional complex vectors where any combination of* M *these vectors* ($M \leq N$) *are independent. Consider two subsets of* $\mathbb{F}$: $\mathbf{S}_D \in \mathrm{C}^{N \times D}$, $\mathbf{S} \in \mathrm{C}^{N \times K}$ *with* $K \geq D$.
If $dim(L[\mathbf{S}_D,\mathbf{S}]) < M$ *and* $\mathbf{S}_D.\underline{\alpha}_D = \mathbf{S}.\underline{\alpha}$, *where dim stands for 'dimension of ...',* $L[.]$ *means 'the subspace spanned by ...',* $\underline{\alpha}_D \in \mathrm{C}^D$ *with (every element of* $\underline{\alpha}_D \neq 0$), $\underline{\alpha} \in \mathrm{C}^K$, *then:*

i) $L[\mathbf{S}_D] \subseteq L[\mathbf{S}]$

ii) K*-*D *elements of* $\underline{\alpha}$ *are zero, and*

iii) D *out of* K *columns of* $\mathbf{S}$ *are the* D *columns of* $\mathbf{S}_D$.

PROOF :

The subspace $L[\mathbf{S}_D,\mathbf{S}]$ is the subspace generated by $\mathbf{S}_D \bigcup \mathbf{S}$. That is,

$$L[\mathbf{S}_D,\mathbf{S}] = L[\mathbf{S}_D] + L[\mathbf{S}] \tag{3.4}$$

However

$$\begin{aligned} dim(L[\mathbf{S}_D] + L[\mathbf{S}]) &= dim(L[\mathbf{S}_D]) + dim(L[\mathbf{S}]) - dim(L[\mathbf{S}_D] \bigcap L[\mathbf{S}]) \\ &= D + K - dim(L[\mathbf{S}_D] \bigcap L[\mathbf{S}]) \\ &< M \end{aligned} \tag{3.5}$$

$D+K-dim(L[\mathbf{S}_D] \bigcap L[\mathbf{S}])<M$ in the last equation means that $\mathbf{S}_D \bigcup \mathbf{S}$ is a basis of the subspace $L[\mathbf{S}_D,\mathbf{S}]$. However,

$$\begin{aligned} \mathbf{S}_D.\underline{\alpha}_D = \mathbf{S}.\underline{\alpha} \quad &\Rightarrow \quad \mathbf{S}_D.\underline{\alpha}_D - \mathbf{S}.\underline{\alpha} = \underline{0} \\ &\Rightarrow \quad \underline{\alpha}_D = \underline{0}\ ,\ \underline{\alpha} = \underline{0} \end{aligned}$$

But, because every element of $\underline{\alpha}_D$ is nonzero, the equation $\mathbf{S}_D.\underline{\alpha}_D - \mathbf{S}.\underline{\alpha} = \underline{0}$ is satisfied only if $L[\mathbf{S}_D] \subseteq L[\mathbf{S}]$ (then $\mathbf{S}_D = \mathbf{S}.\mathbf{A} \Rightarrow \mathbf{S}(\mathbf{A}.\underline{\alpha}_D - \underline{\alpha}) = \underline{0}$ which is valid for $\mathbf{A}.\underline{\alpha}_D - \underline{\alpha} = \underline{0}$). This proves part($i$) of the LEMMA.

However, part(i) of LEMMA implies that $L[\mathbf{S}_D] \subseteq [L[\mathbf{S}]$. It is apparent then that $\mathbf{S}_D$ will belong to a D-dim subspace of $L[\mathbf{S}]$ ($L[\mathbf{S}_{c1}]$, say)

That is,

$$L[\mathbf{S}_D] = L[\mathbf{S}_{c1}] \tag{3.6}$$

Let

$$\mathbf{S}_D = [\![\, \underline{S}_{D_1}, \underline{S}_{D_2}, \ldots\ldots, \underline{S}_{D_D}]\!] \tag{3.7}$$

and let us rearrange the columns of $\mathbf{S}$ and the corresponding elements of $\underline{\alpha}$ in such a way that: *i*) the subspace $L[\mathbf{S}]$ can be decomposed into two complement subspaces as shown in *Figure* 3.3(*a*) and *ii*) the same subspace $L[\mathbf{S}]$ can be decomposed as in *Figure* 3.3(*b*) .

where $$\mathbf{S} = [\![\, \underline{S}_1, \underline{S}_2, \ldots\ldots, \underline{S}_D, \underline{S}_{D+1}, \ldots\ldots, \underline{S}_K \,]\!] \tag{3.8}$$

Let $$\underline{E} = \mathbf{S}_D \cdot \underline{\alpha}_D \tag{3.9}$$

$$= \mathbf{S} \,.\, \underline{\alpha} \tag{3.10}$$

By partitioning the vector $\underline{\alpha}$ into two subvectors, that is, $\underline{\alpha}^T = [\![\, \underline{d}^T, \underline{e}^T]\!]$ with $\underline{d} \in C^D$, $\underline{e} \in C^{K-D}$ *Equation* 3.10 can be written as:

$$\underline{E} = \mathbf{S}_{C1} \cdot \underline{d} + \mathbf{S}_{C2} \cdot \underline{e} \tag{3.11}$$

It needs to be proved that :

$$\underline{e} = \underline{0} \qquad \underline{d} = \underline{\alpha}_D \qquad \mathbf{S}_{C1} = \mathbf{S}_D \tag{3.12}$$

However, because $L[\mathbf{S}_D] = L[\mathbf{S}_{C1}]$ implies that the columns of $\mathbf{S}_D$ and the columns of $\mathbf{S}_{C1}$ are two different bases of the same subspace, it follows that one basis can be written as a linear combination of the other; that is:

$$\mathbf{S}_{C1} = \mathbf{S}_D \cdot \mathbf{A} \qquad \text{with} \qquad \mathbf{A} \in C^{D \times D} \tag{3.13}$$

FIGURE – 3.3

DECOMPOSITION OF THE SUBSPACE $L[S]$ INTO TWO COMPLEMENTS SUBSPACES

a)

$$L[\underline{S}_{c2}] = L[\underline{S}_{D+1}, \underline{S}_{D+2}, \cdots\cdots, \underline{S}_K]$$

$$\dim\{L[\underline{S}_{c2}]\} = K - D$$

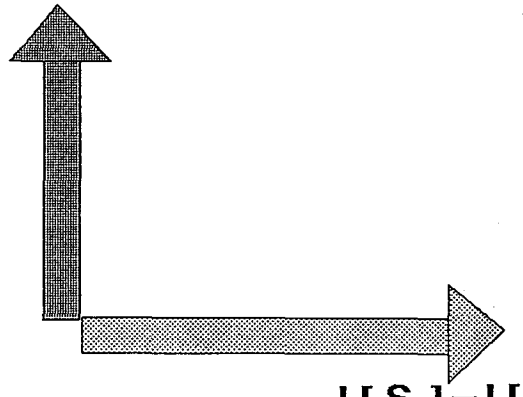

$$L[\underline{S}_{c1}] = L[\underline{S}_1, \underline{S}_2, \cdots\cdots, \underline{S}_D]$$

$$\dim\{L[\underline{S}_{c1}]\} = D$$

b)

$$L[\underline{S}_{c2}] = L[\underline{S}_{D+1}, \underline{S}_{D+2}, \cdots\cdots, \underline{S}_K]$$

$$\dim\{L[\underline{S}_{c2}]\} = K - D$$

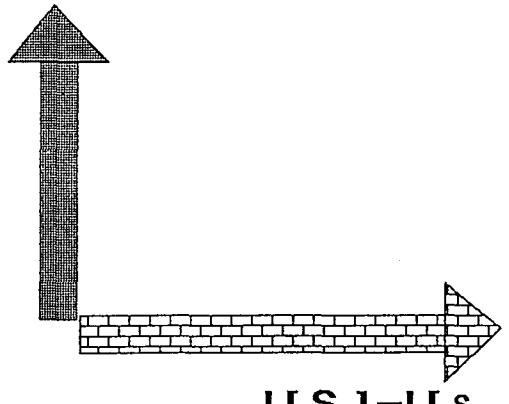

$$L[\underline{S}_D] = L[\underline{S}_{D1}, \underline{S}_{D2}, \cdots\cdots, \underline{S}_{DD}]$$

$$\dim\{L[\underline{S}_D]\} = D$$

Note : $L[.]$ *means 'spanned by ...'*

Then, *Equation* 3.11 becomes:

$$i.e. \quad \underline{E}=\mathbf{S}_D.\underline{b} + \mathbf{S}_{C2}.\underline{e} \qquad (3.14)$$
$$with \quad \underline{b}=\mathbf{A}.\underline{d}\ ,\ \underline{b}\in C^D$$

In addition *Equation* 3.9 can be rewritten as:

$$\underline{E}=\mathbf{S}_D.\underline{\alpha}_D + \mathbf{S}_{C2}.\underline{0} \qquad (3.15)$$

On subtracting *Equation* 3.15 from *Equations*-3.14 it follows that:

$$\underline{0} = \mathbf{S}_D.(\underline{b}-\underline{\alpha}_D) + \mathbf{S}_{C2}.\underline{e} \qquad (3.16)$$

which is true only if:

$$\underline{b}=\underline{\alpha}_D \qquad \underline{e}=\underline{0} \qquad (3.17)$$

This last equation proves part (*ii*) of the LEMMA.
However, because of $\mathbf{S}_{C1}=\mathbf{S}_D.\mathbf{A}$ in conjunction with the fact that any combination of D columns from both matrices $\mathbf{S}_D$ and $\mathbf{S}_{C1}$ are linearly independent, the matrix $\mathbf{A}$ becomes the identity matrix.
Therefore

$$\underline{d} = \underline{\alpha}_D \qquad (3.18)$$

This proves part (*iii*) of the LEMMA.

LEMMA 2: *Consider an Euclidean space* H, $dim[H]=N$ *and any subspace* h, $dim[h]=M\leq N$ *of* H *spanned by* M *independent vectors* $\underline{h}_1,....,\underline{h}_M$. *Then the projection of any vector* $\underline{x}$ *in* H *on to* h *is given by* $\mathbf{P}.\underline{x}$ *where* $\mathbf{P}$ *is the projection operator which maps each vector of* H *onto* h *and which has the following properties:*

- $\mathbf{P} = \mathbf{V}.(\mathbf{V}^H\mathbf{V})^{-1}.\mathbf{V}^H$ *where* $\mathbf{V}=[\underline{h}_1,....,\underline{h}_M]$,
- $\mathbf{P}^2=\mathbf{P}$ *i.e.* $\mathbf{P}$ *is idempotent,*
- $\mathbf{P}^H = \mathbf{P}$

THEOREM 1. : *The number of signals, incident at an array of* N *sensors and arriving from different angles, is given by the number of non-zero elements of the vector* $(\mathbf{S}^H.\mathbf{S})^{-1}.\mathbf{S}^H.\underline{E}$ *at the solution of any of the following minimization problems*

a) $$\min_{\underline{p}} \xi \quad given \quad \xi=trace(\mathbf{P}_{\mathbf{S}}.\mathbf{Q}_{\underline{E}}.\mathbf{P}_{\mathbf{S}}.\mathbf{P}_{\underline{E}}) \tag{3.19}$$

b) $$\min_{\underline{p}} \xi \quad given \quad \xi = \left(\frac{1}{\sqrt{\underline{E}^H\mathbf{P}_{\mathbf{S}}\underline{E}}} \right)^n \tag{3.20}$$

c) $$\min_{\underline{p}} \xi \quad given \quad \xi= trace(\mathbf{Q}_{\mathbf{S}}.\mathbf{P}_{\underline{E}}) \tag{3.21}$$

with $\Re^{2K} \overset{\xi}{\mapsto} \Re$, $K\in\mathcal{N}^+$,$K\in[D,....,N]$ *and*

where:

- $\underline{E}\in C^N$ *is either one*★ *of the signal subspace eigenvectors of the data covariance matrix, or any array input sample vector free of additive noise.*
- $\mathbf{S}\in C^{N\times K}$ *has as columns* K *independent vectors belonging to the array manifold .*

★ Excluding the case where all the SPVs are themselves orthogonal. This special case is covered on page 76 by the Aspect function.

- $\mathbf{P}_{\mathbf{S}}$ *is the projection operator to the subspace spanned by the columns of* $\mathbf{S}$, *that is the 'range space of* $\mathbf{S}$' $R(\mathbf{S})$;
- $\mathbf{Q}_{\underline{E}}$ *is the projection operator to the complement of the subspace spanned by* $\underline{E}$, *that is the 'null space of* $\underline{E}$' $N(\underline{E})$;
- $\mathbf{P}_{\underline{E}}$ *is the projection operator to the subspace spanned by* $\underline{E}$, *that is the 'range space of* $\underline{E}$' $R(\underline{E})$;
- n *integer greater or equal to* 1
- $\underline{p}$ *is the vector of location-parameters* ($\underline{p} \in \Re^{2K}$)

PROOF :

Because $\underline{E}$ belongs to the unknown signal subspace, it follows that it is a linear combination of the unknown D Source Position Vectors of the true sources. This means that

$$\underline{E}=\mathbf{S}_D \cdot \underline{\alpha}_D \tag{3.22}$$

where $\mathbf{S}_D$ is the matrix whose columns are the D source position vectors of the true sources. However,

a)

$$\begin{aligned}
\xi &= trace(\mathbf{P}_{\mathbf{S}} \cdot \mathbf{Q}_{\underline{E}} \cdot \mathbf{P}_{\mathbf{S}} \cdot \mathbf{P}_{\underline{E}}) = \\
&= trace(\mathbf{P}_{\mathbf{S}} \cdot \mathbf{Q}_{\underline{E}} \cdot \mathbf{P}_{\mathbf{S}} \cdot \underline{E} \cdot \underline{E}^{\mathsf{H}}) = \\
&= trace(\underline{E}^{\mathsf{H}} \cdot \mathbf{P}_{\mathbf{S}} \cdot \mathbf{Q}_{\underline{E}} \cdot \mathbf{P}_{\mathbf{S}} \cdot \underline{E}) = \\
&= \underline{E}^{\mathsf{H}} \cdot \mathbf{P}_{\mathbf{S}} \cdot \mathbf{Q}_{\underline{E}} \cdot \mathbf{P}_{\mathbf{S}} \cdot \underline{E} = \\
&= \underline{E}^{\mathsf{H}} \cdot \mathbf{P}_{\mathbf{S}} \cdot \mathbf{Q}_{\underline{E}} \cdot \mathbf{Q}_{\underline{E}} \mathbf{P}_{\mathbf{S}} \cdot \underline{E} = \\
&= \underline{w}^{\mathsf{H}} \cdot \underline{w} \qquad \text{where} \quad \underline{w} = \mathbf{Q}_{\underline{E}} \cdot \mathbf{P}_{\mathbf{S}} \cdot \underline{E}
\end{aligned} \tag{3.23}$$

The last equation shows that the cost function is a positive quantity (square magnitude of a vector), so the global minimum is zero; this is reached when the vector $\underline{w}$ becomes a zero vector. Then the vector $\underline{E}$ belongs to the the range space of the columns of $\mathbf{S}$, that is $\Re(\mathbf{S})$. Thus

$$\mathbf{P}_{\mathbf{S}}.\underline{E} = \underline{E} \quad \textit{which implies } \xi = \underline{E}.\mathbf{Q}_{\underline{E}}.\underline{E}^{H} = 0$$

Let

$$\underline{\alpha} = (\mathbf{S}^{H}.\mathbf{S})^{-1}.\mathbf{S}^{H}.\underline{E} \tag{3.24}$$

By pre-multiplying both sides of Equation-3.24 by $\mathbf{S}$ $\Rightarrow$

$$\begin{aligned} \mathbf{S}.\underline{\alpha} &= \mathbf{S}.(\mathbf{S}^{H}.\mathbf{S})^{-1}.\mathbf{S}^{H}.\underline{E} \quad \Rightarrow \\ \mathbf{S}.\underline{\alpha} &= \mathbf{P}_{\mathbf{S}}.\underline{E} \quad \Rightarrow \\ \mathbf{S}.\underline{\alpha} &= \underline{E} \end{aligned} \tag{3.25}$$

Thus, by combining last equation with *Equation* 3.22:

$$\underline{E} = \mathbf{S}_{D}.\underline{\alpha}_{D} = \mathbf{S}.\underline{\alpha} \tag{3.26}$$

Equation 3.36 in conjunction with part(i) and part(ii) of LEMMA.1 implies that the $K-$dim vector $\underline{\alpha}$ has D non-zero elements.

However, if the assumptions of LEMMA .1 are not valid then there is no guarantee that the solution of the minimization problem *Equation* 3.19 is a unique solution. Theorem-3, which follows, deals with the conditions under which the assumptions of LEMMA.1 are valid.

b)

$$\xi = \left(\frac{1}{\sqrt{\underline{E}^H \mathbf{P}_S \underline{E}}} \right)^n \tag{3.27}$$

on multiplying both the numerator and the denominator by

$\left(\sqrt{\underline{E}^H \mathbf{P}_S \underline{E}} \right)^n$ it follows that

$$\Rightarrow \xi = \left(\frac{\sqrt{\underline{E}^H \mathbf{P}_S \underline{E}}}{\underline{E}^H \mathbf{P}_S \underline{E}} \right)^n \tag{3.28}$$

Now when the numerator is multiplied by $\underline{E}^H \underline{E}$ no change takes place since $\underline{E}^H \underline{E}$ is equal to unity. Thus:

$$\Rightarrow \xi = \left(\frac{\sqrt{\underline{E}^H \mathbf{P}_S \underline{E}} . \underline{E}^H . \underline{E}}{\underline{E}^H \mathbf{P}_S \underline{E}} \right)^n = \left(\frac{\sqrt{\underline{E}^H \mathbf{P}_S \mathbf{P}_S \underline{E}} . \sqrt{\underline{E}^H . \underline{E}}}{\underline{E}^H \mathbf{P}_S \underline{E}} \right)^n \tag{3.29}$$

In *Equation* 3.29 Lemma 2 has been used. On replacing $\mathbf{P}_S . \underline{E}$ by the vector $\underline{w}$ in *Equation* 3.29, that is using

$$\underline{w} = \mathbf{P}_S \underline{E} \tag{3.30}$$

Equation 3.29 becomes

$$\xi = \left(\frac{\sqrt{\underline{w}^H \underline{w}} . \sqrt{\underline{E}^H . \underline{E}}}{\underline{w}^H \underline{E}} \right)^n \tag{3.31}$$

However, it is well known [GOL-83] that the angle between two complex vectors $\underline{w}$ and $\underline{E}$ is given by

$$cos\Theta.e^{\Phi}=\frac{\underline{w}^H\underline{E}}{\sqrt{\underline{w}^H\underline{w}}.\sqrt{\underline{E}^H.\underline{E}}} \tag{3.32}$$

Thus, it is clear that

$$\xi=\left(\frac{1}{cos\Theta.e^{\Phi}}\right)^n \tag{3.33}$$

However $\xi\in$R, therefore $\Phi=0$ which implies

$$\xi=sec^n\Theta \tag{3.34}$$

Thus, when *Equation* 3.20 cost function is minimized the angle Θ will become zero indicating that the vector $\underline{w}$ and $\underline{E}$ span the same one dimensional space; in other words, the two vectors become identical.
This means

$$\begin{aligned}
\underline{w}=\underline{E} \quad &\Rightarrow \\
\mathbf{P}_{\mathbf{S}}\underline{E} = \mathbf{S}_D.\underline{\alpha}_D \quad &\Rightarrow \\
\mathbf{S}.(\mathbf{S}^H.\mathbf{S})^{-1}\mathbf{S}^H.\underline{E} = \mathbf{S}_D.\underline{\alpha}_D \quad &\Rightarrow \\
\mathbf{S}.\underline{\alpha} = \mathbf{S}_D.\underline{\alpha}_D \quad &
\end{aligned} \tag{3.35}$$

where $\underline{\alpha}=(\mathbf{S}^H.\mathbf{S})^{-1}.\mathbf{S}^H.\underline{E}$

Equation 3.35 in conjunction with part(i) and part(ii) of LEMMA.1 implies that the $K-$dim vector $\underline{\alpha}$ has D non-zero elements.

c) proof similar to that of (a).

THEOREM 2. : *if* $(\underline{\theta}^*,\underline{\phi}^*)$ *is a solution to any one of the minimization problems given by Equations* 3.19, 3.20 *or* 3.21 *of Theorem*.1., *then the pair* (θ_i,ϕ_i) *which is formed by the* i^{th} *elements of the vectors* $\underline{\theta}^*,\underline{\phi}^*$ *is the DOA (Direction Of Arrivals) of an incident signal provided that the* i^{th} *element of the vector* $(\mathbf{S}^H.\mathbf{S})^{-1}.\mathbf{S}^H.\underline{E}$ *is not zero*;

PROOF :

Consider K initial directions $(\underline{\theta},\underline{\phi})$ and let $\mathbf{S}$ be the matrix the columns of which are the vectors belonging to the array manifold which correspond to the K initial directions. Let $L[\mathbf{S}]$ be the subspace spanned by the columns of $\mathbf{S}$. *Figure* 3.4(a) illustrates the geometry involved. Also, let $\underline{w}$ be the projection of $\underline{E}$ on to $L[\mathbf{S}]$. By projecting the vector $\underline{w}$ on to the *null-subspace* of $\underline{E}$ the vector $(\underline{\tilde{w}})$ is formed as shown *Figure* 3.4(b). By minimizing the magnitude of $(\underline{\tilde{w}})$, that is *Equation* 3.19 the subspace $L[\mathbf{S}]$ is rotated so as to approach the *range-subspace* of $\underline{E}$. *Figure* 3.4(c) shows the final settled position of the $L[\mathbf{S}]$ at the end of minimization *Equation* 3.19. Thus, at the solution $(\underline{\theta}^*,\underline{\phi}^*)$, the vector $\underline{E}$ belongs to the subspace spanned by the columns of $\mathbf{S}$, that is $\underline{E}\in L[\mathbf{S}]$; this implies that $\underline{E}$ becomes identical to $\underline{w}$ and consequently $\underline{E}$ can be written as a linear combination of the columns of $\mathbf{S}$ which are the K vectors belonging to the array manifold and corresponding to the solution $(\underline{\theta}^*,\underline{\phi}^*)$, that is,

$$E=\mathbf{S}.\underline{\alpha} \tag{3.36}$$

Similar results will be obtained by using *Equations*3.20, 3.21.

FIGURE – 3.4

GEOMETRY INVOLVED IN ASPECT

a)

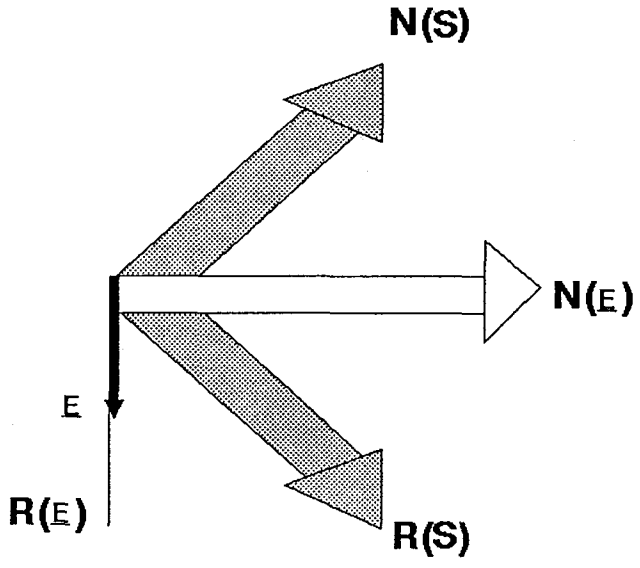

b)

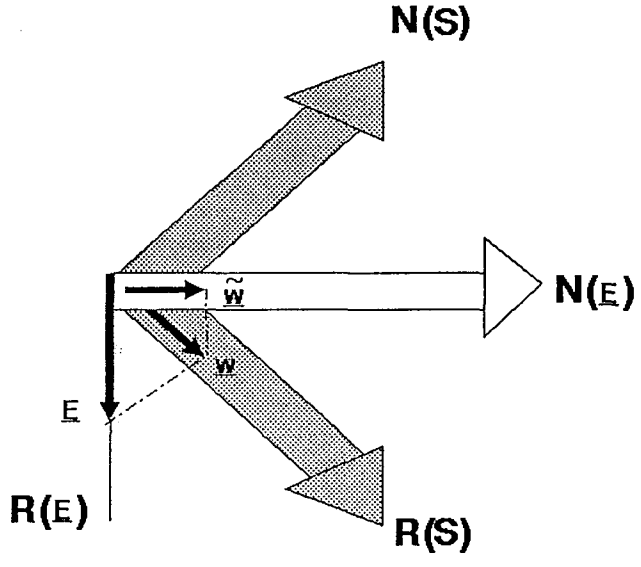

$\dim\{ \mathbf{N(S)} \} = N - K$

$\dim\{ \mathbf{N(E)} \} = N - 1$

$\dim\{ \mathbf{R(S)} \} = K$

$\dim\{ \mathbf{R(E)} \} = 1$

c)

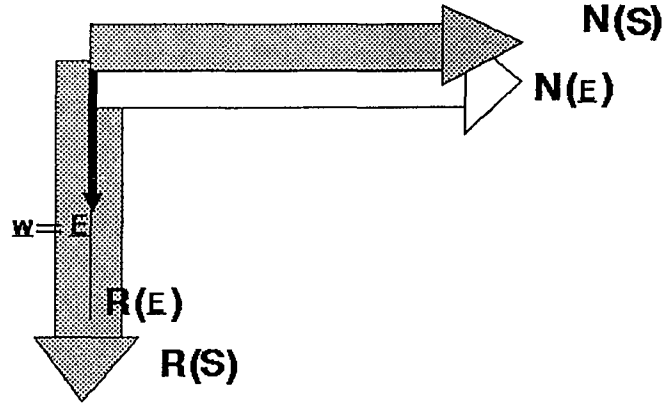

Now,

$$\underline{E}=\mathbf{S}.\underline{\alpha} \Rightarrow \underline{\alpha}=(\mathbf{S}^H.\mathbf{S})^{-1}.\mathbf{S}^H.\underline{E} \tag{3.37}$$

and it has been proved in THEOREM.1. that $\underline{\alpha}$ has D non-zero elements. Thus, in order to prove the THEOREM-2 it is sufficient to prove that the i^{th} column of $\mathbf{S}$ which corresponds to a non-zero elements of $\underline{\alpha}$ is equal to one column of $\mathbf{S}_D$. Proof of this is obtained by using part(iii) of LEMMA .1.

▩

THEOREM .3. : *Theorem.*1. *and Theorem.*2. *have unique solutions as long as the following condition is satisfied:*

$$\textit{the array manifold dimensionality} > K+D \tag{3.38}$$

PROOF :

By assuming that the array manifold dimensionality is greater than $K+D$ ensures that every combination of $K+D$ Source Position Vectors are independent. In other words this ensures that

$$dim(L[\mathbf{S}_D,\mathbf{S}]) < (\textit{array manifold dimensionality}) \tag{3.39}$$

thus validating the assumptions of LEMMA-1. The uniqueness of the solution is then apparent.

However, *Equation* 3.38 is more restricted than is needed. For instance from *Equation* 3.39 it follows that:

$$K+D-dim(L[\mathbf{S}_D]\bigcap L[\mathbf{S}]) < (\textit{array manifold dimensionality}) \tag{3.40}$$

where the maximum value of $dim(L[\mathbf{S}_D] \bigcap L[\mathbf{S}])$ is equal to D. That implies that the minimum value of the array manifold dimensionality is equal to K.

ASPECT COST FUNCTIONS

In the cost function used in the Theorems given above there is one eigenvector in use. This eigenvector should belong to the Signal subspace. One such vector is the eigenvector which corresponds to the maximum eigenvalue of the covariance matrix. This vector belongs to the signal subspace even if all the sources are correlated, or if there is only one signal source and its signal arrives at the array having travelled over a number of different paths (multipath propagation).
If there are a number of eigenvectors which obviously belong to the signal subspace then this additional information can be taken into account as well. This can be done by extending the cost functions given by *Equation* 3.19,3.20, and 3.21 in the following manner:

$$\xi = trace(\mathbf{P_S} \cdot \mathbf{Q_E} \cdot \mathbf{P_S} \cdot \mathbf{P_E})$$

$$\xi = \prod_i \left(\frac{1}{\sqrt{\underline{E}_i^H \mathbf{P_S} \underline{E}_i}} \right)^n$$

$$\xi = \text{trace}(\mathbf{Q_S} \cdot \mathbf{P_E})$$

where $\mathbf{E}$ is the matrix which has as columns the eigenvectors belonging to the Signal Subspace.

3.3 THE ASPECT ALGORITHM

ASPECT is a new algorithm for locating a number of sources correlated or otherwise. This algorithm is not restricted to linear arrays and is based on the Theorems given in the previous section. The algorithm can be expressed as a number of steps appropriate for Single Instruction Multiple Data Computer or for systolic array implementation as follows:

STEP-1: form the data covariance matrix

STEP-2: estimate the eigenvectors $\mathbb{E}$ which corresponds to the largest eigenvalues of the covariance matrix if there is confidence that these eigenvectors belong to the signal subspace.

STEP-3: estimate the Projection Operators of the subspace spanned by the columns of $\mathbb{E}$ (that is $\mathbf{P}_{\mathbb{E}}$)

STEP-4: choose K initial directions with K to be certainly greater than, or equal, to the number of incident signals but less than, or equal, to the array manifold dimensionality.

STEP-5: minimize one of the following cost function:

$$\xi = trace(\mathbf{P}_{\mathbf{S}} \cdot \mathbf{Q}_{\mathbb{E}} \cdot \mathbf{P}_{\mathbf{S}} \cdot \mathbf{P}_{\mathbb{E}}) \tag{3.41}$$

$$\xi = \prod_i \left(\frac{1}{\sqrt{\underline{E}_i^H \mathbf{P}_{\mathbf{S}} \underline{E}_i}} \right)^n \tag{3.42}$$

$$\xi = \text{trace}(\mathbf{Q}_{\mathbf{S}} \cdot \mathbf{P}_{\mathbb{E}}) \tag{3.43}$$

where $\mathbb{E}$ is the matrix which has as columns the eigenvectors belonging to the Signal Subspace.

5.a: For instance for *Equation* 3.42:

1 form the matrices:

$\mathbb{K}_0=[\underline{k}_0,\underline{k}_0, .., \underline{k}_0]$ ($3\times K$ matrix)

(That is a vector expanding to a matrix)

$\mathbb{L}=[\underline{r}_1,\underline{r}_2,....,\underline{r}_N]^T$ ($N\times 3$ matrix)

2. at time n update :

$\underline{v}_n^T = [\![\ \underline{\theta}_n^T\ ,\ \underline{\phi}_n^T\ ]\!]$ ($2K\times 1$ vector)

$\mathbb{K}=[\underline{k}_1,\underline{k}_2, .., \underline{k}_K]$ ($3\times K$ matrix)

and also update the following sub-*STEPS 2a* to *2p*

2a. $\mathbf{G}$, $\mathbf{G}_\theta$, $\mathbf{G}_\phi$, $\mathbf{G}_{\theta\phi}$ ($N\times K$ matrices)

$\mathbb{K}_\theta$, $\mathbb{K}_\phi$, $\mathbb{K}_{\theta\phi}$ ($N\times K$ matrices)

$\mathbf{U}= -j.\mathbb{L}.(\mathbb{K}-\mathbb{K}_0)$ ($N\times K$ matrix)

2b. $\mathbf{U}=exp(\mathbf{U})$ $\mathbf{U}_\theta=-j.\mathbb{L}.\mathbb{K}_\theta$ $\mathbf{U}_\phi=-j.\mathbb{L}.\mathbb{K}_\phi$

$\mathbf{U}_{\theta\phi}=j.\mathbb{L}.\mathbb{K}_{\theta\phi}$

2c. $\mathbf{S} = \mathbf{G}*\mathbf{U}$ $\mathbf{G}_\theta = \mathbf{G}_\theta*\mathbf{U}$ $\mathbf{G}_\phi = \mathbf{G}_\phi*\mathbf{U}$

2d. $\mathbf{S}_\theta = \mathbf{G}_\theta+ \mathbf{U}_\theta*\mathbf{S}$ $\mathbf{S}_\phi = \mathbf{G}_\phi + \mathbf{U}_\phi*\mathbf{S}$

2e. $\mathbf{S}_{\theta\phi}= \mathbf{G}_{\theta\phi}*\mathbf{U}+\mathbf{U}_\phi*\mathbf{G}_\theta+ \mathbf{U}_{\theta\phi}*\mathbf{S} + \mathbf{U}_\theta*\mathbf{S}_\phi$

2f. $\mathbb{A}_\mathbf{S}=(\mathbf{S}^H.\mathbf{S})^{-1}$

2g. $\mathbb{B}_\mathbf{S}=\mathbb{A}_\mathbf{S}.\mathbf{S}^H$

2h. $\underline{\alpha}= \mathbb{B}_\mathbf{S}.\underline{E}$ $\mathbf{P}_\mathbf{S}=\mathbf{S}.\mathbb{B}_\mathbf{S}$

2i. $\mathbf{Q}_\mathbf{S}=\mathbf{I}-\mathbf{P}_\mathbf{S}$

2j. $\underline{c}= diag(\mathbb{E}^H.\mathbf{P}_\mathbf{S}.\mathbb{E})$

2k. $\underline{h}=[1,1,..,1]^T\bigstar\sqrt{\underline{c}}$

2l. ξ=product of elements of $\underline{h}$

2m. for every ij where $i,j\in[1,..,M]$ estimate:

$\mathbf{C}_{\theta_i}=\mathbf{S}_\theta^{*i}.\mathbf{B}^{i*}$ $\mathbf{C}_{\phi_i}=\mathbf{S}_\phi^{*i}.\mathbf{B}^{i*}$ $\mathbf{C}_{\theta_i\phi_i}=\mathbf{S}_{\theta\phi}^{*i}.\mathbf{B}^{i*}$

where the superscripts $*i$ or $i*$ above mean the i^{th} column or row respectively of their matrix.

$$\mathbf{A}_{\theta_i} = \mathbf{Q}_{\mathbf{S}}.\mathbf{C}_{\theta_i} \qquad \mathbf{A}_{\phi_i} = \mathbf{Q}_{\mathbf{S}}.\mathbf{C}_{\phi_i}$$

$$\mathbf{P}_{\mathbf{S}_{\theta_i}} = \mathbf{A}_{\theta_i} + \mathbf{A}_{\theta_i}^H \qquad \mathbf{P}_{\mathbf{S}_{\phi_i}} = \mathbf{A}_{\phi_i} + \mathbf{A}_{\phi_i}^H$$

$$\mathbf{P}_{\mathbf{S}_{\theta_i\phi_j}} = -\mathbf{P}_{\mathbf{S}_{\phi_j}}.\mathbf{C}_{\theta_i} - \mathbf{A}_{\theta_i}.\mathbf{C}_{\phi_j} + \mathbf{A}_{\theta_i}.\mathbf{A}_{\phi_j} - l.\mathbf{Q}_{\mathbf{S}}.\mathbf{C}_{\theta_i\phi_j}$$

where $l=0$ *if* $i \neq j$ *and* $l=-1$ *if* $i=j$

2n. $\mathbf{M}=[diag\left(\mathbf{E}^H.\mathbf{P}_{\mathbf{S}_{\theta_1}}.\mathbf{E}\right),\ldots,diag\left(\mathbf{E}^H.\mathbf{P}_{\mathbf{S}_{\theta_K}}.\mathbf{E}\right),$
$diag\left(\mathbf{E}^H.\mathbf{P}_{\mathbf{S}_{\phi_1}}.\mathbf{E}\right),\ldots,diag\left(\mathbf{E}^H.\mathbf{P}_{\mathbf{S}_{\phi_K}}.\mathbf{E}\right)]$

2o. $\mathbf{M}=-0.5*n*\mathbf{M}*[\underline{h}, \underline{h},\ldots, \underline{h}]^{2+n}$

2p. $\underline{\nabla}\xi^T =$ sum the element of each column of $\mathbf{M}$

$\underline{\nabla}^2\xi =$ its elements are given by *Equation-A3.9* of Appendix 3.

5.b: evaluate the direction of search $dv=\underline{\nabla}^2\xi^{-1}.\ \underline{\nabla}\xi$

5.c: perform a line search across the direction $-\underline{dv}$ in order to estimate a constant l indicating how far to move along the current direction.

5.d: update $\underline{v}$ at time $n+1$ via: $\underline{v}_{n+1} := \underline{v}_n + l.\underline{\nabla}_n$

5.e: $n:=n+1$

5.f: check if a selected stop criterion is satisfied.

If not satisfied then goto *STEP 5.a.2b*

else goto *STEP 6.*

STEP-6: find the non zero elements of the vector $(\mathbf{S}^H.\mathbf{S})^{-1}.\mathbf{S}^H.\underline{E}$ and accept

i) the number of signals incident to the array, from different direction of arrivals, to be the number of those non-zero elements;

ii) the directions of arrival, to be the directions related to the vectors which correspond to non-zero elements of $(\mathbf{S}^H.\mathbf{S})^{-1}.\mathbf{S}^H.\underline{E}$ where $\underline{E}$ is one of the columns of $\mathbf{E}$.

N.B.: the operators $*$ and $\not*$ implies element by element operations (multiplication and division respectively).

The above algorithm as has been presented above is in a form appropriate for VLSI implementation. *Figure* 3.5 gives an example of the implementation for the *SPVs* and their derivatives in a block diagram form. In addition, the *Appendices* 3 and 4 provide the basic mathematical tools of ASPECT algorithm for the three cost functions given by *Equations* 3.41,3.42,3.43.

It is also important to point out that the process could be applied to individual samples at the input of the array and then to average the results of, say, every q samples in order to subtract the effects of noise from the original samples. Also the ***STEP-1*** and ***STEP-2*** can be replaced by one step which will estimate the Right Singular Vector which corresponds to the largest singular value of a block of samples.

— Since the material presented in this chapter was developed and the thesis was written and submitted a paper by Cadjow [CAD-88] has appeared in the technical literature. This paper deals with the problem of located correlated sources. The approach is, however, funtamentally different from that developed in this thesis.

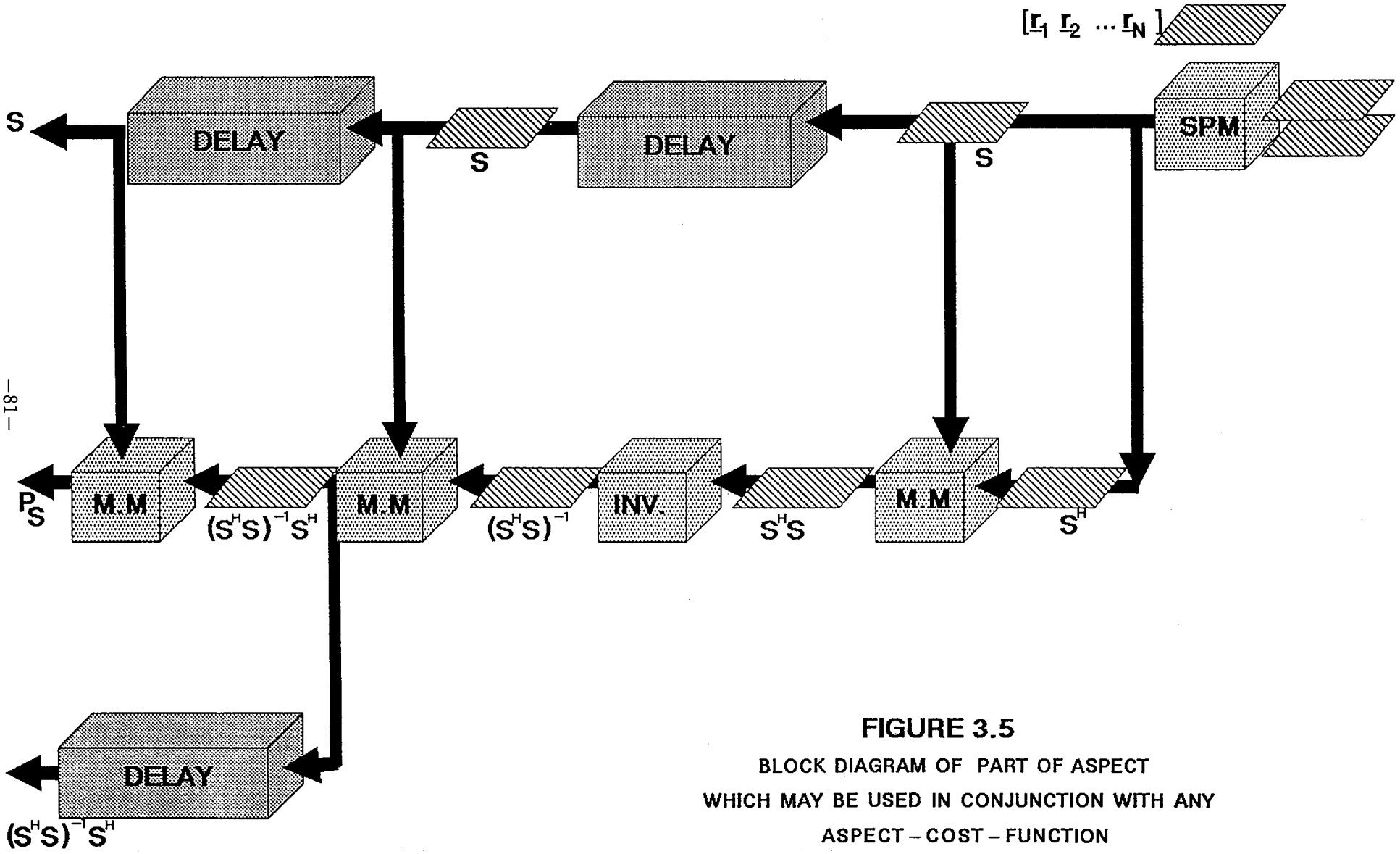

FIGURE 3.5

BLOCK DIAGRAM OF PART OF ASPECT
WHICH MAY BE USED IN CONJUNCTION WITH ANY
ASPECT – COST – FUNCTION

CHAPTER 4

COMPUTER SIMULATION STUDIES of ASPECT ALGORITHM

4.1 INTRODUCTION

In this chapter the results of a series of computer simulations are presented. The simulations were carried out in order to assess the performance and limitations of ASPECT algorithm, under various signal scenarios. The number of sources is considered to be less than the array manifold dimensionality.

The ASPECT algorithm which is based on the Theorems presented in the previous chapter has been coded in PASCAL and MATLAB.

For the whole set of simulations it is assumed that the signal environment involves three directional emitting sources in the presence of non-directional noise. Since the number of sources is not a prior piece of information to ASPECT, the algorithm will start with an assumed number of sources, which will be four (say) for the whole set simulation.

At the end of its operational processing ASPECT should provide the information as to the fact that the number of emitting sources is three not four.

Series of tests were carried out assuming plane wave propagation and then repeated for spherical wave propagation. In each of the two series of tests the performance of ASPECT was considered with respect to range of points. In the first tests the resolving power of ASPECT and its robustness to noise is examined. Thus, two of the three sources (the trial pair) are brought together with angle separations of 10°,5°,2° and 1° under various noise levels. In these tests it was assumed that sources are uncorrelated and then correlated (coherent). Also it was assumed that sources are of equal power. Tests were generalized and repeated in order to determine the performance of ASPECT when emitting sources of widely differing power levels are involved.

The array is assumed that has steered its main lobe toward the direction (0°,95°).

The whole set of simulations, concerning the planewave approximation situation, is performed under the same initial guesses of ASPECT, which are chosen to be: four signals incident to the array from the following four directions: (10°,20°), (7°,50°), (0°,95°) i.e the steering vector direction, and (20°,165°). On the other hand, a self-initialized ASPECT is used in the spherical-wave situation.

The computer simulations were carried out using an APRICOT XEN-*i* 386/30 with 80387 co-processor and Cyber-855 main frame.

4.2 ARRAY MODEL

For the whole set of simulations concerning planewave approximation, an array of eight isotropic elements was deployed with seven of the eight elements are uniformly distributed on a semi-circle of radius R=1.93$\frac{\lambda}{2}$ located in the X-Y plane and the 8^{th} element being located at the point (x=0,y=R,z=$\frac{\lambda}{2}$). The situation is illustrated in *Figure* 4.1*a*. In the case of spherical wave propagation a different array configuration was deployed. This array has twelve elements. Eight of those elements are located as in *Figure* 4.1*a*. The remaining four are located as shown in *Figure* 4.1*b*.

As was mentioned above the array is assumed that has steered its main lobe toward the direction (0°,95°).

4.3 PLANE WAVE SITUATION

4.3.1 Angular Resolution Tests With Uncorrelated Sources

Initial tests were performed in order to assess the performance of ASPECT in resolving closely spaced incident signals. In every case the incident signals are assumed to be three in number, of equal power and uncorrelated. The noise is assumed to be thermal plus isotropic of power −40dB. In each case the *directions of incidence* of third and first signals are (10°,90°), and (0°,30°) correspondingly. The second signal, which together with the first signal constitute a trial pair, is located in

FIGURE – 4.1

ARRAY MODELS USED IN THE SIMULATIONS CARRIED OUT IN THIS CHAPTER

a) FOR PLANE WAVE PROPAGATION

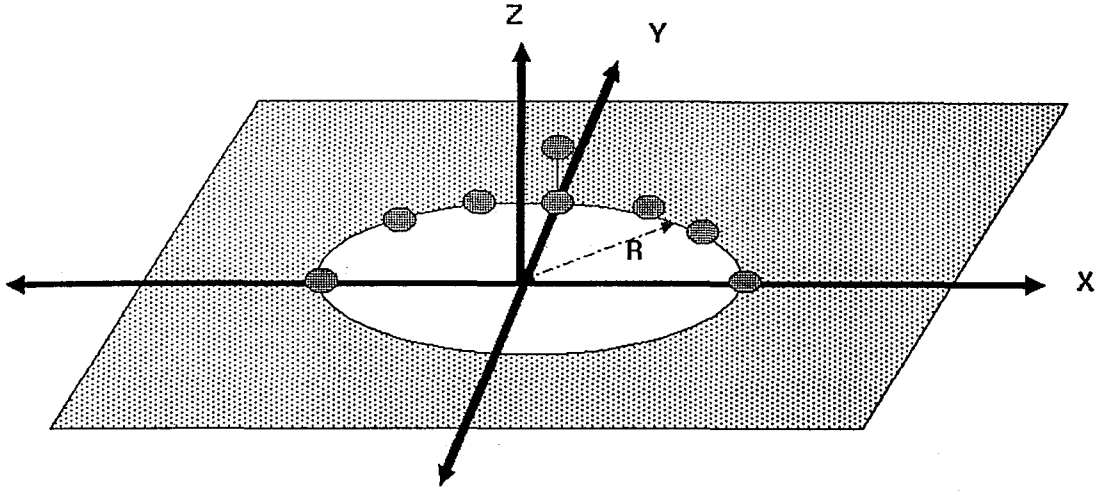

b) FOR SPHERICAL WAVE PROPAGATION

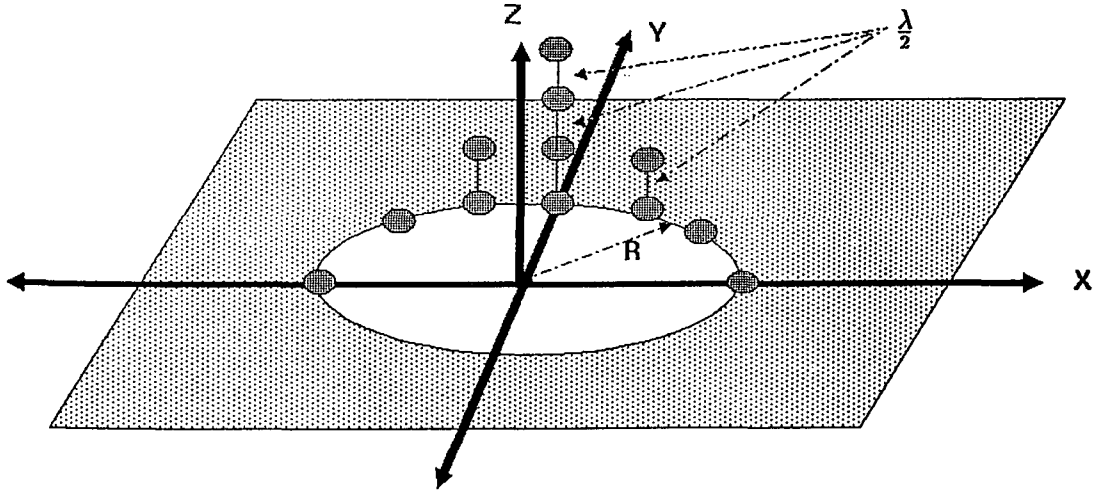

positions which provide 10°, 5°, 2° and 1° angle separation from the *direction of incidence* of the first signal. Thus, the directions of the second signal are chosen to be the following: (0°,40°), (0°,35°), (0°,32°), (0°,31°).

The results of the simulations are shown in *Figures* 4.2-4.5. These results show that ASPECT correctly and accurately resolves and estimates the number and the directions of the incident signals for every case. It is important to note the pattern of behavior of ASPECT with regard to the detection of the signals. In *Figure* 4.2, for instance, Source No.4 disappears after 7 iterations. Thus the algorithm ends with 3 sources having been correctly detected.

From *Figures* 4.2-4.5 it is also clear that the number of iterations (keeping the same initial directions) increases as the angle separation of the trial pair decreases.

FIGURE – 4.2 (Uncorrelated Sources)

	TRUE directions	INITIAL directions	directions estimated by ASPECT
source No.1	(0.0, 30.0)	(10.0, 20.0)	(0.0000, 30.0000)
source No.2	(0.0, 40.0)	(7.0, 50.0)	(–0.0000, 40.0000)
source No.3	(10.0, 90.0)	(0.0, 95.0)	(10.0000, 90.0000)
source No.4	———	(20.0,165.0)	———

cost: 1.000000000000000e+000

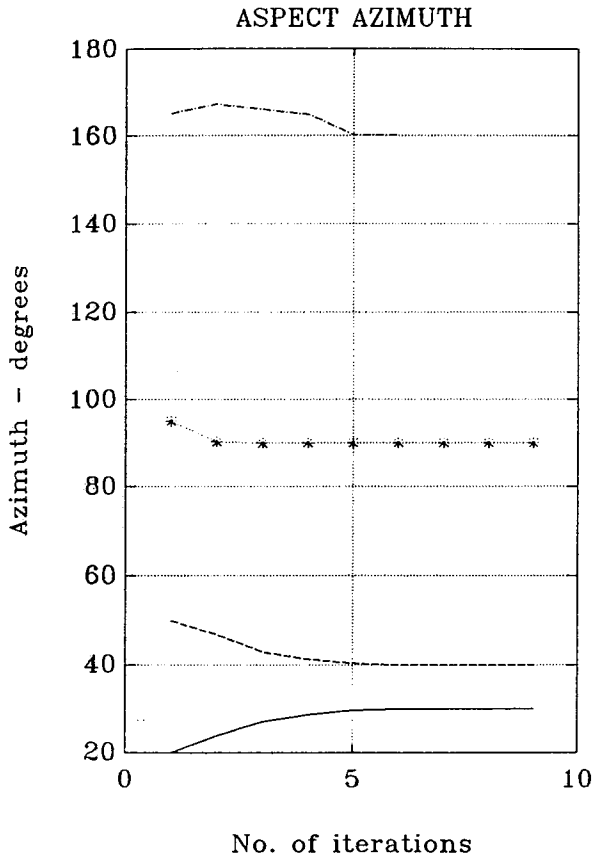

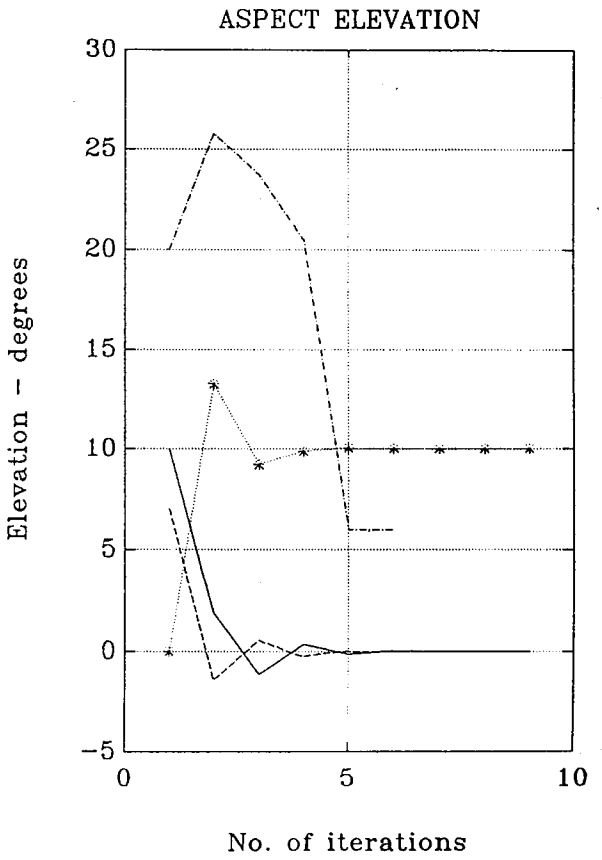

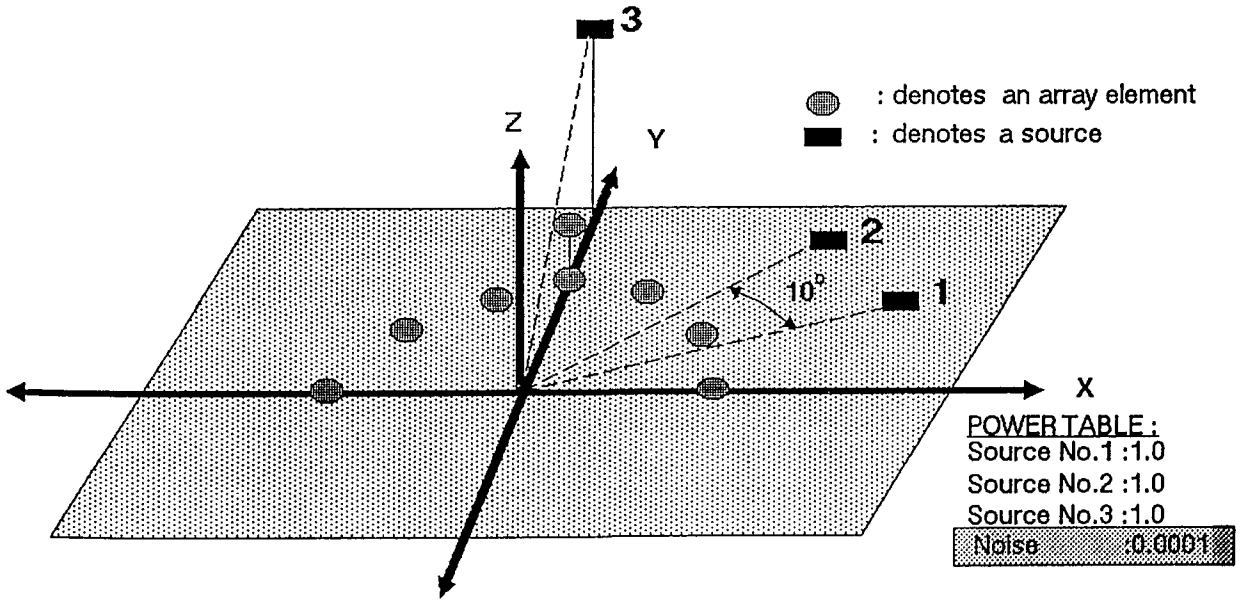

FIGURE – 4.3 (Uncorrelated Sources)

	TRUE directions	INITIAL directions	directions estimated by ASPECT
source No.1	(0.0, 30.0)	(10.0, 20.0)	(0.0000, 30.0000)
source No.2	(0.0, 35.0)	(7.0, 50.0)	(0.0000, 35.0000)
source No.3	(10.0, 90.0)	(0.0, 95.0)	(10.0000, 90.0000)
source No.4	———	(20.0,165.0)	———

cost:1.000000000000000e+000

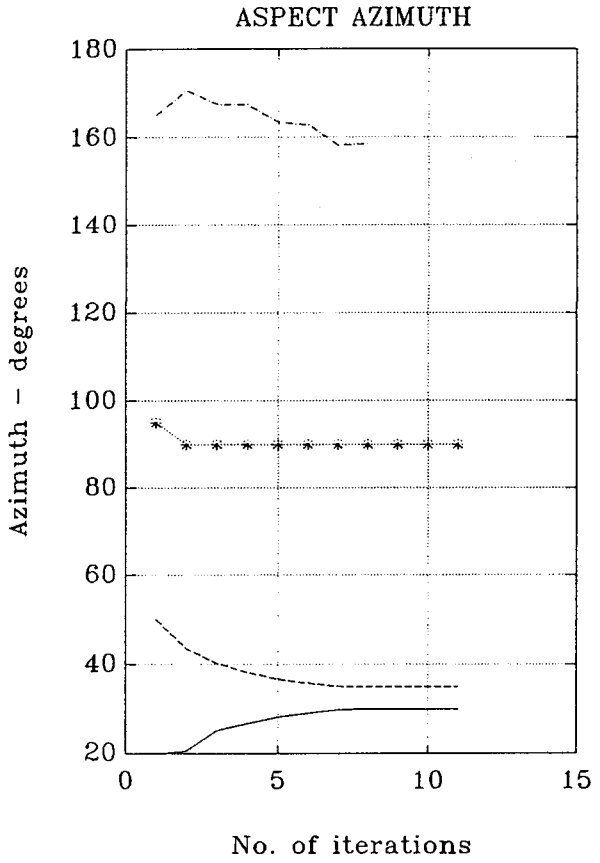

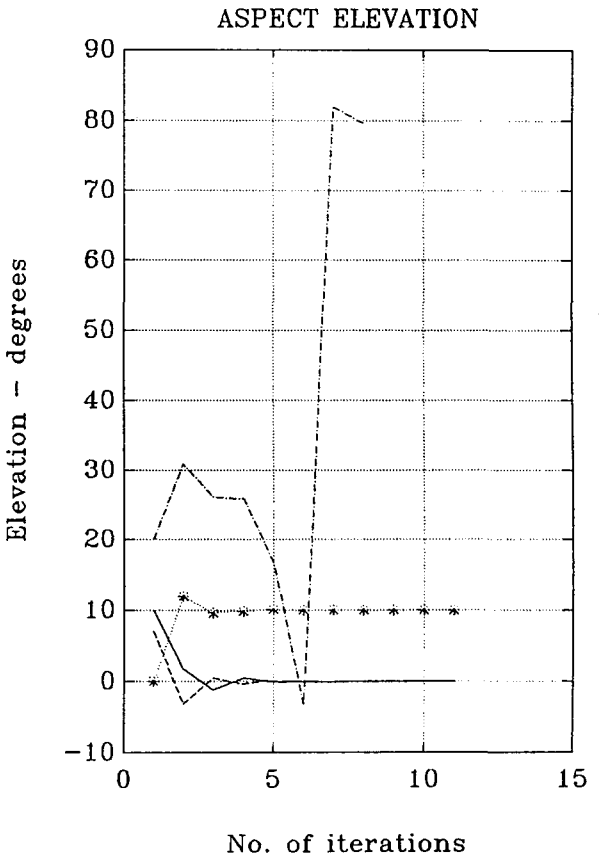

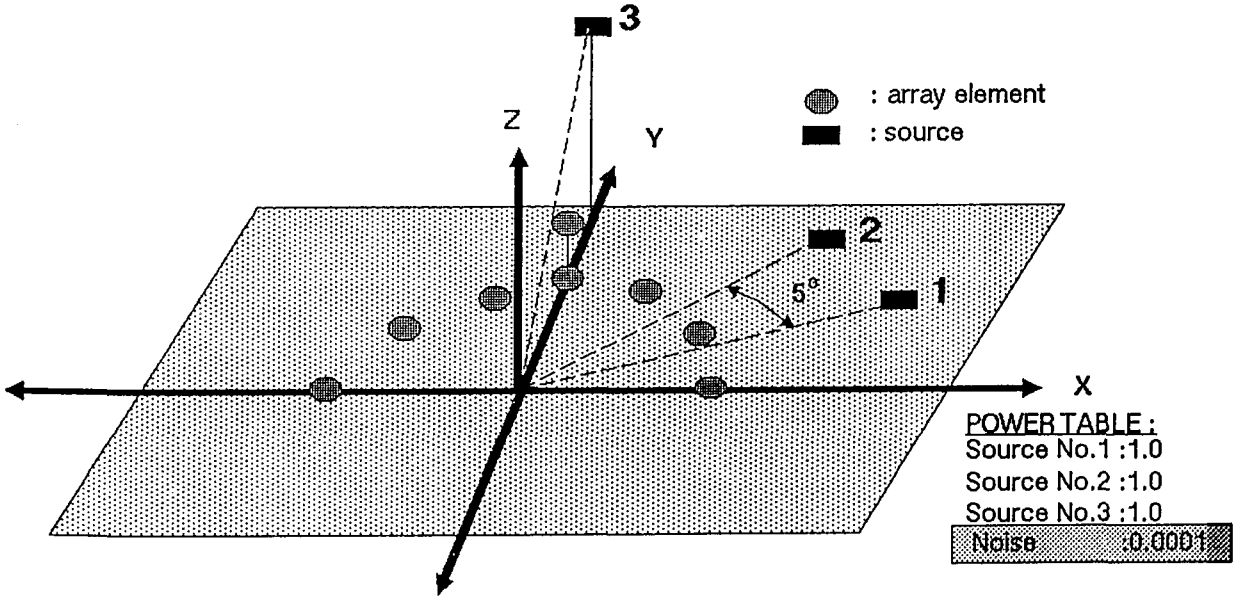

FIGURE – 4.4 (Uncorrelated Sources)

	TRUE directions	INITIAL directions	directions estimated by ASPECT
source No.1	(0.0, 30.0)	(10.0, 20.0)	(−0.0000, 30.0000)
source No.2	(0.0, 32.0)	(7.0, 50.0)	(0.0000, 32.0000)
source No.3	(10.0, 90.0)	(0.0, 95.0)	(10.0000, 90.0000)
source No.4	———	(20.0,165.0)	———

cost: 1.000000000000000e + 000

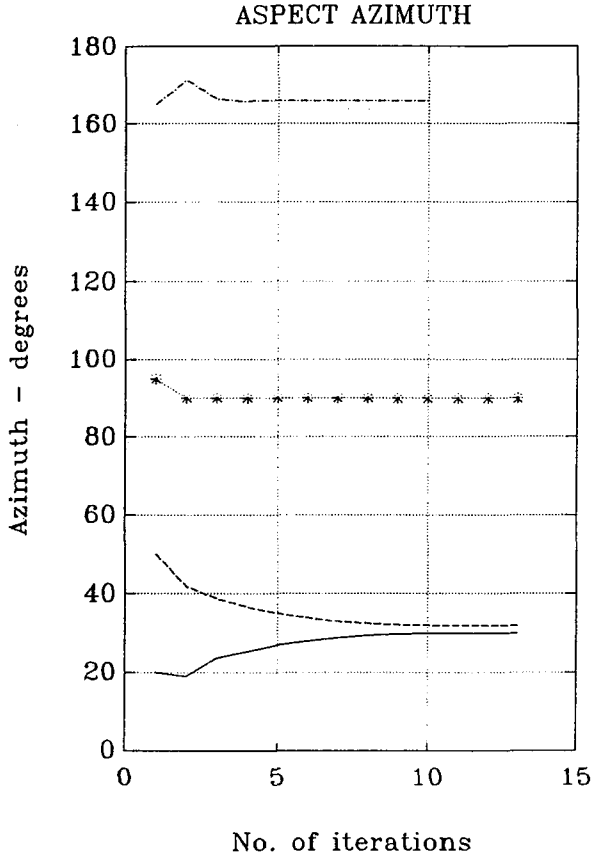

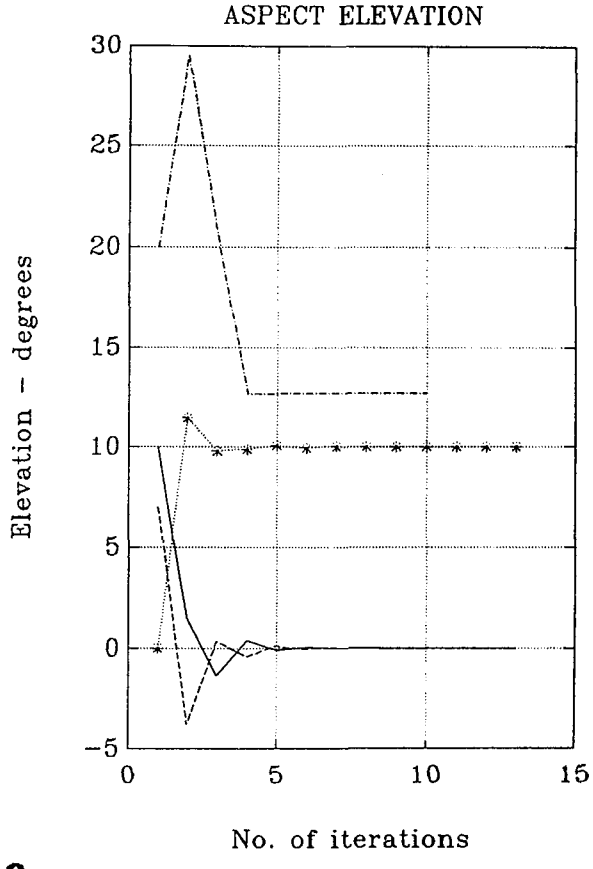

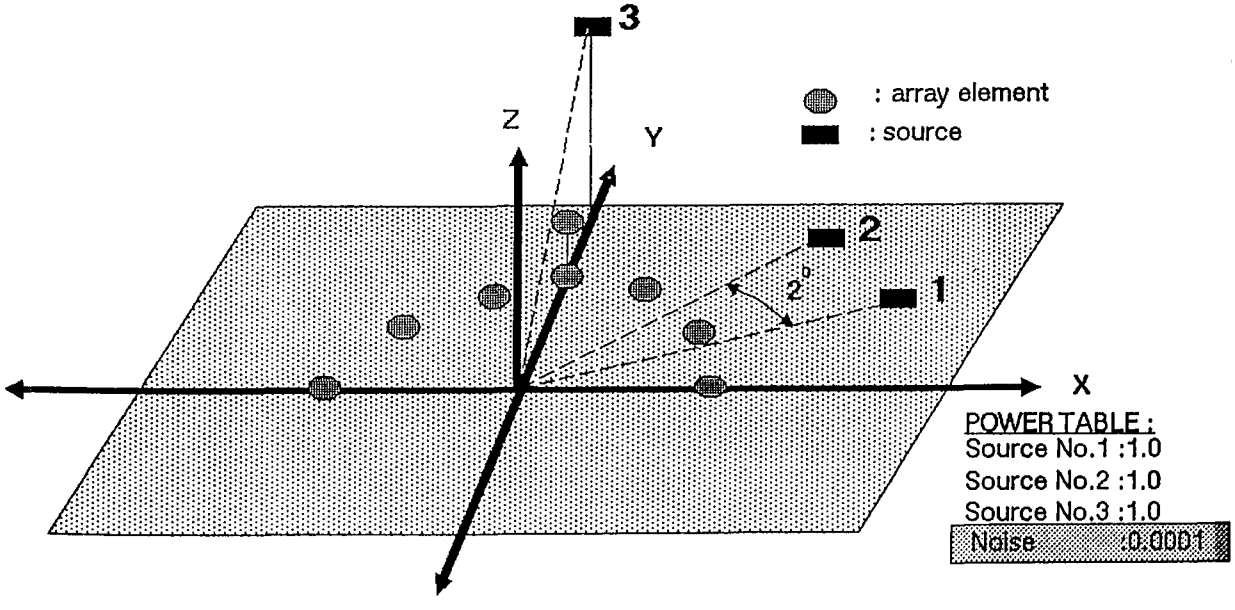

FIGURE – 4.5 (Uncorrelated Sources)

	TRUE directions	INITIAL directions	directions estimated by ASPECT
source No.1	(0.0, 30.0)	(10.0, 20.0)	(–0.0000, 30.0000)
source No.2	(0.0, 31.0)	(7.0, 50.0)	(0.0000, 31.0000)
source No.3	(10.0, 90.0)	(0.0, 95.0)	(10.0000, 90.0000)
source No.4	———	(20.0,165.0)	———

cost: 1.000000000000000e+000

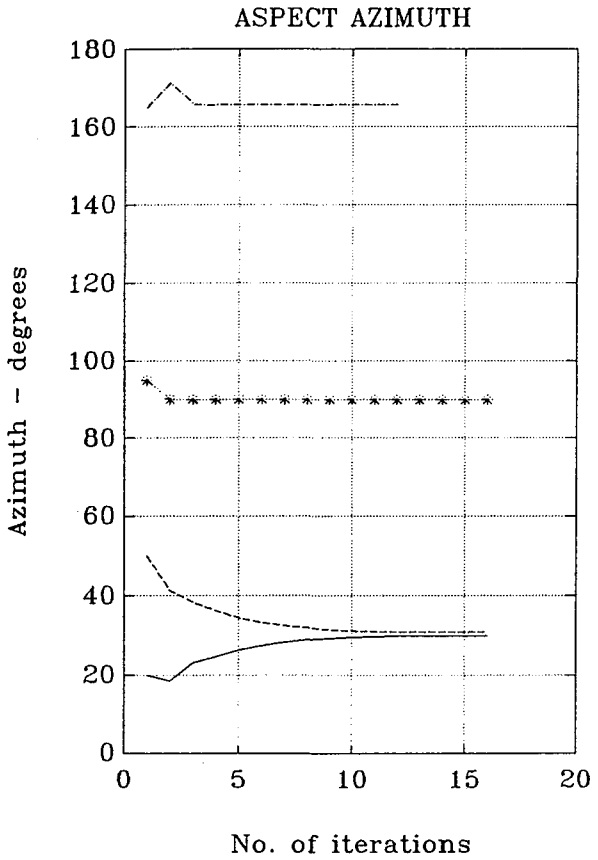

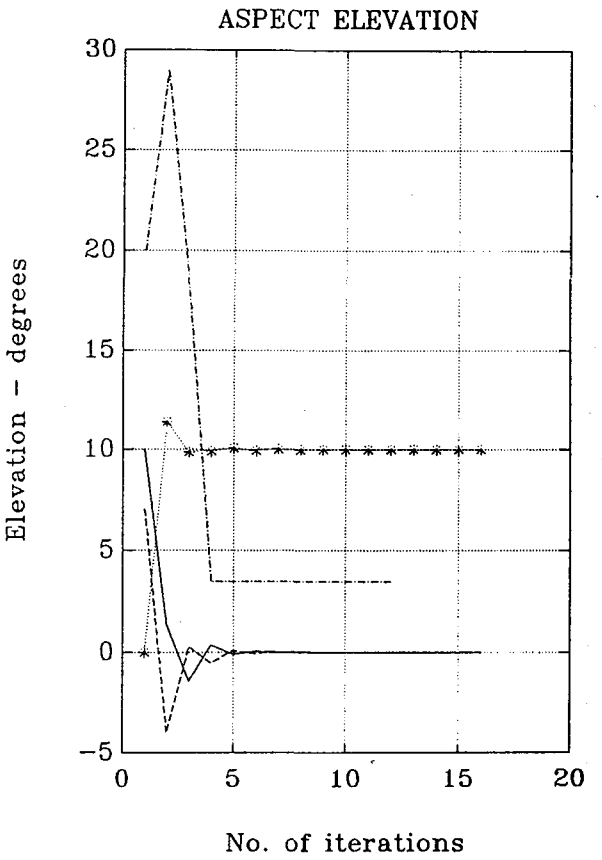

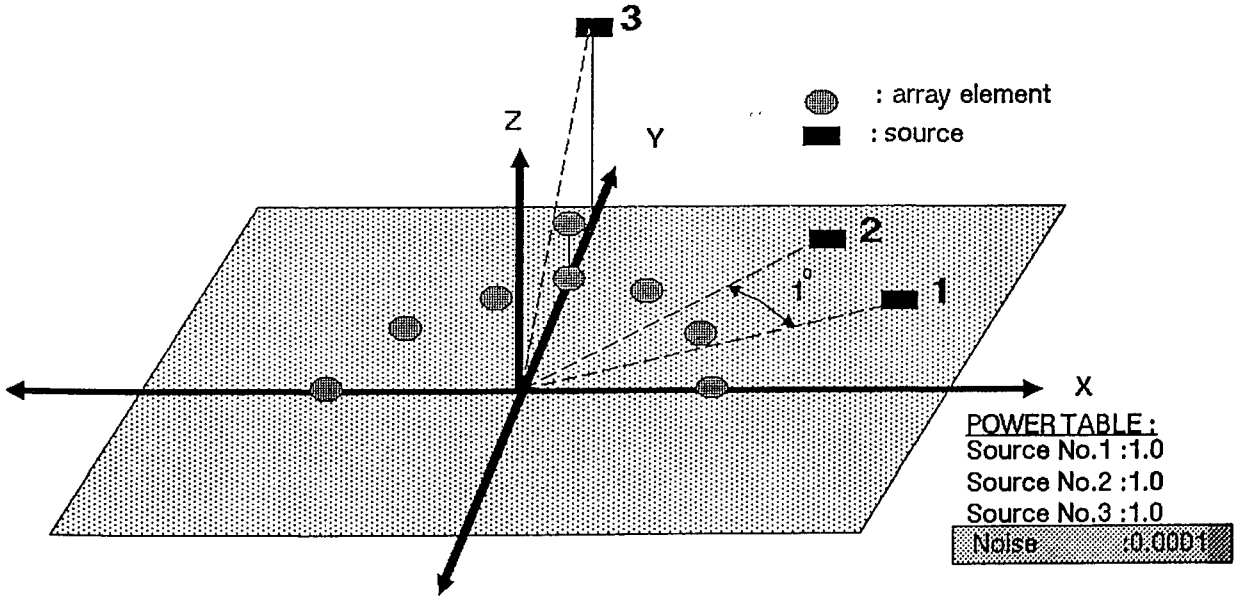

4.3.2 Noise Effects

In this section the effect of omni-directional additive Gaussian noise on the performance of the ASPECT is considered. The noise power is brought up from -40dB to -20dB and -10dB. The array environment described in the previous section remains unchanged. For every power level the performance of ASPECT is assessed with respect to space resolution, by repeating the whole set of tests of the *Angular Resolution* section. The results are shown in Figures 4.6 to 4.13. By comparing the set of figures *Figures* 4.6-4.9 which correspond to -20dB noise level with the set *Figures* 4.10-4.13 (that is for -10dB noise level) it is concluded that these two sets are identical. In addition the above two sets of figures are identical to Figures 4.2-4.5 (-40dB noise) showing the robustness of ASPECT with respect to noise level.

FIGURE – 4.6 (Uncorrelated Sources)

	TRUE directions	INITIAL directions	directions estimated by ASPECT
source No.1	(0.0, 30.0)	(10.0, 20.0)	(0.0000, 30.0000)
source No.2	(0.0, 40.0)	(7.0, 50.0)	(0.0000, 40.0000)
source No.3	(10.0, 90.0)	(0.0, 95.0)	(10.0000, 90.0000)
source No.4	———	(20.0,165.0)	———

cost:1.000000000000000e+000

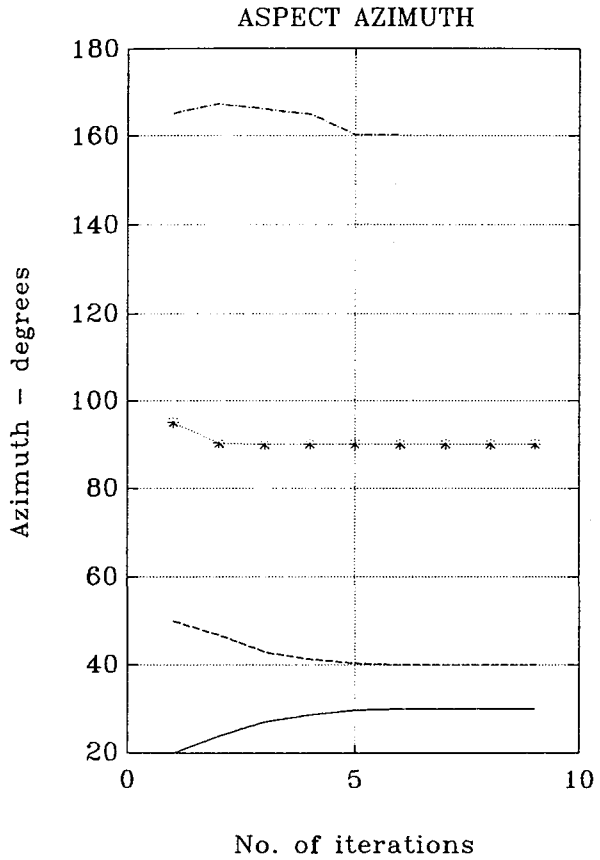

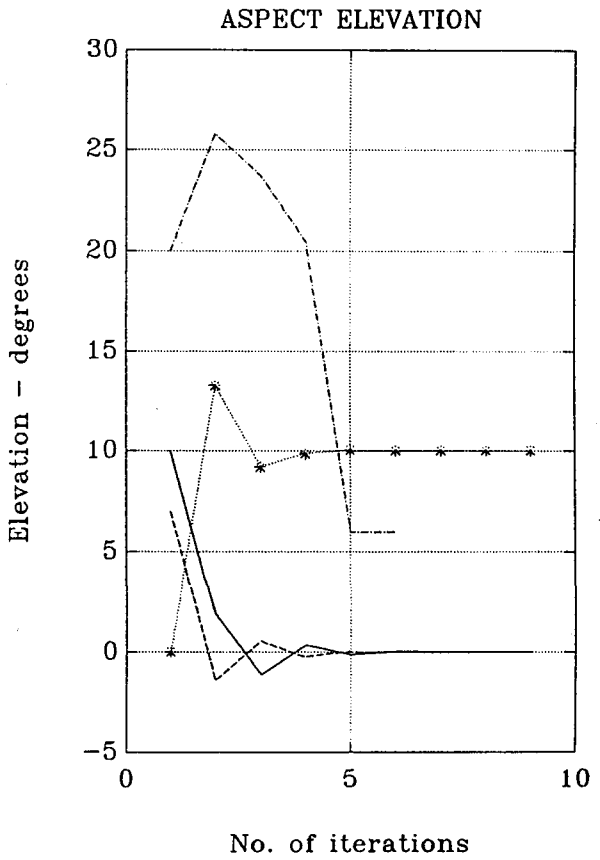

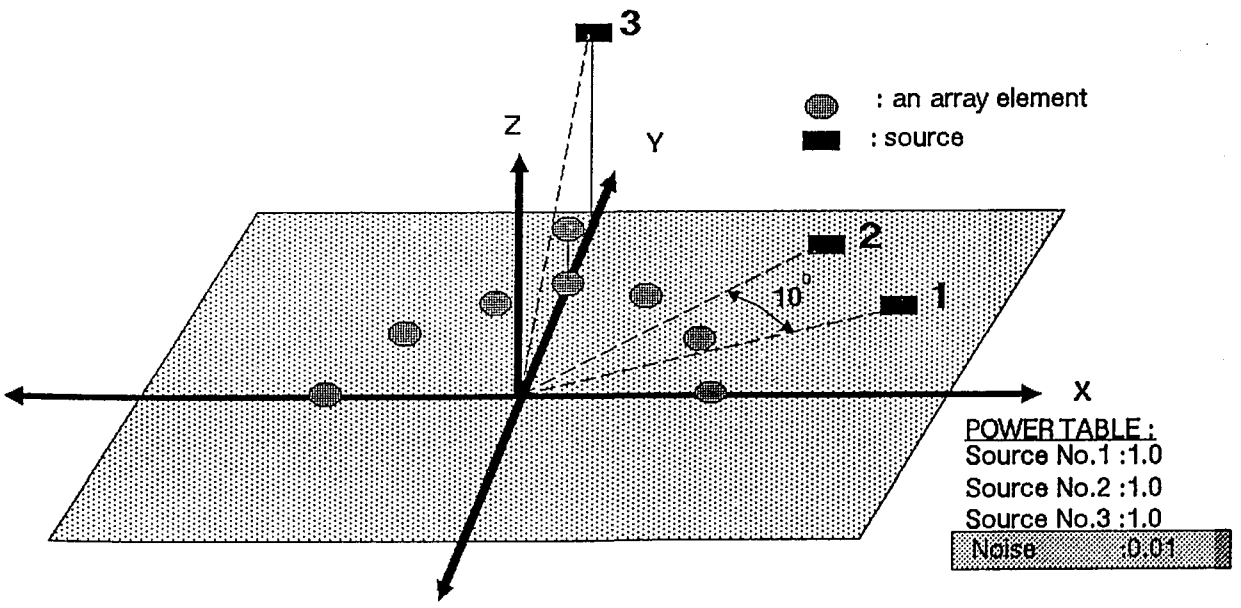

POWER TABLE :
Source No.1 :1.0
Source No.2 :1.0
Source No.3 :1.0
Noise :0.01

FIGURE – 4.7 (Uncorrelated Sources)

	TRUE directions	INITIAL directions	directions estimated by ASPECT
source No.1	(0.0, 30.0)	(10.0, 20.0)	(0.0000, 30.0000)
source No.2	(0.0, 35.0)	(7.0, 50.0)	(0.0000, 35.0000)
source No.3	(10.0, 90.0)	(0.0, 95.0)	(10.0000, 90.0000)
source No.4	———	(20.0,165.0)	———

cost:1.000000000000000e+000

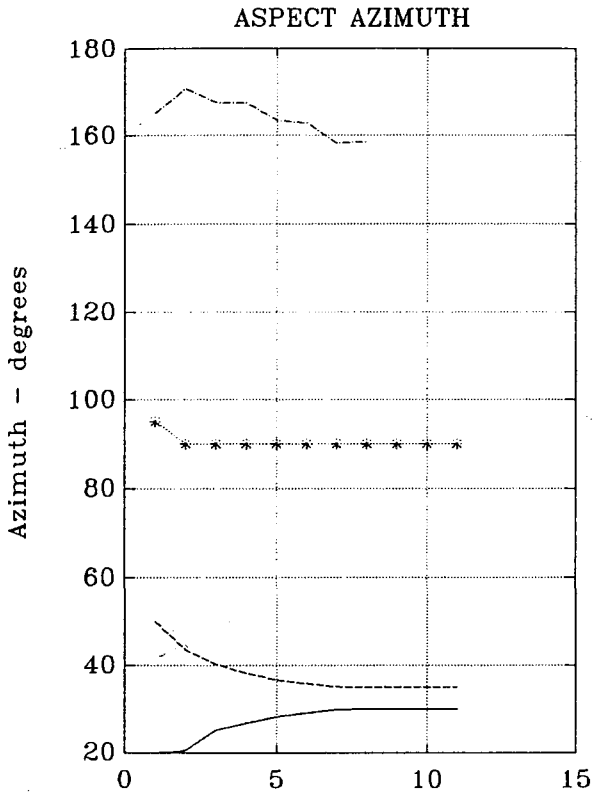

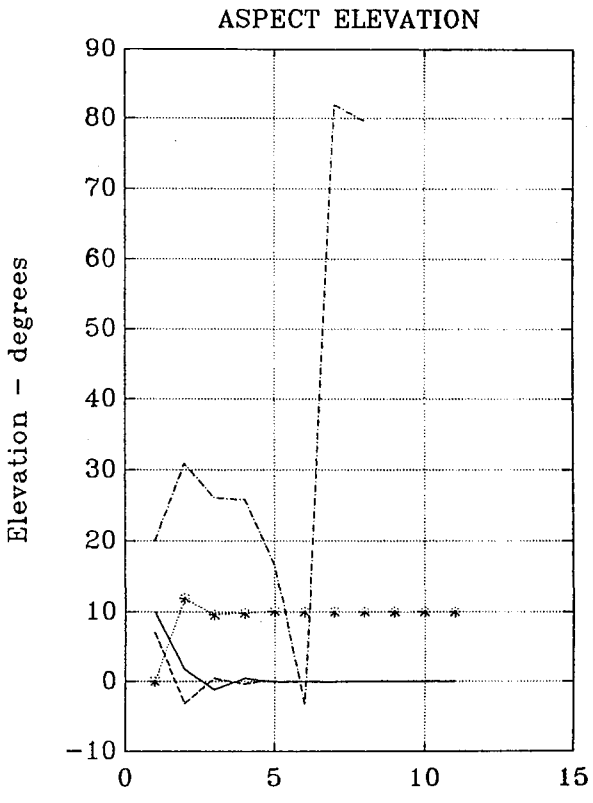

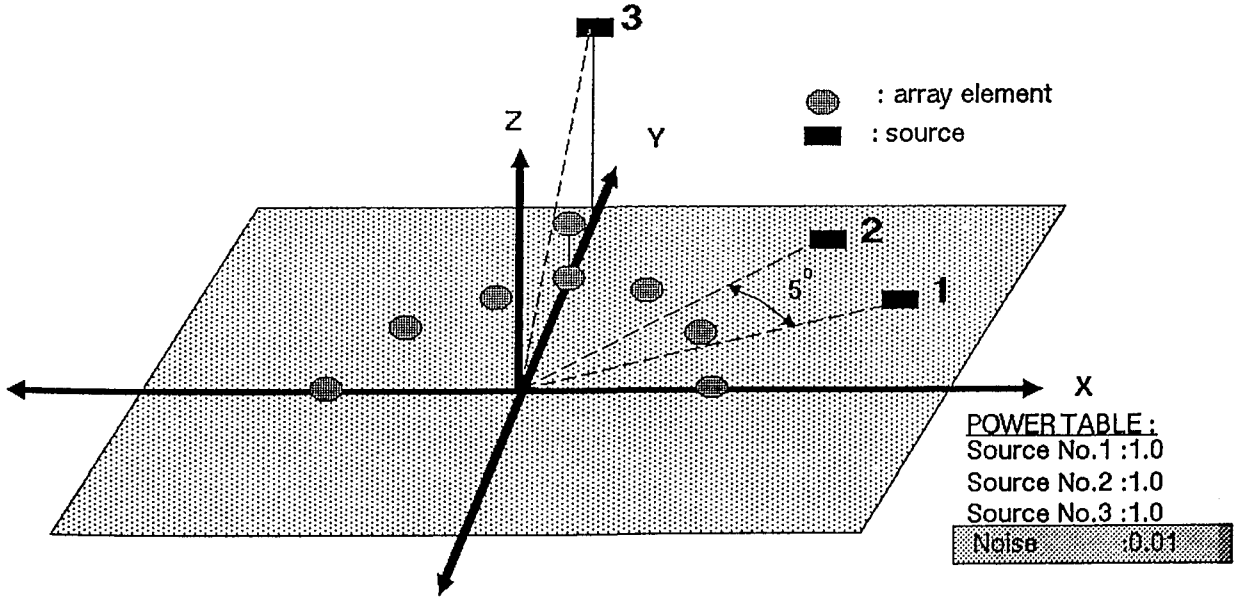

FIGURE – 4.8 (Uncorrelated Sources)

	TRUE directions	INITIAL directions	directions estimated by ASPECT
source No.1	(0.0, 30.0)	(10.0, 20.0)	(0.0000, 30.0000)
source No.2	(0.0, 32.0)	(7.0, 50.0)	(0.0000, 32.0000)
source No.3	(10.0, 90.0)	(0.0, 95.0)	(10.0000, 90.0000)
source No.4	———	(20.0,165.0)	———

cost:1.0000000000000000e+000

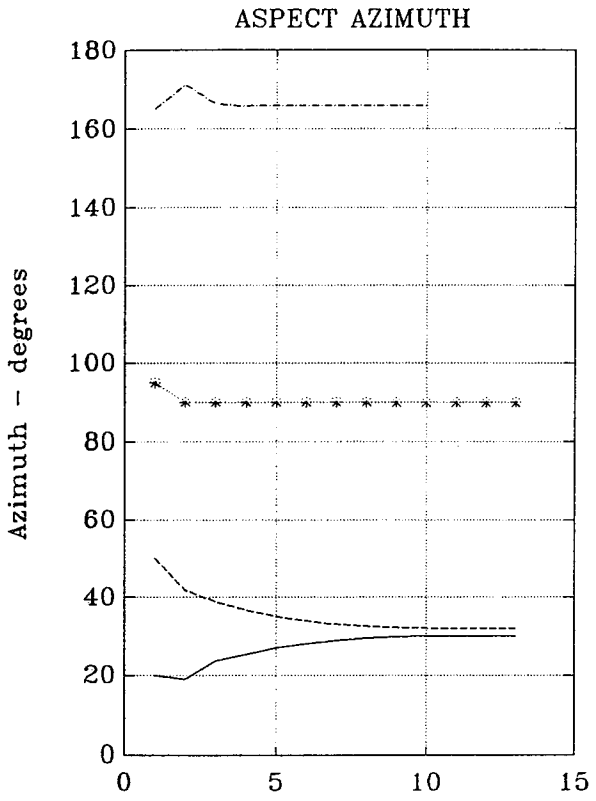

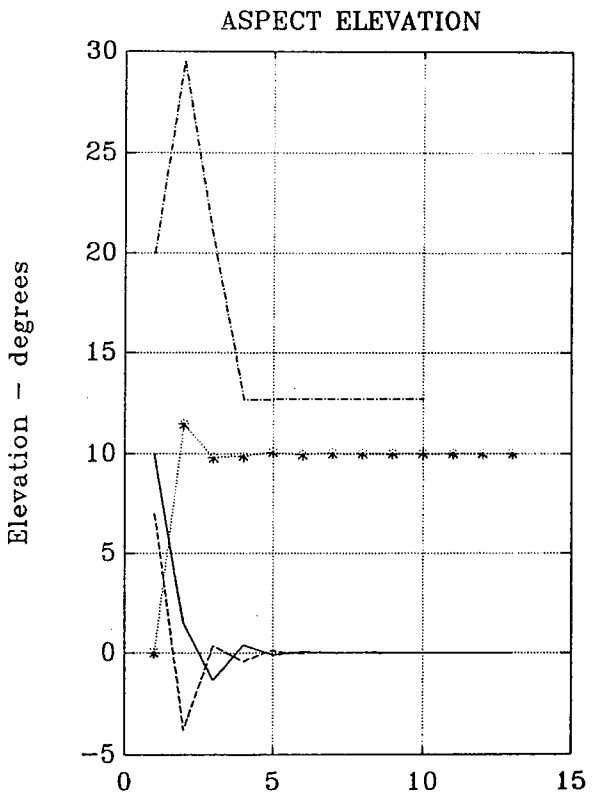

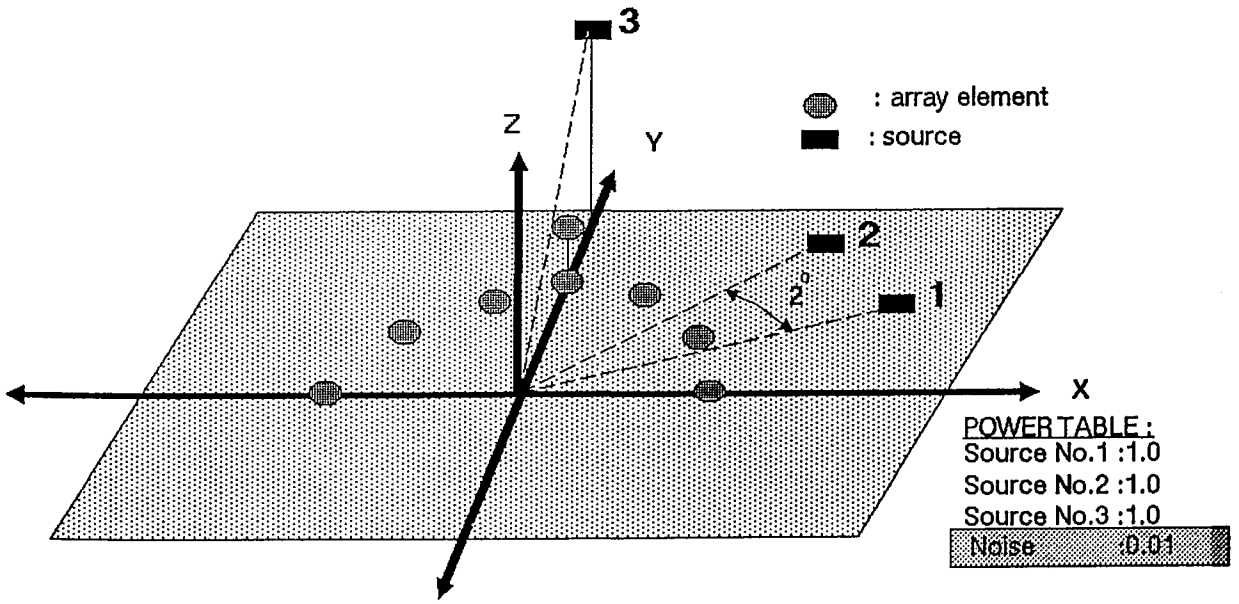

FIGURE－4.9 (Uncorrelated Sources)

	TRUE directions	INITIAL directions	directions estimated by ASPECT
source No.1	(0.0, 30.0)	(10.0, 20.0)	(－0.0000, 30.0000)
source No.2	(0.0, 31.0)	(7.0, 50.0)	(0.0000, 31.0000)
source No.3	(10.0, 90.0)	(0.0, 95.0)	(10.0000, 90.0000)
source No.4	———	(20.0,165.0)	———

cost:1.000000000000001e＋000

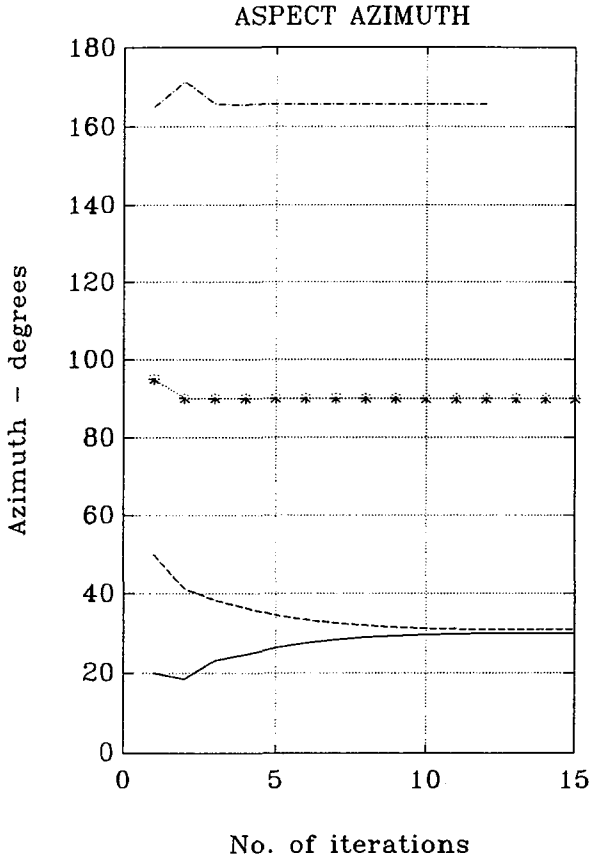

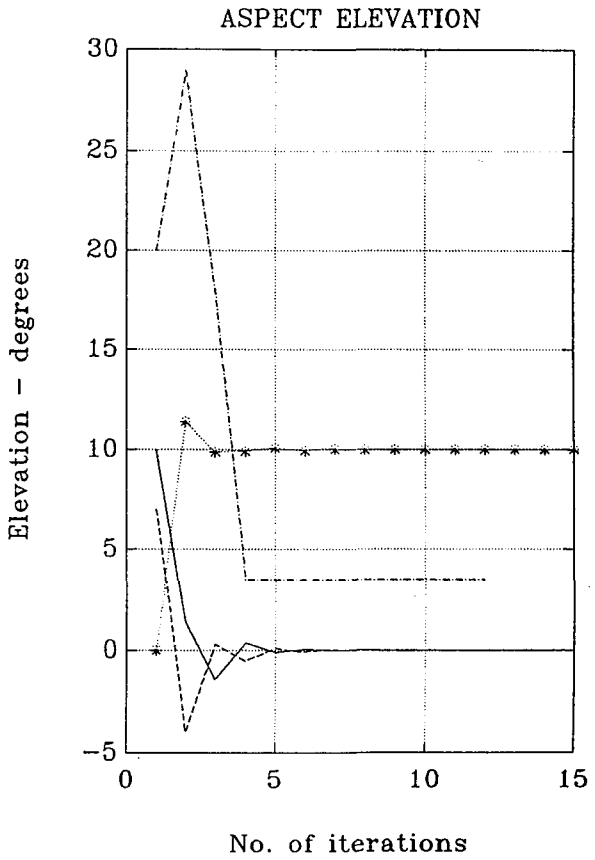

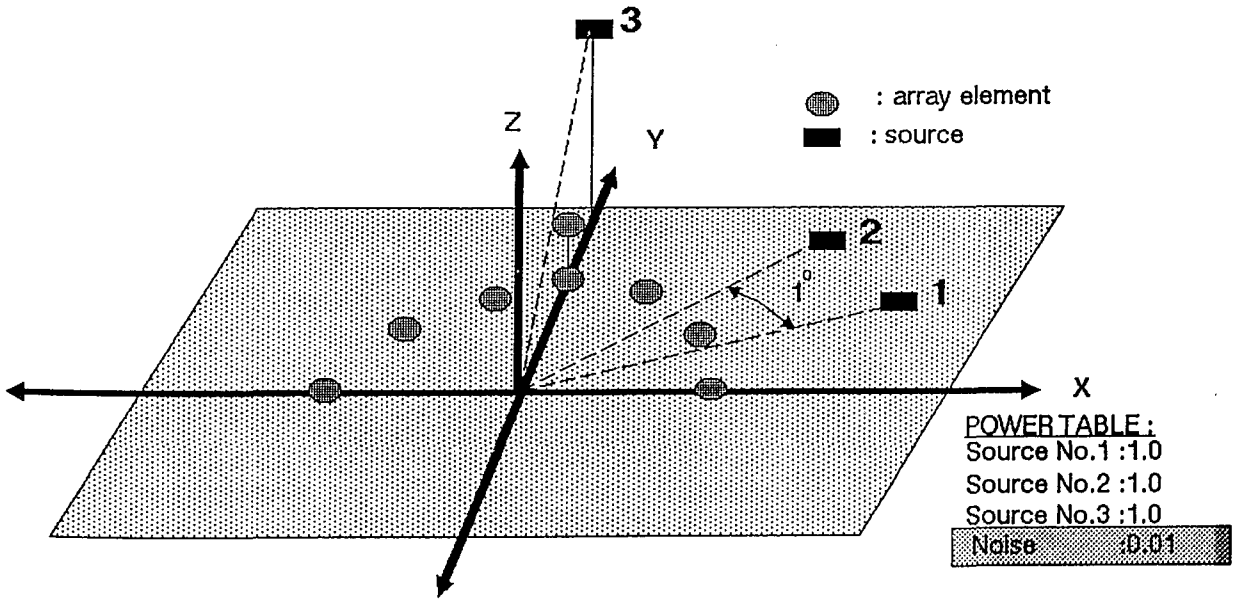

FIGURE – 4.10 (Uncorrelated Sources)

	TRUE directions	INITIAL directions	directions estimated by ASPECT
source No.1	(0.0, 30.0)	(10.0, 20.0)	(0.0000, 30.0000)
source No.2	(0.0, 40.0)	(7.0, 50.0)	(–0.0000, 40.0000)
source No.3	(10.0, 90.0)	(0.0, 95.0)	(10.0000, 90.0000)
source No.4	———	(20.0,165.0)	———

cost: 1.000000000000001e+000

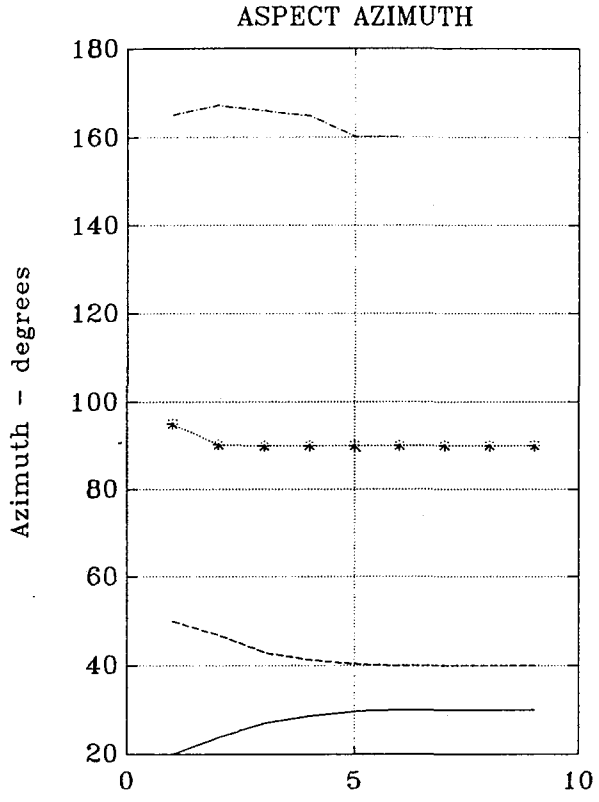

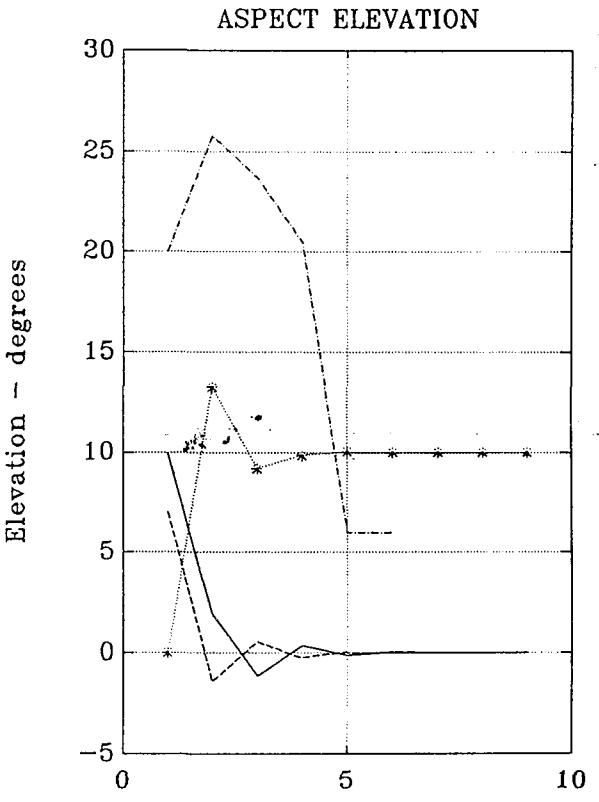

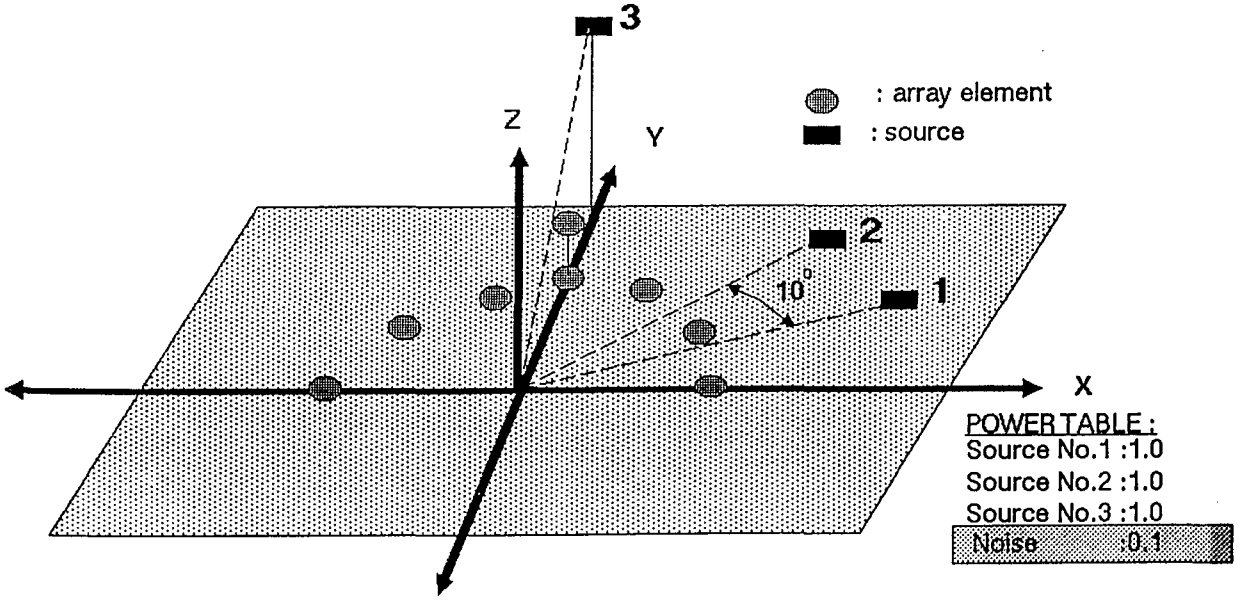

FIGURE－4.11 (Uncorrelated Sources)

	TRUE directions	INITIAL directions	directions estimated by ASPECT
source No.1	(0.0, 30.0)	(10.0, 20.0)	(－0.0000, 30.0000)
source No.2	(0.0, 35.0)	(7.0, 50.0)	(－0.0000, 35.0000)
source No.3	(10.0, 90.0)	(0.0, 95.0)	(10.0000, 90.0000)
source No.4	———	(20.0,165.0)	———

cost:1.0000000000000000e＋000

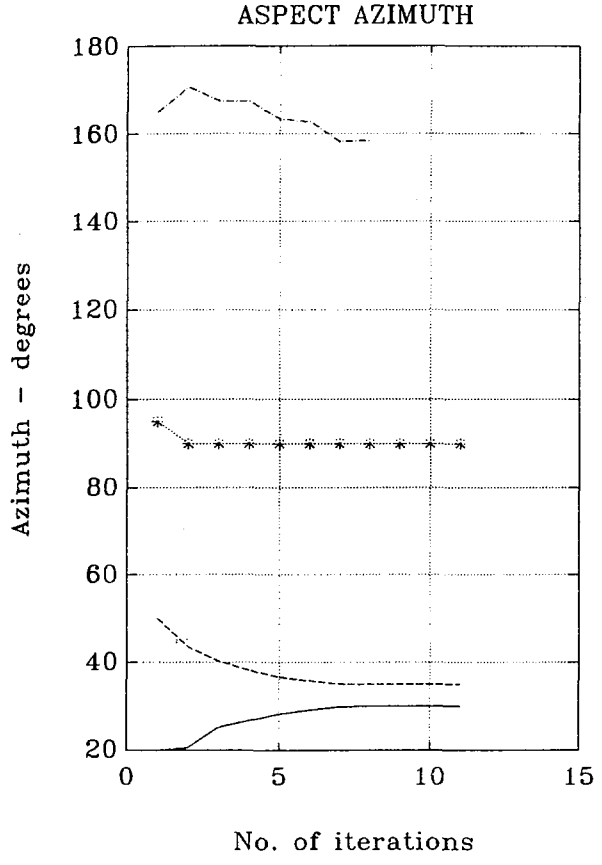

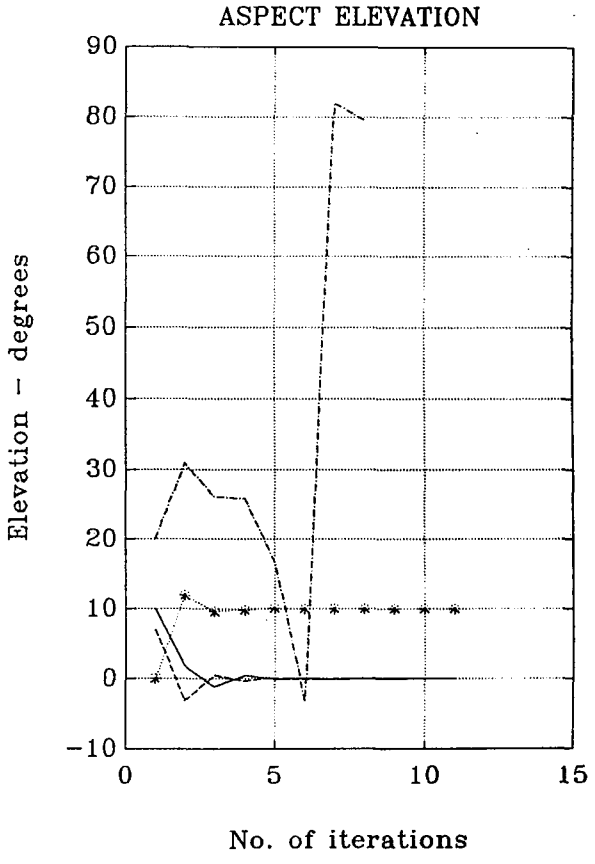

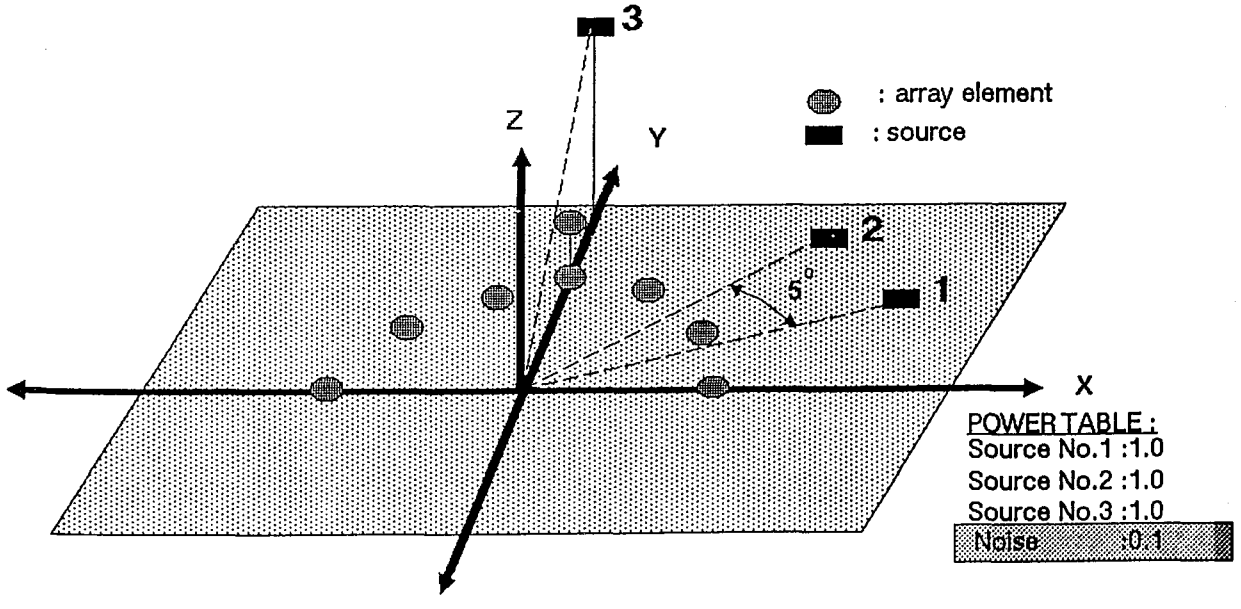

FIGURE – 4.12 (Uncorrelated Sources)

	TRUE directions	INITIAL directions	directions estimated by ASPECT
source No.1	(0.0, 30.0)	(10.0, 20.0)	(0.0000, 30.0000)
source No.2	(0.0, 32.0)	(7.0, 50.0)	(0.0000, 32.0000)
source No.3	(10.0, 90.0)	(0.0, 95.0)	(10.0000, 90.0000)
source No.4	———	(20.0,165.0)	———

cost: 1.000000000000000e+000

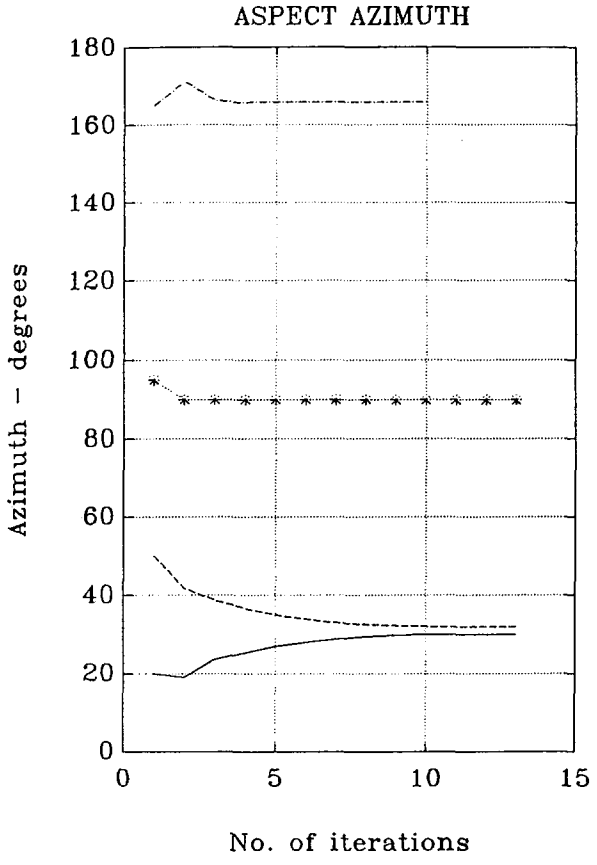

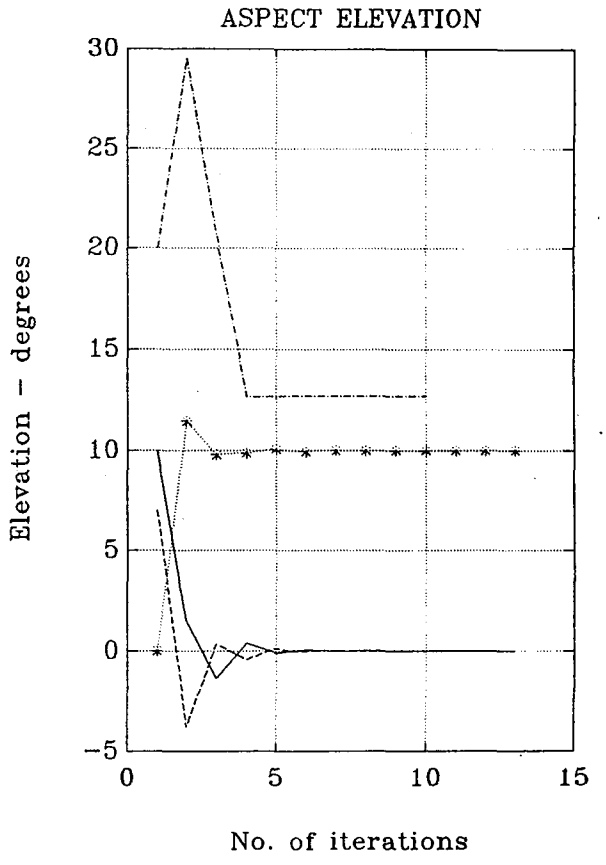

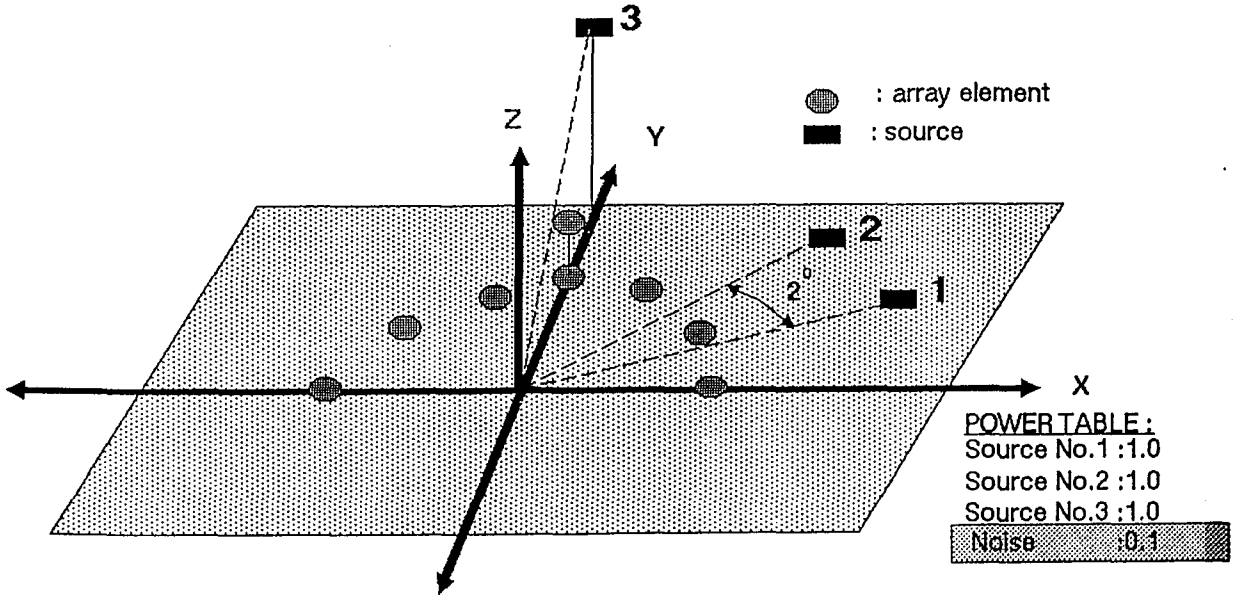

FIGURE – 4.13 (Uncorrelated Sources)

	TRUE directions	INITIAL directions	directions estimated by ASPECT
source No.1	(0.0, 30.0)	(10.0, 20.0)	(−0.0000, 30.0000)
source No.2	(0.0, 31.0)	(7.0, 50.0)	(0.0000, 31.0000)
source No.3	(10.0, 90.0)	(0.0, 95.0)	(10.0000, 90.0000)
source No.4	———	(20.0,165.0)	———

cost:1.000000000000001e+000

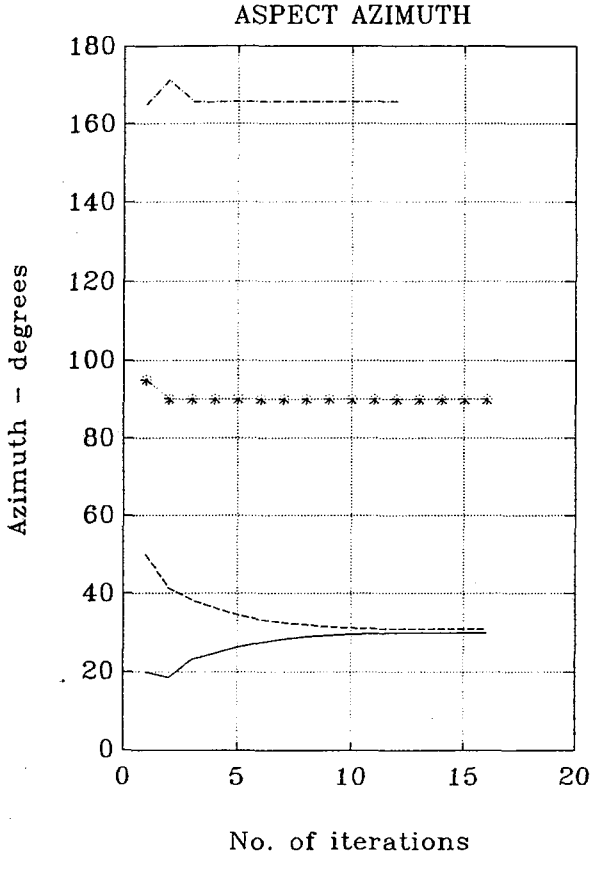

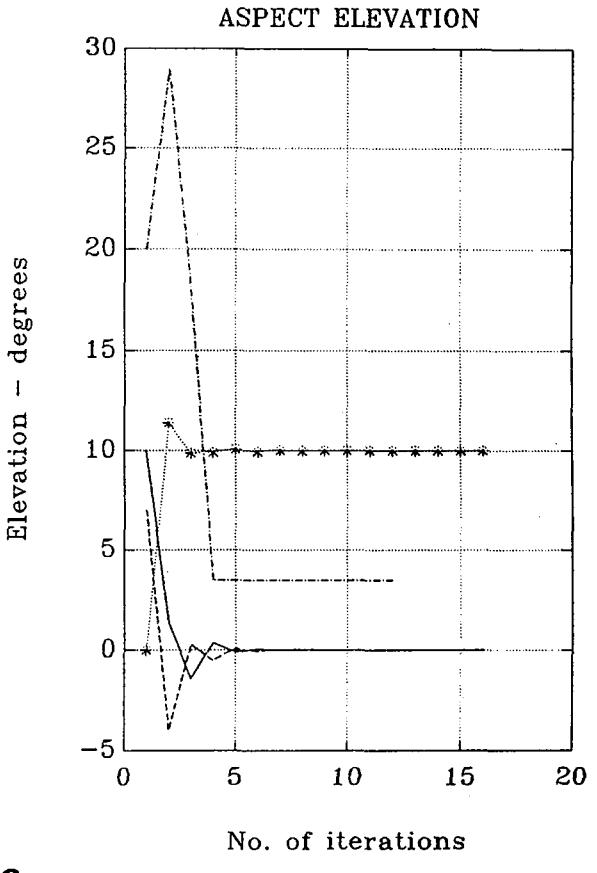

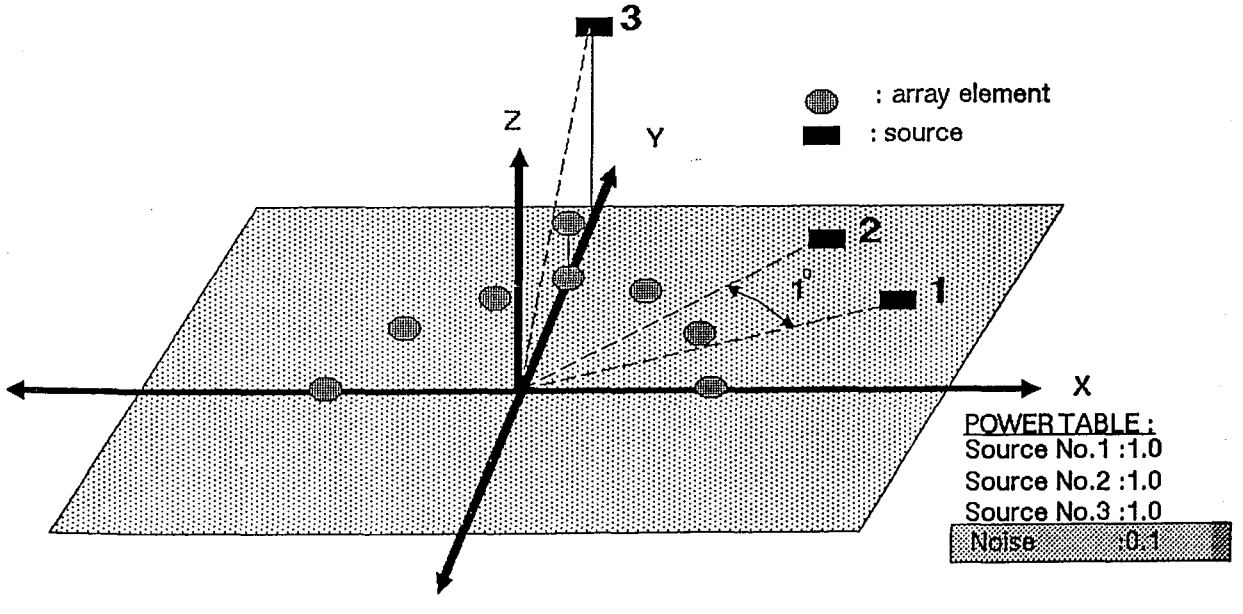

4.3.3 Power Resolution

In this section ASPECT is tested in a signal environment where there are present both *strong* and *weak* signals. Consider that the noise power is -40dB. Then, one of the trial pair, that is the second source, is taken from 0dB down to -20dB, -40dB (i.e equal to noise power). For each selected level the trial pair is located in positions which provide 10°, 5°, 2° and 1° angle separation. The results are shown in:

- *Figures* 4.14-4.17 for -20dB trial pair differing power level and
- *Figures* 4.18-4.21 for -40dB (that is one source of the trial pair has a power level equal to noisel).

These results show that ASPECT is able to resolve a trial pair with widely differing power levels wihout any particular problem.

FIGURE – 4.14 (Uncorrelated Sources)

	TRUE directions	INITIAL directions	directions estimated by ASPECT
source No.1	(0.0, 30.0)	(10.0, 20.0)	(0.0000, 30.0000)
source No.2	(0.0, 40.0)	(7.0, 50.0)	(0.0000, 40.0000)
source No.3	(10.0, 90.0)	(0.0, 95.0)	(10.0000, 90.0000)
source No.4	———	(20.0,165.0)	———

cost:1.000000000000000e+000

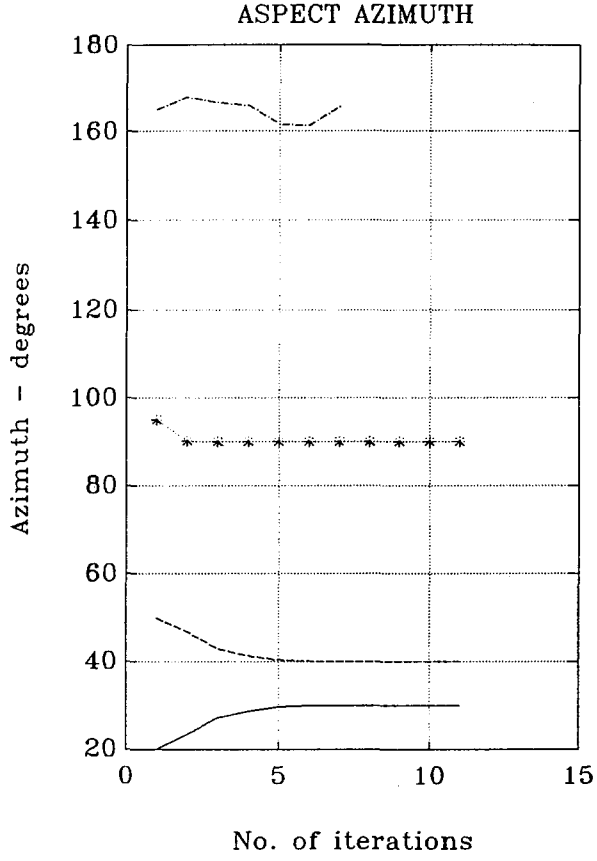

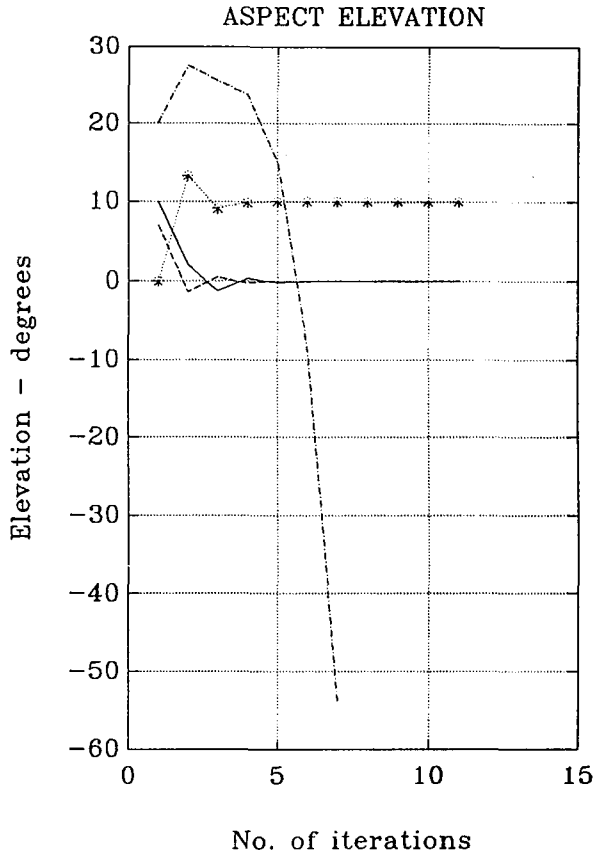

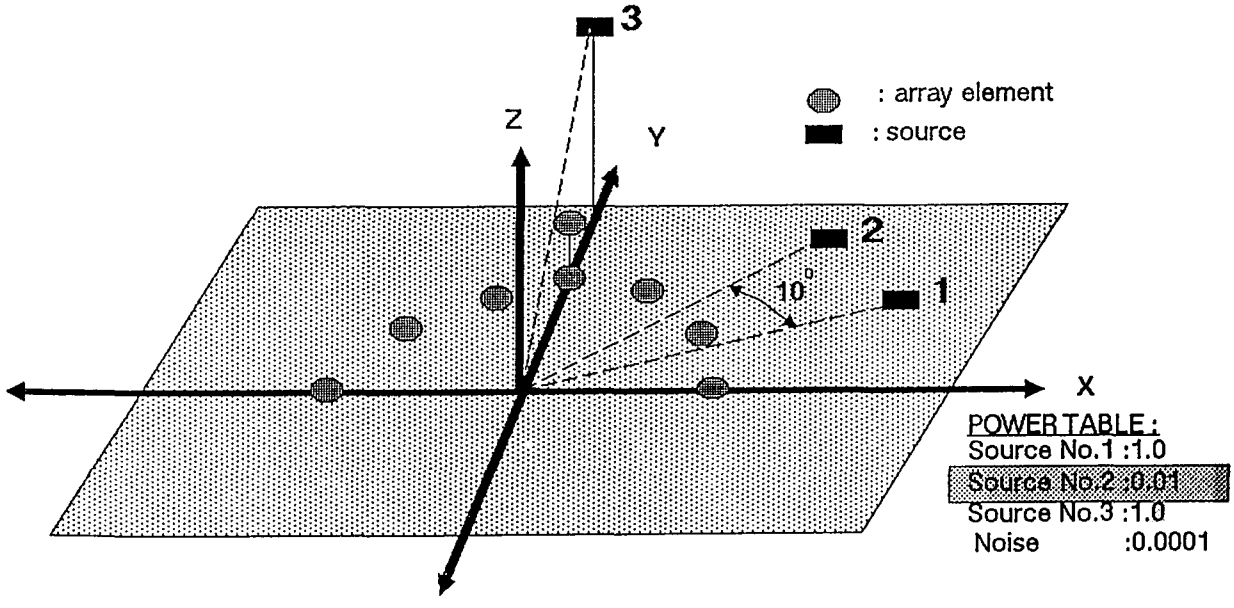

FIGURE – 4.15 (Uncorrelated Sources)

	TRUE directions	INITIAL directions	directions estimated by ASPECT
source No.1	(0.0, 30.0)	(10.0, 20.0)	(– 0.0000, 30.0000)
source No.2	(0.0, 35.0)	(7.0, 50.0)	(0.0000, 35.0000)
source No.3	(10.0, 90.0)	(0.0, 95.0)	(10.0000, 90.0000)
source No.4	———	(20.0,165.0)	———

cost:1.000000000000000e + 000

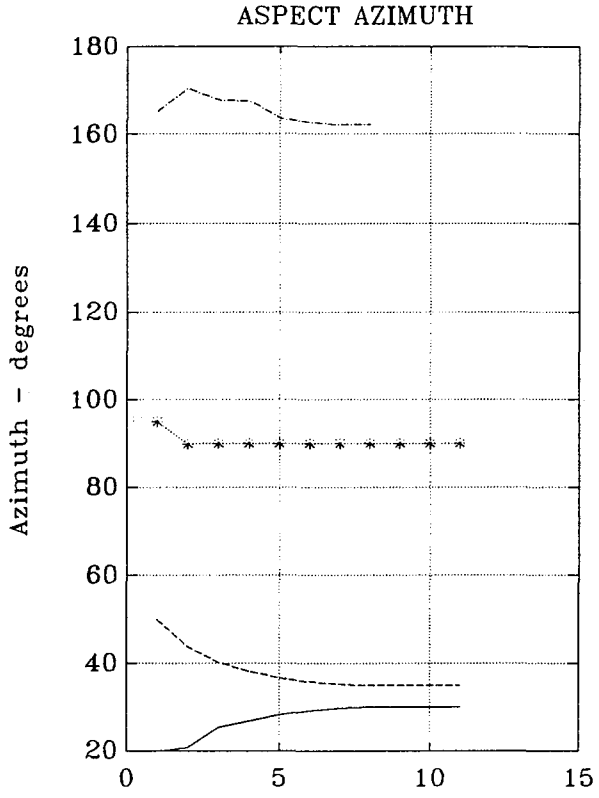

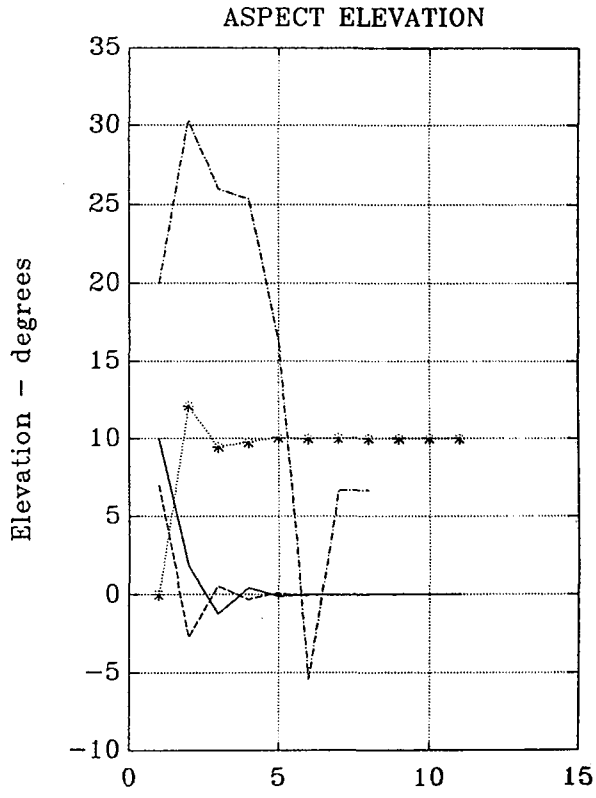

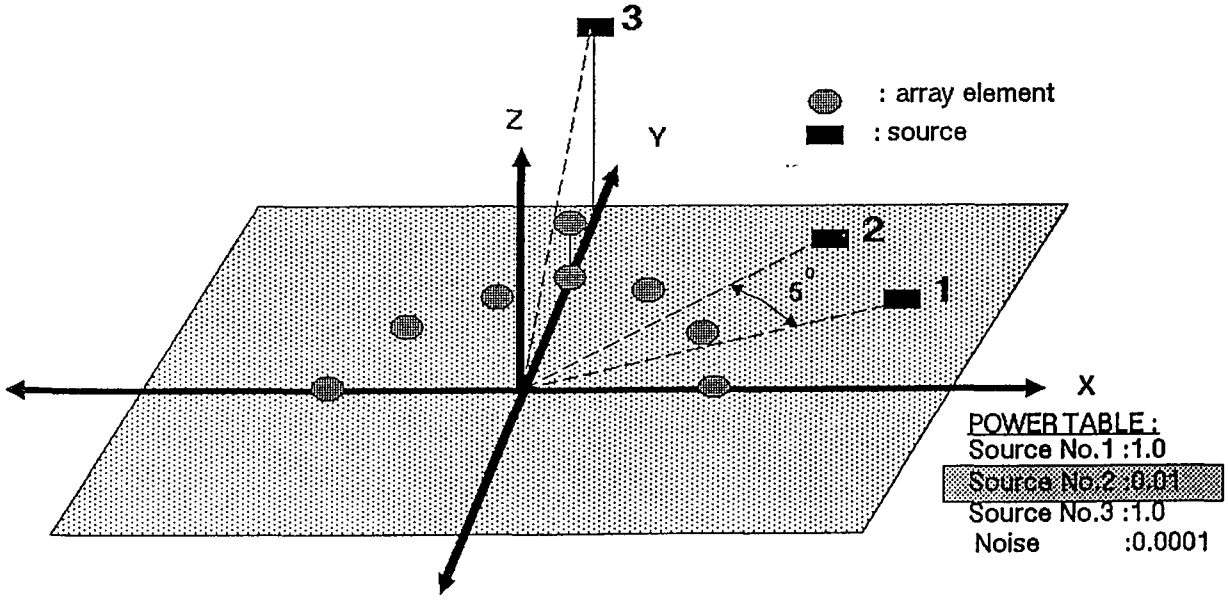

FIGURE – 4.16 (Uncorrelated Sources)

	TRUE directions	INITIAL directions	directions estimated by ASPECT
source No.1	(0.0, 30.0)	(10.0, 20.0)	(0.0000, 30.0000)
source No.2	(0.0, 32.0)	(7.0, 50.0)	(–0.0000, 32.0000)
source No.3	(10.0, 90.0)	(0.0, 95.0)	(10.0000, 90.0000)
source No.4	———	(20.0,165.0)	———

cost:1.000000000000000e+000

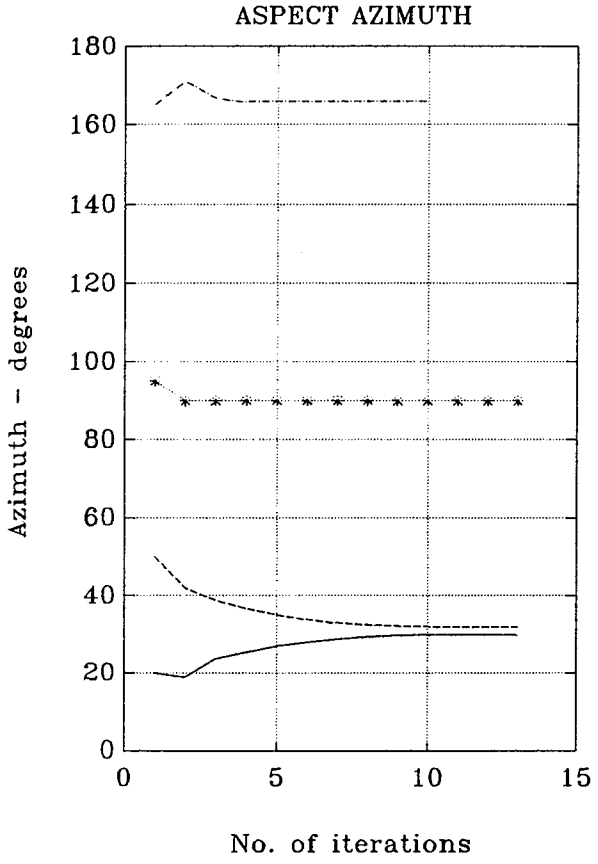

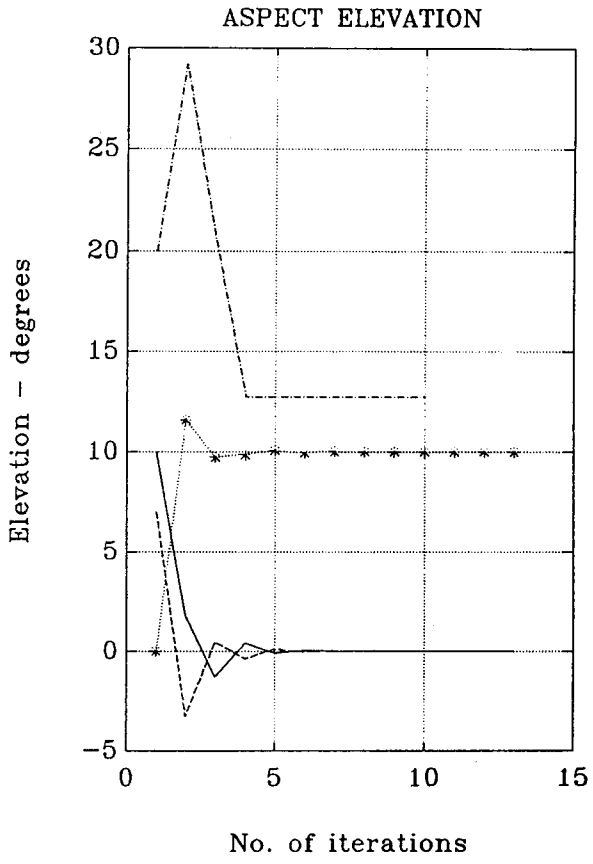

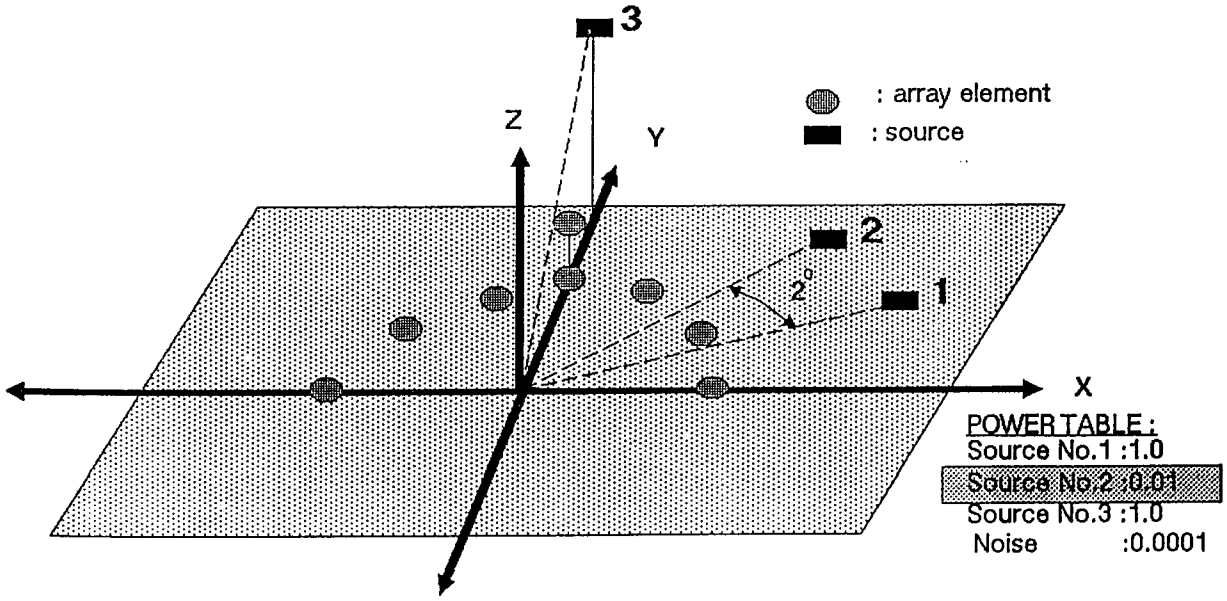

FIGURE – 4.17 (Uncorrelated Sources)

	TRUE directions	INITIAL directions	directions estimated by ASPECT
source No.1	(0.0, 30.0)	(10.0, 20.0)	(–0.0000, 30.0002)
source No.2	(0.0, 31.0)	(7.0, 50.0)	(–0.0000, 30.9998)
source No.3	(10.0, 90.0)	(0.0, 95.0)	(10.0000, 90.0000)
source No.4	———	(20.0,165.0)	———

cost:1.000000000000002e+000

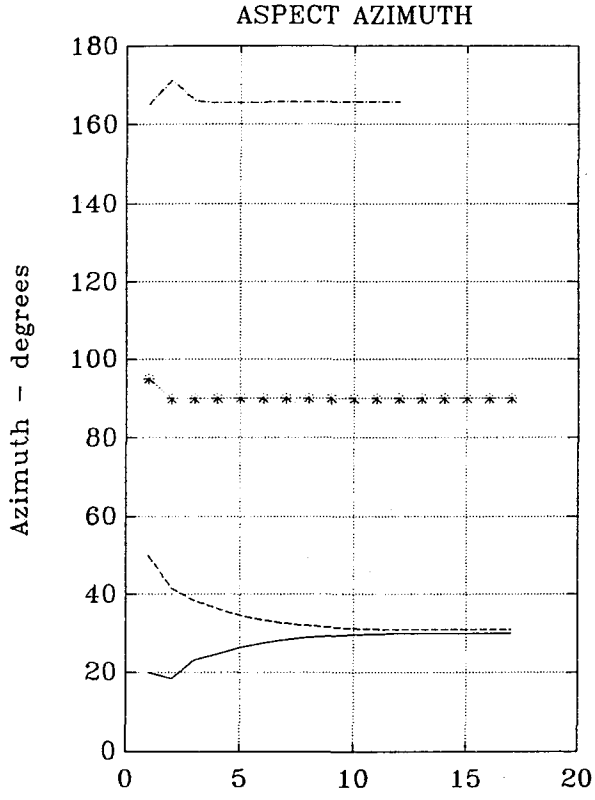

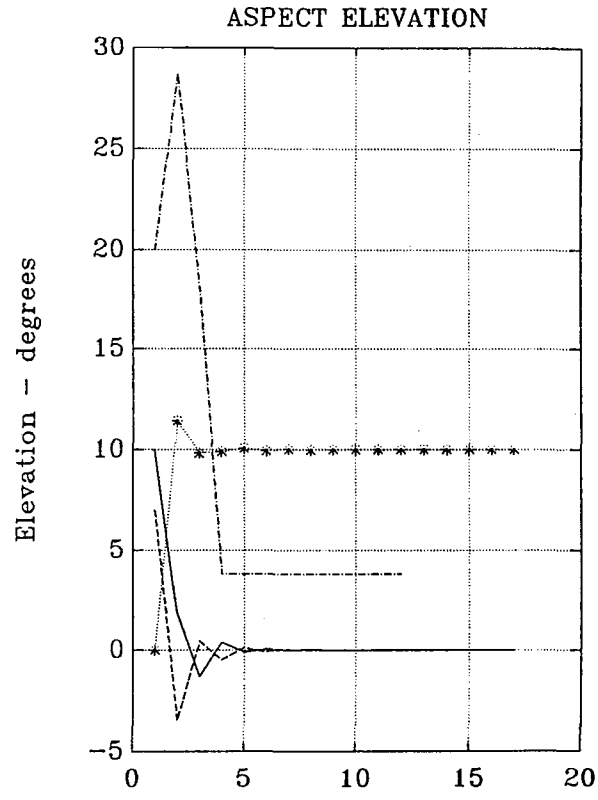

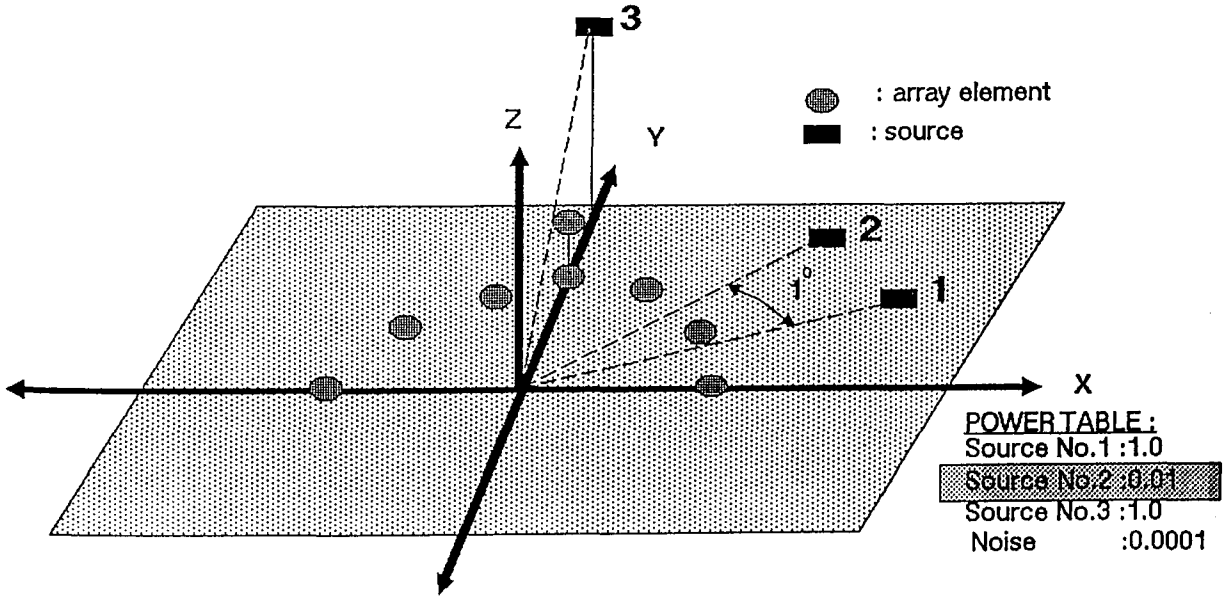

FIGURE – 4.18 (Uncorrelated Sources)

	TRUE directions	INITIAL directions	directions estimated by ASPECT
source No.1	(0.0, 30.0)	(10.0, 20.0)	(0.0000, 30.0000)
source No.2	(0.0, 40.0)	(7.0, 50.0)	(-0.0000, 40.0000)
source No.3	(10.0, 90.0)	(0.0, 95.0)	(10.0000, 90.0000)
source No.4	———	(20.0,165.0)	———

cost:1.000000000000000e+000

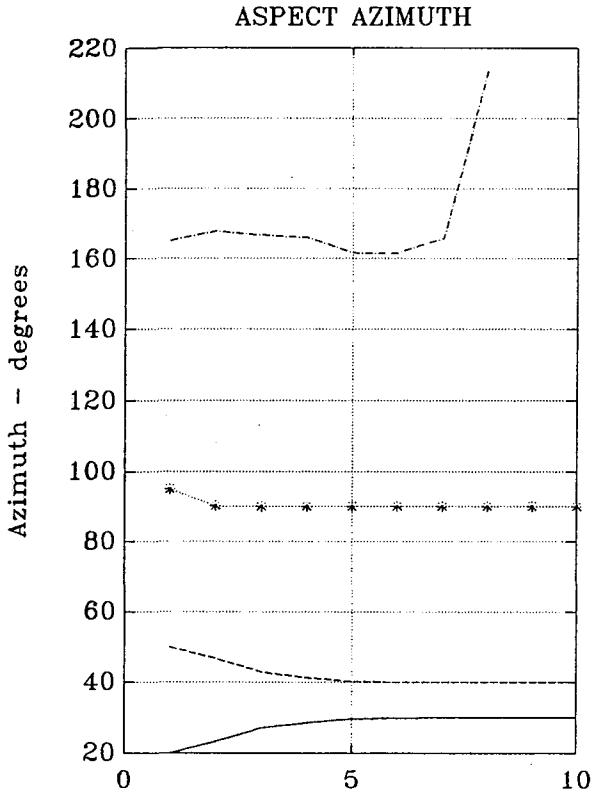

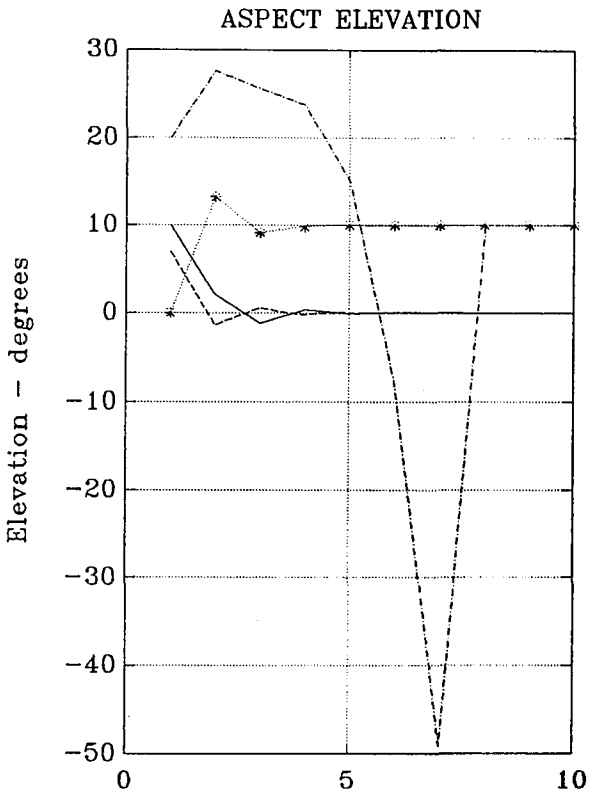

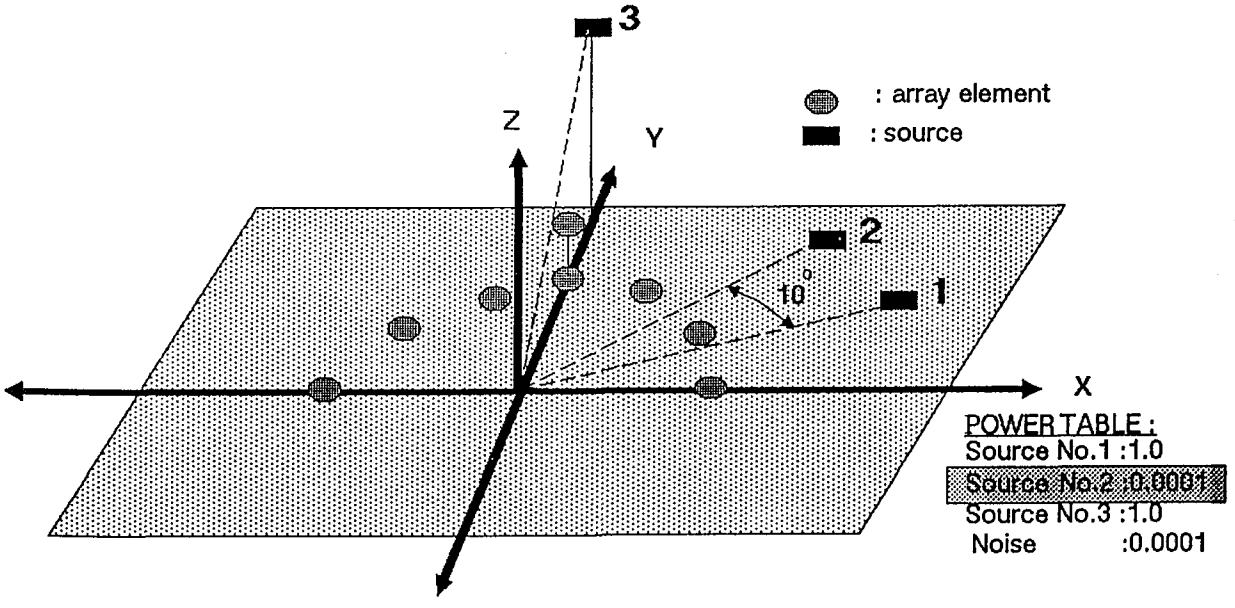

FIGURE – 4.19 (Uncorrelated Sources)

	TRUE directions	INITIAL directions	directions estimated by ASPECT
source No.1	(0.0, 30.0)	(10.0, 20.0)	(–0.0000, 30.0000)
source No.2	(0.0, 35.0)	(7.0, 50.0)	(0.0000, 35.0000)
source No.3	(10.0, 90.0)	(0.0, 95.0)	(10.0000, 90.0000)
source No.4	———	(20.0,165.0)	———

cost:1.000000000000000e+000

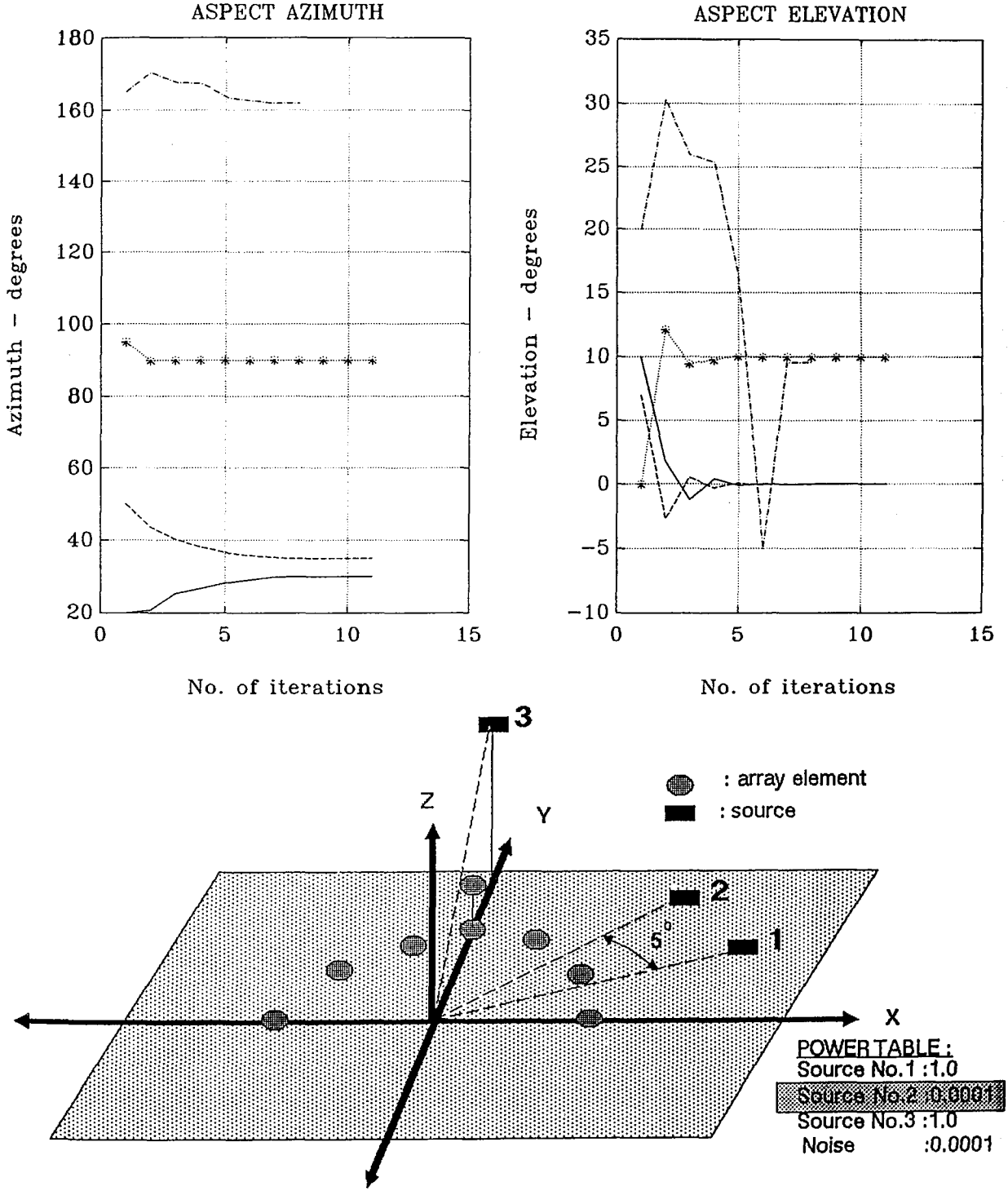

FIGURE – 4.20 (Uncorrelated Sources)

	TRUE directions	INITIAL directions	directions estimated by ASPECT
source No.1	(0.0, 30.0)	(10.0, 20.0)	(0.0000, 30.0000)
source No.2	(0.0, 32.0)	(7.0, 50.0)	(−0.0000, 32.0000)
source No.3	(10.0, 90.0)	(0.0, 95.0)	(10.0000, 90.0000)
source No.4	———	(20.0,165.0)	———

cost:1.000000000000000e+000

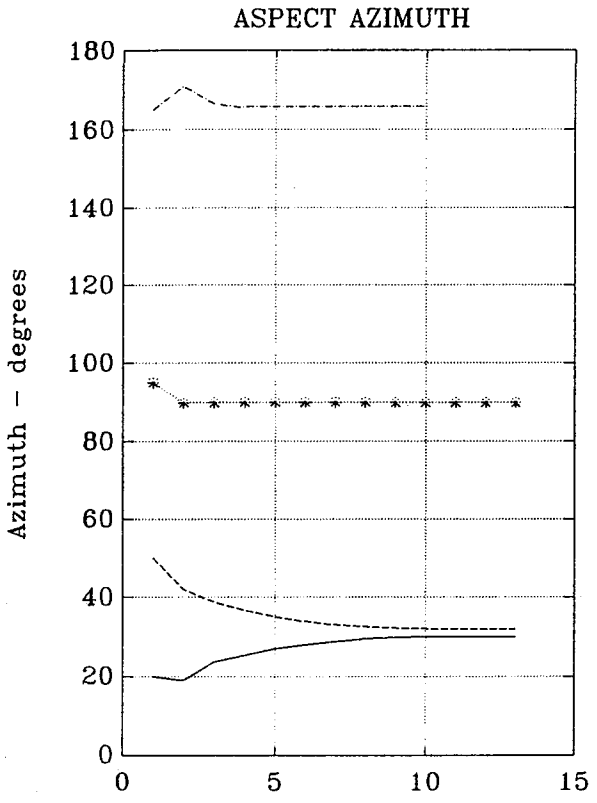

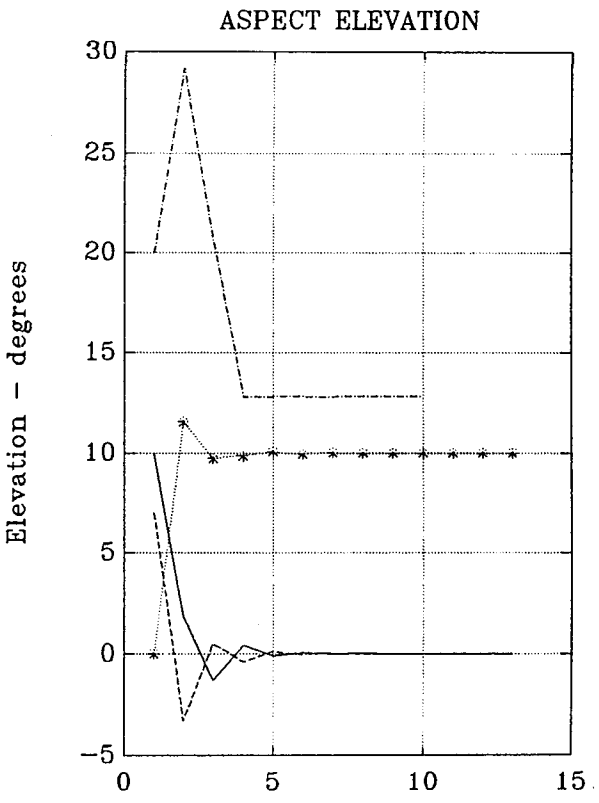

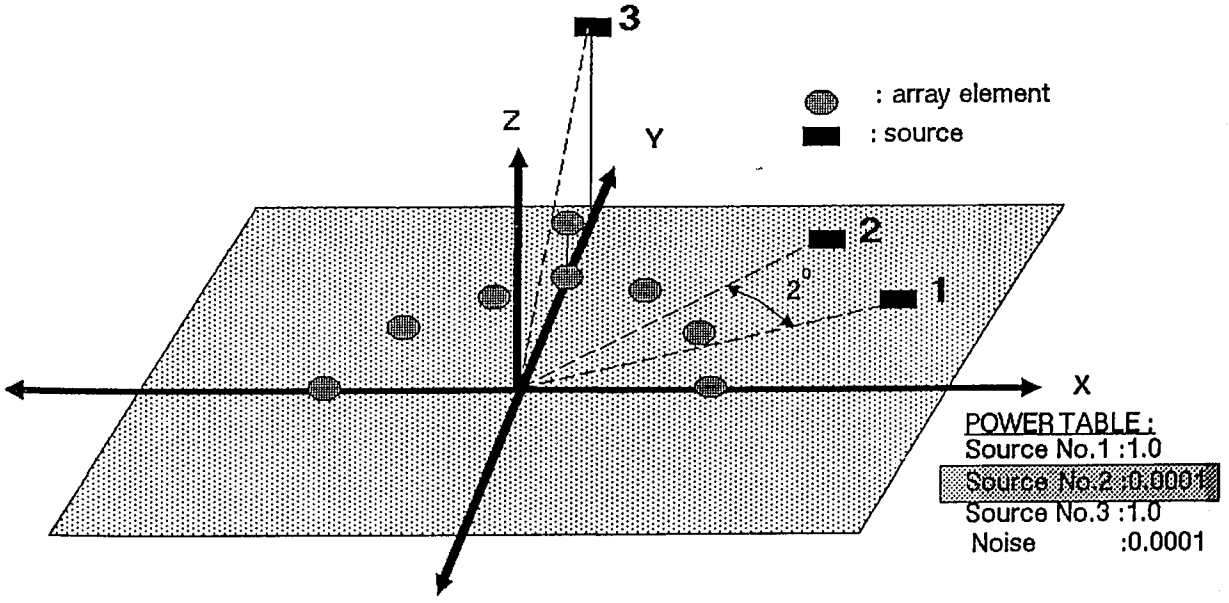

POWER TABLE :
Source No.1 :1.0
Source No.2 :0.0001
Source No.3 :1.0
Noise :0.0001

FIGURE – 4.21 (Uncorrelated Sources)

	TRUE directions	INITIAL directions	directions estimated by ASPECT
source No.1	(0.0, 30.0)	(10.0, 20.0)	(– 0.0000, 30.0000)
source No.2	(0.0, 31.0)	(7.0, 50.0)	(0.0000, 31.0000)
source No.3	(10.0, 90.0)	(0.0, 95.0)	(10.0000, 90.0000)
source No.4	———	(20.0,165.0)	———

cost:1.000000000000000e + 000

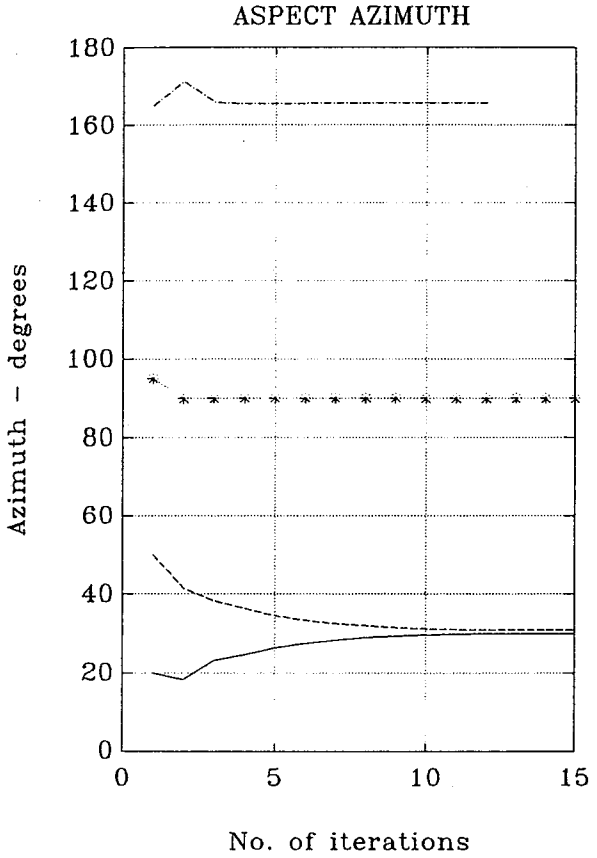

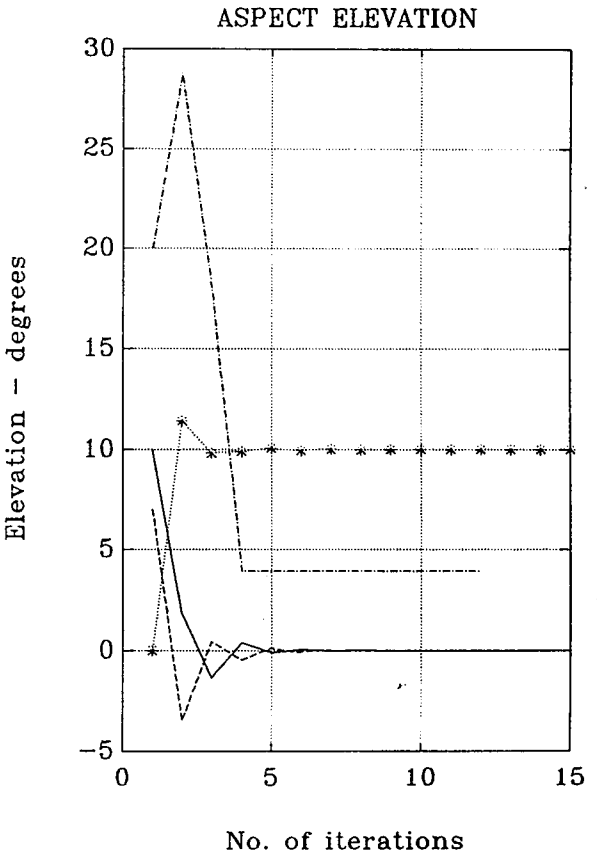

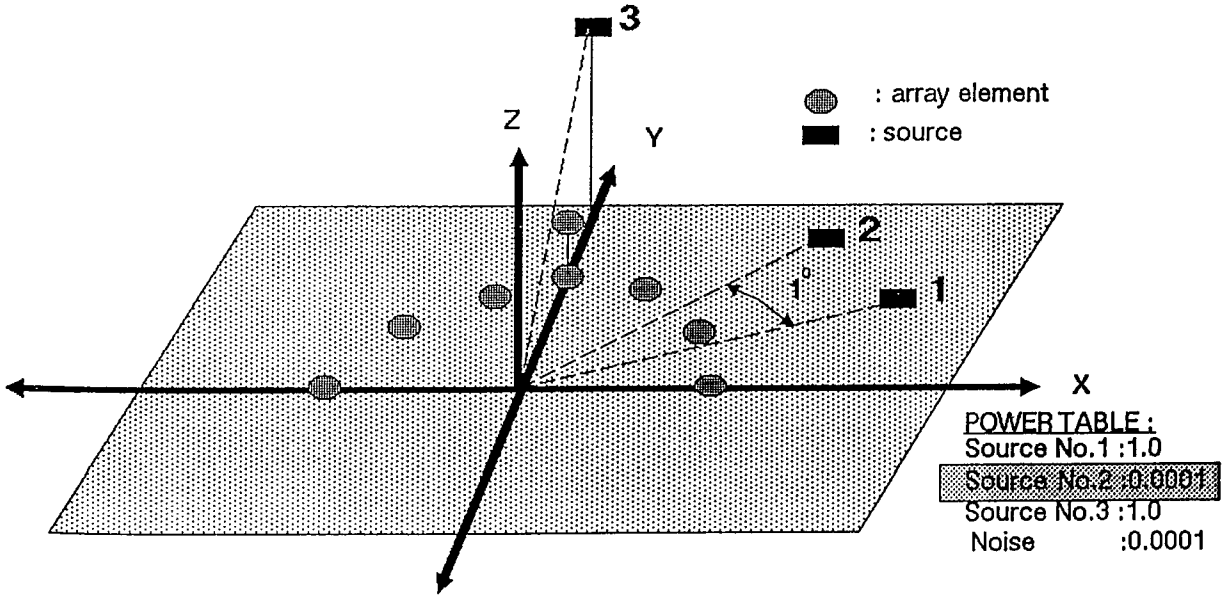

4.3.4 Signal Correlation

So far simulations results heve been presented dealing with uncorrelated signal situations. These results show that ASPECT can adequately handle these signal environments which can be also handled by the existing Signal Subspace Techniques (e.g. MUSIC). However, this section is concerned with signal environments which involve correlated (coherent) sources and it is well known that these environments cannot be treated by the existing signal subspace techniques (see *Figure* 3.2 for illustration of the failure of the MUSIC algorithm).

The results of the previous sections indicate the robustness of ASPECT with respect to noise power level. One of the questions which this section is concerned with is to examine if that robustness to noise power is maintained in correlated or coherent signal environments. Thus, the simulations carried out in *Sections* 4.3.1 and 4.3.2 will be reconsidered here, but this time with the trial pair to be fully correlated. Firstly, the effects of angular resolution with noise levels from -40dB up to -20dB and -10dB is considered for 10°, 5°, 2° and 1° angle separation in the trial pair. The effects of correlation on the performance of ASPECT, for every signal environment referred to above, are shown:

- in *Figures* 4.22-4.25 (for -40dB)
- in *Figures* 4.26-4.29 (for -20dB)
- in *Figures* 4.30-4.33 (for -10dB).

Figures 4.22 to 4.33 shows that ASPECT keeps its robustness properties

with respect to noise level in fully correlated situations. However, although it performs satisfactorily in almost every case, it loses accuracy when two correlated sources are close together (see for example *Figures* 4.25, 4.29 and 4.33).

Next, the effects of sources with widely differing power levels is considered for 10°, 5°, 2° and 1° angle separation in the trial pair. The performance of ASPECT when one of the trial pair is taken down from 0dB to −20dB, −40dB, with −40dB noise power, is illustated in

- *Figures* 4.34-4.37 (for −20dB) and
- *Figures* 4.38-4.41 (for −40dB, that is, equal to the noise level)

The results are satisfactory with the exception of the reduction of the bearing accuracy when the array environment involves some signals which are close together and, at the same time with widely differing power levels. This reduction of accuracy is slightly more significant than it is in the uncorrelated situation. *Figure* 4.41 presents the worst case where for signals directions (0°,30°) and (0°,31°) ASPECT provides the directions (0.0000°,30.0042°) and (0.0076°,31.7027°). However, in all the cases the third independent source is estimated with accuracy.

Finally, it is important to point out that by comparing *Figures* 4.2-4.21 (uncorrelated situations) with *Figures* 4.22-4.41 (correlated situations) it can be seen that the number of iterations increases when signal correlation is involved.

FIGURE – 4.22 (Sources No.1 and No.2 are correlated)

	TRUE directions	INITIAL directions	directions estimated by ASPECT
source No.1	(0.0, 30.0)	(10.0, 20.0)	(0.0000, 30.0000)
source No.2	(0.0, 40.0)	(7.0, 50.0)	(–0.0000, 40.0000)
source No.3	(10.0, 90.0)	(0.0, 95.0)	(10.0000, 90.0000)
source No.4	———	(20.0,165.0)	———

cost: 1.000000000000000e+000

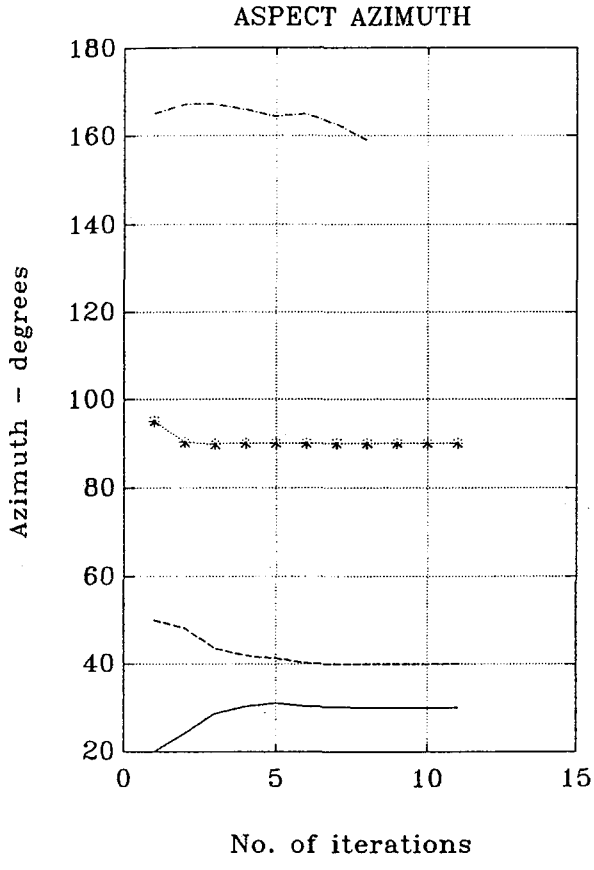

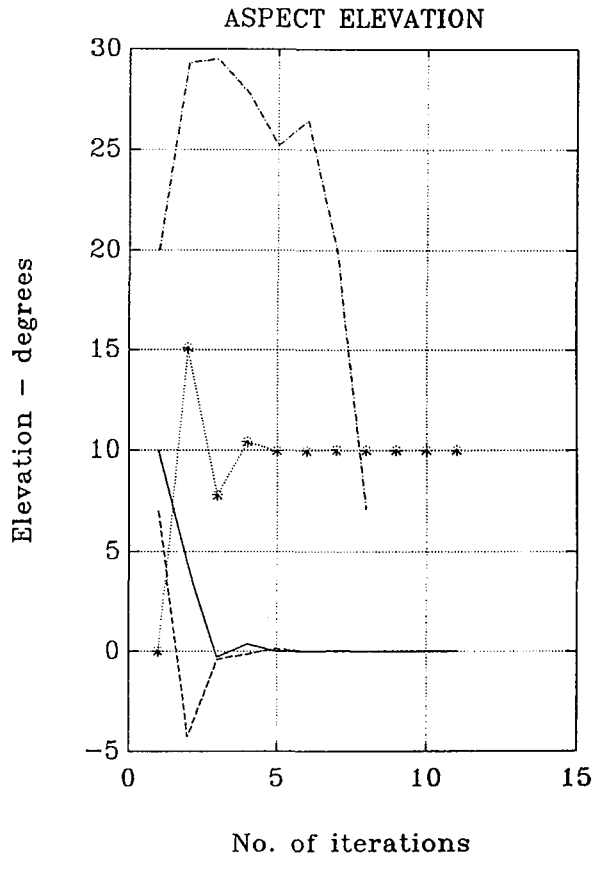

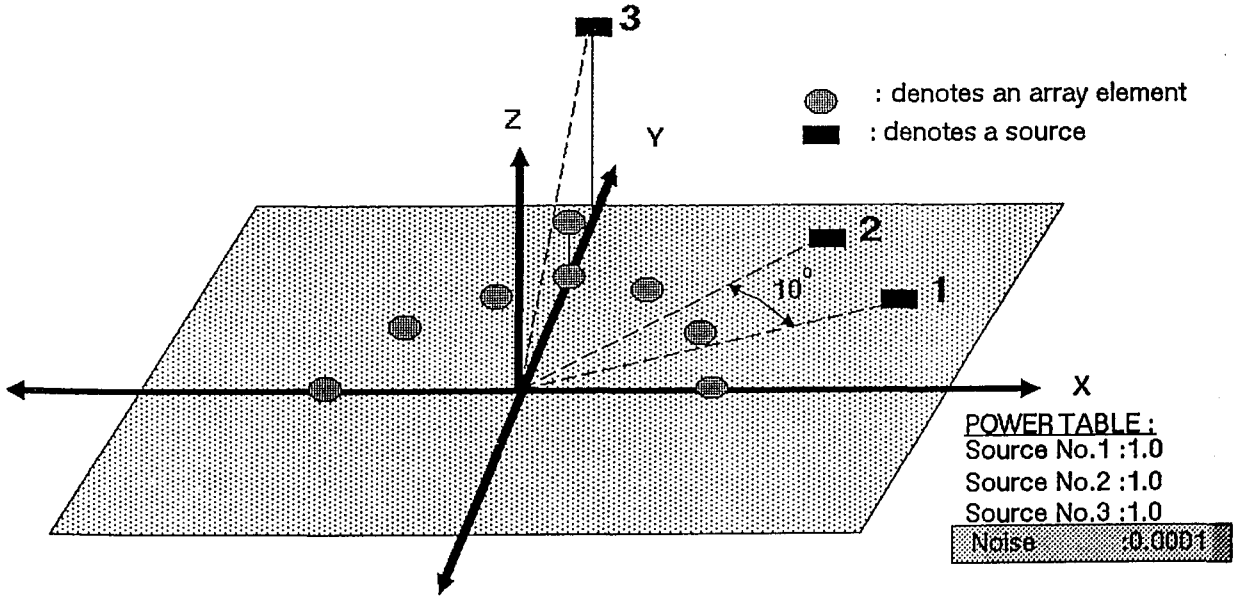

FIGURE – 4.23 (Sources No.1 and No.2 are correlated)

	TRUE directions	INITIAL directions	directions estimated by ASPECT
source No.1	(0.0, 30.0)	(10.0, 20.0)	(–0.0000, 30.0000)
source No.2	(0.0, 35.0)	(7.0, 50.0)	(0.0000, 35.0000)
source No.3	(10.0, 90.0)	(0.0, 95.0)	(10.0000, 90.0000)
source No.4	———	(20.0,165.0)	———

cost: 1.000000000000000e + 000

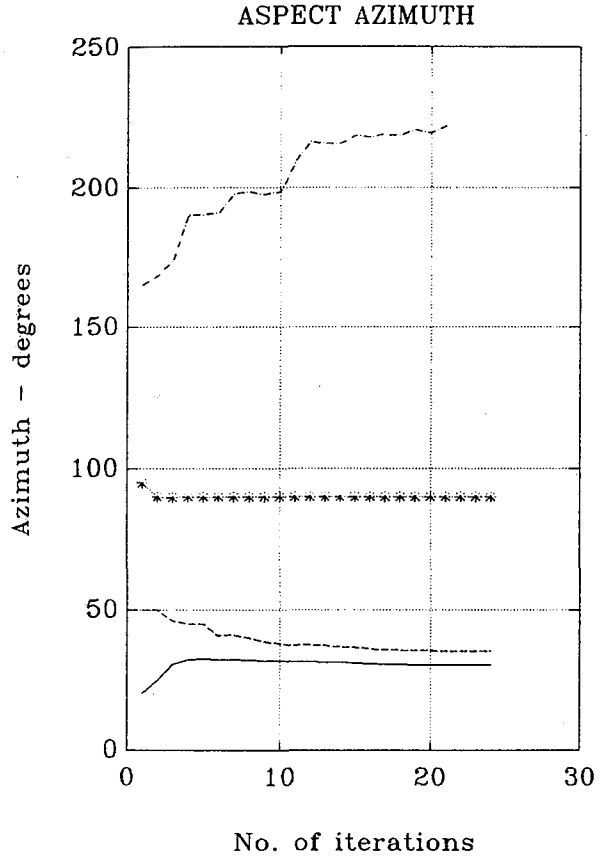

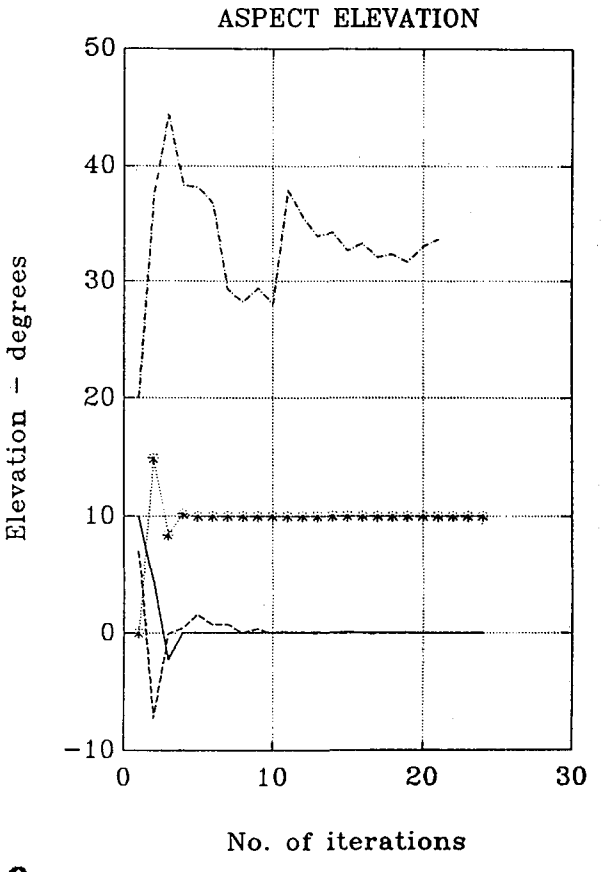

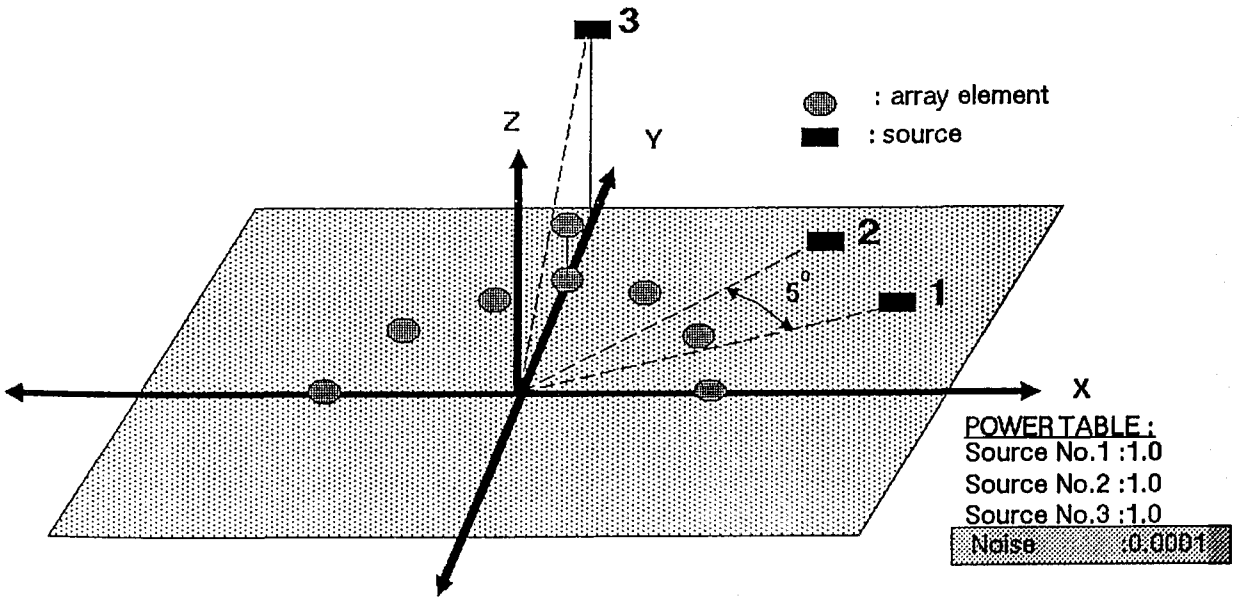

FIGURE – 4.24 (Sources No.1 and No.2 are correlated)

	TRUE directions	INITIAL directions	directions estimated by ASPECT
source No.1	(0.0, 30.0)	(10.0, 20.0)	(0.0000, 30.0000)
source No.2	(0.0, 32.0)	(7.0, 50.0)	(–0.0000, 32.0000)
source No.3	(10.0, 90.0)	(0.0, 95.0)	(10.0000, 90.0000)
source No.4	———	(20.0,165.0)	———

cost: 1.00000000000000e+000

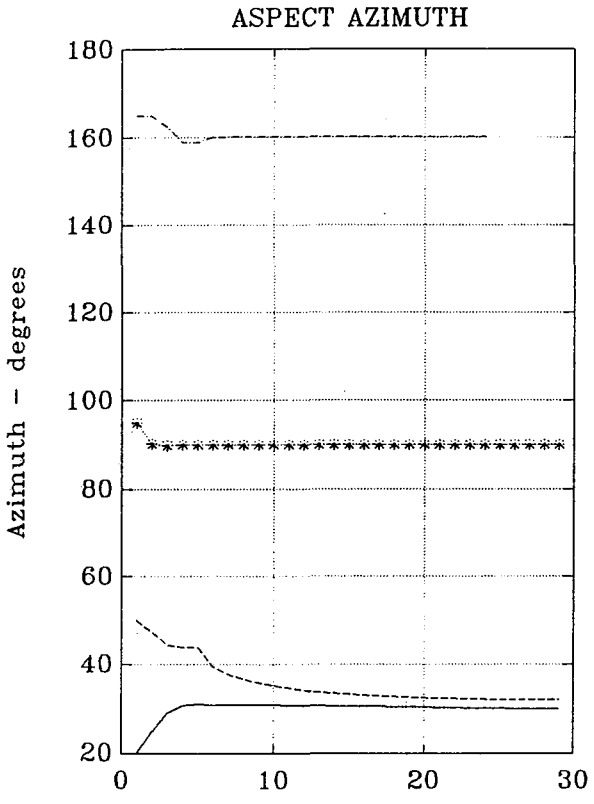

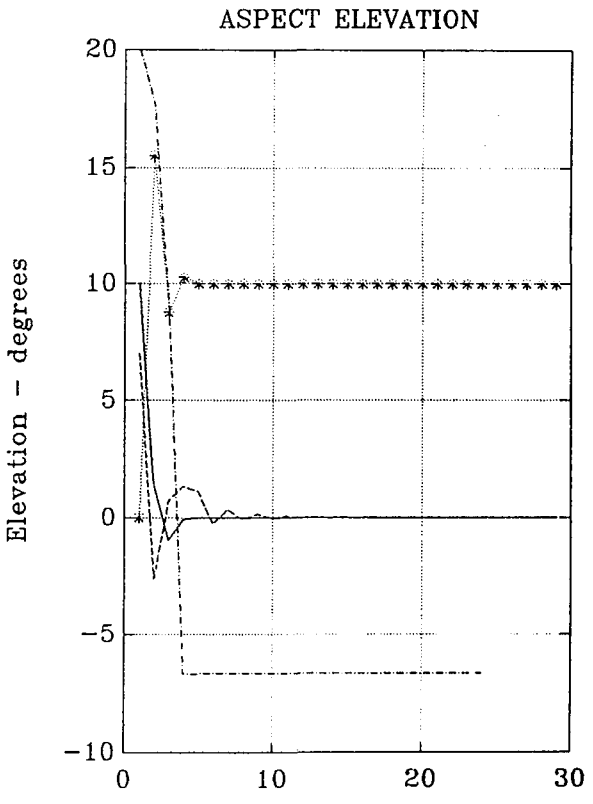

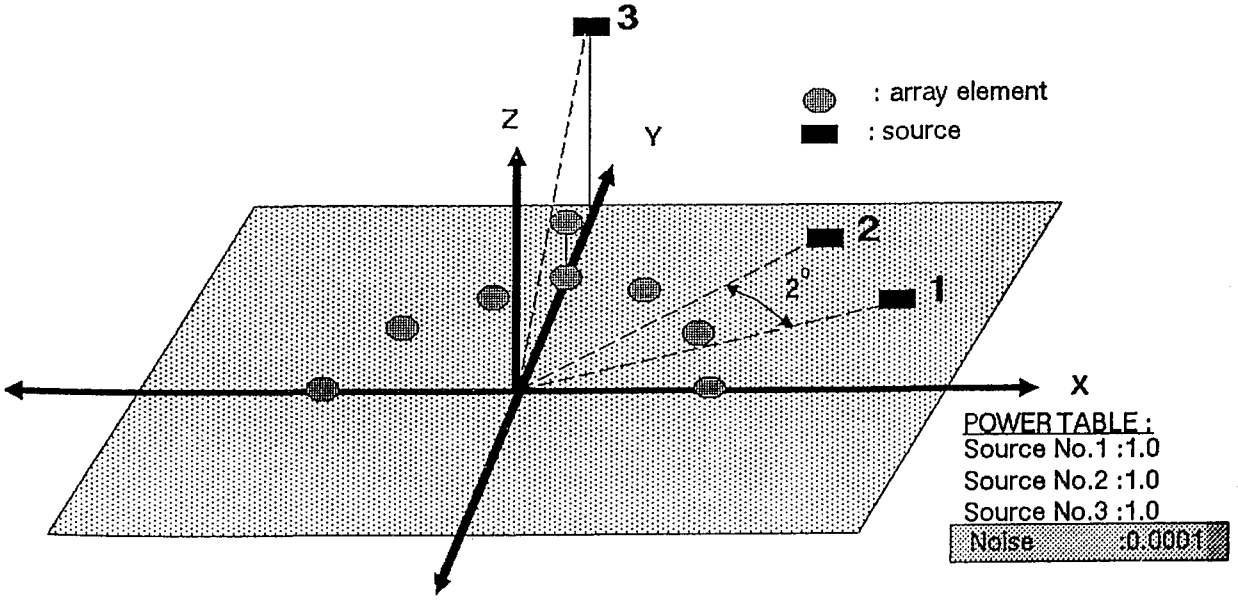

FIGURE – 4.25 (Sources No.1 and No.2 are correlated)

	TRUE directions	INITIAL directions	directions estimated by ASPECT
source No.1	(0.0, 30.0)	(10.0, 20.0)	(0.0001, 30.0031)
source No.2	(0.0, 31.0)	(7.0, 50.0)	(–0.0001, 31.0031)
source No.3	(10.0, 90.0)	(0.0, 95.0)	(10.0000, 90.0000)
source No.4	———	(20.0,165.0)	———

cost:1.000000000000000e+000

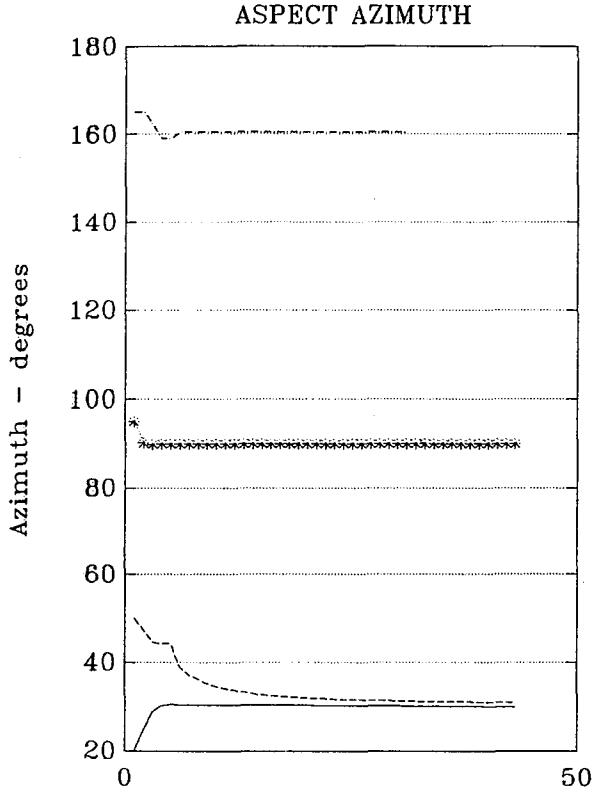

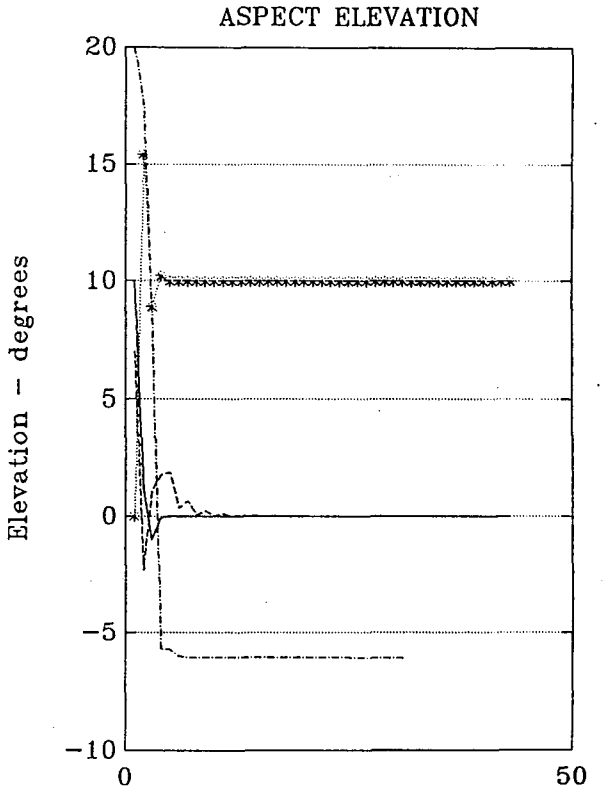

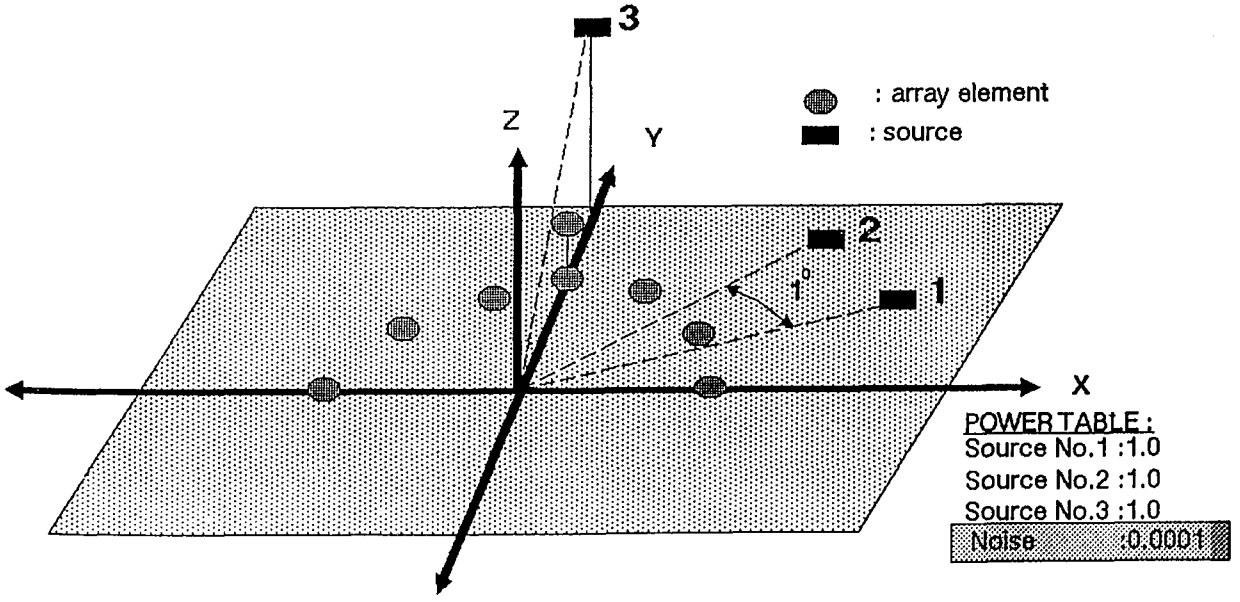

FIGURE – 4.26 (Sources No.1 and No.2 are correlated)

	TRUE directions	INITIAL directions	directions estimated by ASPECT
source No.1	(0.0, 30.0)	(10.0, 20.0)	(0.0000, 30.0000)
source No.2	(0.0, 40.0)	(7.0, 50.0)	(–0.0000, 40.0000)
source No.3	(10.0, 90.0)	(0.0, 95.0)	(10.0000, 90.0000)
source No.4	———	(20.0,165.0)	———

cost:1.000000000000000e+000

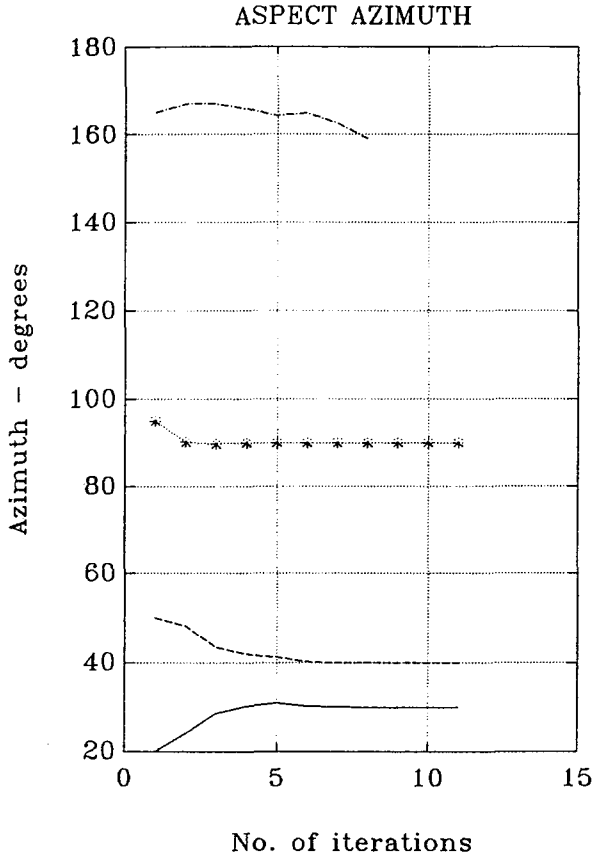

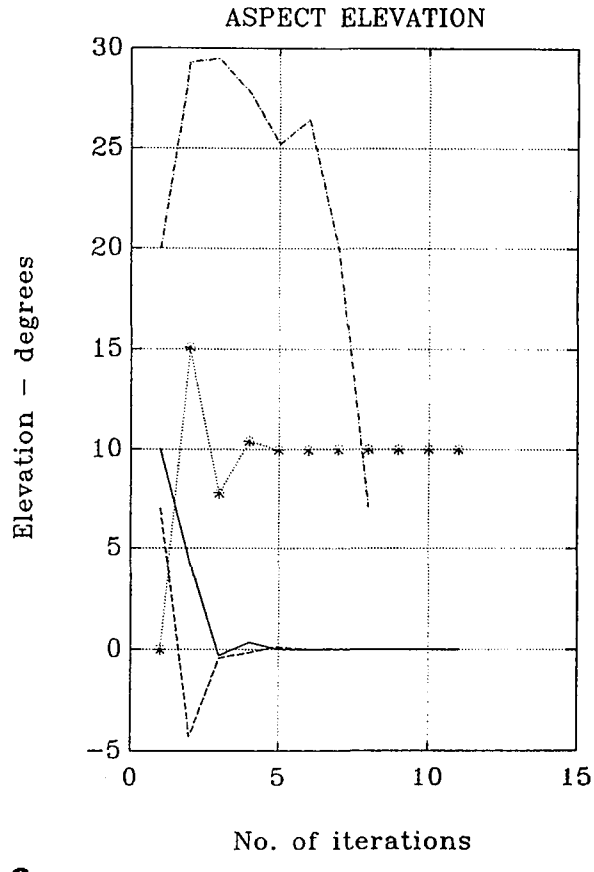

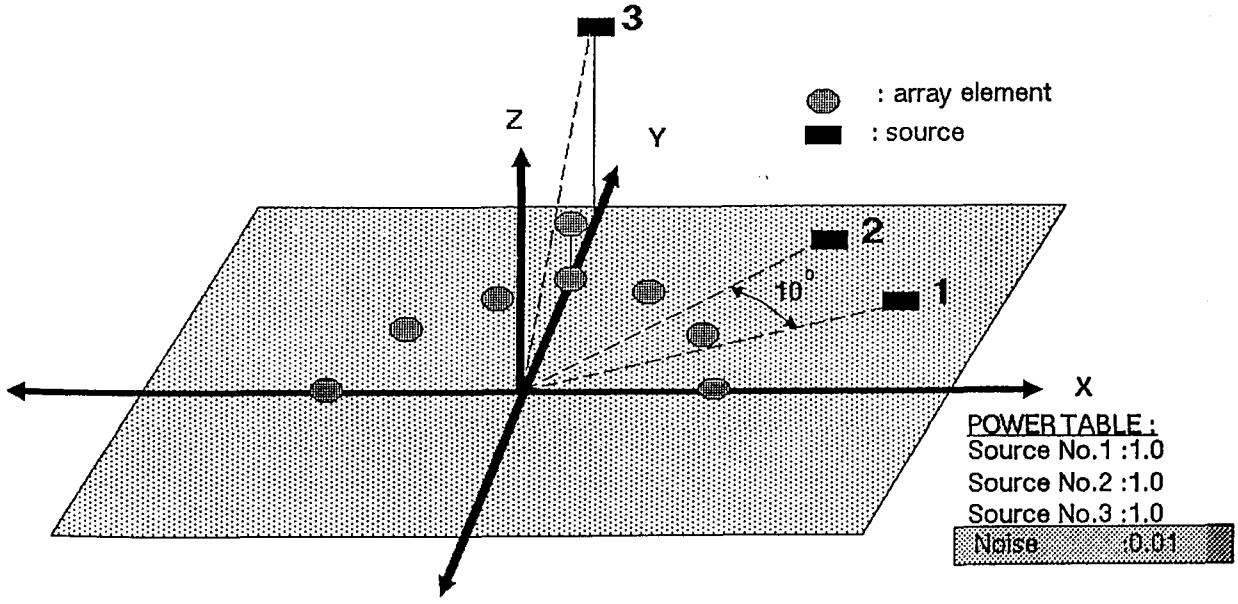

POWER TABLE :
Source No.1 :1.0
Source No.2 :1.0
Source No.3 :1.0
Noise :0.01

FIGURE – 4.27 (Sources No.1 and No.2 are correlated)

	TRUE directions	INITIAL directions	directions estimated by ASPECT
source No.1	(0.0, 30.0)	(10.0, 20.0)	(–0.0000, 30.0000)
source No.2	(0.0, 35.0)	(7.0, 50.0)	(0.0000, 35.0000)
source No.3	(10.0, 90.0)	(0.0, 95.0)	(10.0000, 90.0000)
source No.4	———	(20.0,165.0)	———

cost:1.000000000000000e+000

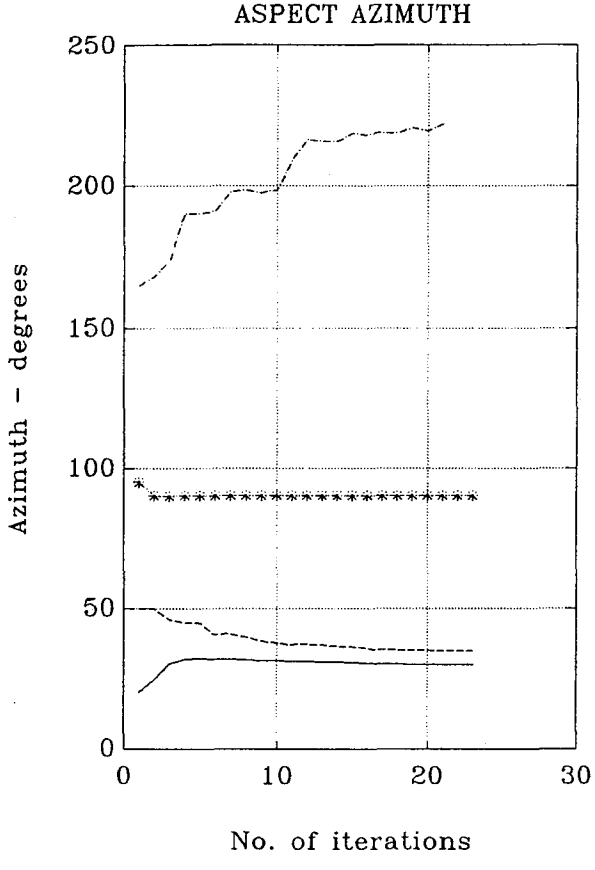

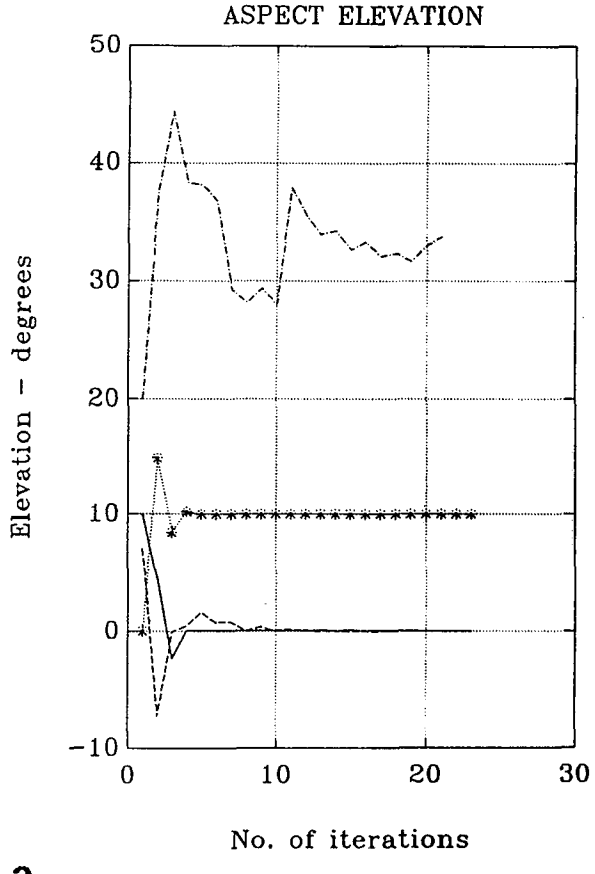

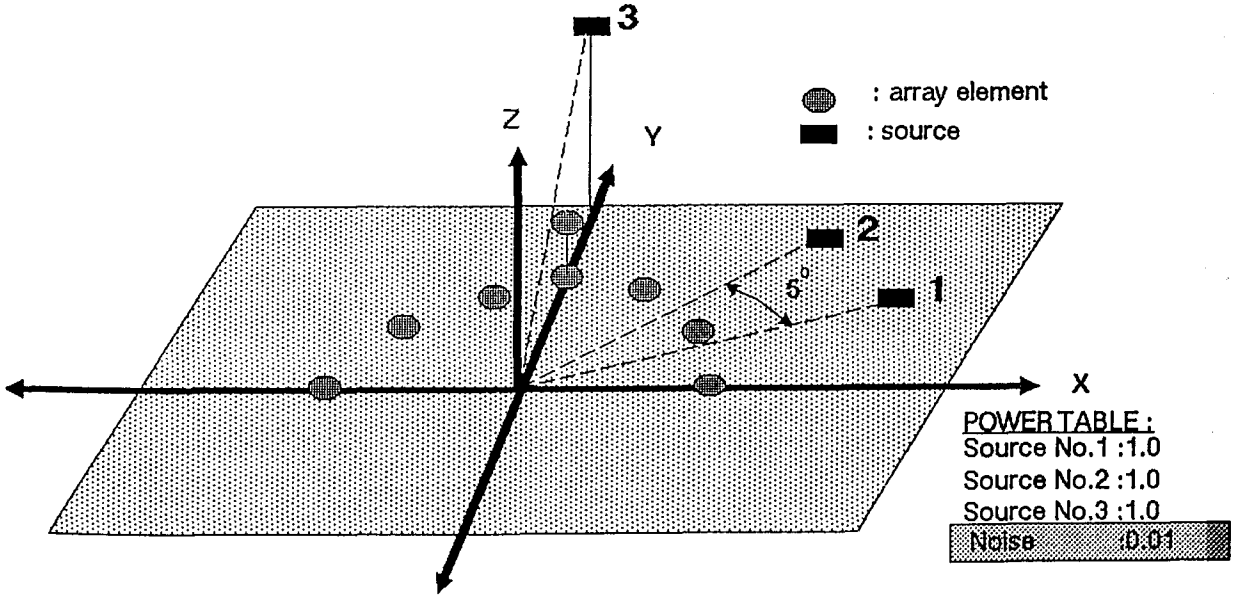

FIGURE – 4.28 (Sources No.1 and No.2 are correlated)

	TRUE directions	INITIAL directions	directions estimated by ASPECT
source No.1	(0.0, 30.0)	(10.0, 20.0)	(– 0.0000, 30.0000)
source No.2	(0.0, 32.0)	(7.0, 50.0)	(0.0000, 32.0000)
source No.3	(10.0, 90.0)	(0.0, 95.0)	(10.0000, 90.0000)
source No.4	———	(20.0,165.0)	———

cost:1.000000000000000e + 000

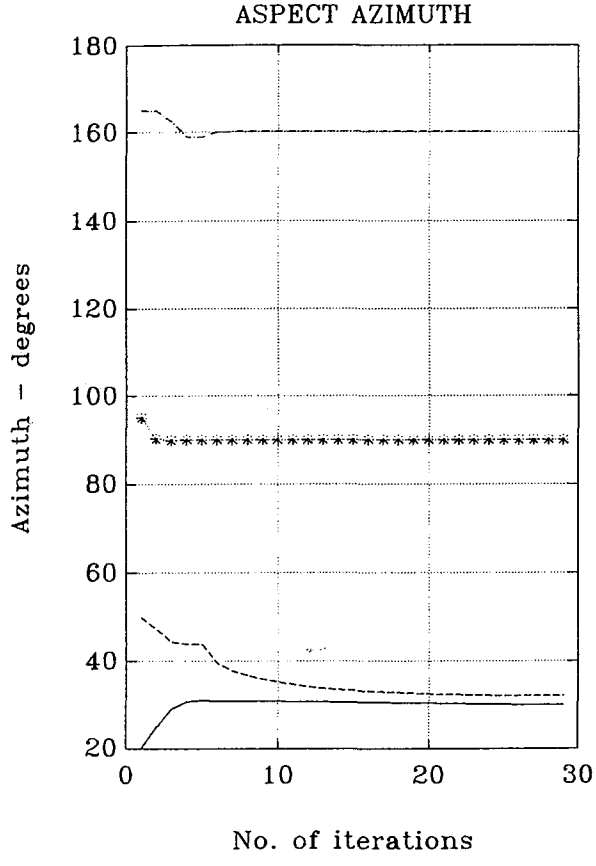

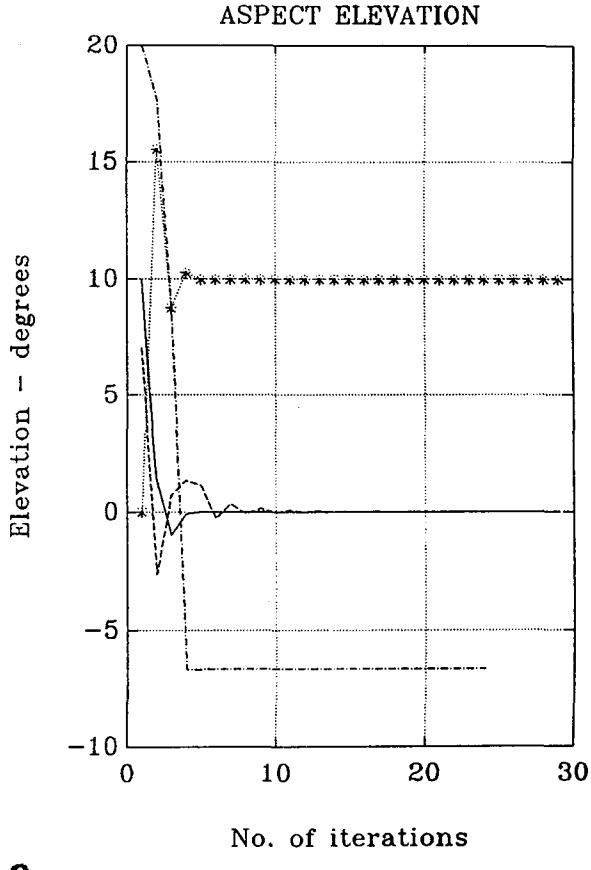

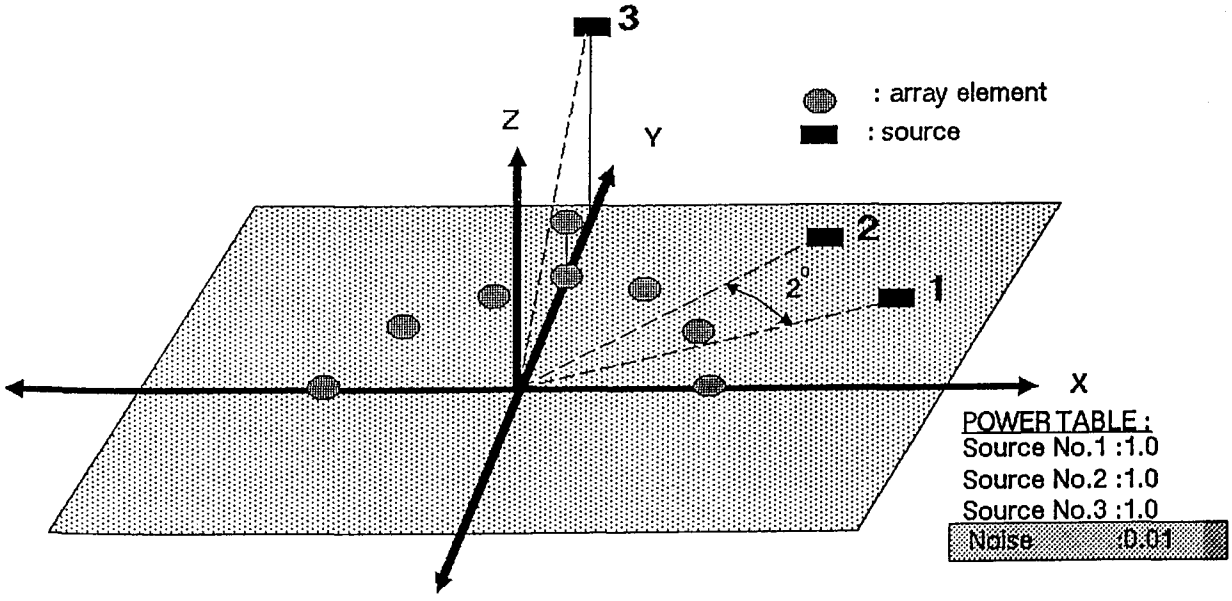

FIGURE — 4.29 (Sources No.1 and No.2 are correlated)

	TRUE directions	INITIAL directions	directions estimated by ASPECT
source No.1	(0.0, 30.0)	(10.0, 20.0)	(0.0000, 30.0069)
source No.2	(0.0, 31.0)	(7.0, 50.0)	(−0.0001, 31.0069)
source No.3	(10.0, 90.0)	(0.0, 95.0)	(10.0000, 90.0000)
source No.4	———	(20.0,165.0)	———

cost:1.00000000000001e+000

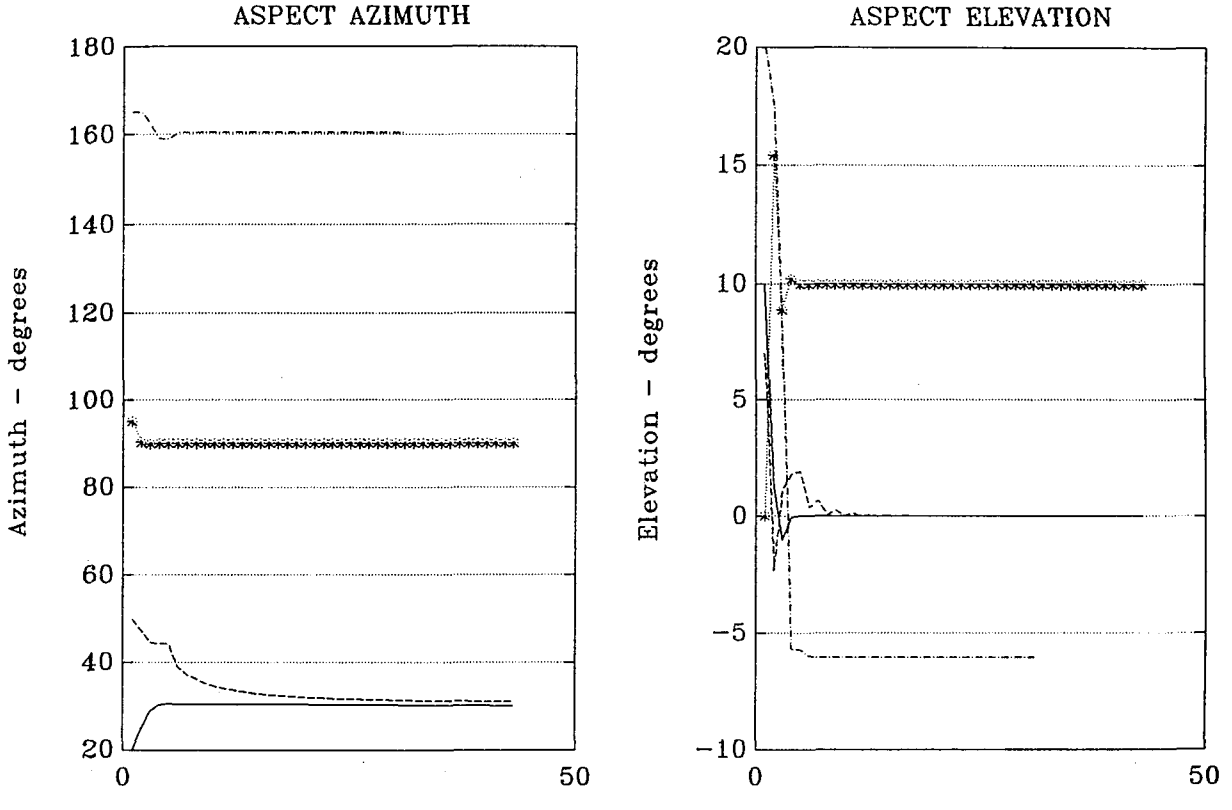

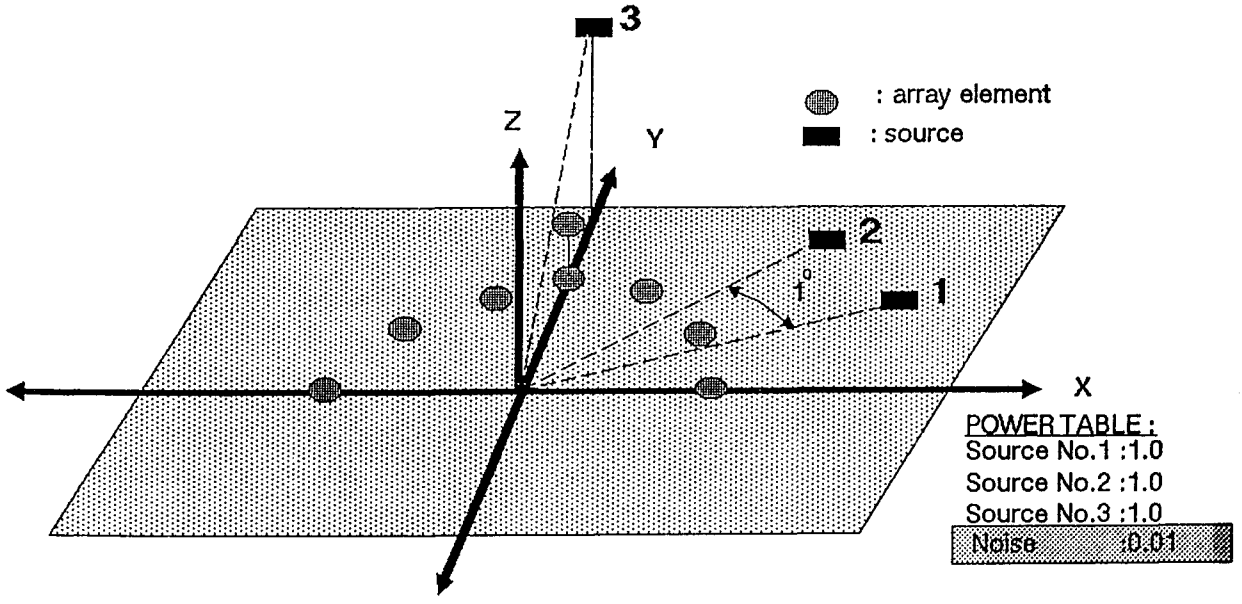

FIGURE – 4.30 (Sources No.1 and No.2 are correlated)

	TRUE directions	INITIAL directions	directions estimated by ASPECT
source No.1	(0.0, 30.0)	(10.0, 20.0)	(0.0000, 30.0000)
source No.2	(0.0, 40.0)	(7.0, 50.0)	(–0.0000, 40.0000)
source No.3	(10.0, 90.0)	(0.0, 95.0)	(10.0000, 90.0000)
source No.4	———	(20.0,165.0)	———

cost:1.00000000000001e+000

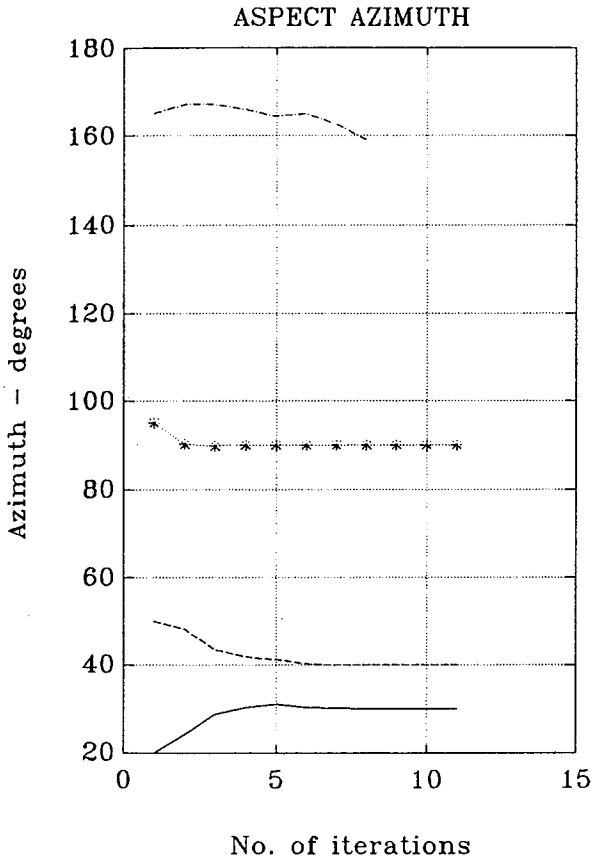

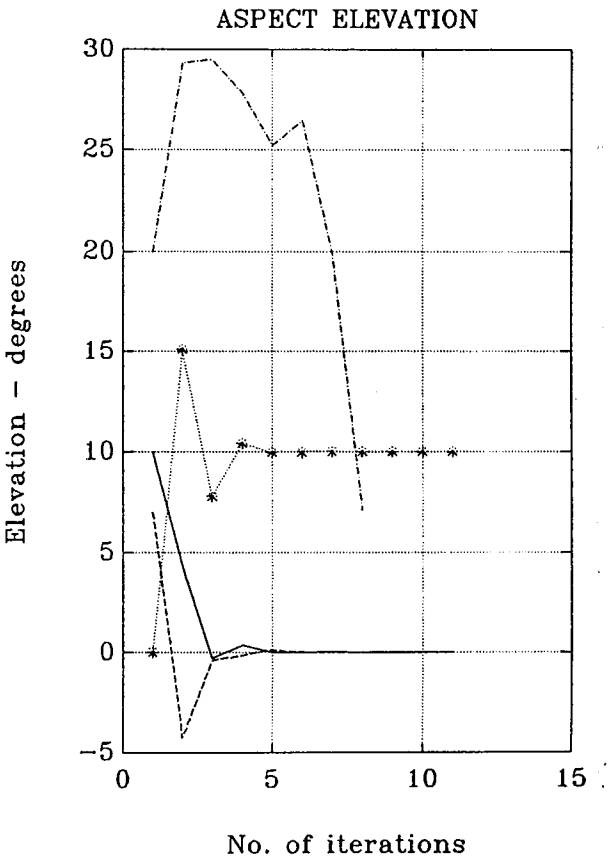

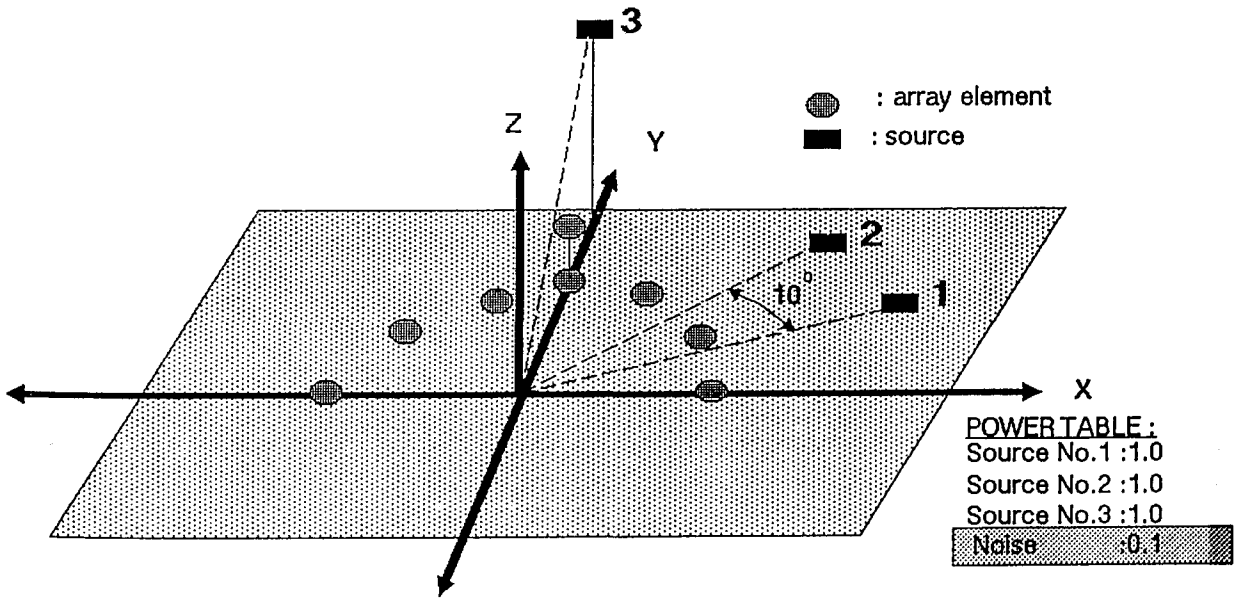

POWER TABLE :
Source No.1 :1.0
Source No.2 :1.0
Source No.3 :1.0
Noise :0.1

FIGURE – 4.31 (Sources No.1 and No.2 are correlated)

	TRUE directions	INITIAL directions	directions estimated by ASPECT
source No.1	(0.0, 30.0)	(10.0, 20.0)	(−0.0000, 30.0000)
source No.2	(0.0, 35.0)	(7.0, 50.0)	(0.0000, 35.0000)
source No.3	(10.0, 90.0)	(0.0, 95.0)	(10.0000, 90.0000)
source No.4	———	(20.0,165.0)	———

cost:1.000000000000000e+000

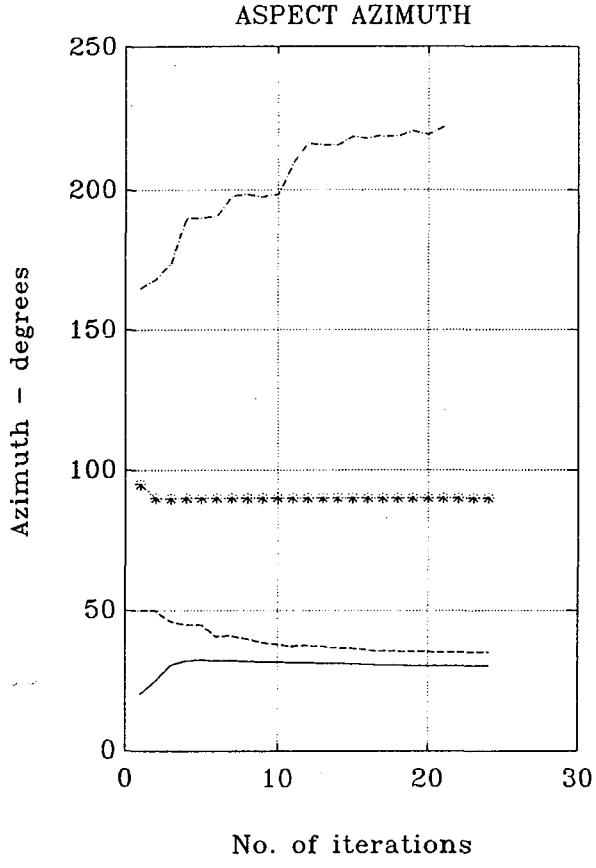

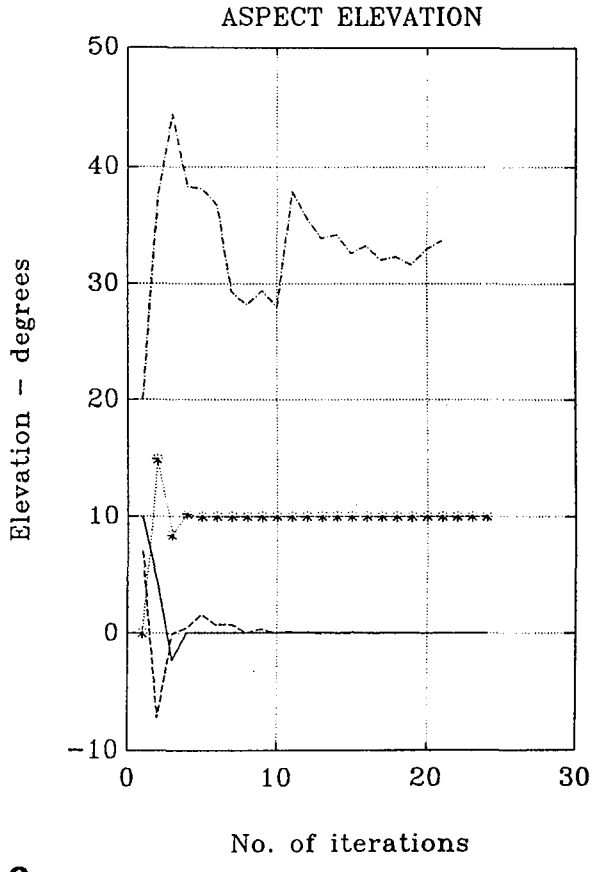

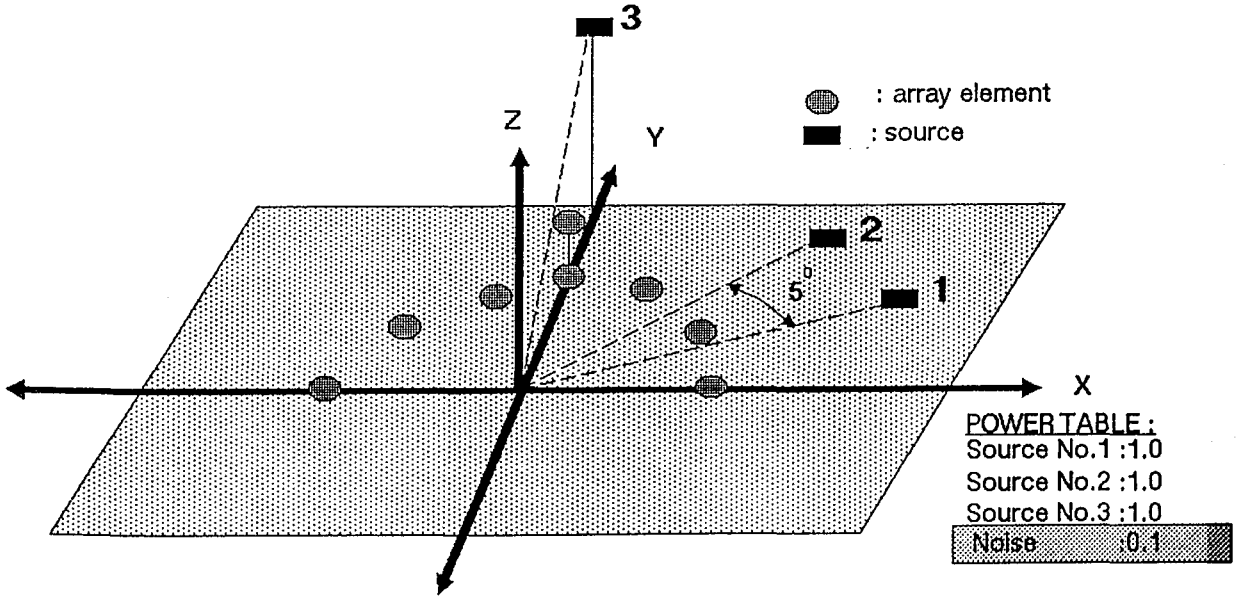

FIGURE — 4.32 (Sources No.1 and No.2 are correlated)

	TRUE directions	INITIAL directions	directions estimated by ASPECT
source No.1	(0.0, 30.0)	(10.0, 20.0)	(0.0000, 29.9999)
source No.2	(0.0, 32.0)	(7.0, 50.0)	(−0.0000, 31.9999)
source No.3	(10.0, 90.0)	(0.0, 95.0)	(10.0000, 90.0000)
source No.4	———	(20.0,165.0)	———

cost:1.000000000000000e+000

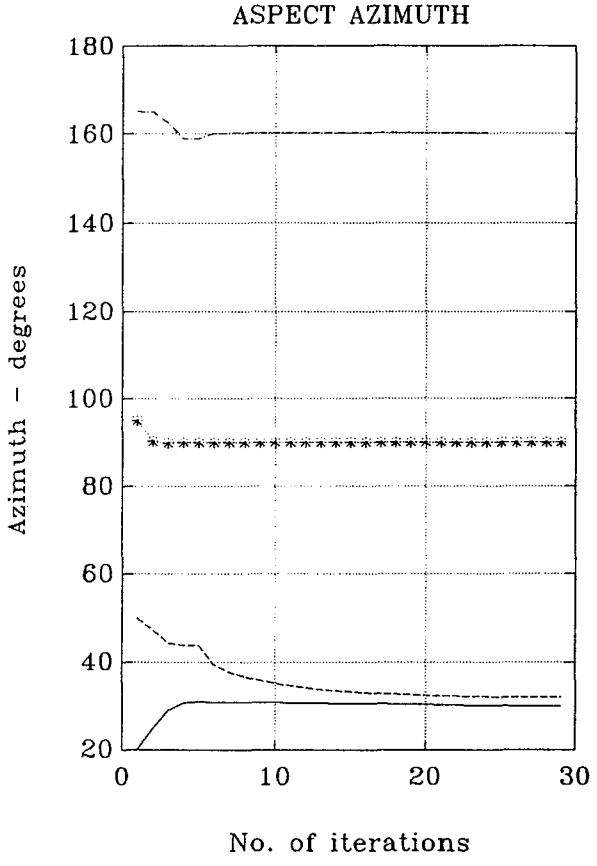

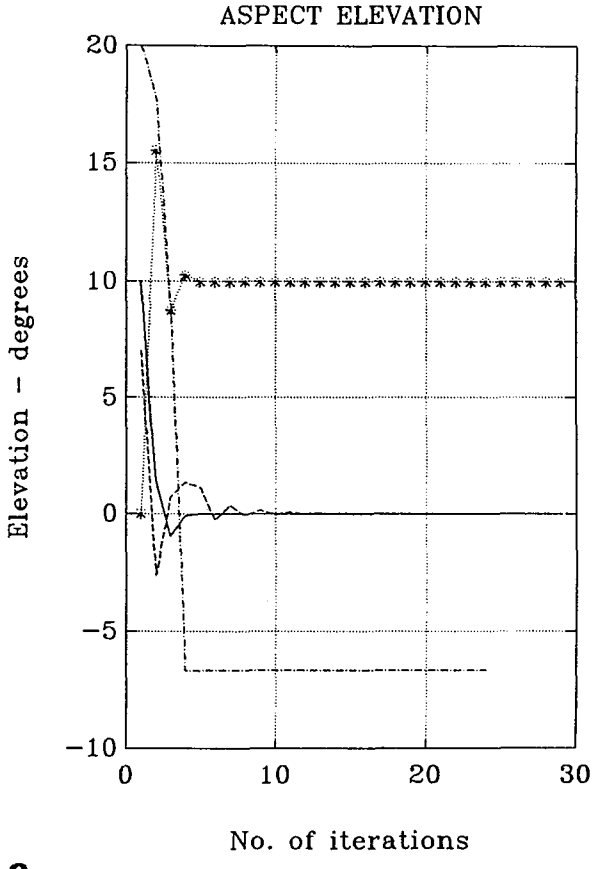

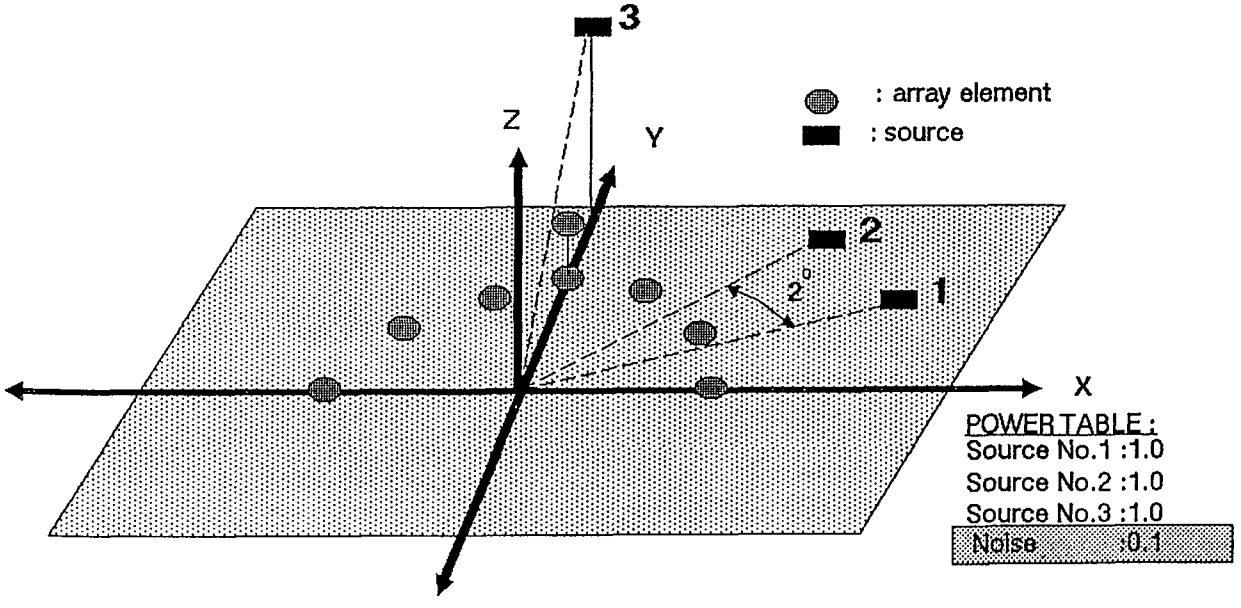

FIGURE – 4.33 (Sources No.1 and No.2 are correlated)

	TRUE directions	INITIAL directions	directions estimated by ASPECT
source No.1	(0.0, 30.0)	(10.0, 20.0)	(0.0000, 30.0071)
source No.2	(0.0, 31.0)	(7.0, 50.0)	(–0.0000, 31.0070)
source No.3	(10.0, 90.0)	(0.0, 95.0)	(10.0000, 90.0000)
source No.4	———	(20.0,165.0)	———

cost:1.000000000000001e+000

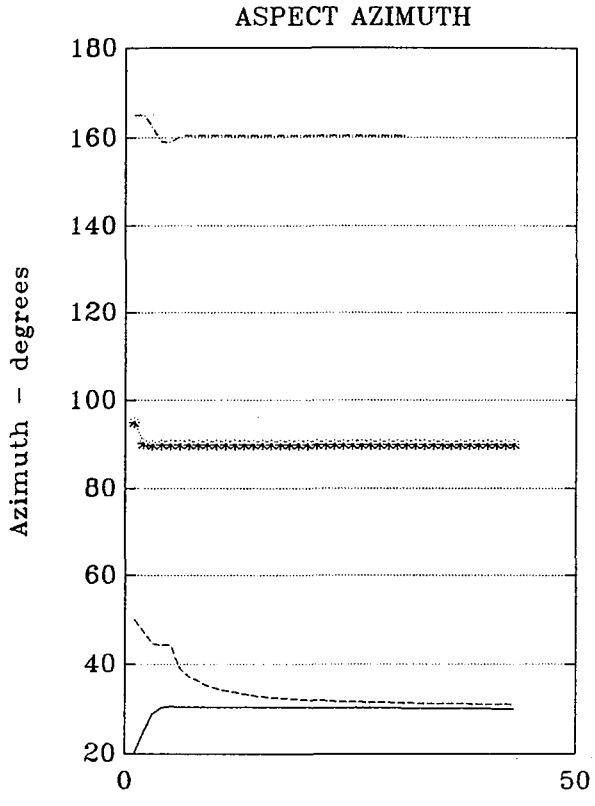

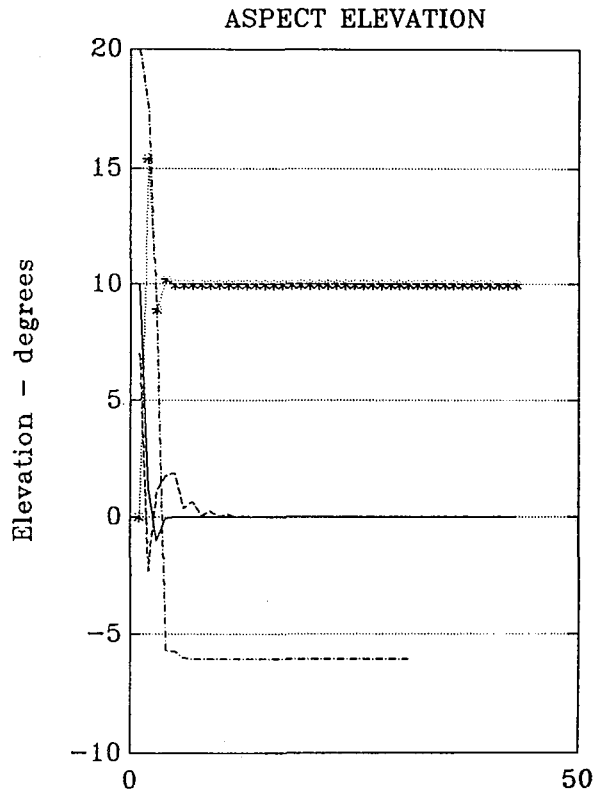

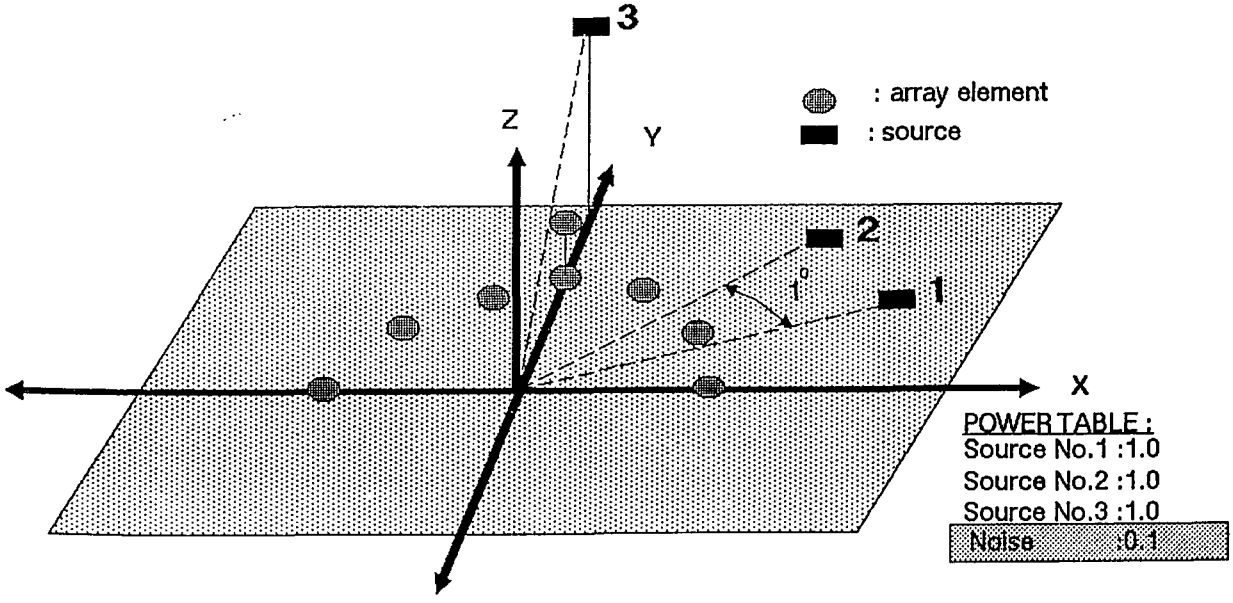

POWER TABLE :
Source No.1 :1.0
Source No.2 :1.0
Source No.3 :1.0
Noise :0.1

FIGURE – 4.34 (Sources No.1 and No.2 are correlated)

	TRUE directions	INITIAL directions	directions estimated by ASPECT
source No.1	(0.0, 30.0)	(10.0, 20.0)	(– 0.0000, 30.0000)
source No.2	(0.0, 40.0)	(7.0, 50.0)	(0.0000, 40.0000)
source No.3	(10.0, 90.0)	(0.0, 95.0)	(10.0000, 90.0000)
source No.4	———	(20.0,165.0)	———

cost: 1.000000000000000e + 000

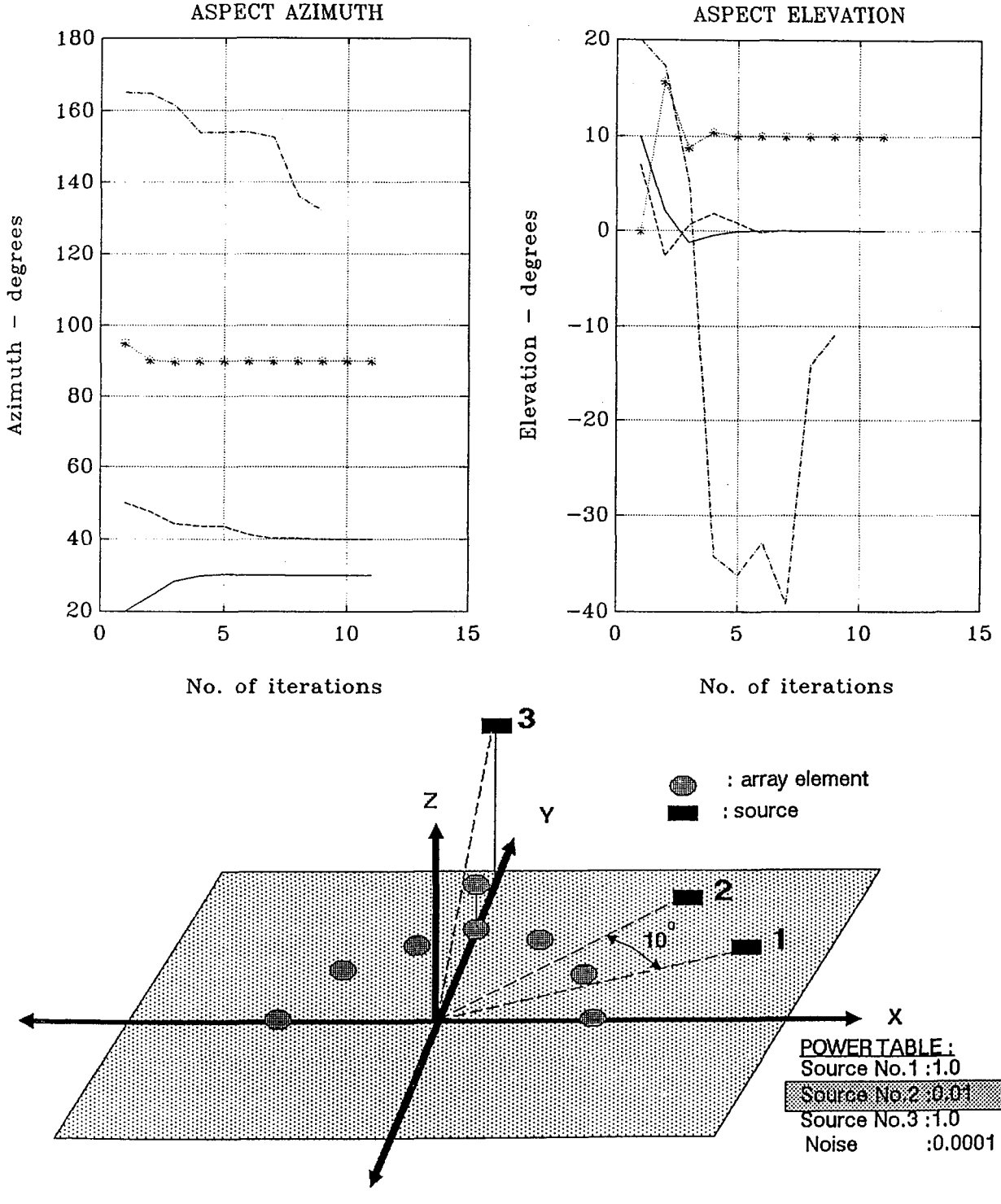

FIGURE – 4.35 (Sources No.1 and No.2 are correlated)

	TRUE directions	INITIAL directions	directions estimated by ASPECT
source No.1	(0.0, 30.0)	(10.0, 20.0)	(– 0.0000, 30.0000)
source No.2	(0.0, 35.0)	(7.0, 50.0)	(0.0000, 35.0001)
source No.3	(10.0, 90.0)	(0.0, 95.0)	(10.0000, 90.0000)
source No.4	———	(20.0,165.0)	———

cost:1.000000000000000e+000

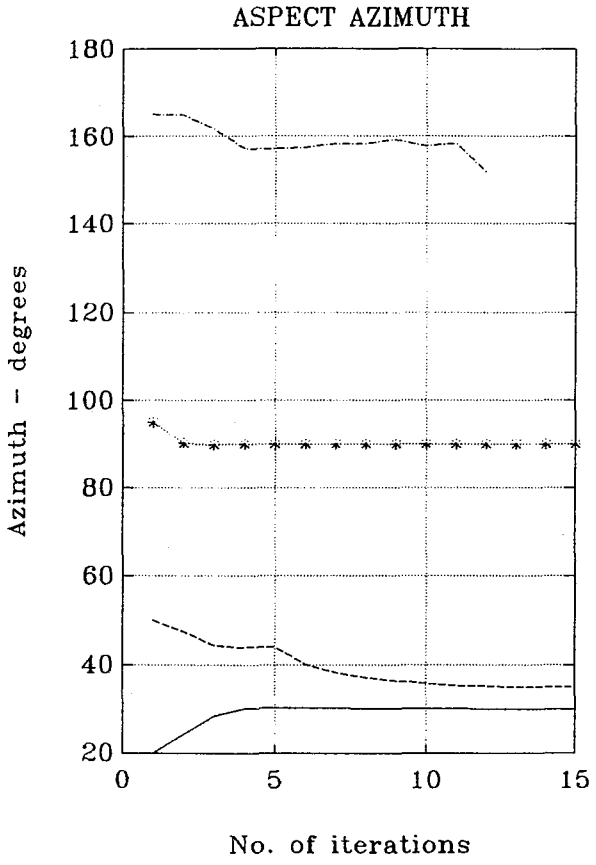

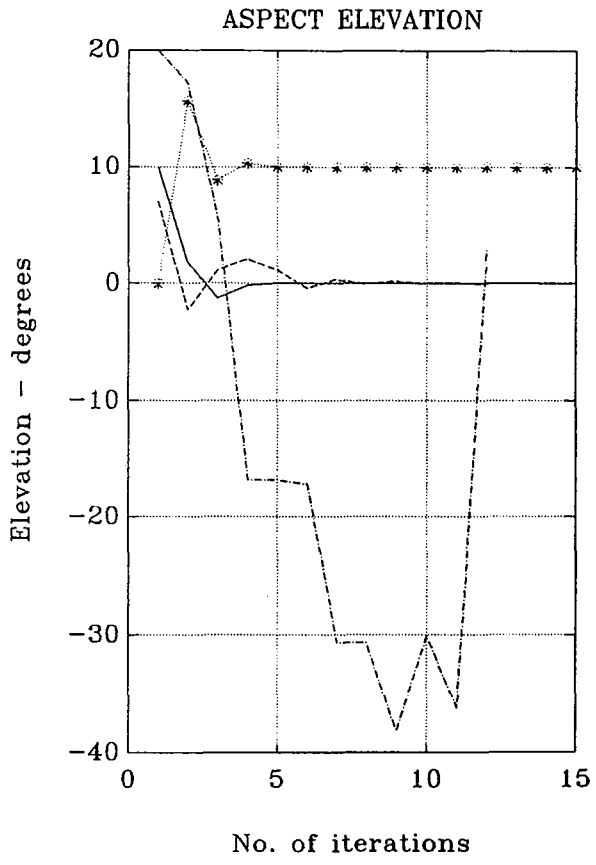

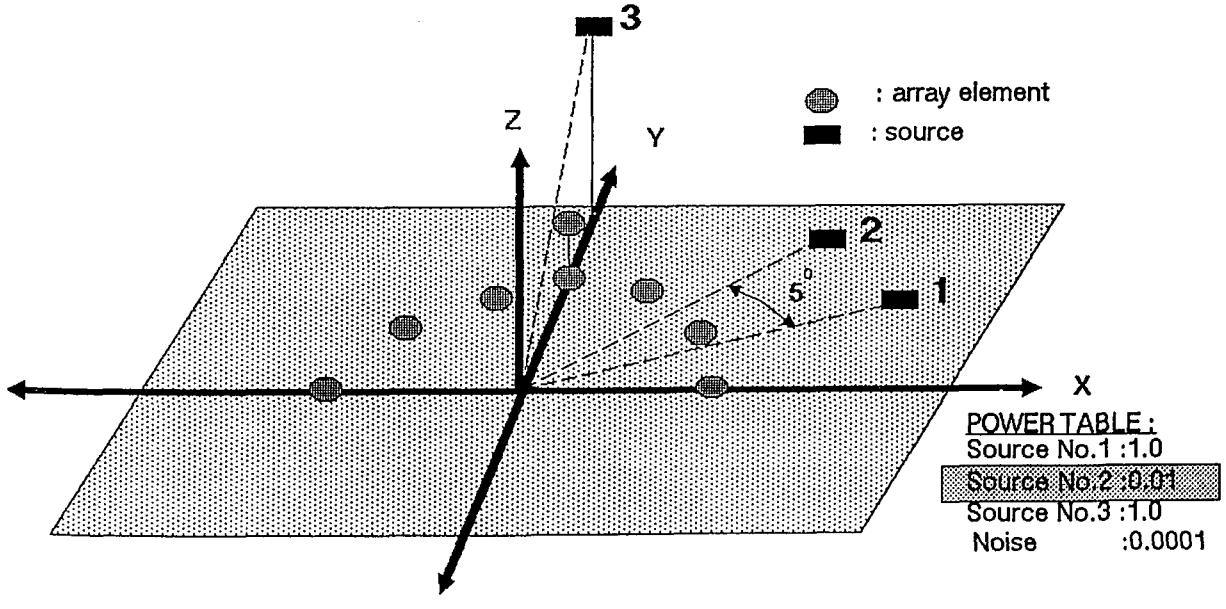

FIGURE – 4.36 (Sources No.1 and No.2 are correlated)

	TRUE directions	INITIAL directions	directions estimated by ASPECT
source No.1	(0.0, 30.0)	(10.0, 20.0)	(0.0000, 30.0001)
source No.2	(0.0, 32.0)	(7.0, 50.0)	(–0.0000, 32.0012)
source No.3	(10.0, 90.0)	(0.0, 95.0)	(10.0000, 90.0000)
source No.4	———	(20.0,165.0)	———

cost: 1.000000000000000e+000

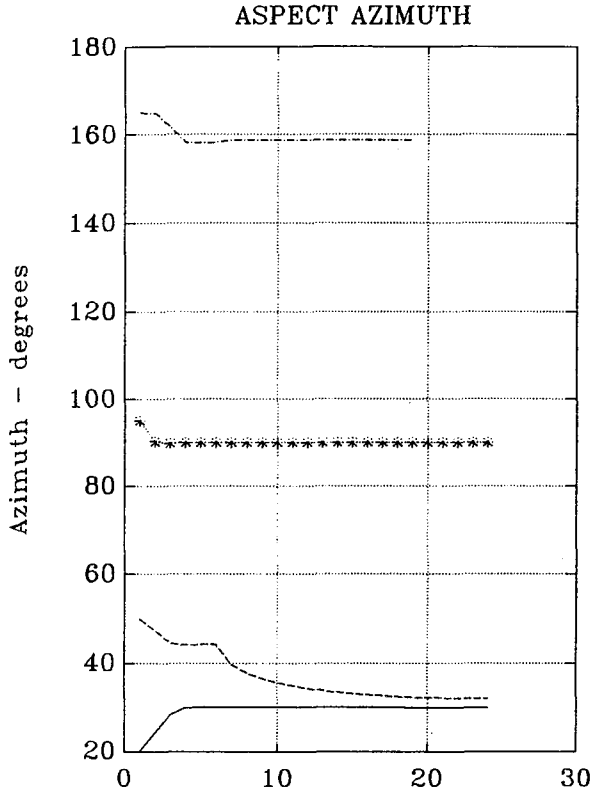

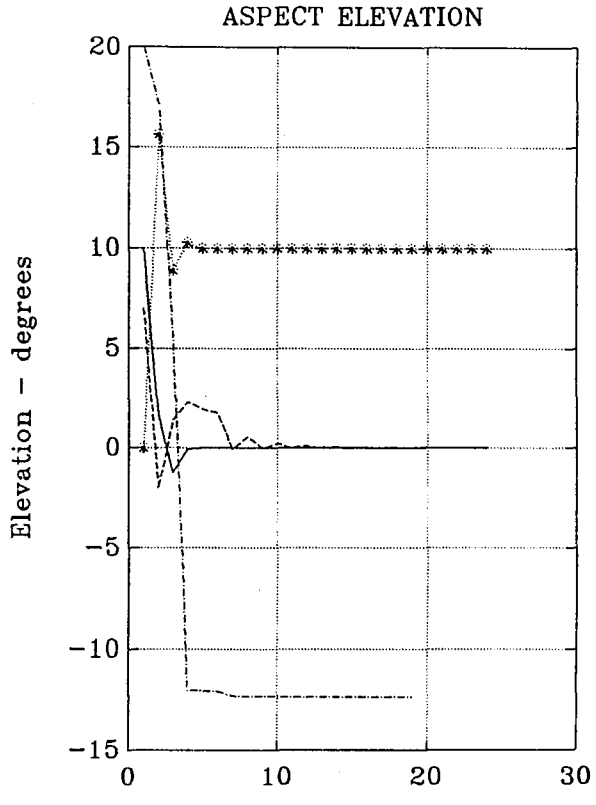

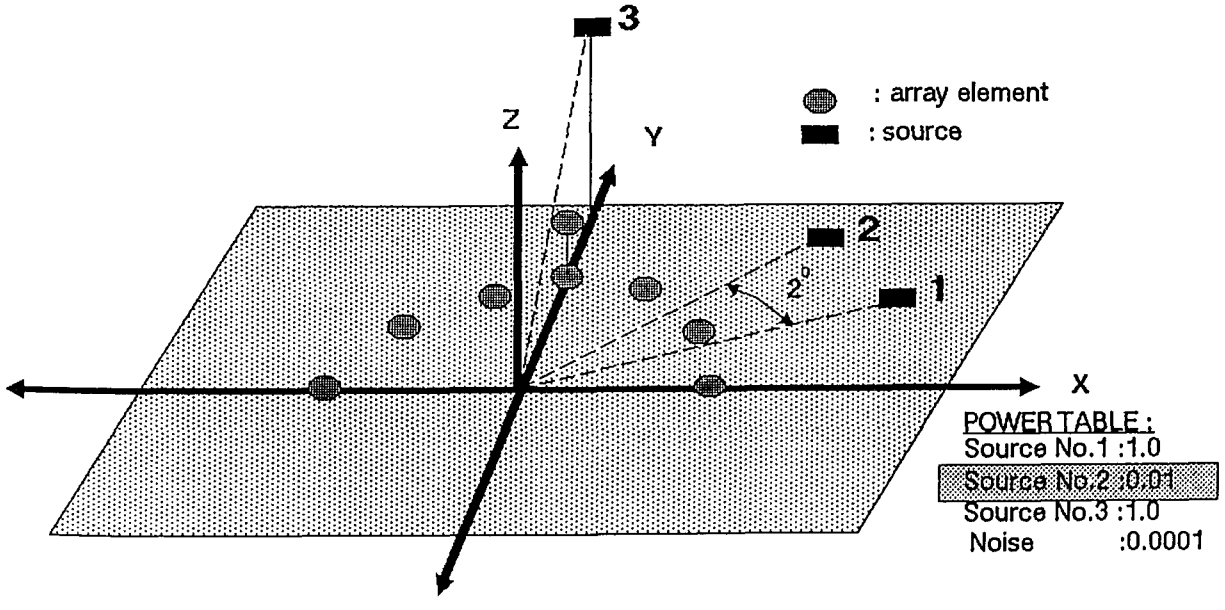

FIGURE – 4.37 (Sources No.1 and No.2 are correlated)

	TRUE directions	INITIAL directions	directions estimated by ASPECT
source No.1	(0.0, 30.0)	(10.0, 20.0)	(0.0000, 30.0048)
source No.2	(0.0, 31.0)	(7.0, 50.0)	(−0.0002, 31.0489)
source No.3	(10.0, 90.0)	(0.0, 95.0)	(10.0000, 90.0000)
source No.4	———	(20.0,165.0)	———

cost: 1.00000000000002e+000

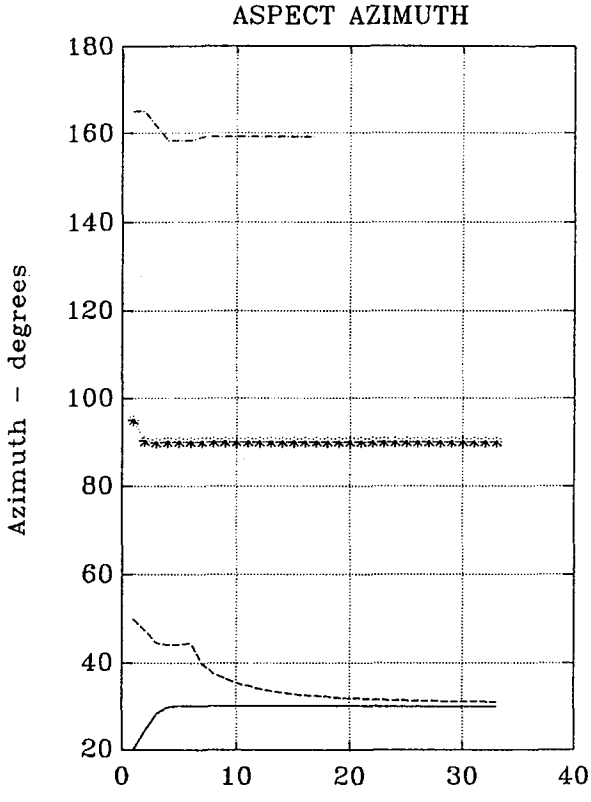

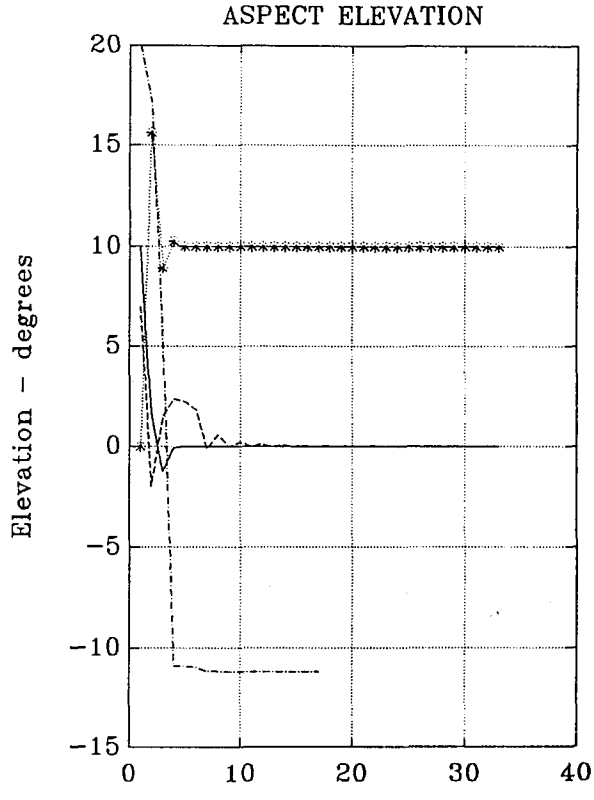

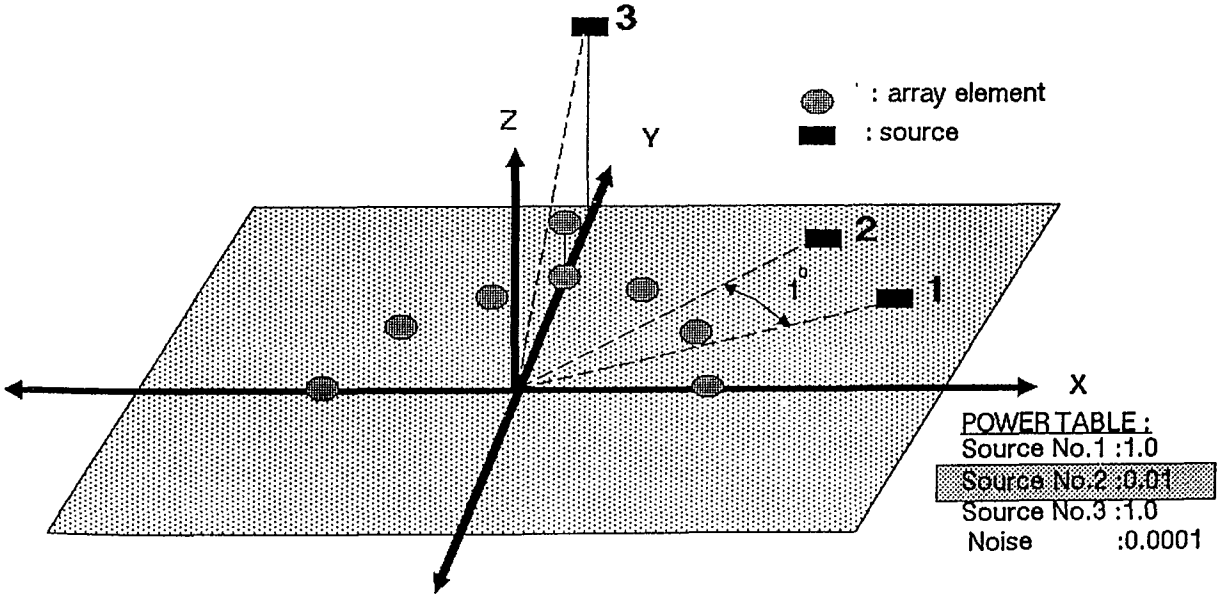

POWER TABLE :
Source No.1 :1.0
Source No.2 :0.01
Source No.3 :1.0
Noise :0.0001

FIGURE – 4.38 (Sources No.1 and No.2 are correlated)

	TRUE directions	INITIAL directions	directions estimated by ASPECT
source No.1	(0.0, 30.0)	(10.0, 20.0)	(– 0.0000, 30.0000)
source No.2	(0.0, 40.0)	(7.0, 50.0)	(0.0001, 40.0005)
source No.3	(10.0, 90.0)	(0.0, 95.0)	(10.0000, 90.0000)
source No.4	———	(20.0,165.0)	———

cost:1.000000000000000e + 000

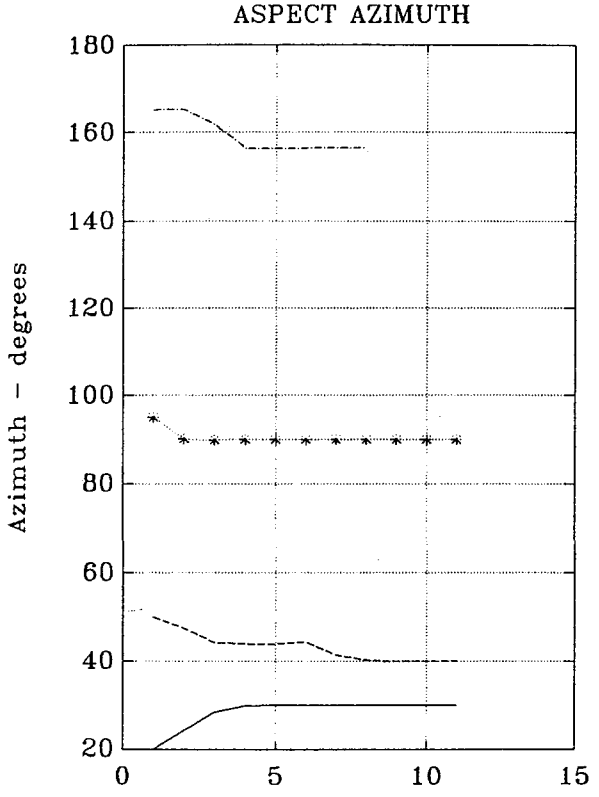

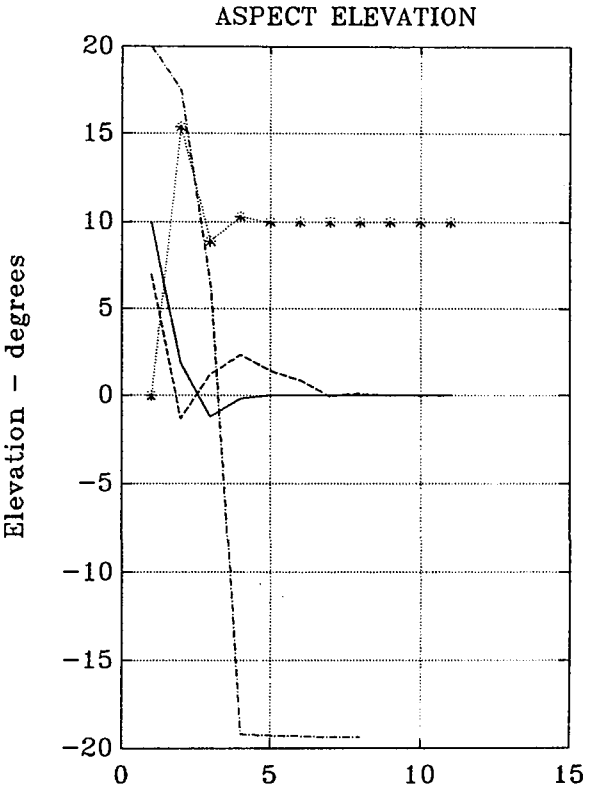

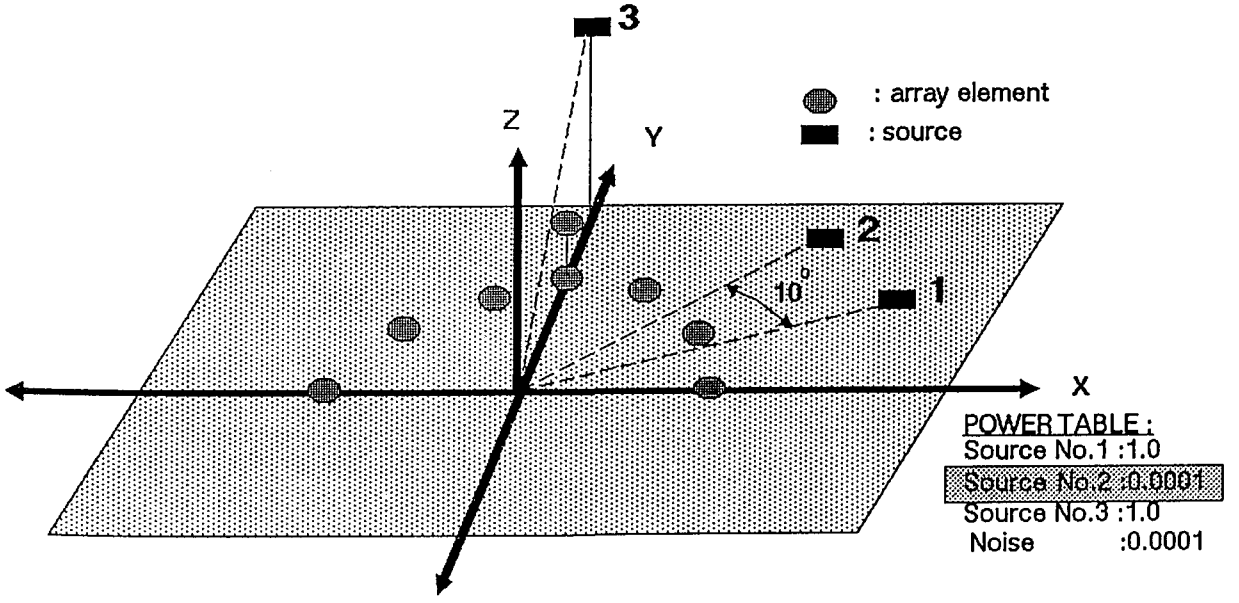

POWER TABLE :
Source No.1 :1.0
Source No.2 :0.0001
Source No.3 :1.0
Noise :0.0001

FIGURE – 4.39 (Sources No.1 and No.2 are correlated)

	TRUE directions	INITIAL directions	directions estimated by ASPECT
source No.1	(0.0, 30.0)	(10.0, 20.0)	(0.0000, 30.0000)
source No.2	(0.0, 35.0)	(7.0, 50.0)	(–0.0000, 35.0001)
source No.3	(10.0, 90.0)	(0.0, 95.0)	(10.0000, 90.0000)
source No.4	———	(20.0,165.0)	———

cost: 1.000000000000000e+000

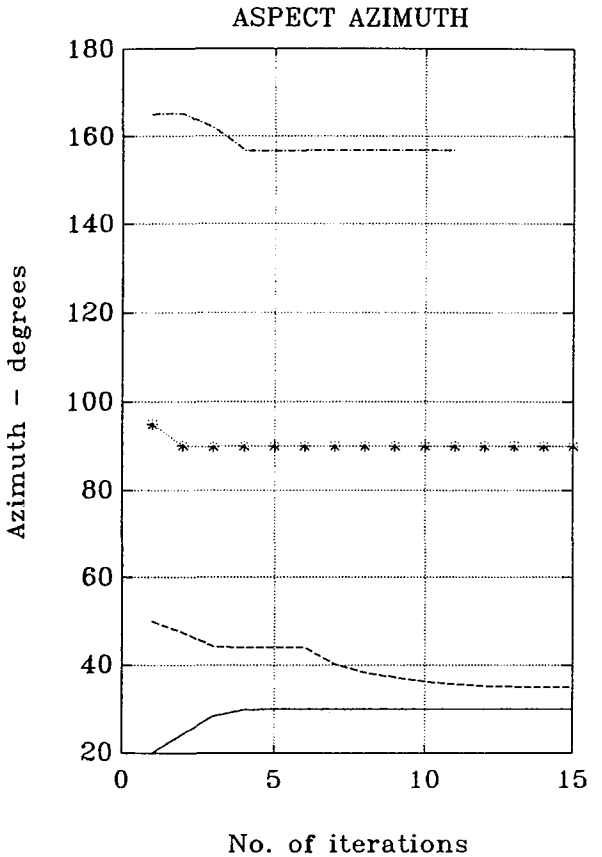

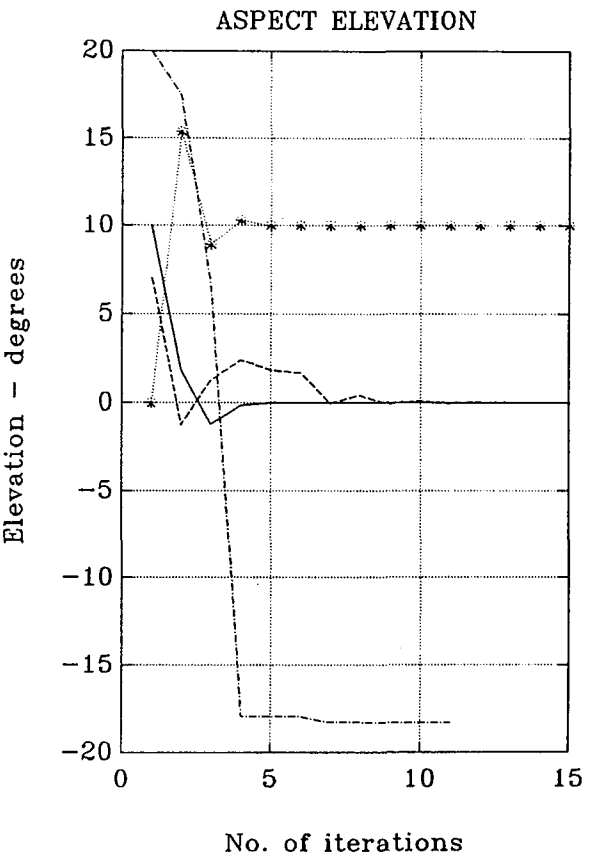

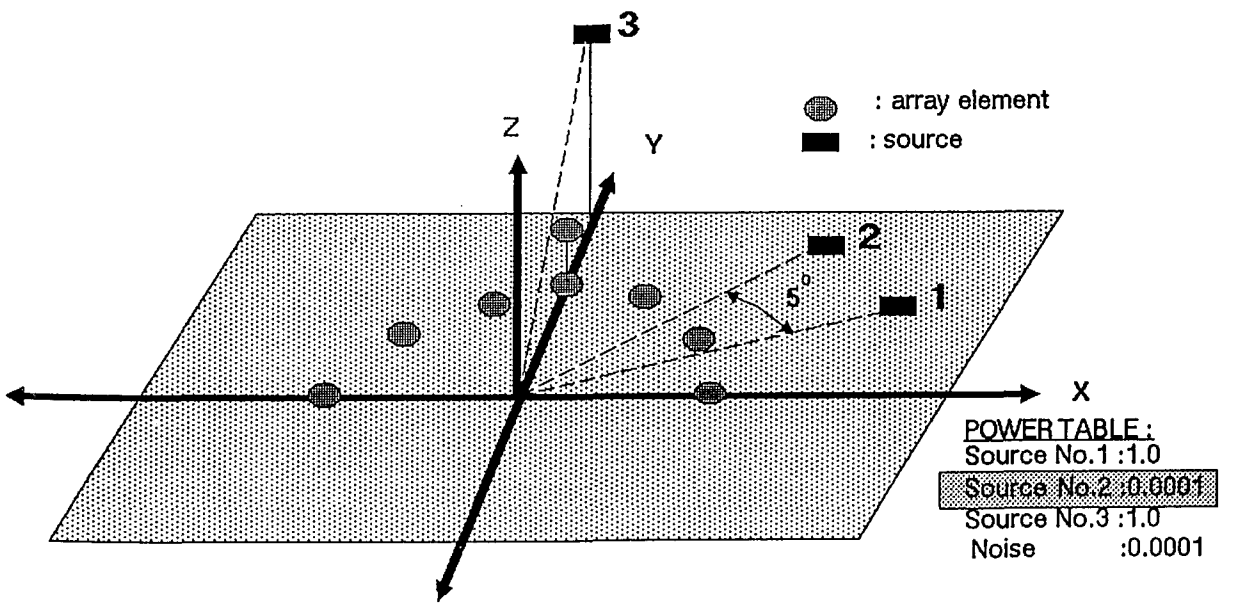

FIGURE – 4.40 (Sources No.1 and No.2 are correlated)

	TRUE directions	INITIAL directions	directions estimated by ASPECT
source No.1	(0.0, 30.0)	(10.0, 20.0)	(0.0000, 30.0009)
source No.2	(0.0, 32.0)	(7.0, 50.0)	(−0.0004, 32.0920)
source No.3	(10.0, 90.0)	(0.0, 95.0)	(10.0000, 90.0000)
source No.4	———	(20.0,165.0)	———

cost:1.00000000000001e+000

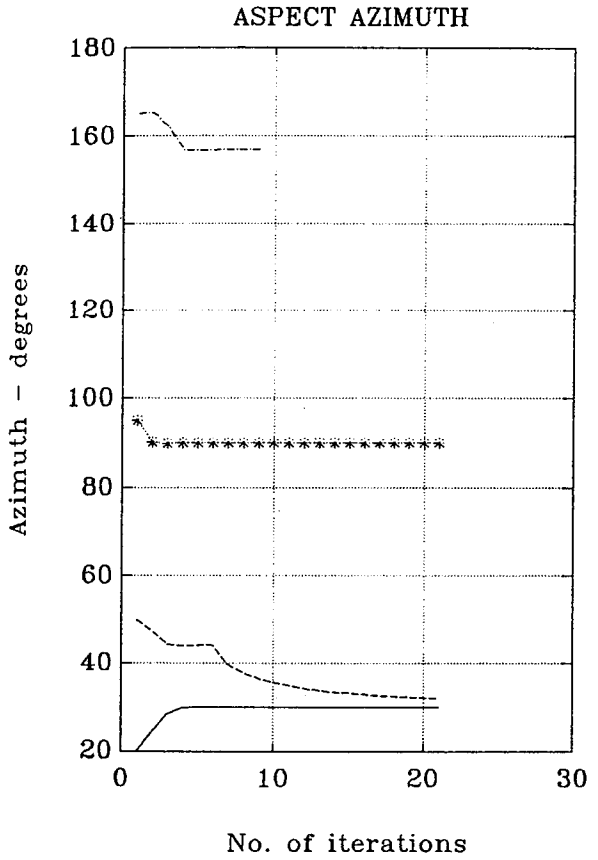

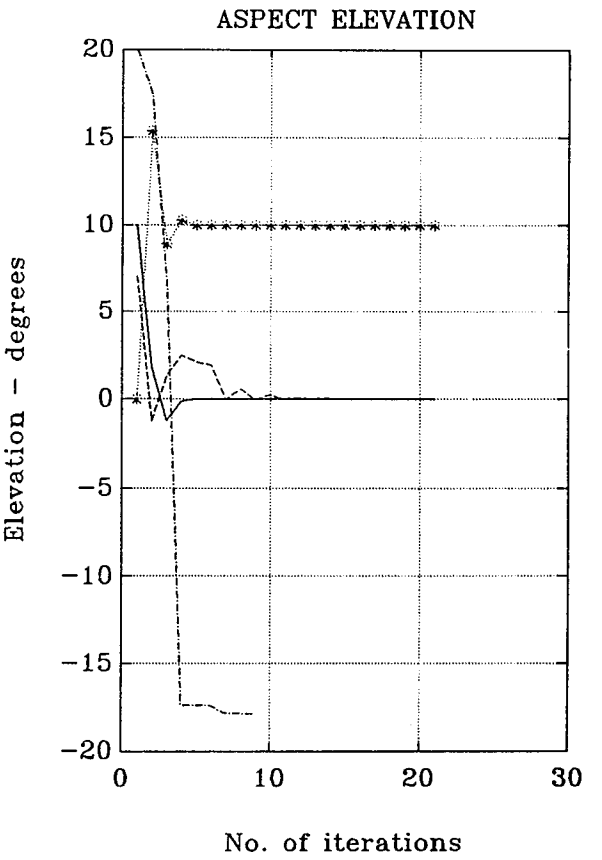

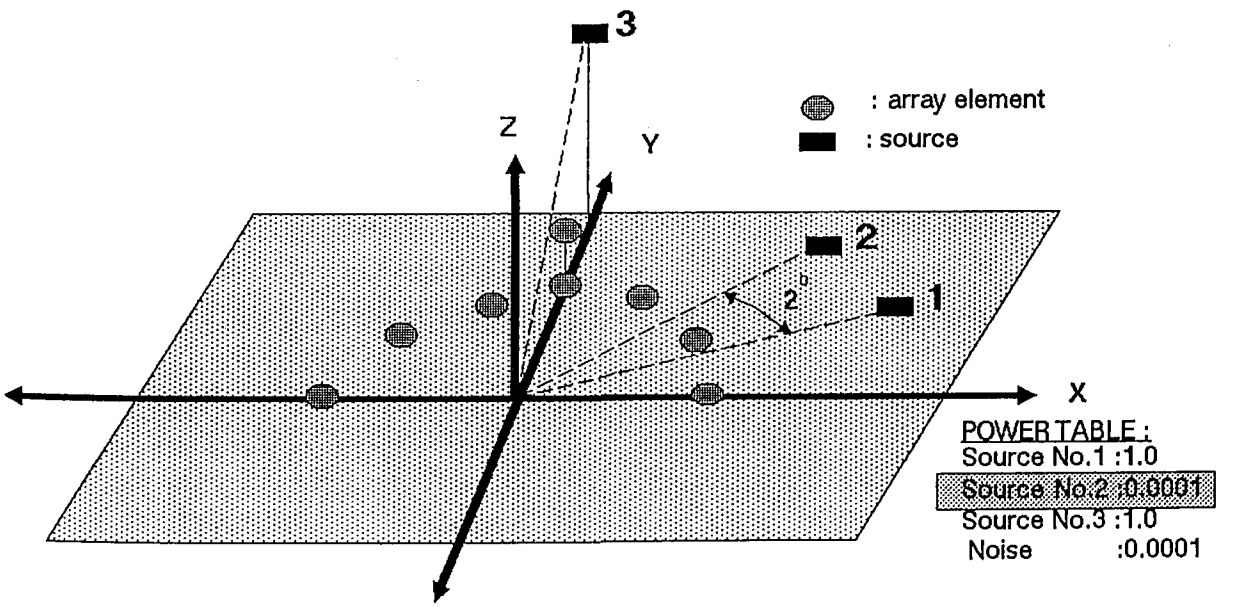

FIGURE—4.41 (Sources No.1 and No.2 are correlated)

	TRUE directions	INITIAL directions	directions estimated by ASPECT
source No.1	(0.0, 30.0)	(10.0, 20.0)	(−0.0000, 30.0042)
source No.2	(0.0, 31.0)	(7.0, 50.0)	(0.0076, 31.7027)
source No.3	(10.0, 90.0)	(0.0, 95.0)	(10.0000, 90.0000)
source No.4	———	(20.0,165.0)	———

cost:1.000000000000004e+000

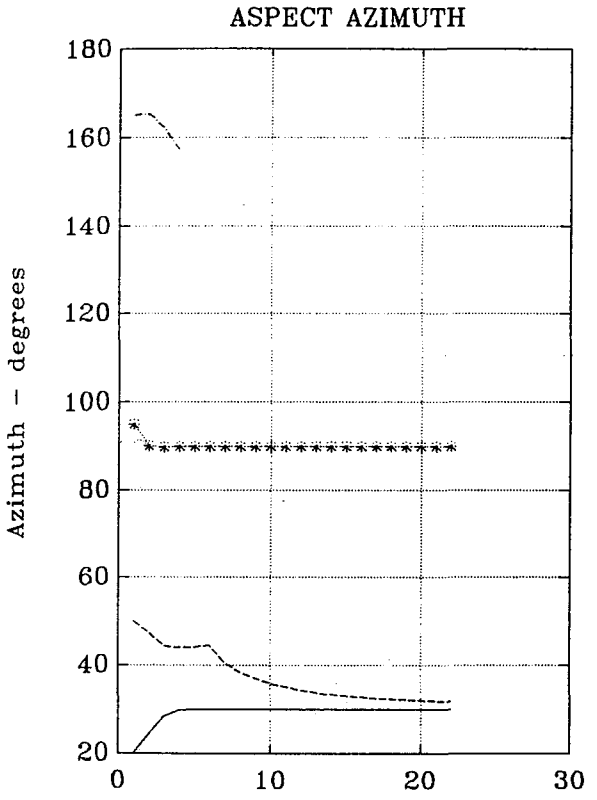

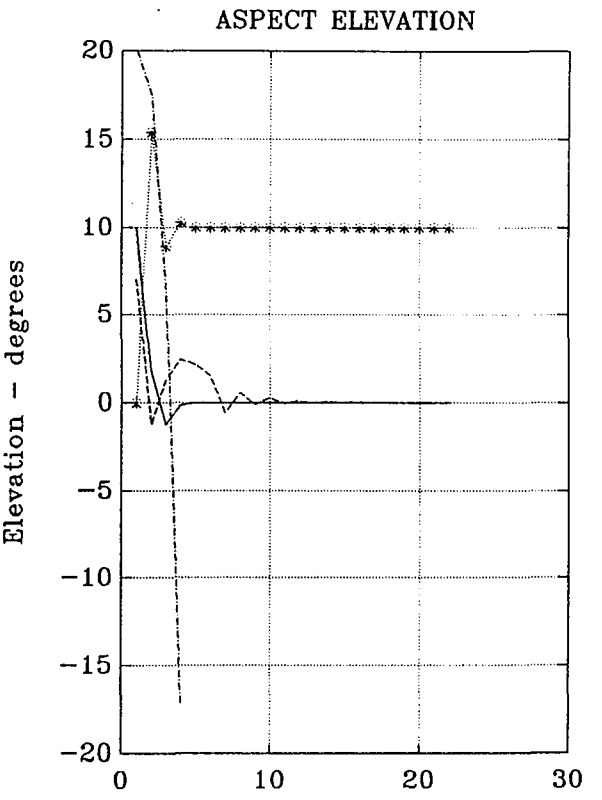

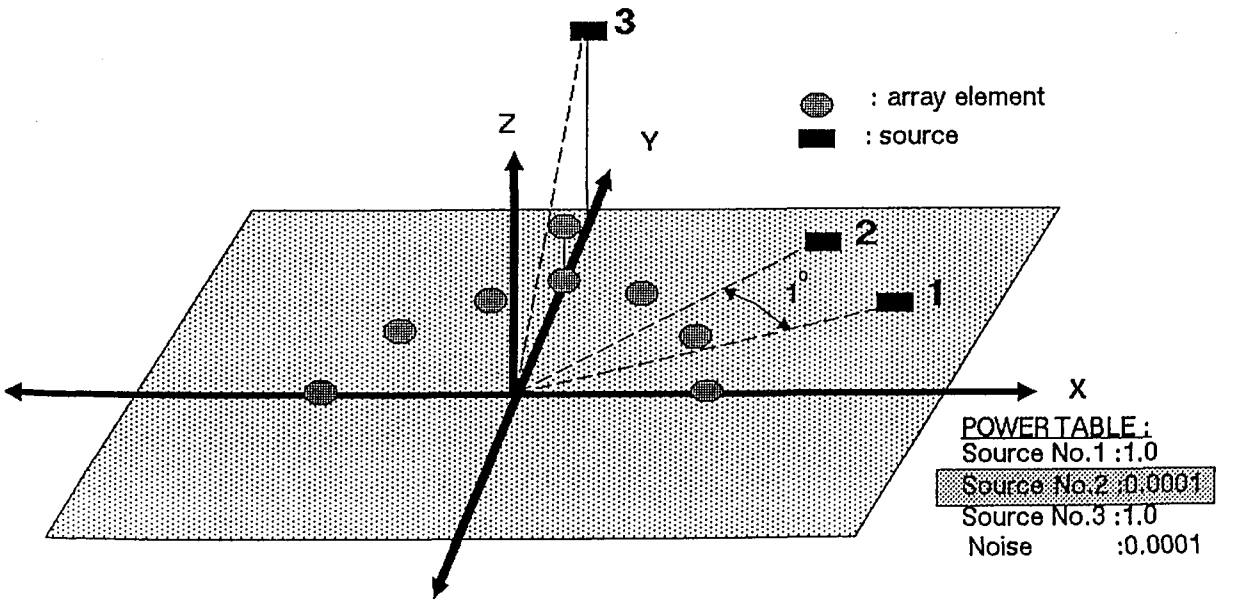

4.4. SPHERICAL WAVE PROPAGATION

The application of ASPECT in a spherical wave propagation environment can be achieved by modelling the received signals (and particularly the Source Position Vectors) with *Equation* 2.16 and by including the *range* as a variable of the *cost function.* This has been done by using the array model specified in *Figure* 4.1*b*. Simulations were performed for both uncorrelated and correlated cases. For every considered case the signal environment is assumed to involve three signals incident to the array from the following positions: (15°, 20°, $30\frac{\lambda}{2}$), (15°, variable, $45\frac{\lambda}{2}$), and (10°, 90°, $65\frac{\lambda}{2}$) where the first element of the above triplet represents the elevation angle, the second element represents the azimuth angle and the third element represents the range in half wave-lengths. The trial pair is formed by the first and second sources where the azimuth angle of the second source is such that the angle separation is 10°, 5°, 2°, 1°. Since it has already been established from the previous simulations in the situations involving plane waves that ASPECT is robust to noise level, the noise effects are not going to be examined in the spherical wave situation. However, the effects of presence of both "weak" and "strong" signals are examined for both correlated and uncorrelated cases. Thus, *Figures* 4.42-4.45 illustrate the results produced by ASPECT for uncorrelated sources of equal power with noise level at −40dB. *Figures* 4.46-4.49 shows the ASPECT's performance when the trial pair is brought down from 0dB to −30dB. For the correlated situation the noise level remains at −40dB and the trial pair is of equal power but fully correlated. The results are shown in

Figures 4.50-4.53 indicating that ASPECT resolves and estimates the positions of the sources with accuracy. When the trial pair is brought down from 0dB to −30dB the algorithm provides the results given in *Figures* 4.54-4.57. *Figure* 4.57 illustrates the lose of accuracy of the estimates, when the trial pair is close together.

FIGURE – 4.42 (Uncorrelated Sources; Spherical Wave Propagation)

	TRUE directions	INITIAL directions	directions estimated by ASPECT
source No.1	(15.0, 20.0, 30.0)	(0.0, 12.0, 100)	(15.0000,20.0000,30.0000)
source No.2	(15.0, 30.0, 45.0)	(0.0, 47.0, 100)	(15.0000,30.0000,45.0000)
source No.3	(10.0, 90.0, 65.0)	(0.0, 76.0, 100)	(10.0000,90.0000,65.0000)
source No.4	———	(0.0, 95.0, 100)	———

cost: 1.000000000000000e + 000

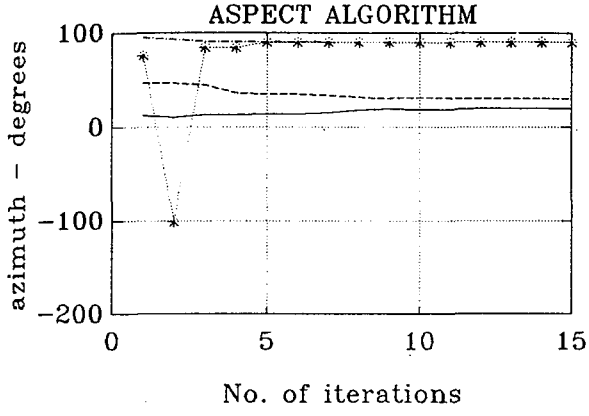

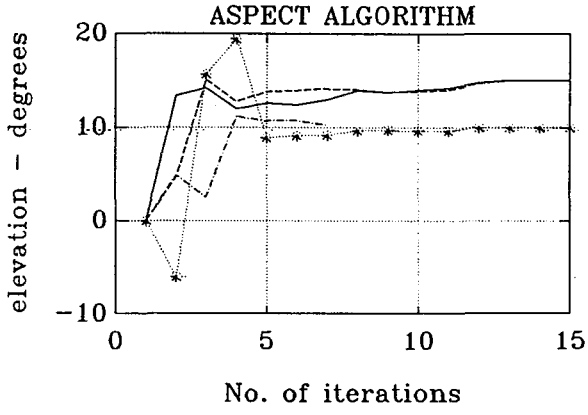

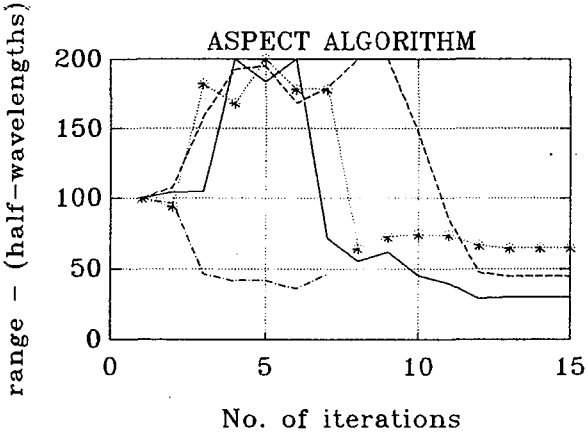

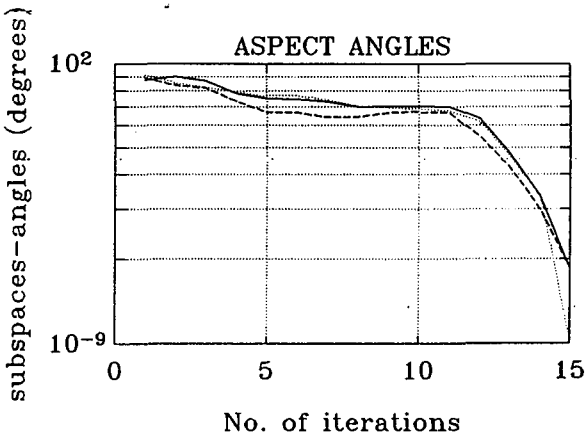

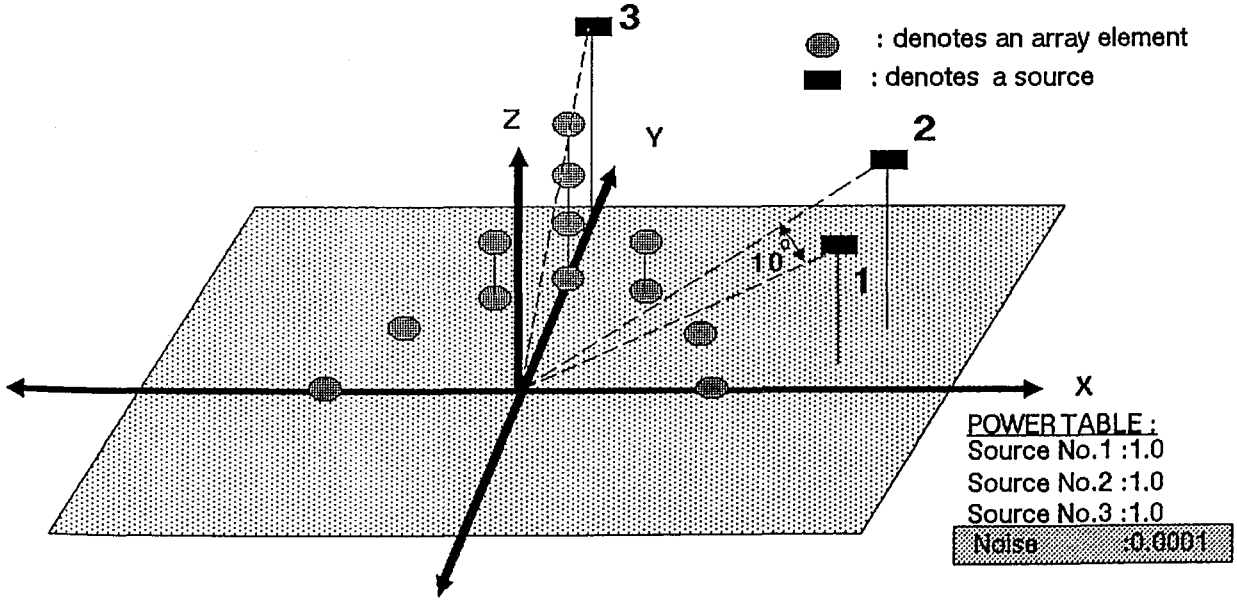

FIGURE – 4.43 (Uncorrelated Sources; Spherical Wave propagation)

	TRUE directions	INITIAL directions	directions estimated by ASPECT
source No.1	(15.0, 20.0, 30.0)	(0.0, 11.0, 100)	(15.0000,20.0000,30.0000)
source No.2	(15.0, 25.0, 45.0)	(0.0, 46.0, 100)	(15.0000,25.0000,45.0000)
source No.3	(10.0, 90.0, 65.0)	(0.0, 75.0, 100)	———
source No.4	———	(0.0, 98.0, 100)	(10.0000,90.0000,65.0000)

cost: 1.000000000000000e+000

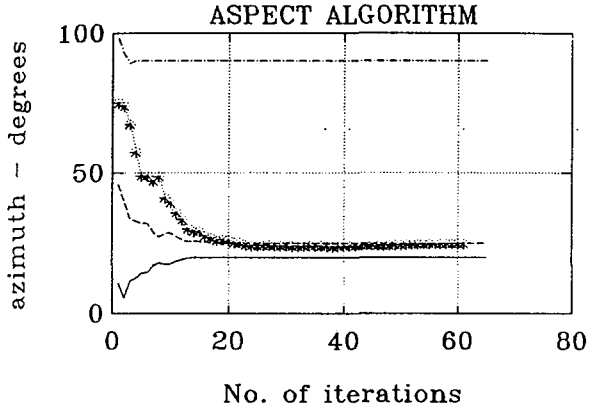

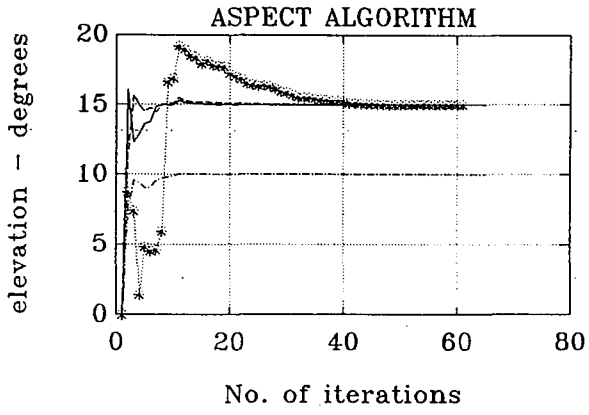

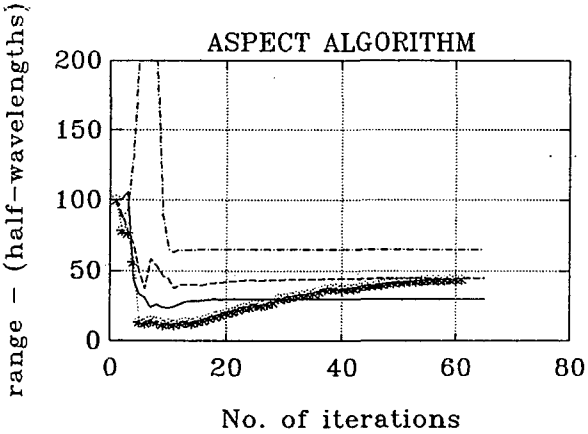

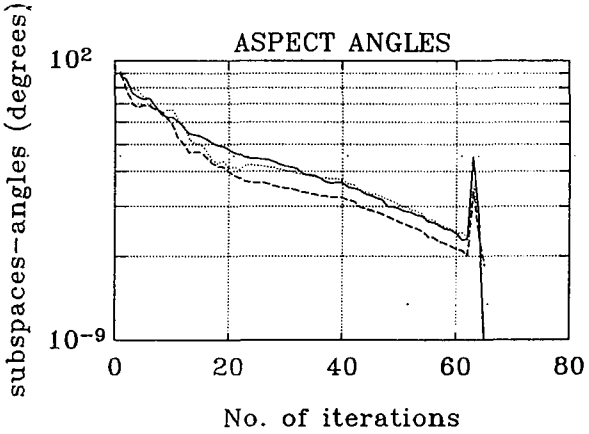

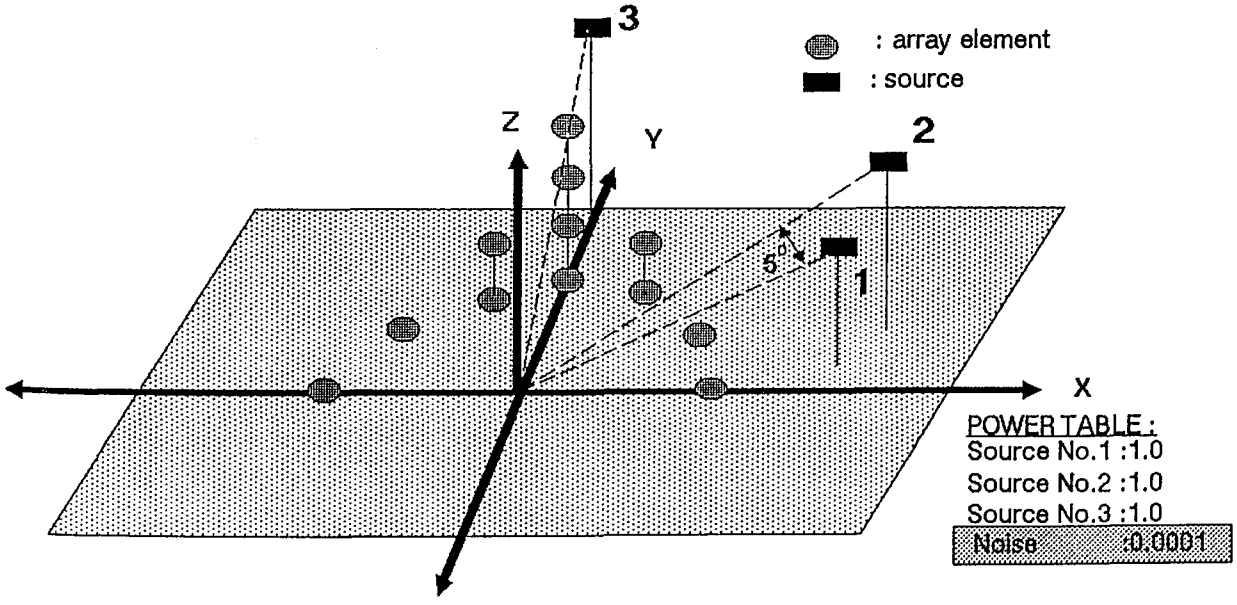

FIGURE—4.44 (Uncorrelated Sources; Spherical Wave Propagation)

	TRUE directions	INITIAL directions	directions estimated by ASPECT
source No.1	(15.0, 20.0, 30.0)	(0.0, 11.0, 100)	(15.0000,20.0000,30.0000)
source No.2	(15.0, 22.0, 45.0)	(0.0, 45.0, 100)	(15.0000,22.0000,45.0000)
source No.3	(10.0, 90.0, 65.0)	(0.0, 74.0, 100)	———
source No.4	———	(0.0, 96.0, 100)	(10.0000,90.0000,65.0000)

cost: 1.000000000000000e+000

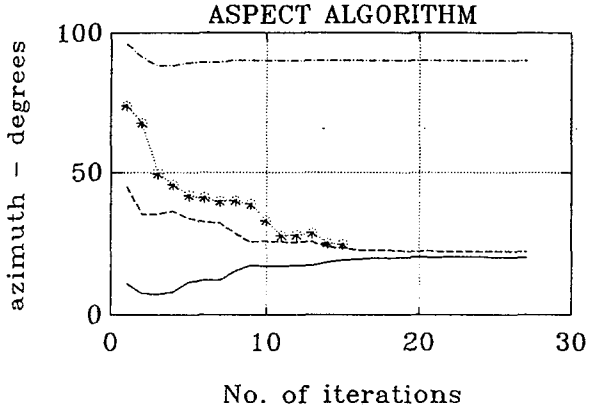

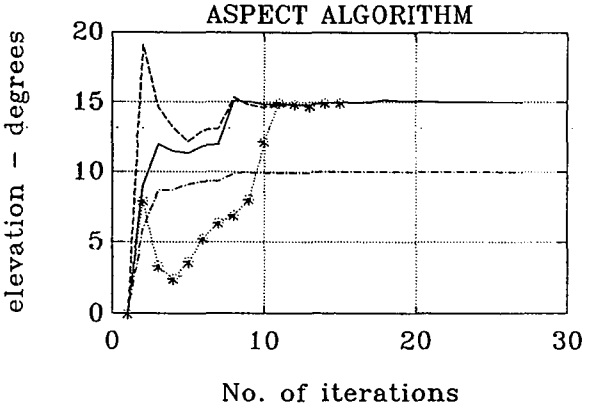

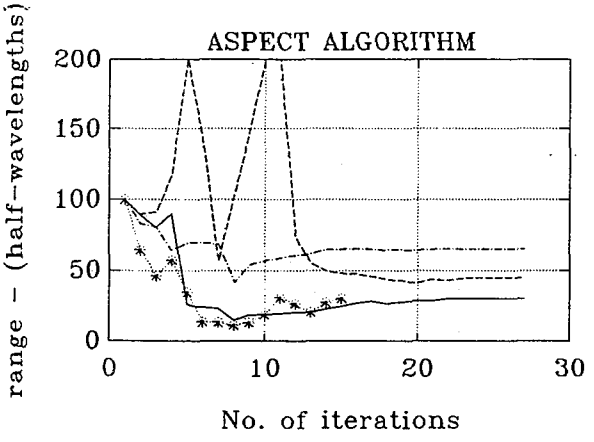

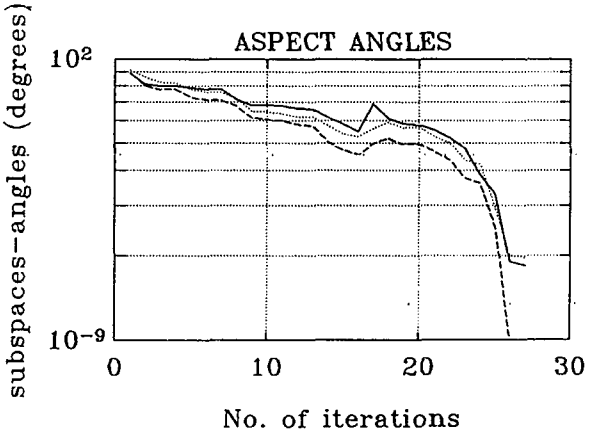

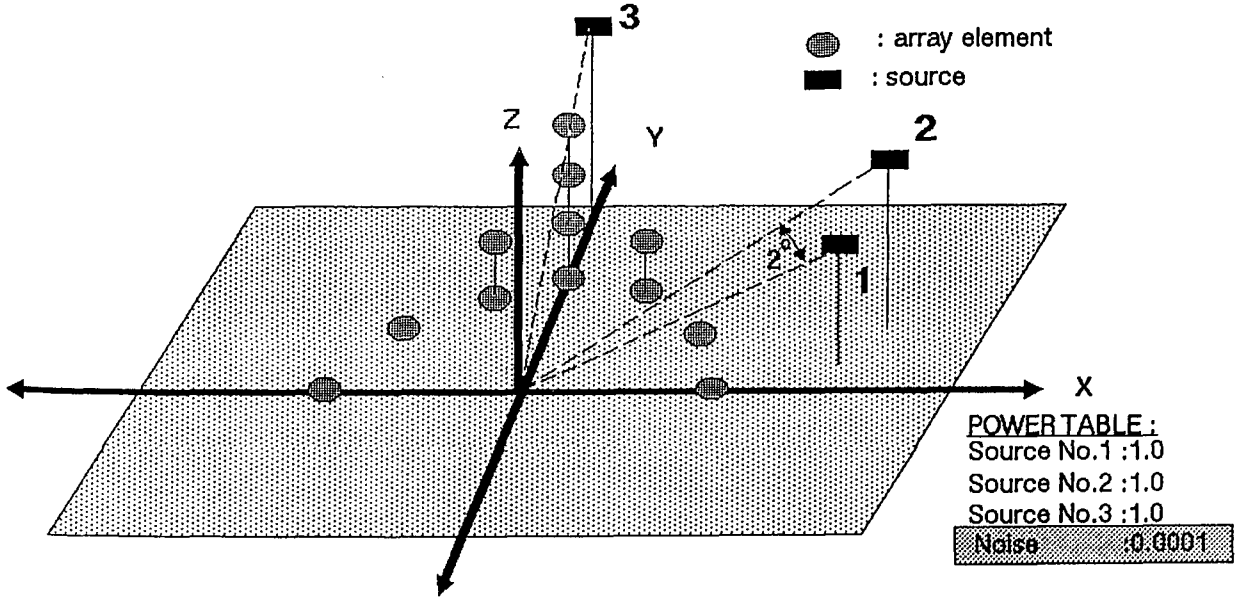

FIGURE – 4.45 (Uncorrelated Sources; Spherical Wave Propagation)

	TRUE directions	INITIAL directions	directions estimated by ASPECT
source No.1	(15.0, 20.0, 30.0)	(0.0, 12.0, 100)	(15.0000,20.0000,30.0000)
source No.2	(15.0, 21.0, 45.0)	(0.0, 45.0, 100)	(15.0000,21.0000,45.0000)
source No.3	(10.0, 90.0, 65.0)	(0.0, 74.0, 100)	———
source No.4	———	(0.0, 94.0, 100)	(10.0000,90.0000,65.0000)

cost: 1.00000000000000e + 000

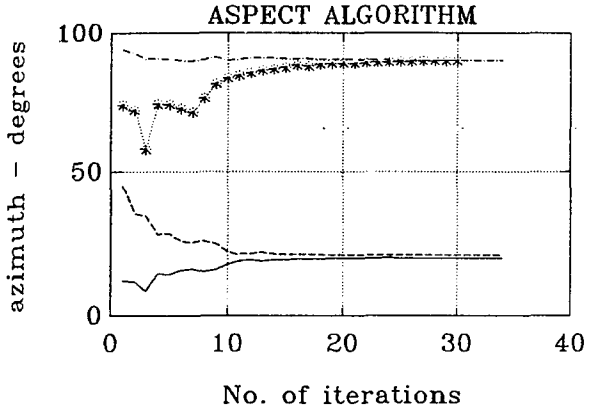

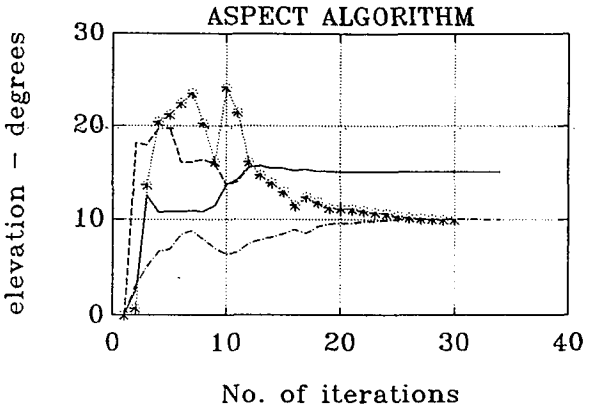

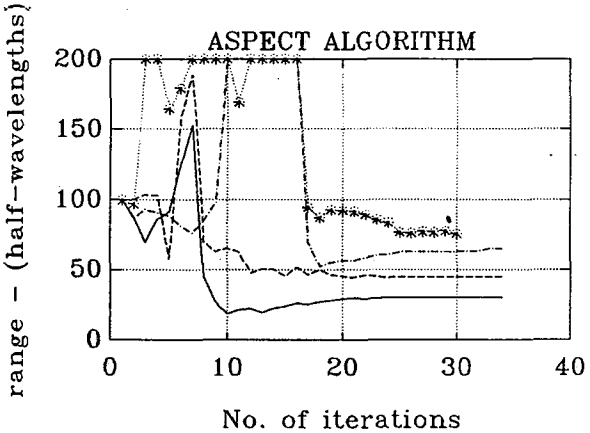

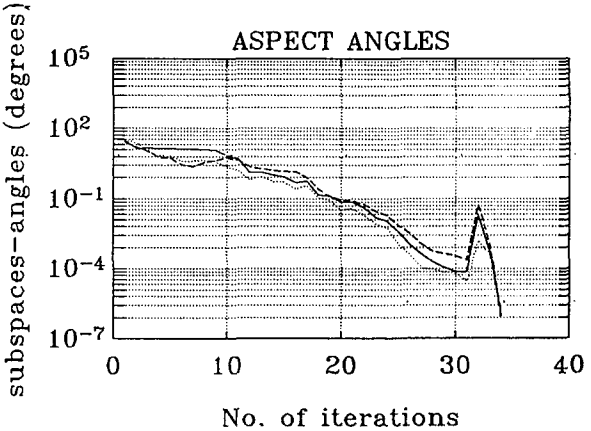

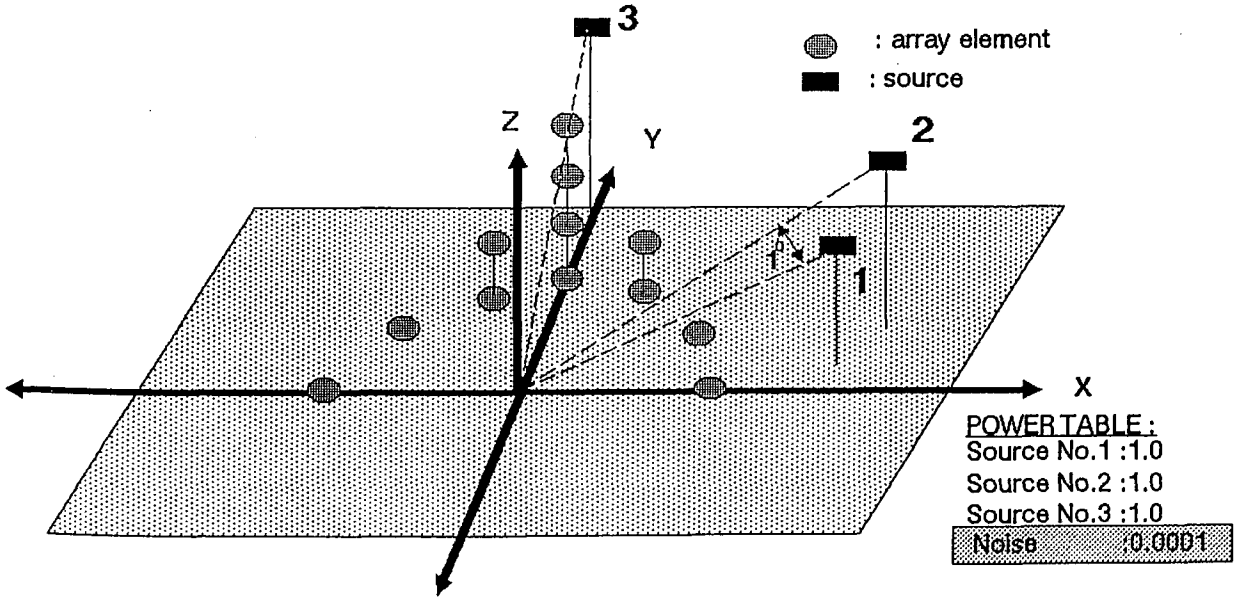

POWER TABLE :
Source No.1 :1.0
Source No.2 :1.0
Source No.3 :1.0
Noise :0.0001

FIGURE—4.46 (Uncorrelated Sources. Power resolution: −30dB)

	TRUE directions	INITIAL directions	directions estimated by ASPECT
source No.1	(15.0, 20.0, 30.0)	(0.0, 10.0, 100)	(15.0000,20.0000,30.0000)
source No.2	(15.0, 30.0, 45.0)	(0.0, 45.0, 100)	(15.0000,30.0000,45.0000)
source No.3	(10.0, 90.0, 65.0)	(0.0, 75.0, 100)	———
source No.4	———	(0.0, 99.0, 100)	(10.0000,90.0000,65.0000)

cost:1.000000000000000e+000

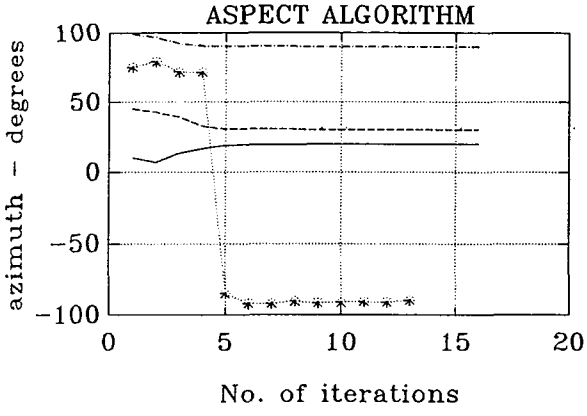

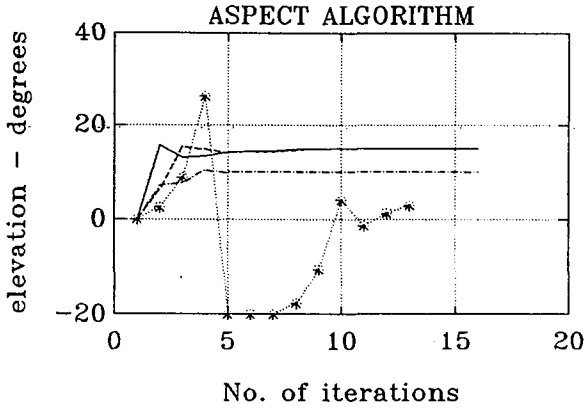

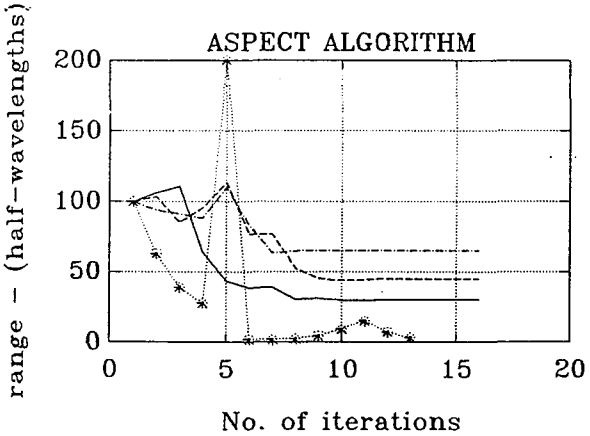

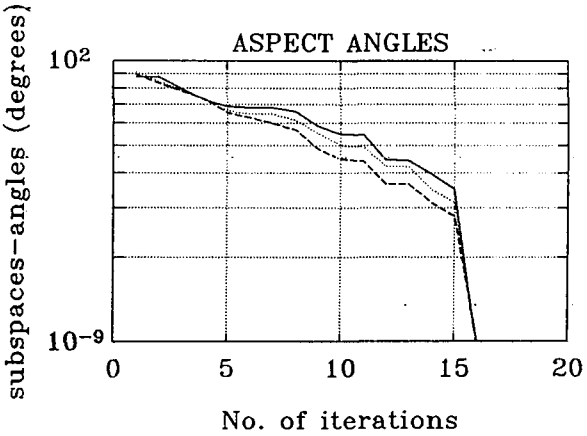

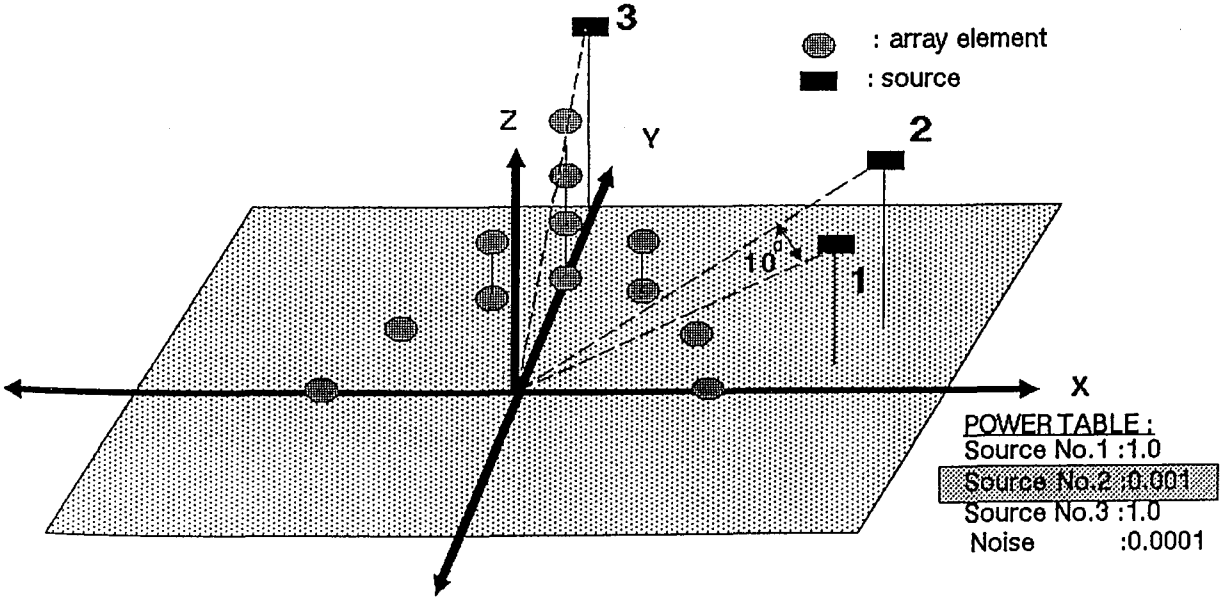

FIGURE – 4.47 (Uncorrelated Sources. Power resolution: – 30dB)

	TRUE directions	INITIAL directions	directions estimated by ASPECT
source No.1	(15.0, 20.0, 30.0)	(0.0, 14.0, 100)	(14.9997,24.9890,44.8352)
source No.2	(15.0, 25.0, 45.0)	(0.0, 45.0, 100)	(15.0000,20.0000,30.0000)
source No.3	(10.0, 90.0, 65.0)	(0.0, 95.0, 100)	(10.0000,90.0000,65.0000)
source No.4	———	(0.0, 169.0, 100)	———

cost:1.000000000000000e+000

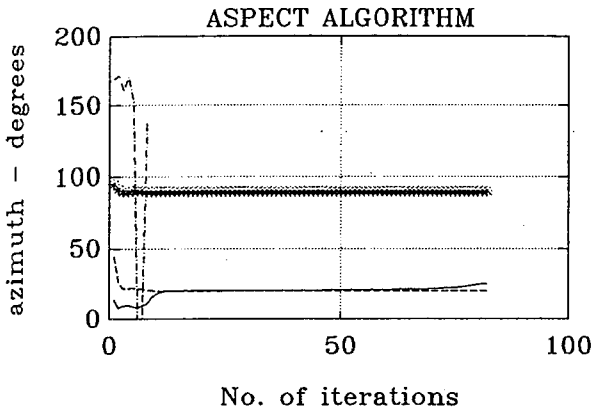

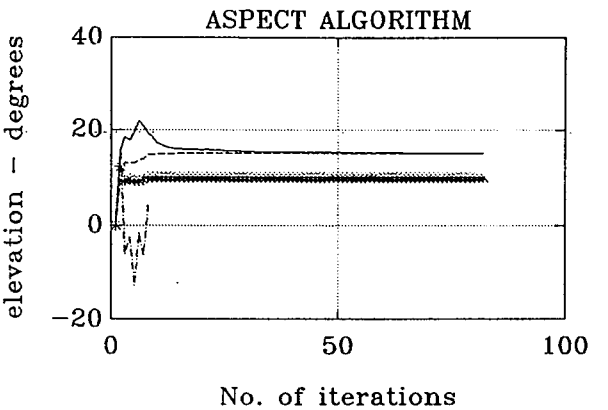

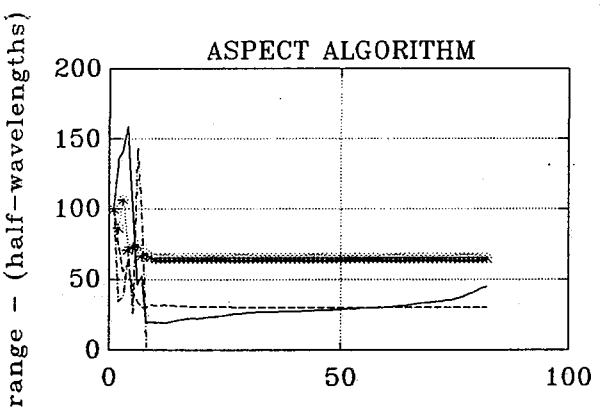

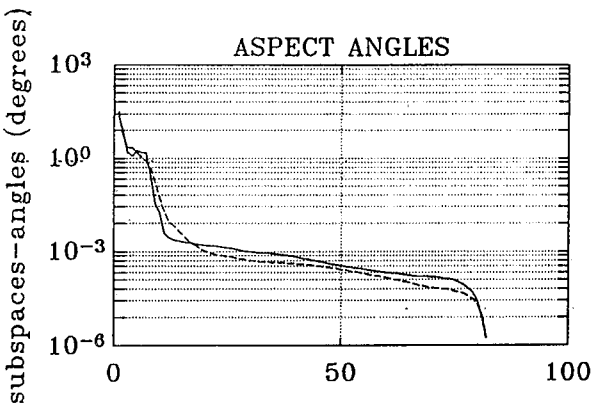

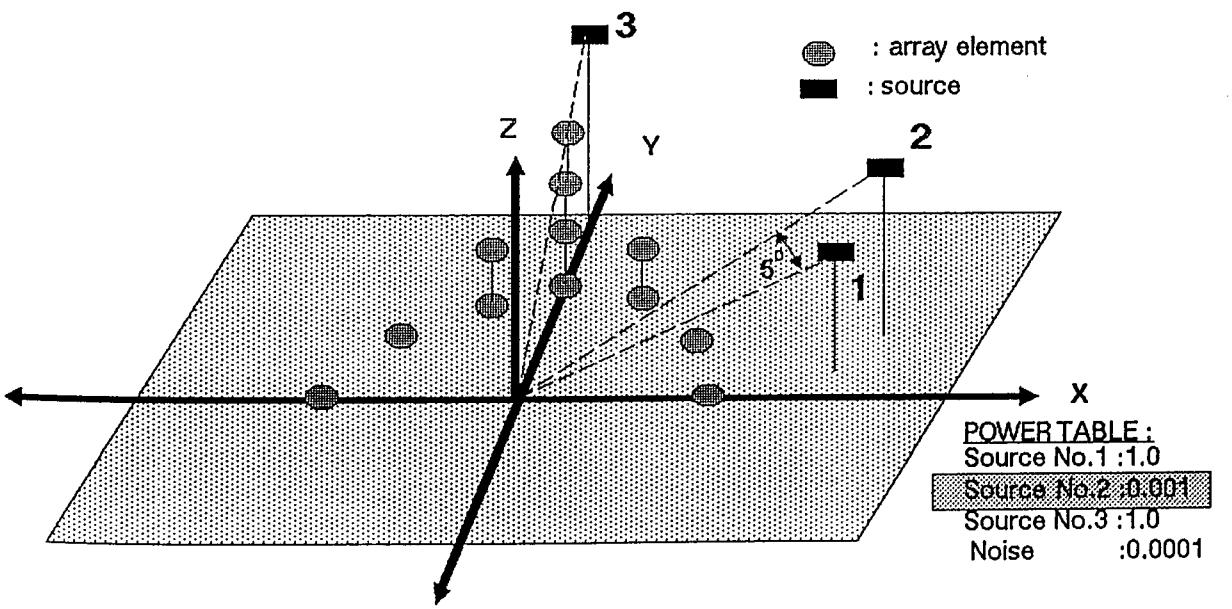

FIGURE – 4.48 (Uncorrelated Sources. Power resolution: –30dB))

	TRUE directions	INITIAL directions	directions estimated by ASPECT
source No.1	(15.0, 20.0, 30.0)	(0.0, 11.0, 100)	(15.0000,20.0000,30.0000)
source No.2	(15.0, 22.0, 45.0)	(0.0, 45.0, 100)	(15.0000,22.0000,45.0000)
source No.3	(10.0, 90.0, 65.0)	(0.0, 74.0, 100)	———
source No.4	———	(0.0, 96.0, 100)	(10.0000,90.0000,65.0000)

cost: 1.000000000000000e+000

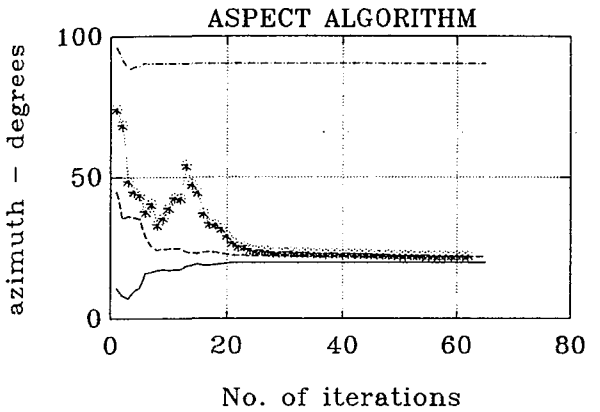

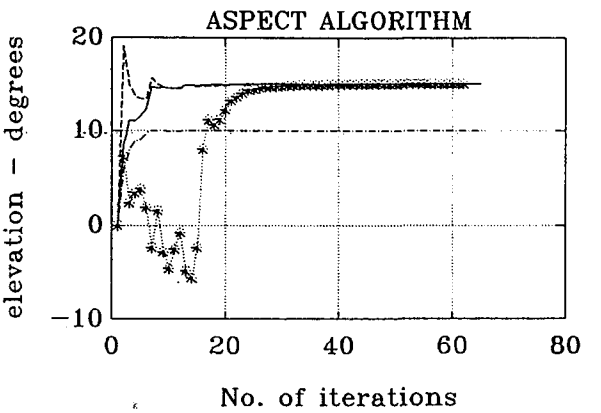

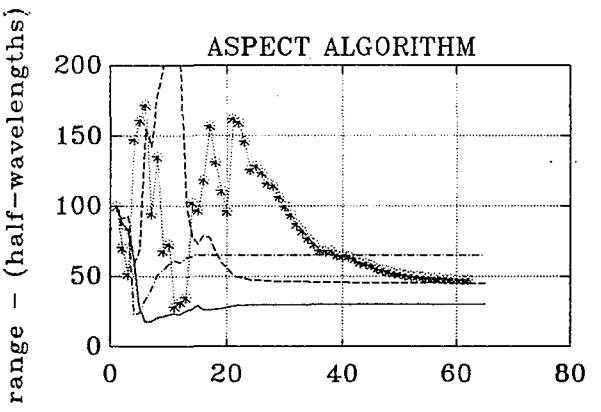

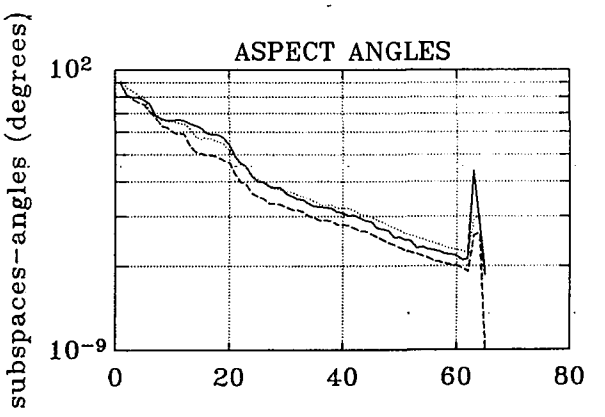

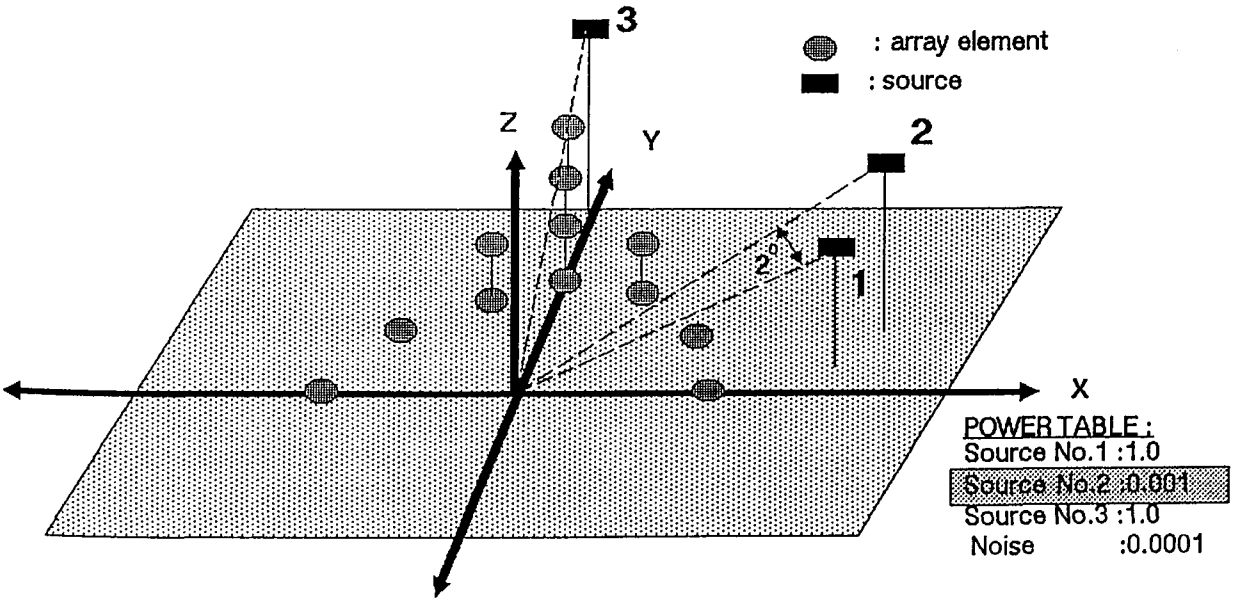

FIGURE – 4.49 (Uncorrelated Sources. Power resolution: –30dB)

	TRUE directions	INITIAL directions	directions estimated by ASPECT
source No.1	(15.0, 20.0, 30.0)	(0.0, 12.0, 100)	(15.0000,20.0000,30.0000)
source No.2	(15.0, 21.0, 45.0)	(0.0, 45.0, 100)	———
source No.3	(10.0, 90.0, 65.0)	(0.0, 74.0, 100)	(15.0000,21.0000,45.0000)
source No.4	———	(0.0, 94.0, 100)	(10.0000,90.0000,65.0000)

cost:1.000000000000000e+000

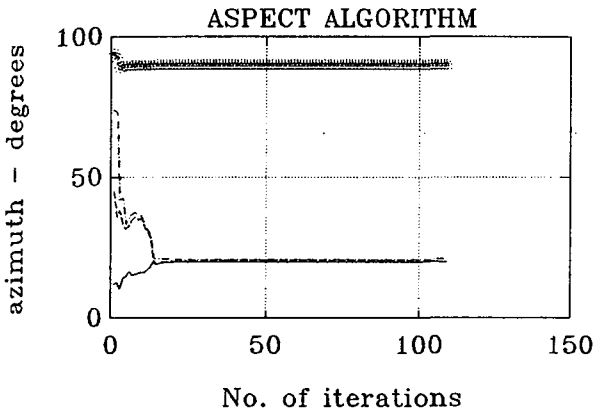

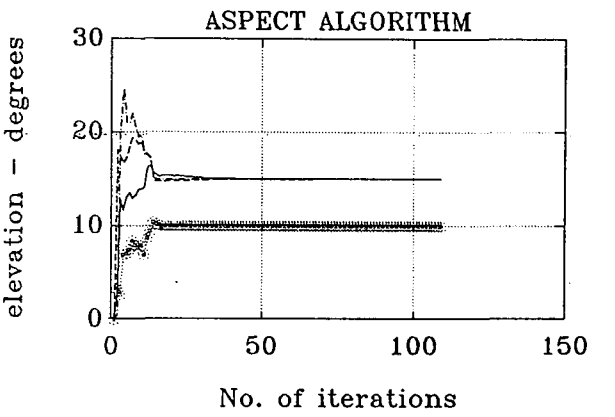

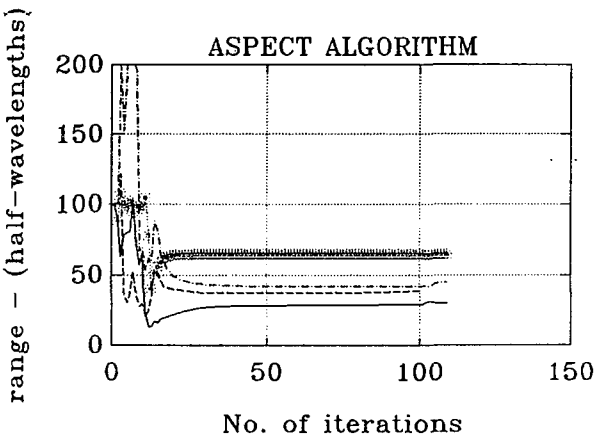

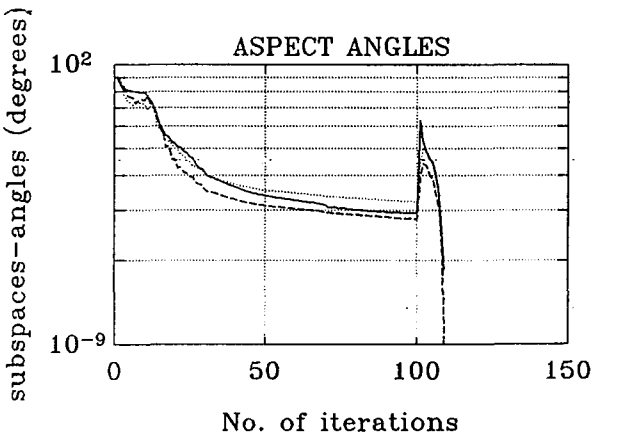

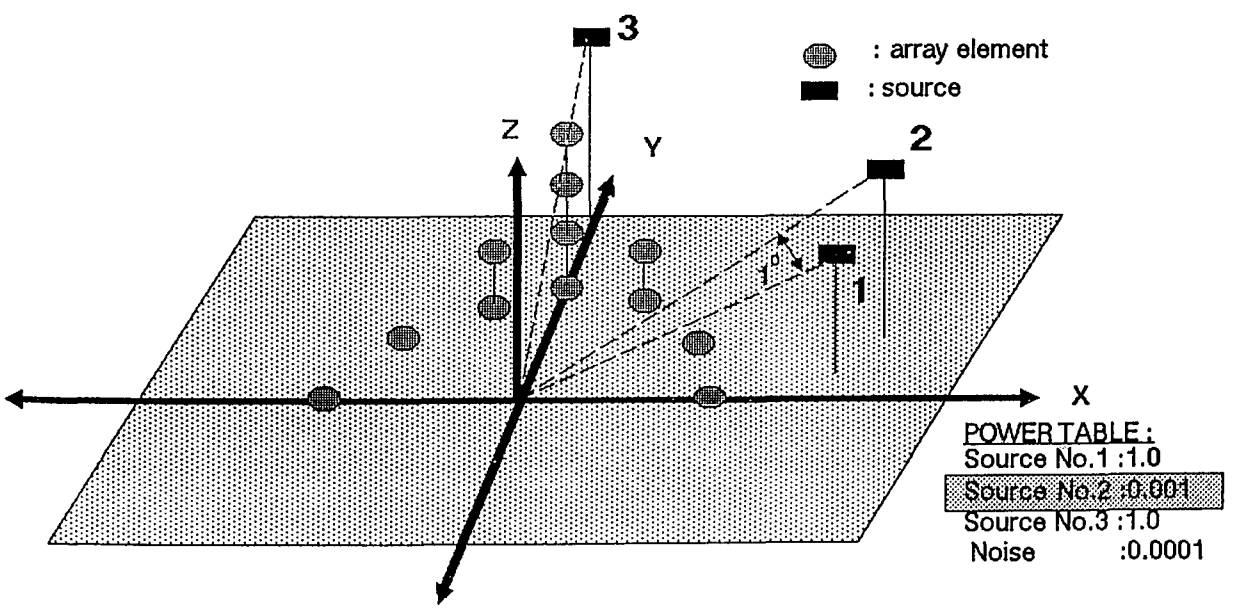

FIGURE – 4.50 (Sources No.1 and No.2 are correlated)

	TRUE directions	INITIAL directions	directions estimated by ASPECT
source No.1	(15.0, 20.0, 30.0)	(0.0, 16.0, 100)	———
source No.2	(15.0, 30.0, 45.0)	(0.0, 45.0, 100)	(15.0000,30.0000,45.0000)
source No.3	(10.0, 90.0, 65.0)	(0.0, 96.0, 100)	(10.0000,90.0000,65.0000)
source No.4	———	(0.0, 170.0, 100)	(15.0000,20.0000,30.0000)

cost:1.000000000000000e+000

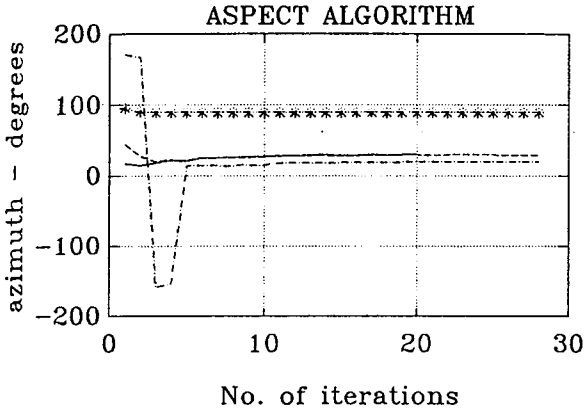

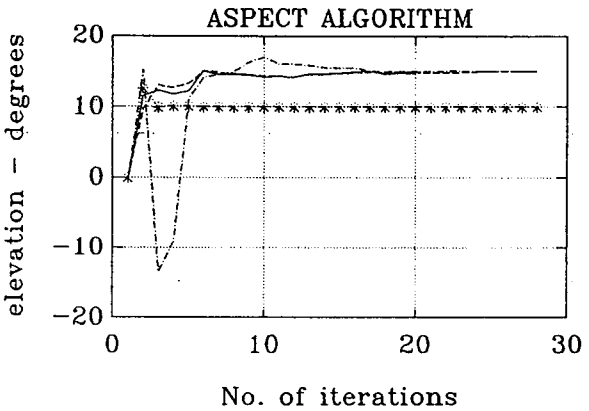

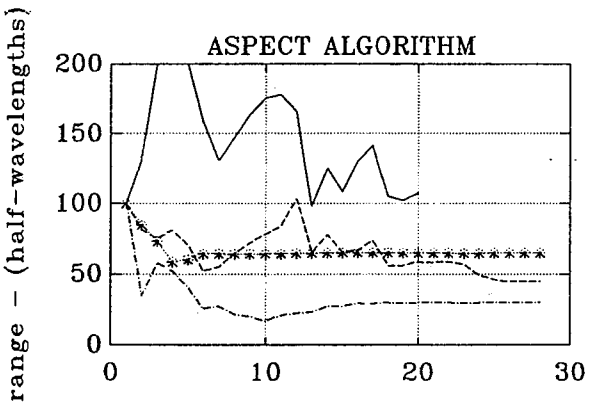

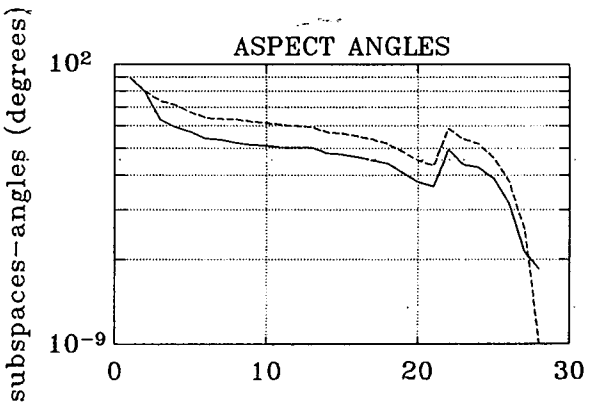

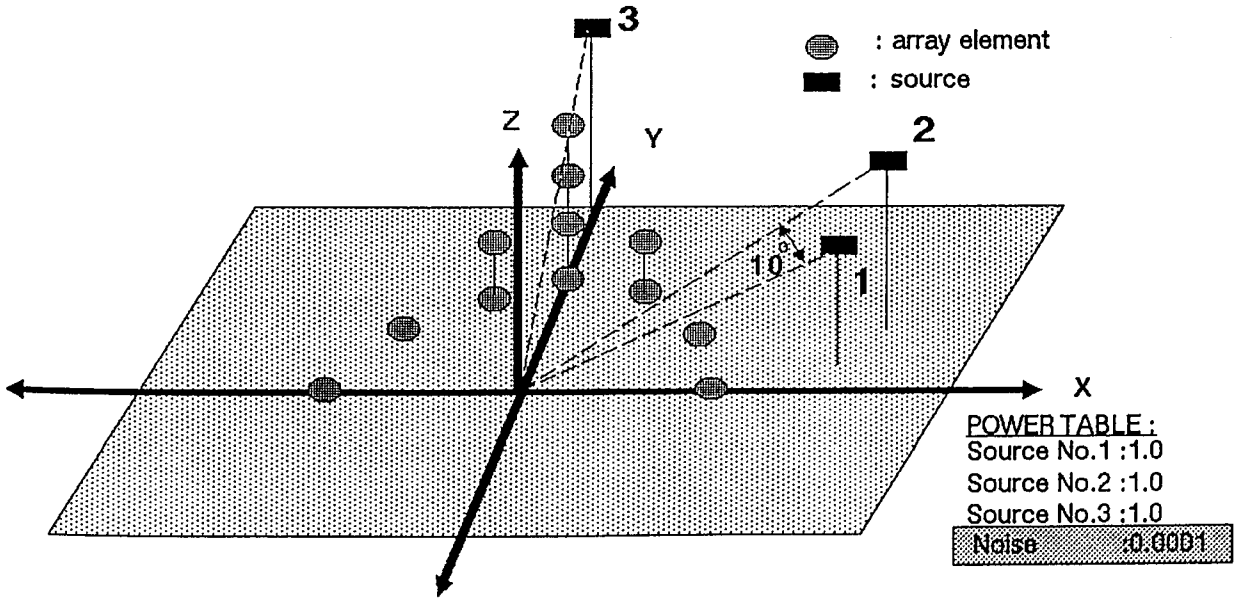

FIGURE – 4.51 (Sources No.1 and No.2 are correlated)

	TRUE directions	INITIAL directions	directions estimated by ASPECT
source No.1	(15.0, 20.0, 30.0)	(0.0, 16.0, 100)	(15.0000,20.0000,30.0000)
source No.2	(15.0, 25.0, 45.0)	(0.0, 45.0, 100)	(15.0000,25.0000,45.0000)
source No.3	(10.0, 90.0, 65.0)	(0.0, 96.0, 100)	(10.0000,90.0000,65.0000)
source No.4	———	(0.0, 169.0, 100)	———

cost:1.000000000000000e+000

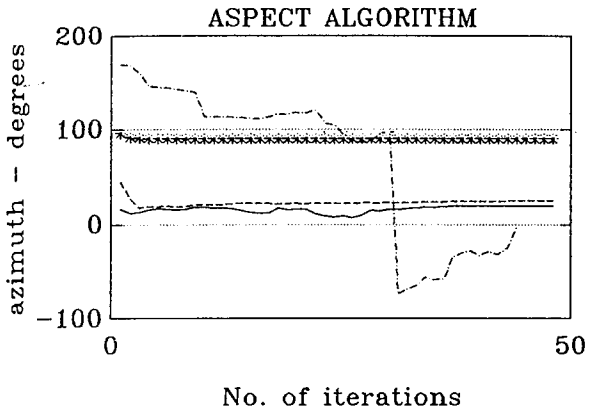

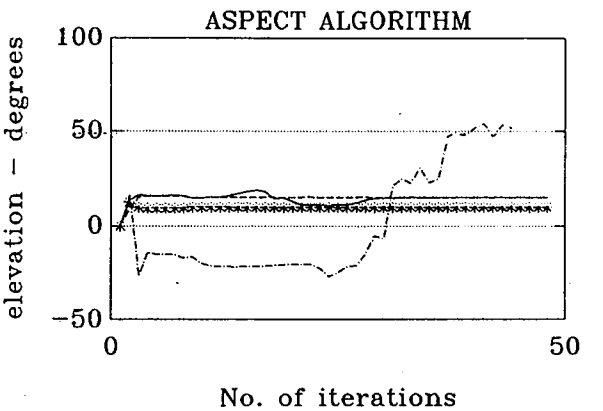

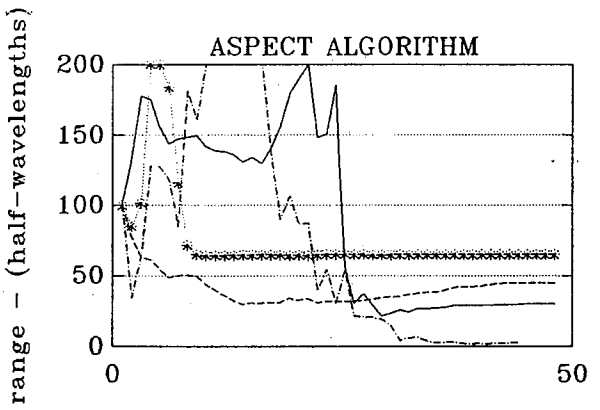

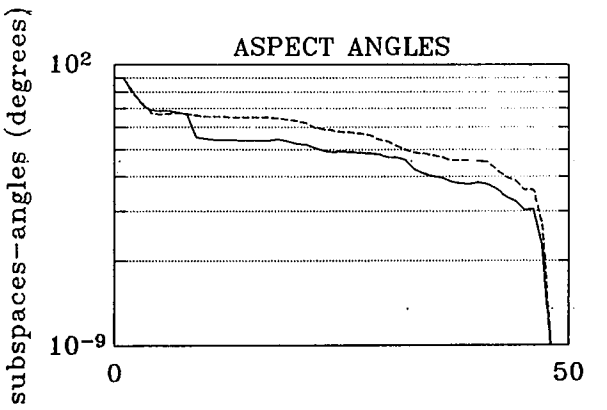

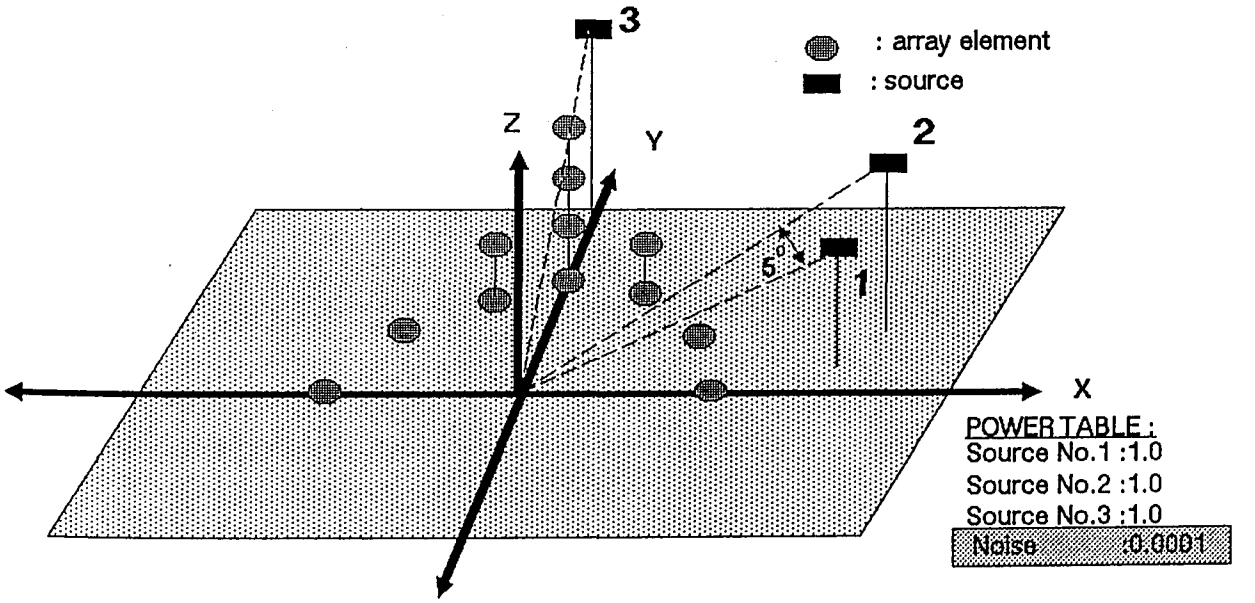

FIGURE – 4.52 (Sources No.1 and No.2 are correlated)

	TRUE directions	INITIAL directions	directions estimated by ASPECT
source No.1	(15.0, 20.0, 30.0)	(0.0, 16.0, 100)	(15.0000,19.9999,29.9998)
source No.2	(15.0, 22.0, 45.0)	(0.0, 45.0, 100)	(15.0000,21.9999,44.9989)
source No.3	(10.0, 90.0, 65.0)	(0.0, 95.0, 100)	(10.0000,90.0000,65.0000)
source No.4	———	(0.0, 169.0, 100)	———

cost:1.000000000000000e+000

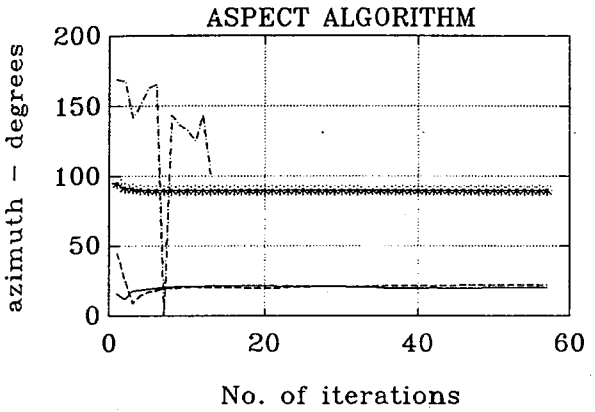

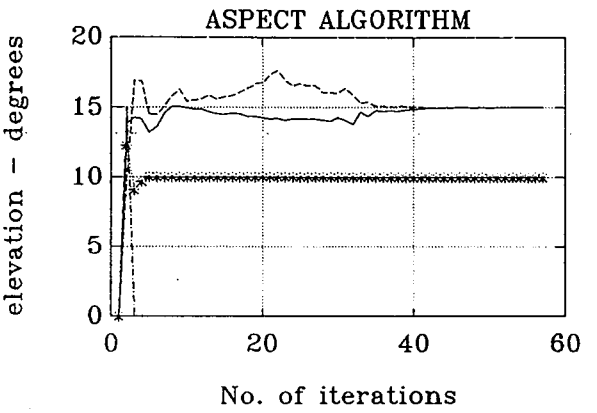

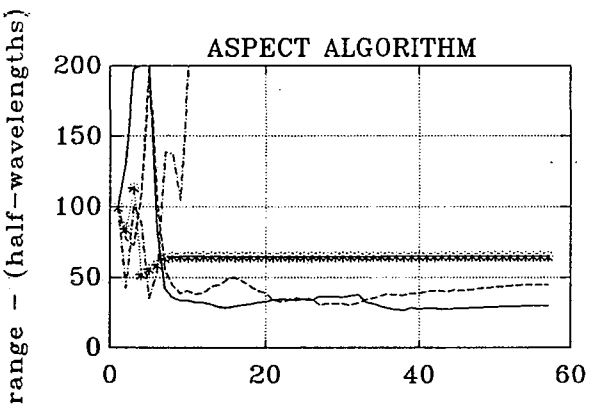

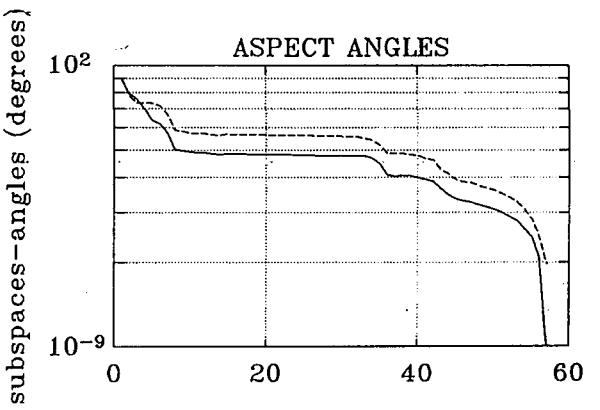

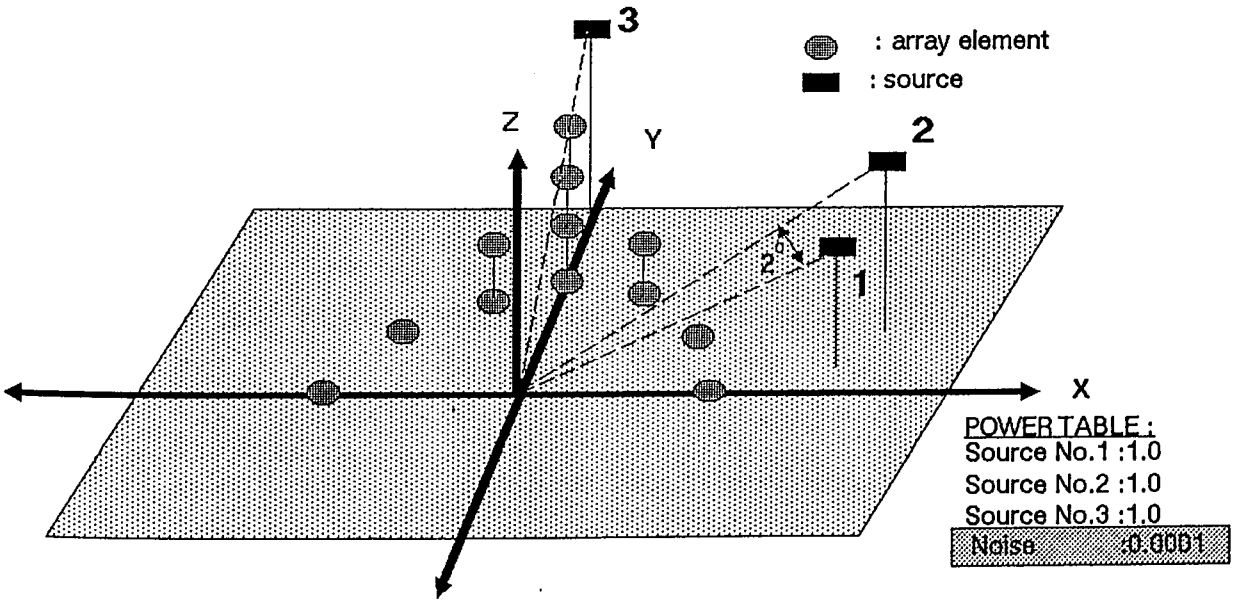

FIGURE – 4.53 (Sources No.1 and No.2 are correlated)

	TRUE directions	INITIAL directions	directions estimated by ASPECT
source No.1	(15.0, 20.0, 30.0)	(0.0, 16.0, 100)	(15.0000,20.0000,30.0000)
source No.2	(15.0, 21.0, 45.0)	(0.0, 45.0, 100)	(15.0000,21.0000,44.9999)
source No.3	(10.0, 90.0, 65.0)	(0.0, 95.0, 100)	(10.0000,90.0000,65.0000)
source No.4	———	(0.0,169.0,100)	———

cost:1.000000000000000e+000

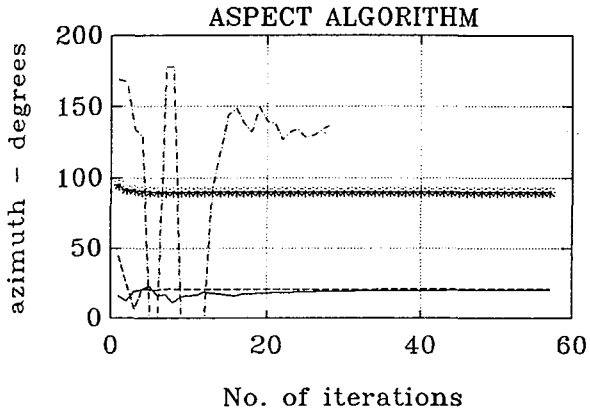

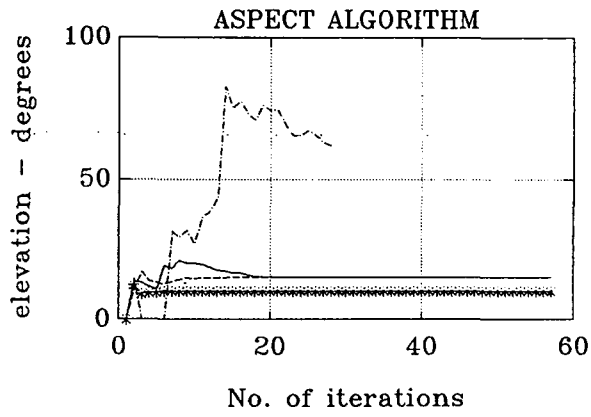

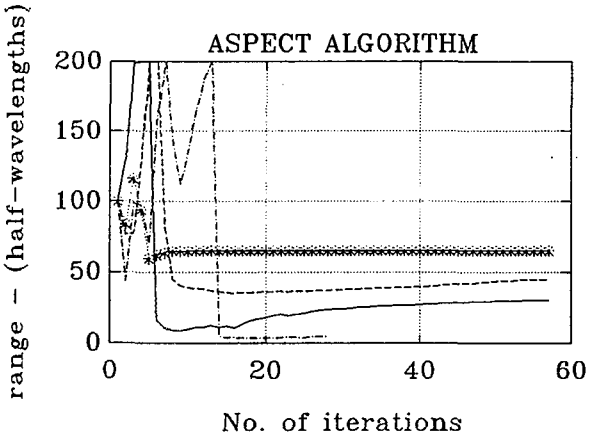

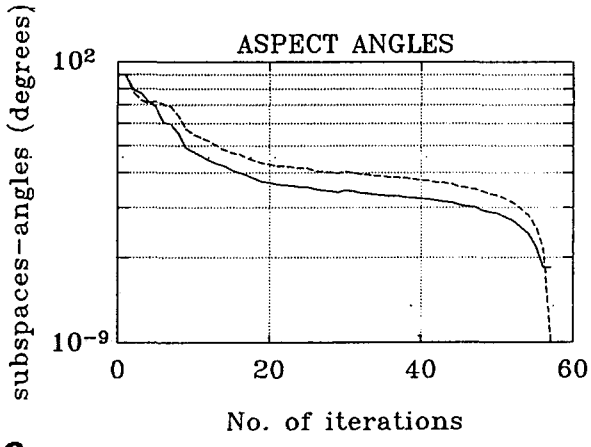

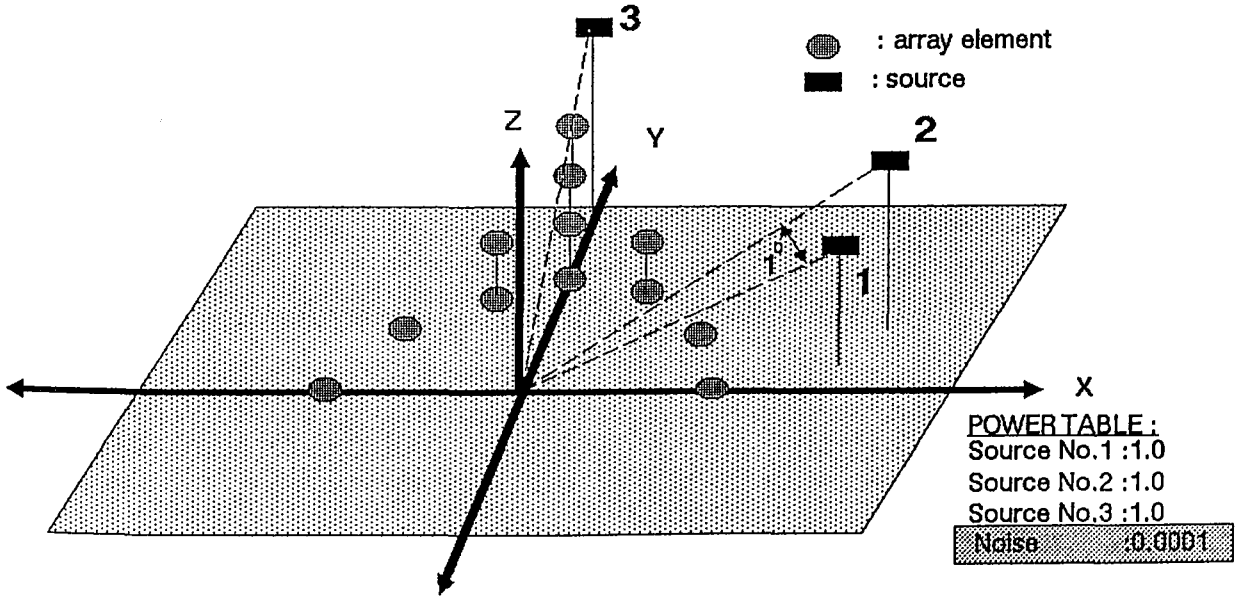

FIGURE – 4.54 (Sources No.1 and No.2 are correlated. Power Resolution: –30dB)

	TRUE directions	INITIAL directions	directions estimated by ASPECT
source No.1	(15.0, 20.0, 30.0)	(0.0, 14.0, 100)	(15.0000,30.0000,45.0000)
source No.2	(15.0, 30.0, 45.0)	(0.0, 45.0, 100)	(15.0000,20.0000,30.0000)
source No.3	(10.0, 90.0, 65.0)	(0.0, 95.0, 100)	(10.0000,90.0000,65.0000)
source No.4	———	(0.0, 169.0,100)	———

cost:1.000000000000000e+000

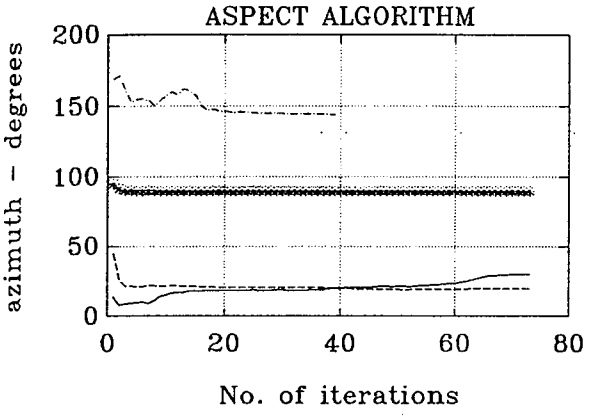

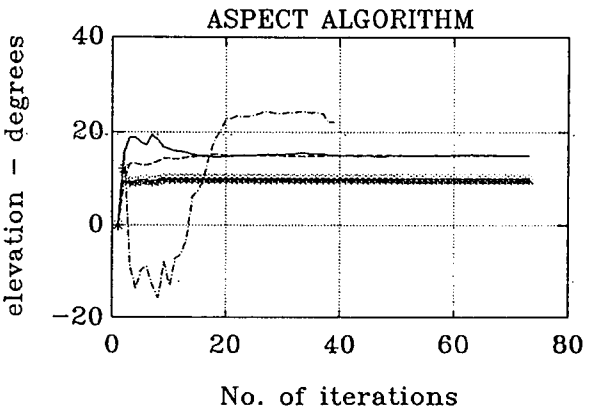

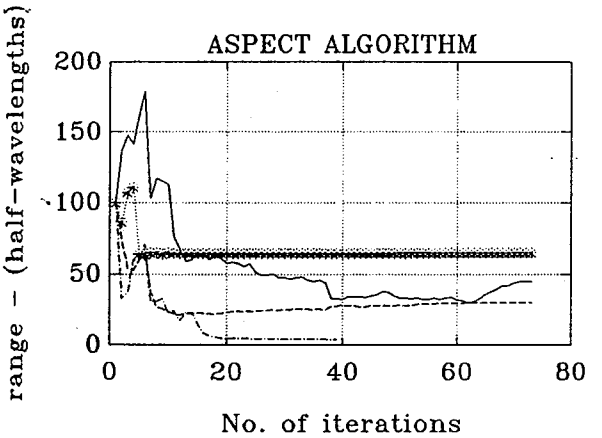

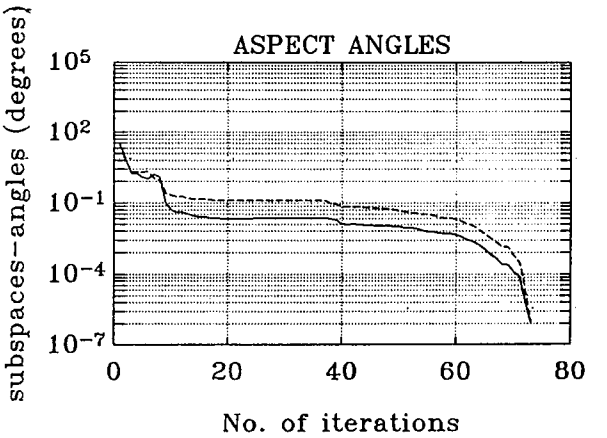

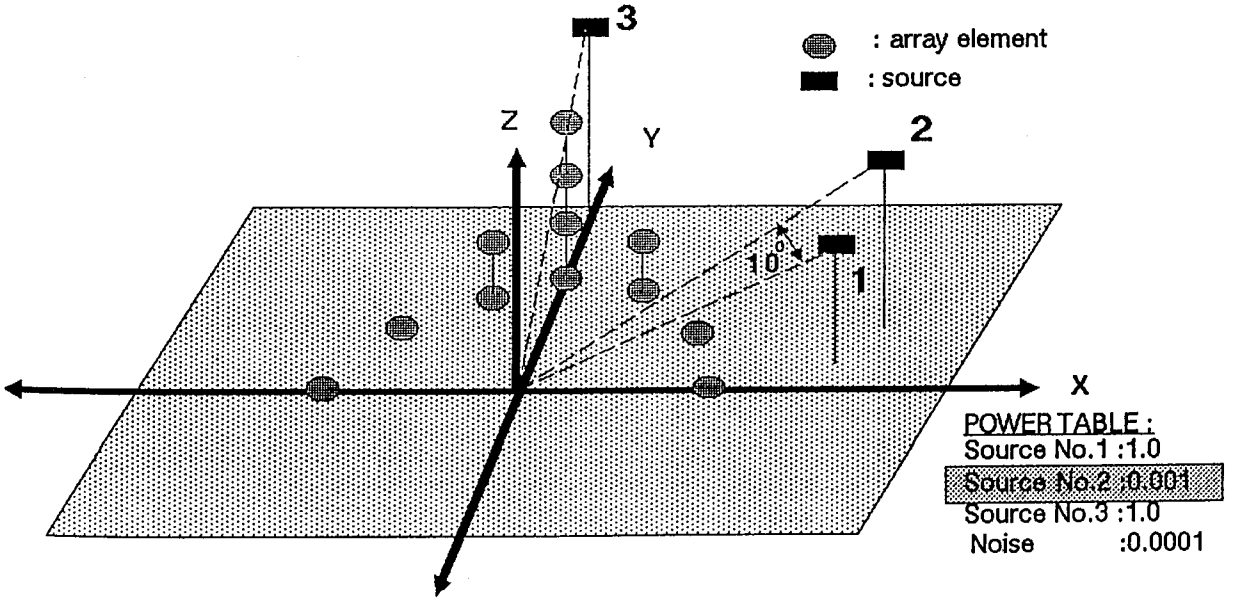

FIGURE – 4.55 (Sources No.1 and No.2 are correlated. Power resolution: –30dB)

	TRUE directions	INITIAL directions	directions estimated by ASPECT
source No.1	(15.0, 20.0, 30.0)	(0.0, 14.0, 100)	(15.0000,20.0000,30.0000)
source No.2	(15.0, 25.0, 45.0)	(0.0, 45.0, 100)	(15.0000,25.0004,45.0031)
source No.3	(10.0, 90.0, 65.0)	(0.0, 95.0, 100)	(10.0000,90.0000,65.0000)
source No.4	———	(0.0, 169.0,100)	———

cost: 1.000000000000000e+000

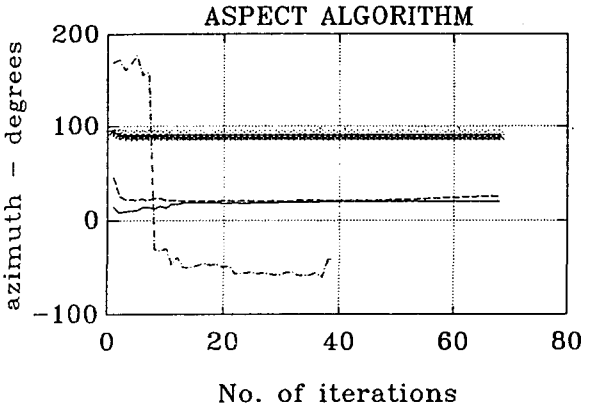

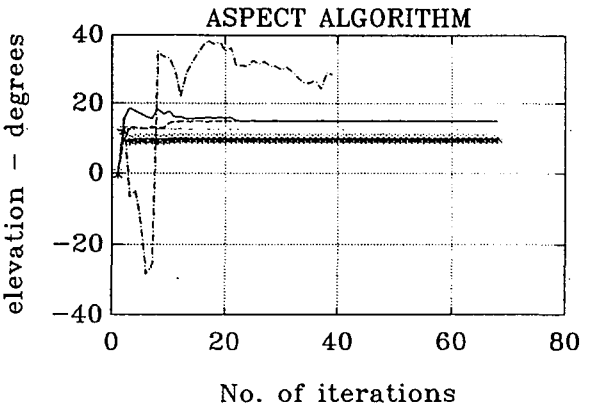

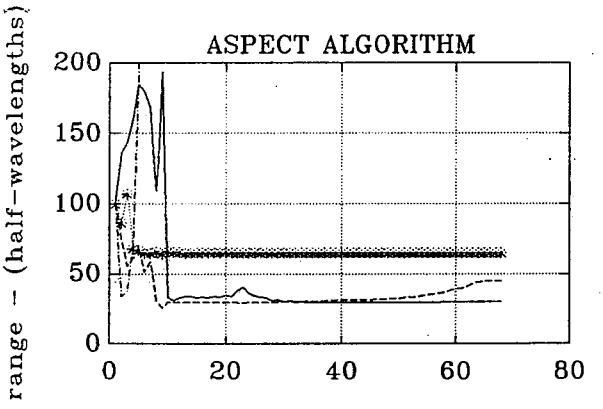

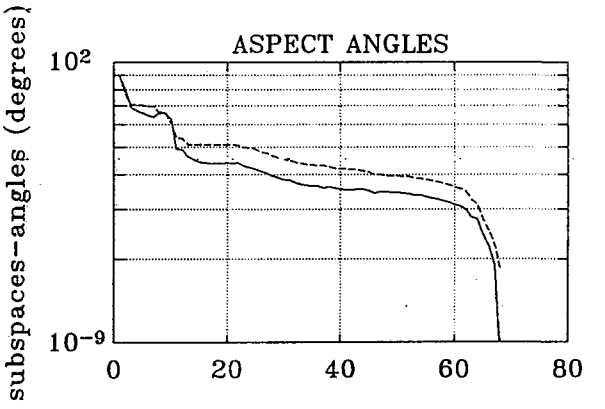

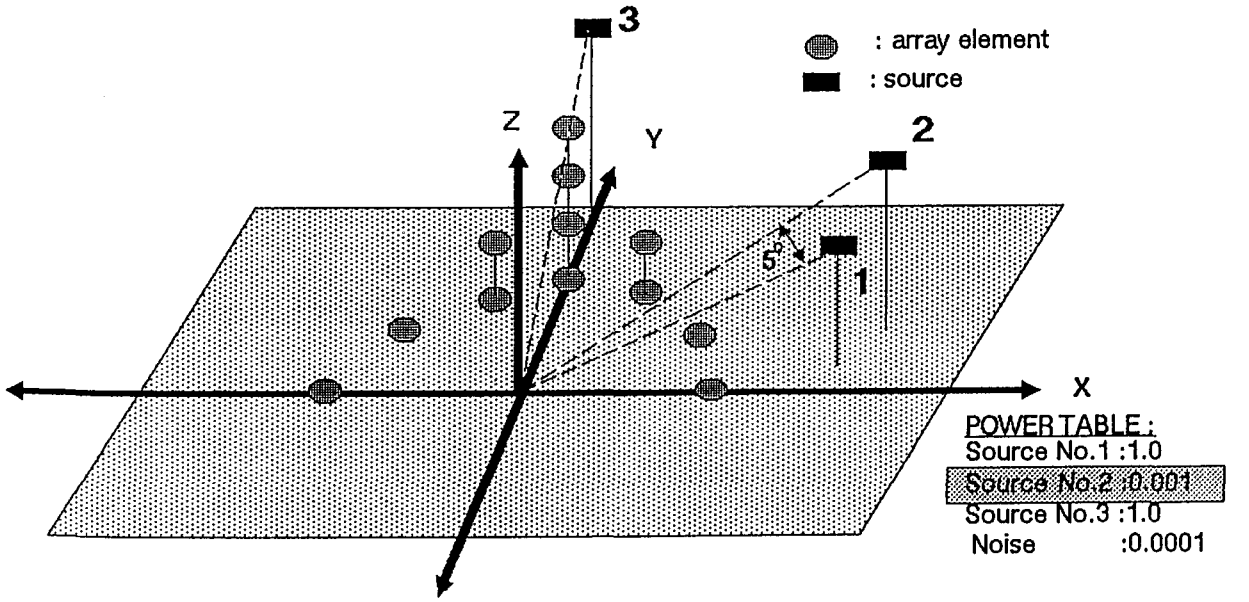

FIGURE – 4.56 (Sources No.1 and No.2 are correlated. Power Resolution: –30dB)

	TRUE directions	INITIAL directions	directions estimated by ASPECT
source No.1	(15.0, 20.0, 30.0)	(0.0, 14.0, 100)	(15.0000,22.0005,45.0053)
source No.2	(15.0, 22.0, 45.0)	(0.0, 45.0, 100)	(15.0000,20.0000,30.0000)
source No.3	(10.0, 90.0, 65.0)	(0.0, 95.0, 100)	(10.0000,90.0000,65.0000)
source No.4	——	(0.0, 169.0, 100)	——

cost:1.000000000000000e+000

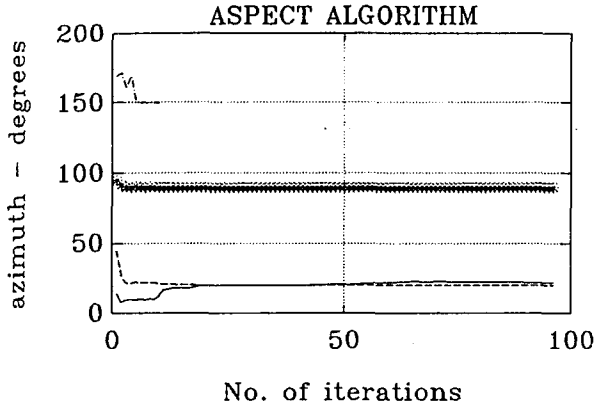

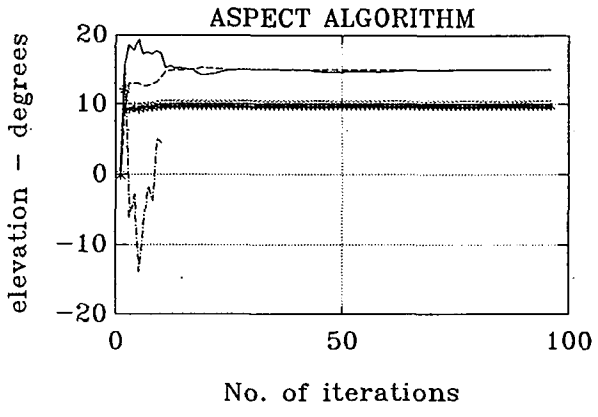

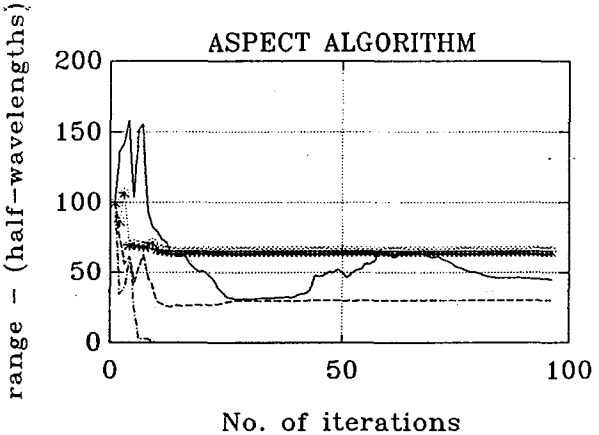

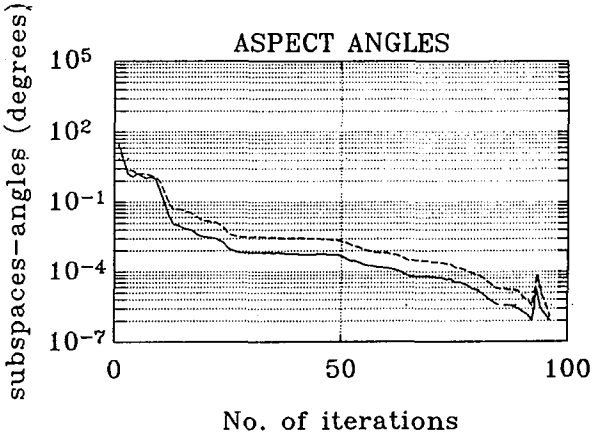

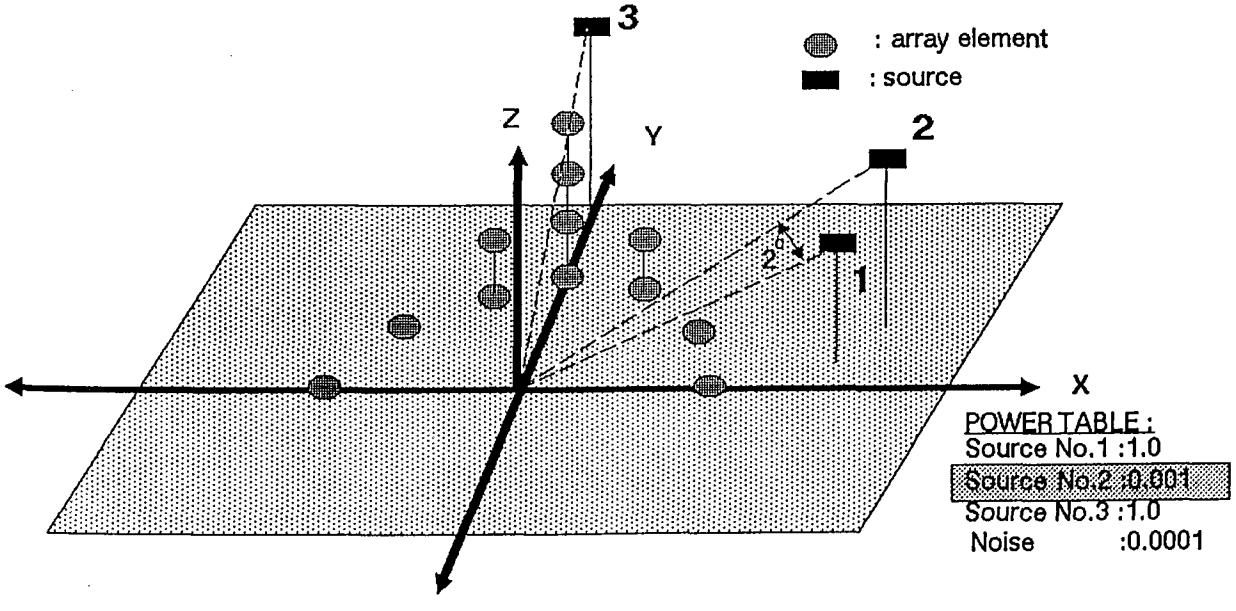

FIGURE – 4.57 (Sources No.1 and No.2 are correlated. Power resolution: – 30dB)

	TRUE directions	INITIAL directions	directions estimated by ASPECT
source No.1	(15.0, 20.0, 30.0)	(0.0, 14.0, 100)	(14.9999,21.0018,45.0540)
source No.2	(15.0, 21.0, 45.0)	(0.0, 45.0, 100)	(15.0000,20.0001,30.0004)
source No.3	(10.0, 90.0, 65.0)	(0.0, 95.0, 100)	(10.0000,90.0000,65.0000)
source No.4	———	(0.0,169.0,100)	———

cost: 1.000000000000000e + 000

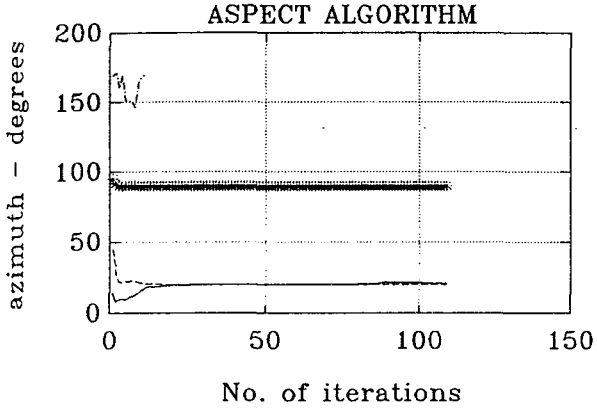

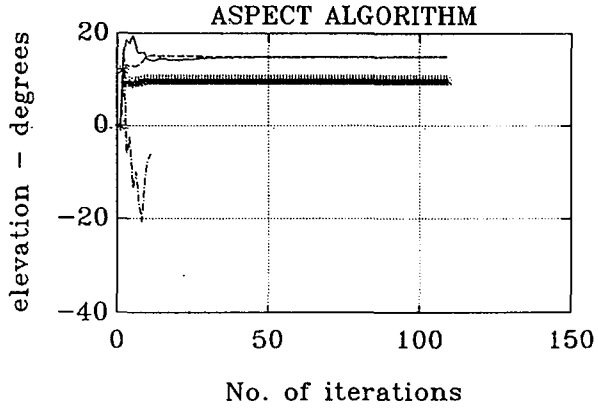

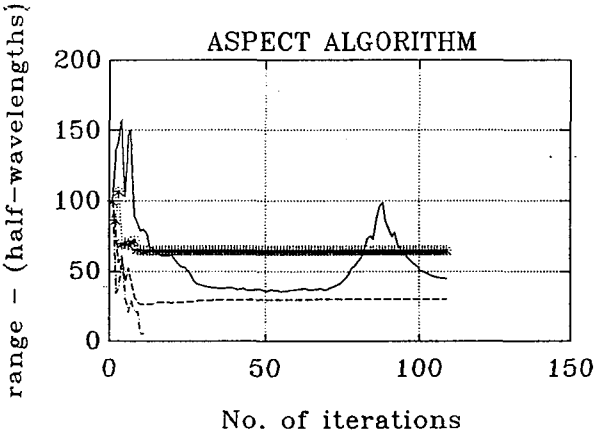

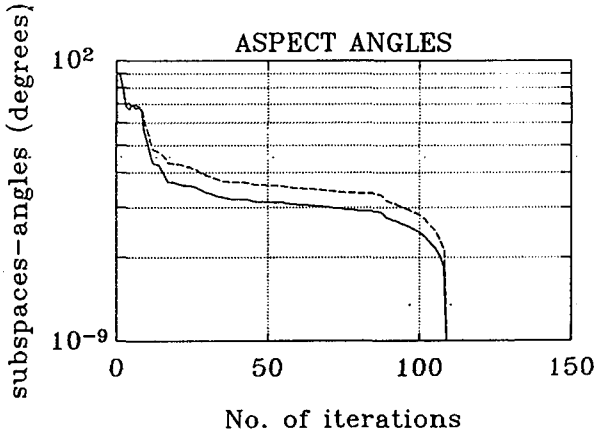

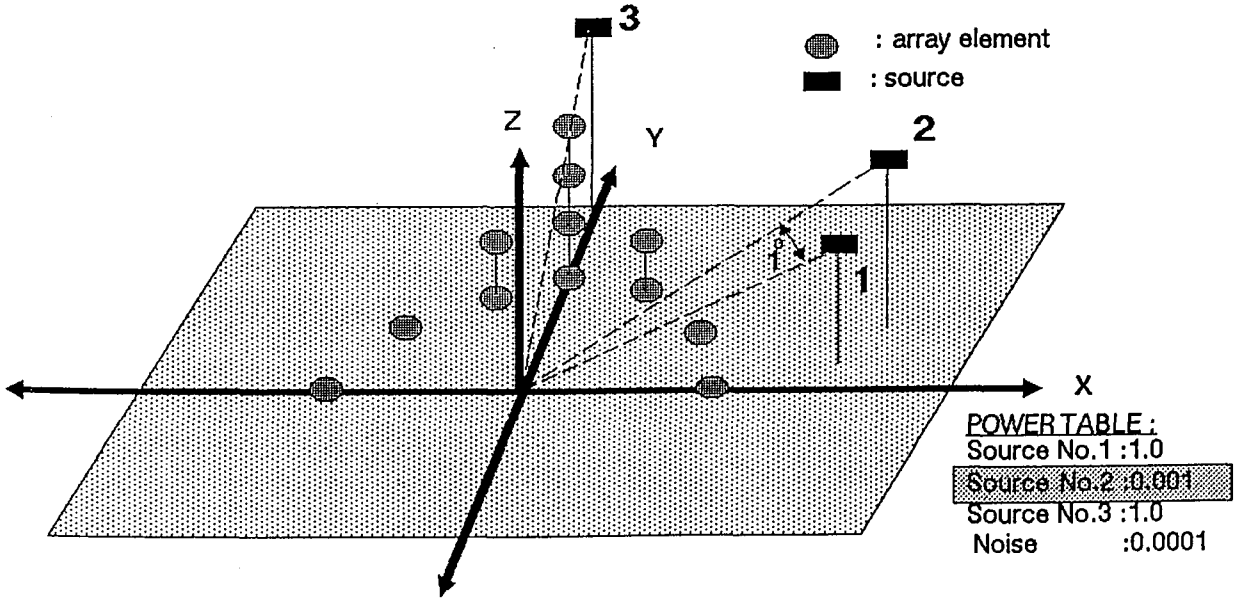

4.6 SPATIAL SMOOTHING

In this section an example of Spatial Smoothing Technique, as it has proposed by Shan, Wax and Kailath [SHA-85], is presented and compared with ASPECT. Since Shan's technique operates only in a linear array environment, an array of seven uniformly distributed isotropic elemements is considered in the presence of three coherent signals incident to the array from direction, originally, 40°, 90°, and 135° and then from directions 40°, 42° and 90°. The array elements were spaced one half wavelength apart. The algorithm uses four subarrays, with each subarray having four elements. The results are shown in *Figure* 4.58 and 4.59 together with results for MUSIC algorithm for those two set of incident signals. *Figure* 4.58 shows that when the sources are well separated the Spatial Smoothing Technique restores the rank of the matrix $\mathbf{R}_{mm}$ and provides unbiased estimates of the locations of the emitting sources. However when these sources are close together this restoration of the rank is not very good as that illustrated by the eigenvalues provided in *Figure* 4.59. This leads to failure of *Spatial Smoothing Technique* to detect and locate some of the incident. Thus in the current example this technique fails to detect and estimate the signal incident from 40° and 42° althought it detects and estimated the location of the third one. In both the above mentioned figures, the failure of MUSIC is illustrated clearly. Next ASPECT is tested for the above two signal environments. Its behaviour is illustrated in *Figures* 4.61 and 4.62 showing that ASPECT outperforms to *Spatial Smoothing Technique* in a linear array situation.

FIGURE – 4.58

MUSIC ALGORITHM and SPATIAL SMOOTHING TECHNIQUE
FOR THREE FULLY CORRELATED SOURCES, WELL SEPARATED IN SPACE

eigen-values of $\mathbf{R}_{xx}$ when the MUSIC algorithm is used :

13.9150 0.1000 0.1000 0.1000 0.1000 0.1000 0.1000

signal subspace ←↑→noise subspace

eigen-values of $\mathbf{R}_{xx}$ when spatial smoothing technique is used :

5.963 3.5953 0.6027 0.1000

signal subspace ←↑→noise subspace

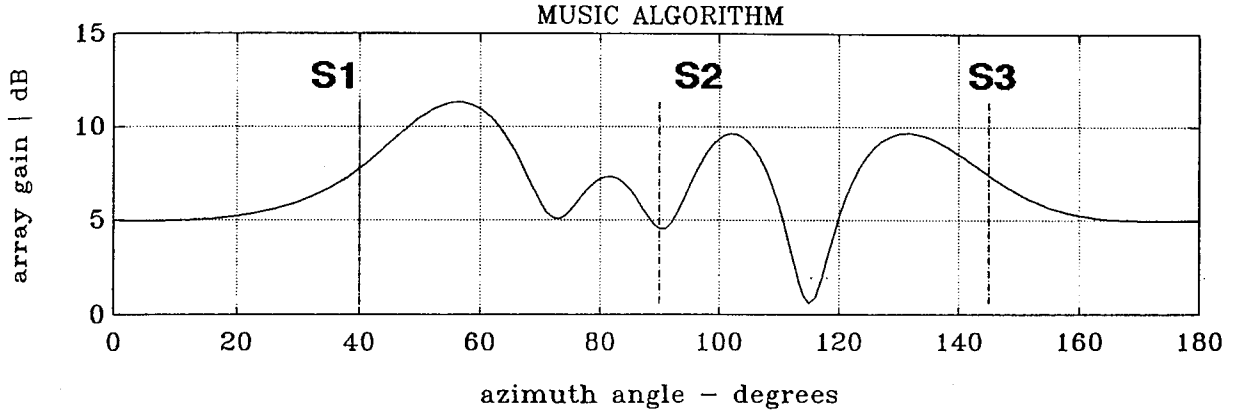

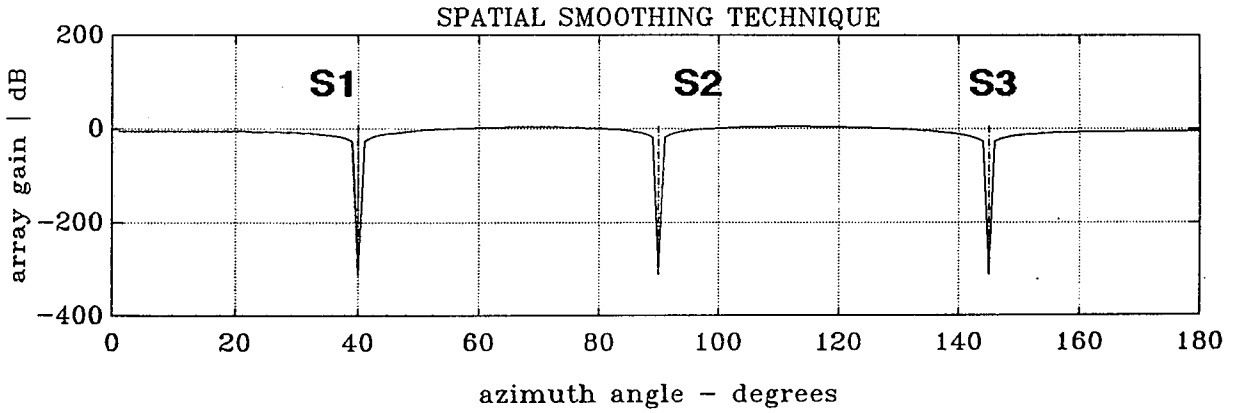

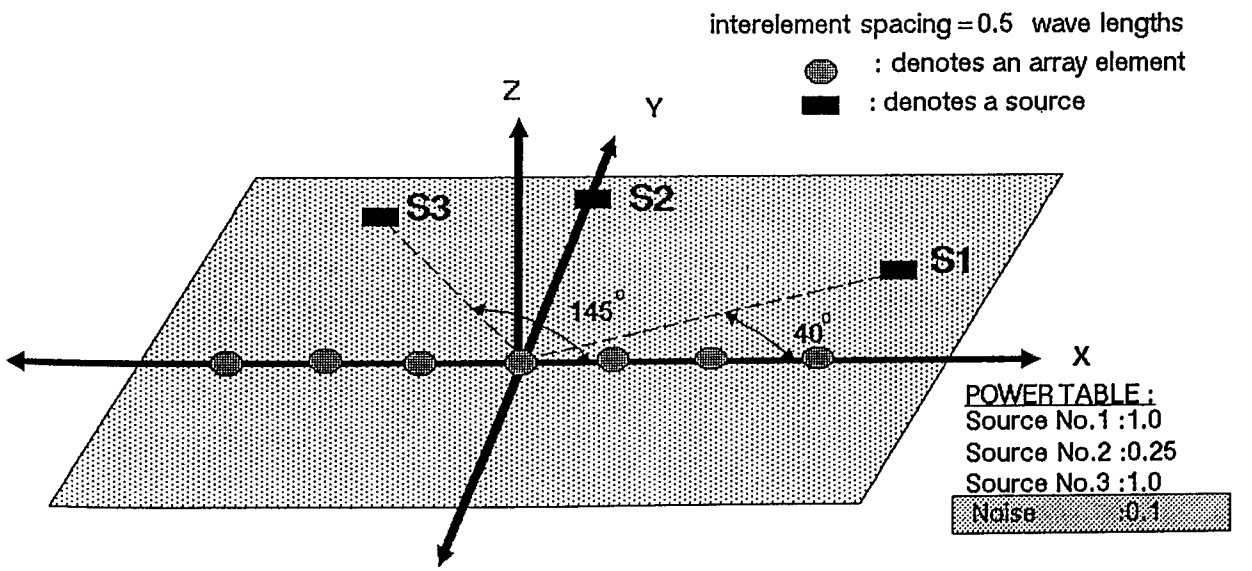

FIGURE – 4.59

MUSIC ALGORITHM and SPATIAL SMOOTHING TECHNIQUE
FOR THREE FULLY CORRELATED SOURCES
(Two of the sources are located close together)

eigen-values of $\mathbf{R}_{xx}$ when the MUSIC algorithm is used :

31.6412 0.1000 0.1000 0.1000 0.1000 0.1000 0.1000

signal subspace ←↑→noise subspace

eigen-values of $\mathbf{R}_{xx}$ when spatial smoothing technique is used :

16.8062 0.9213 0.1000 0.1000

signal subspace ←↑→noise subspace

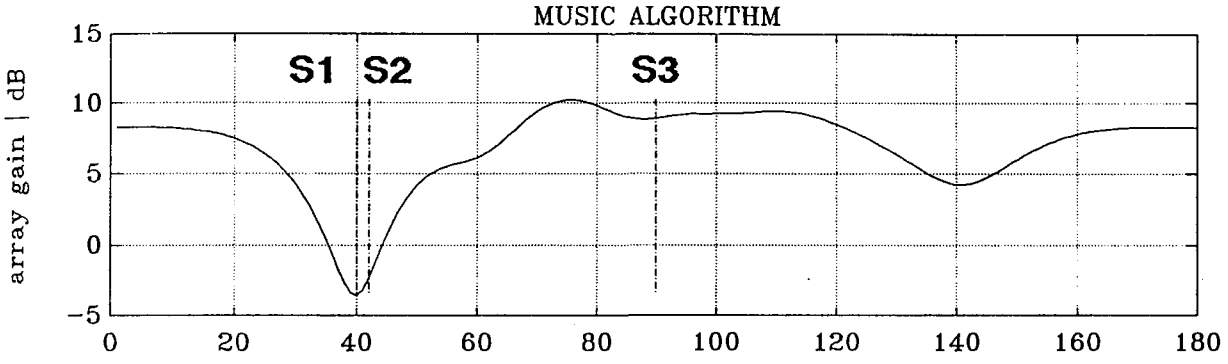

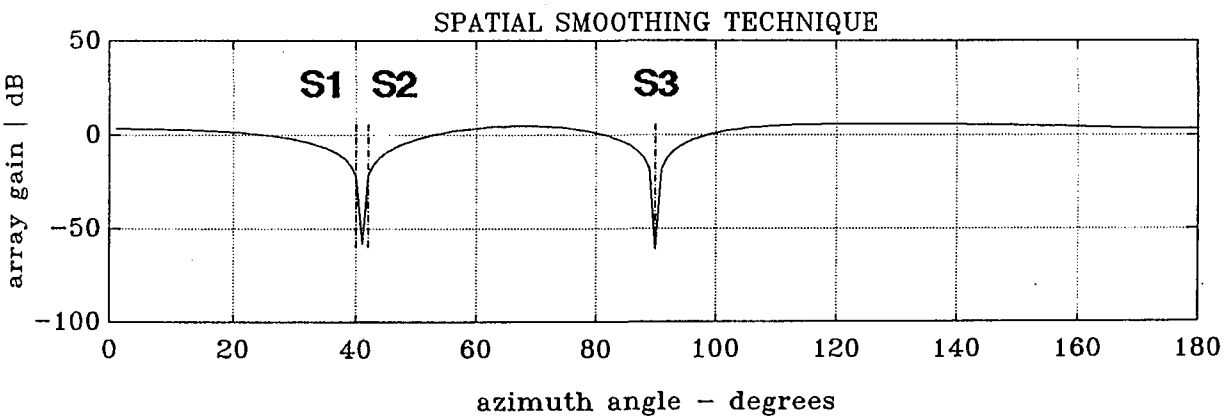

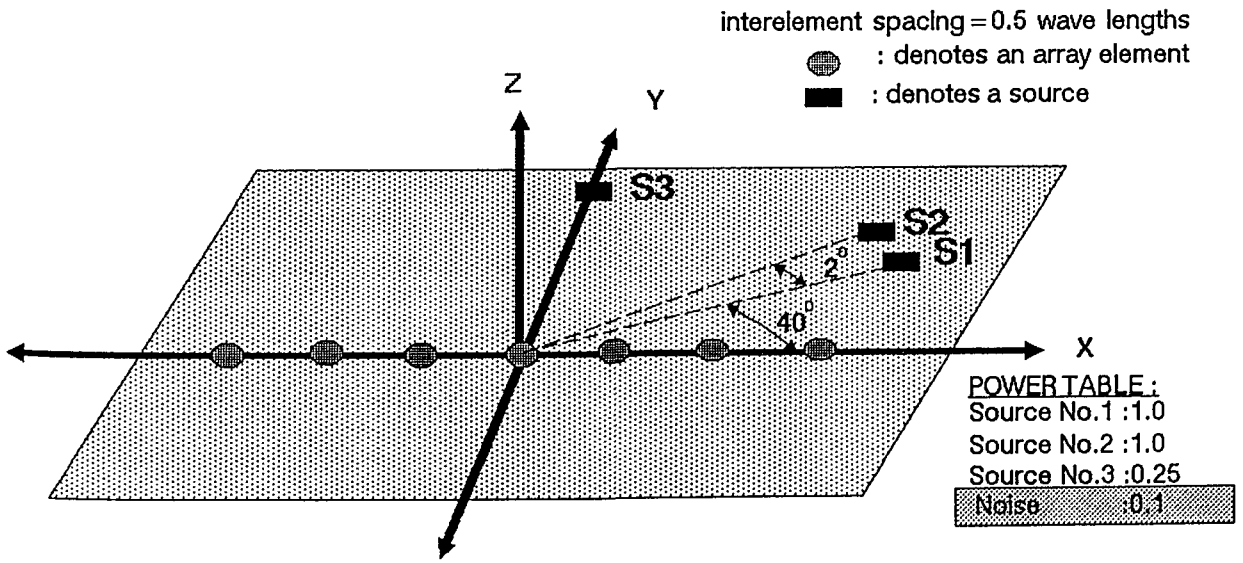

FIGURE – 4.60 ASPECT FOR THREE FULLY CORRELATED SOURCES, WELL SEPARATED IN SPACE

	TRUE directions	INITIAL directions	directions estimated by ASPECT
source No.1	(0.0, 40.0)	(0.0,15.0)	(0.0000, 40.0000)
source No.2	(0.0, 90.0)	(0.0,65.0)	———
source No.3	(0.0,145.0)	(0.0,100.0)	(0.0000, 90.0000)
source No.4	———	(0.0,165.0)	(0.0000, 145.0000)

cost:1.000000000000000e+000

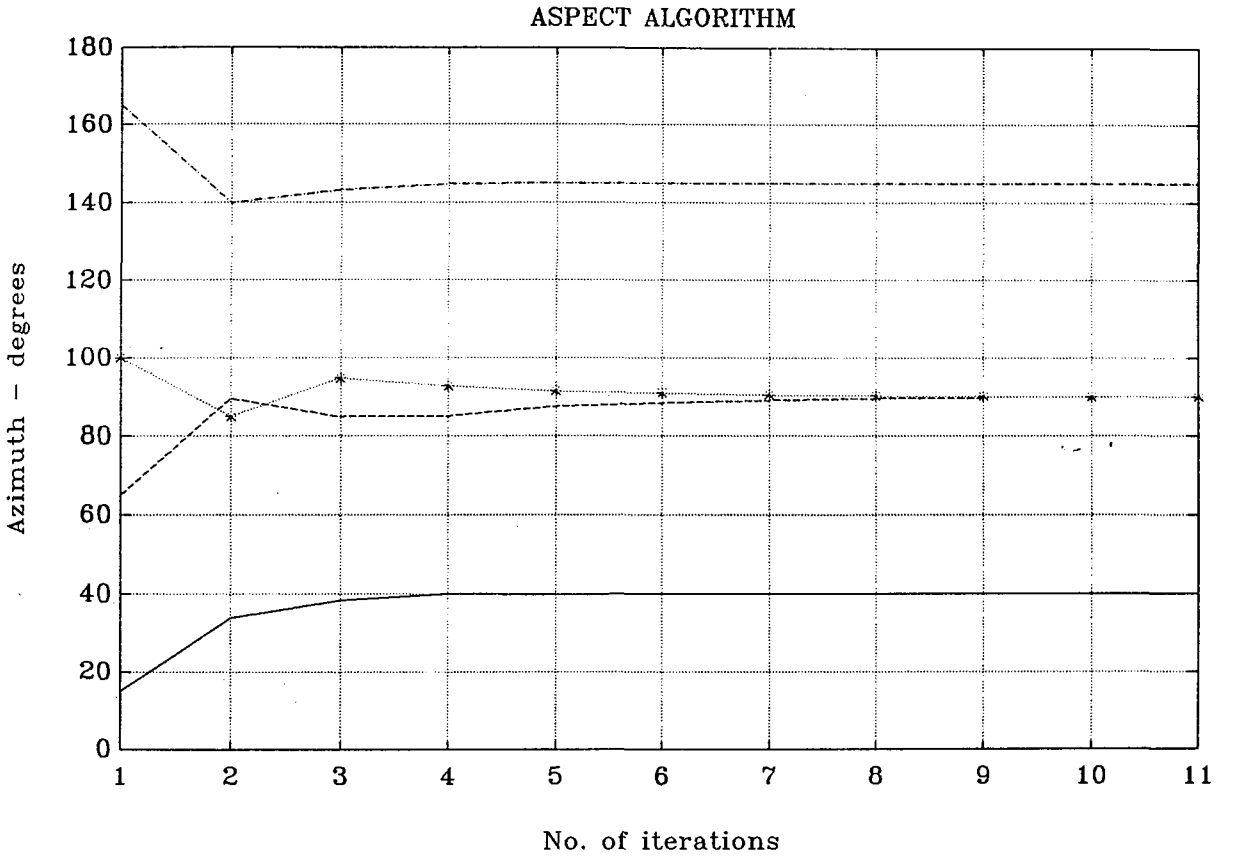

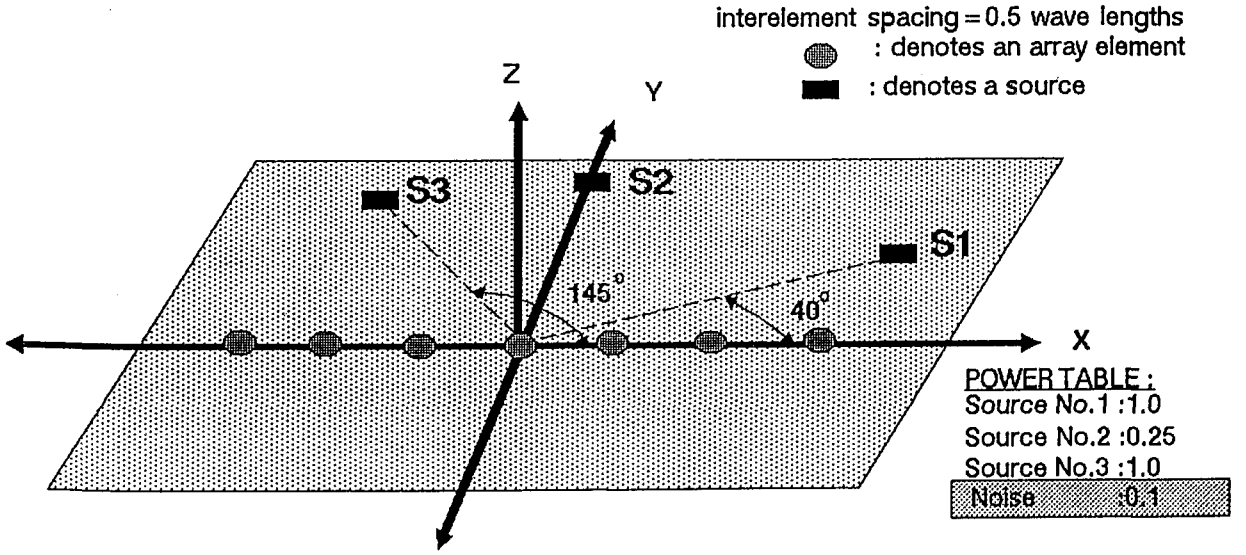

FIGURE – 4.61 ASPECT FOR THREE FULLY CORRELATED SOURCES
(two of the sources are located close together)

	TRUE directions	INITIAL directions	directions estimated by ASPECT
source No.1	(0.0, 40.0)	(0.0,15.0)	(0.0000, 40.0000)
source No.2	(0.0, 42.0)	(0.0,65.0)	(0.0000, 42.0000)
source No.3	(0.0, 90.0)	(0.0,100.0)	(0.0000, 90.0000)
source No.4	———	(0.0,165.0)	———

cost: 1.000000000000000e+000

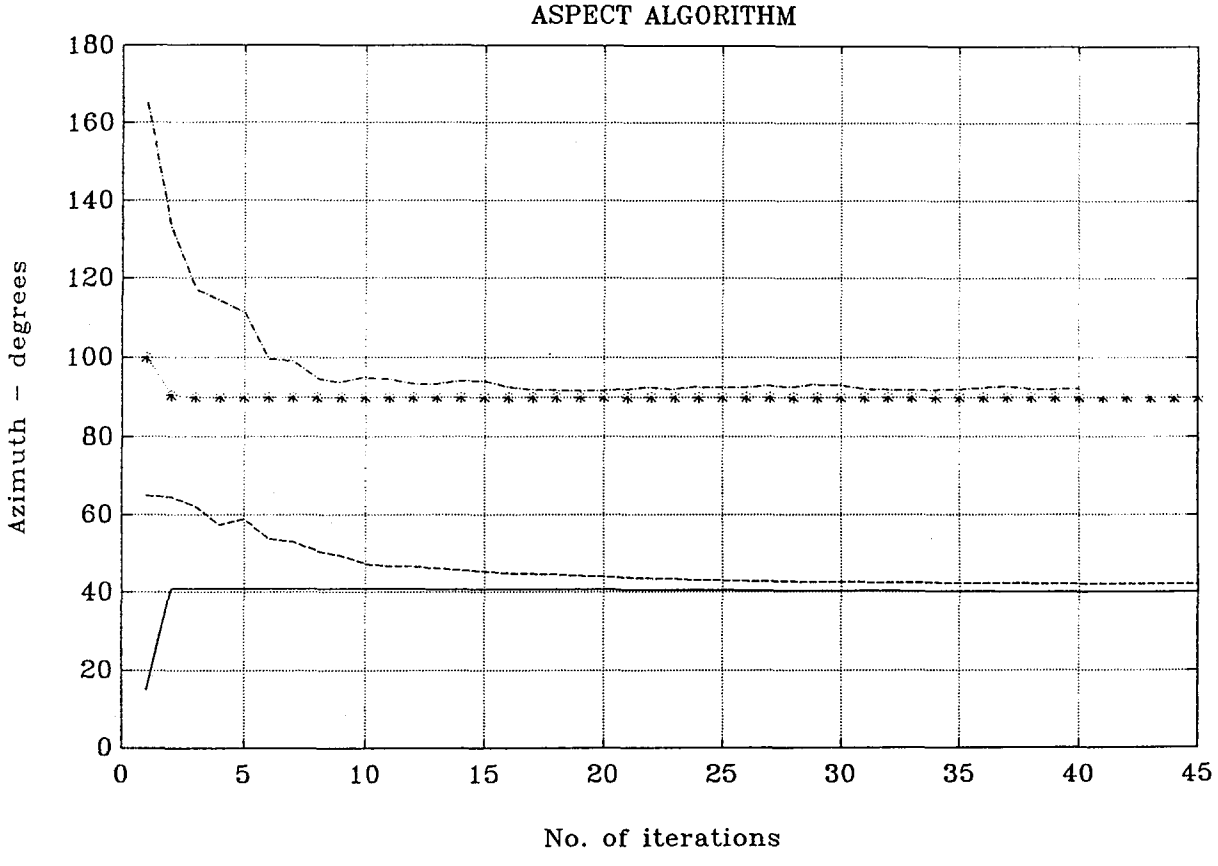

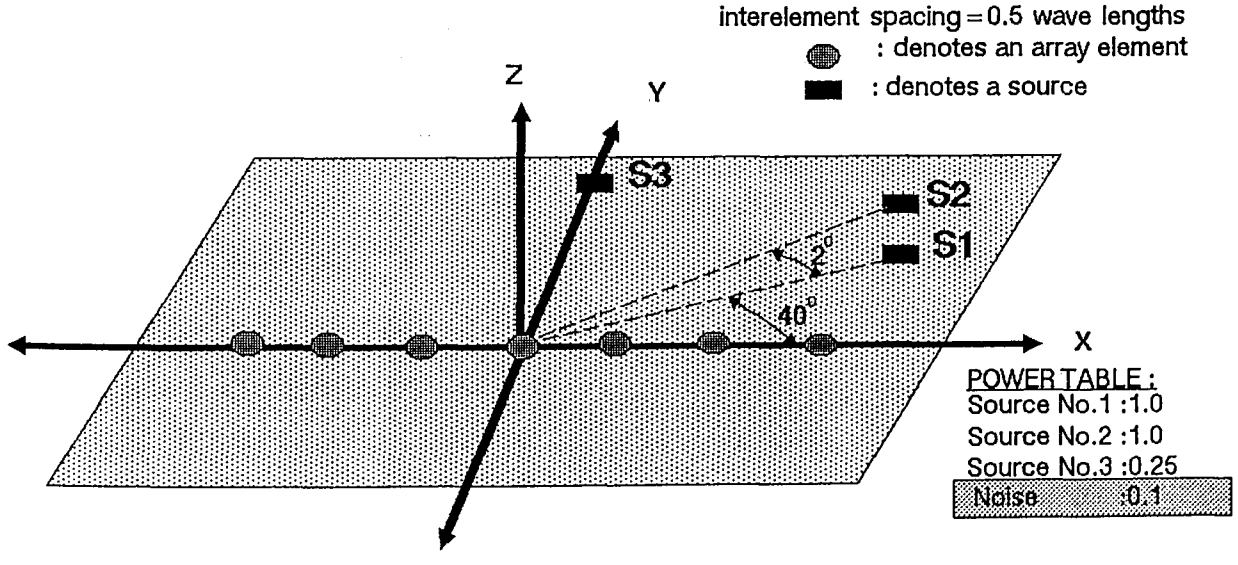

4.7 CONCLUSIONS

This chapter reports on a number of computer simulation tests that have been performed in order to assess the performance and limitations of the ASPECT algorithm presented in the previous chapter. Examples of signal environments examined are concerned with *i*) a number of uncorrelated emitting signal sources and *ii*) a mix of correlated and uncorrelated emitting signal sources.

In the majority of tests which involve uncorrelated sources, ASPECT correctly detects, resolves and estimates the directions of incident signals. However, when there are incident signals which are located close together and at the same time of widelly differing power levels then ASPECT detects the weak signal but loses accuracy when estimating its direction. However, it provides accurate estimates of the remaining sources.

In an environment involving correlated (coherent), sources ASPECT maintains its immunity with respect to noise level. In addition when there are weak and strong correlated signals present ASPECT, although detecting these signals, seems to looses accuracy when it estimates the direction of the weak signal. The loss of accuracy is greater than in the uncorrelated case.

Summarising the results obtained so far, it can be said that this precision is altered when

- the angle separation between sources is small,
- the sources are correlated,
- the sources are of widely differing power levels,

• the observation time is small (see an example in *Appendix* 4).

The problem is further complicated by the parallel existance of more than one of the above cases.

The limitations imposed on the algorithm are as a result of two factors:

1) by the accuracy of the estimated eigenvectors which anyway depends on the conditioning of the covariance matrix and the multiplicity of their roots, as well as by the particular eigenvector estimation algorithm used, and

2) by the computer constant *EPSILON*, that is the smallest positive real value number such that $1.0+EPSILON>1.0$. Thus, it can be said that the smaller the EPSILON is the higher space and signal-power resolution obtainable.

The Performance of ASPECT is also affected by the *array manifold dimensionality*, which is a function of the array geometry and the characteristics of individual sensors in the array. This array manifold dimensionality provides the condition under which the solution of ASPECT with respect to a particular environment is unique; it also provides the maximum number of signals which can be resolved by the algorithm without any ambiguity problem.

It should also be noted that, the limitations of the optimization method used for minimizing the ASPECT cost function influence the rate of convergence of ASPECT.

CHAPTER 5

STEERED VECTOR ADAPTIVE ARRAY PROCESSING

5.0 INTRODUCTION

The previous two chapters addressed the problem of locating a number of emitting sources. This chapter is concerned with the problem of isolating an emitting source in the presence of interference and noise (see *Figure*-1.4 *problem*-2) and obtaining information about the unknown interference environment. An array scheme capable of isolating an emitting source is the so called *steered vector adaptive array*. In this array processing scheme, an array of N sensors operates in a completely unknown interference environment. Its main function is the adjustment of the array pattern so as to receive a signal coming from a known direction, in the presence of M unknown interferences or jammers (with $N \geq M$) which are spatially distributed in unknown directions. Its aim is the reception of the desired signal and maximum suppression of unwanted interferences (ideally to zero).

However, this array technique is willing to compromise on

interference suppression and allow some interference to pass at the output of the array (contaminating the desired signal) in order to obtain maximization of the signal-to-noise ratio. That is, it does not provide complete suppression of unwanted interferences. In addition, the direction of arrival (DOA) of the desired signal should be known a priori as accurately as possible since the pointing errors affect significantly the performance of the array. Furthermore, the larger the power of the desired signal at the input of the array is the smaller the power of the desired signal is provided at the output of the array. This is known as the *power inversion problem-* (see for example [APP-76], [AP2-76]) and it may result in desired-signal cancellation.

A partial solution to the above mentioned problems, is given by the modified Applebaum loop [GUP-84]. This is based on the idea of filtering the desired signal. Thus, by forming a covariance matrix which does not include the desired signal one can make a new adaptive array which is more robust to pointing errors and overcomes the drawback of power inversion mentioned above.

All the same, the performance of adaptive arrays is significantly degraded as the number of jammers increases, with deteriorated results when some of them are close together or when they are located at less than half the array beam-width away from the desired signal. Thus, the performance of adaptive arrays is governed by the geometry involved in the array and signal environment, as well as by the powers of the directional sources.

All the above mensioned problems in conjunction with the resolving power limitations of conventional adaptive array techniques make this array scheme incapable of handling many real world problems.

In this chapter it will be shown how the concepts of signal subspace methods can be extended into conventional steered vector adaptive arrays in order

- to analyse their behavior and highlight the problems mentioned above;
- to present a new algorithm capable of receiving a desired signal in the presence of unknown non-coherent interferences and, which at the same time, is:
    - capable of providing completely interference cancellation
    - capable of locating the positions of interfering sources
    - less susceptible to pointing errors and without the disadvantage of power inversion problems.

Then, the ASPECT algorithm will be slightly modified in order to provide a *weight vector* capable for achieving the above aims even if fully correlated (coherent) signals are involved.

5.1 ARRAY - PROCESSING MODELS

When dealing with broadband signals the array processor can usually be represented by a transfer function as shown in *Figure* 5.1*a*. However, the transfer function is not generally suitable for adaptive processing and, therefore, discrete time approximations for this model can be established using *tapped delay line* (*TDL*) filters (*Figure* 5.1*b*), where each of the tap weights can be considered to be adjustable. The *TDL*, when it is used for narrowband applications, can be reduced to a

FIGURE – 5.1
ARRAY PROCESSING MODELS

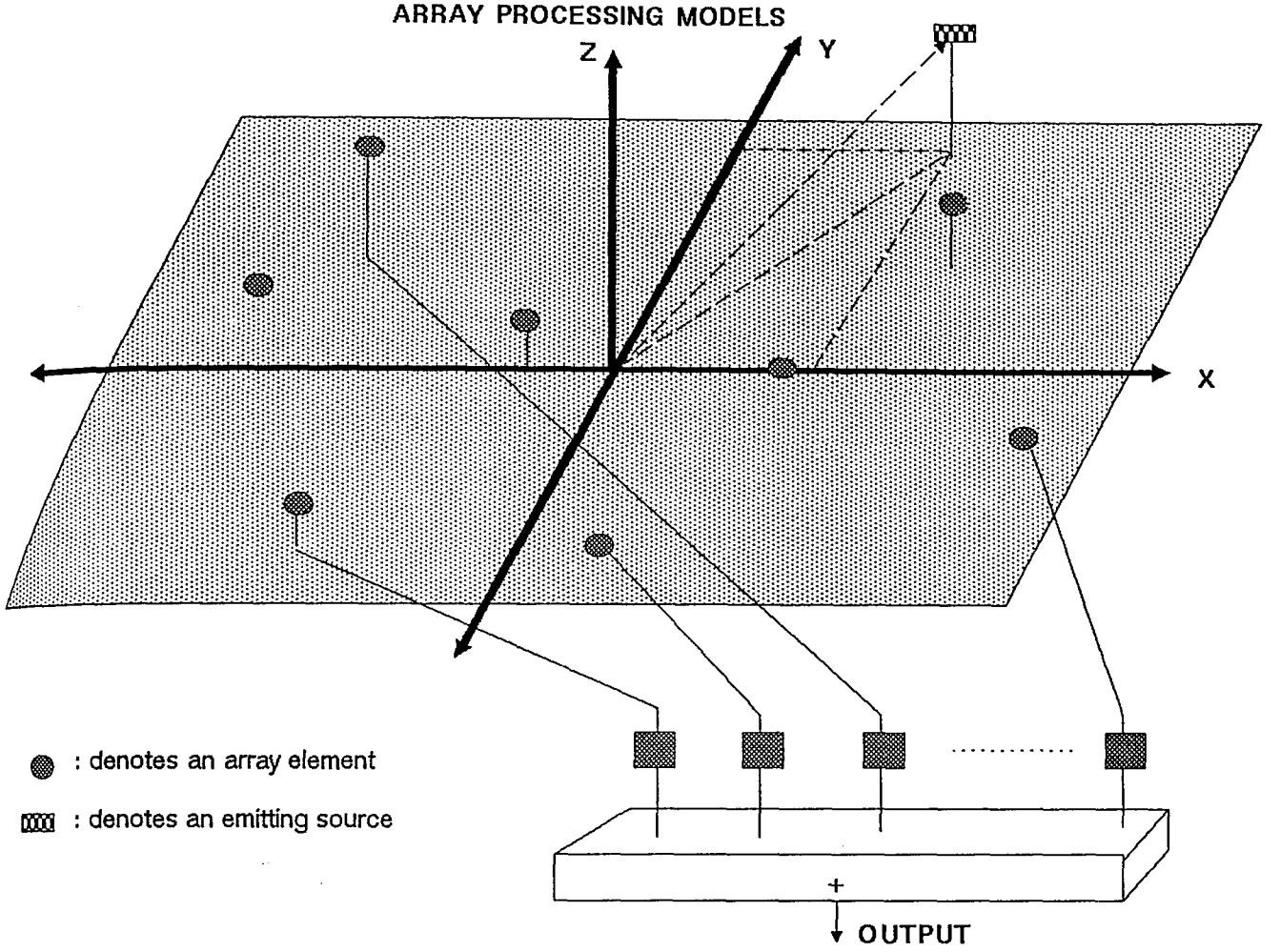

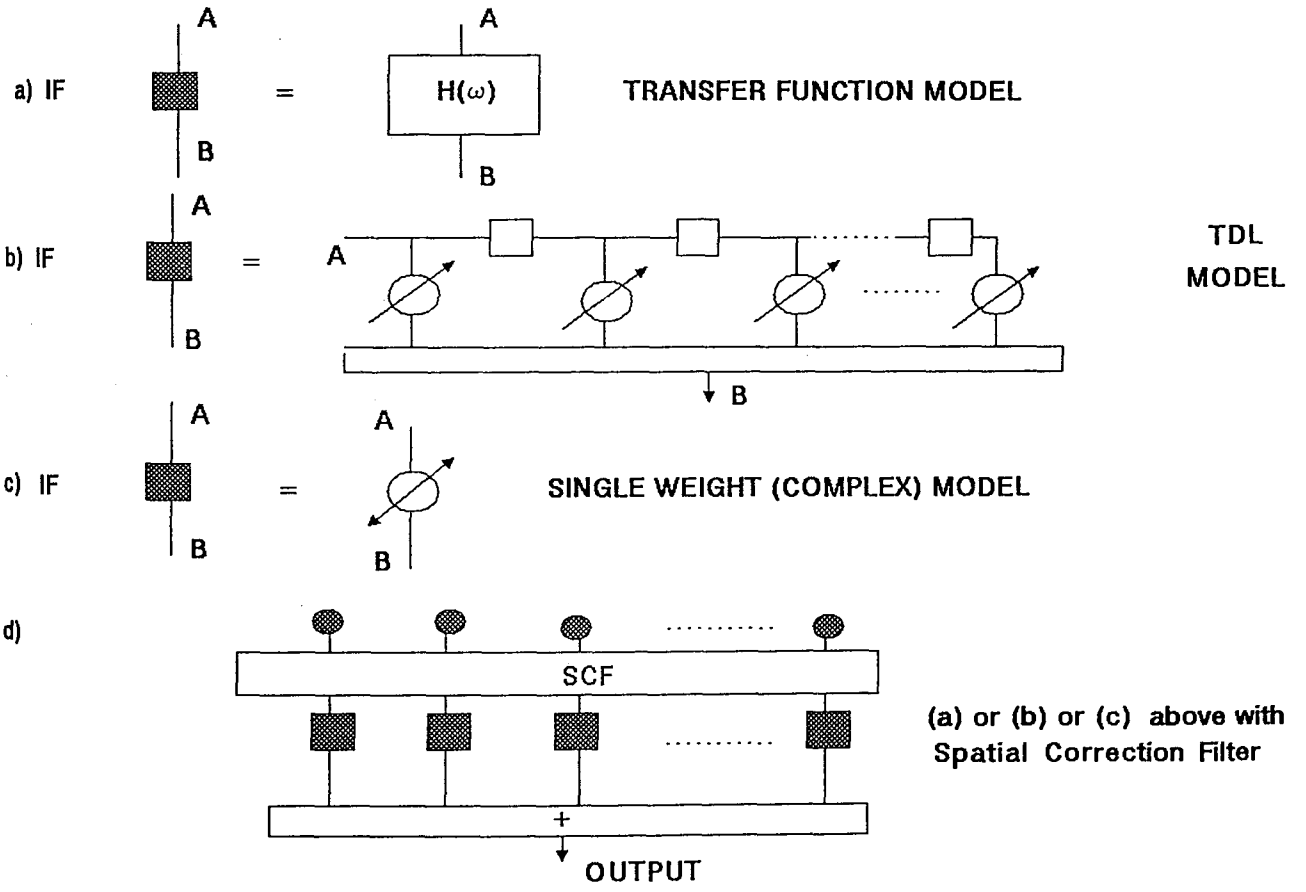

narrowband TDL model which ideally can be represented by a single time delay per channel. This single time delay per channel can then be approximated by a complex weight in each channel and this last model is known as the *single complex weight model* (*Figure* 5.1*c*).

Finally, in many array applications the direction of arrival of the desired signal is known or can be measured. In such a case, the time delays needed to align the desired signal terms in each channel can be computed and this function can be modelled by a *spatial correction filter* as shown in *Figure* 5.1*d*. In the following sections, the single complex weight model (with or without *spatial correction filter*) is going to be used.

In the following two sections the basic concepts necessary to analyse the behaviour of an array, such as array output and array pattern, will be discussed. Since these parameters are well known [HUD-81] the discussion will be kept brief.

5.2 ARRAY OUTPUT

Consider the array as shown in *Figure* 5.2 at some time t. At this time, the output $y(t)$ of the array will be the contribution of all the $x_k(t)$'s weighted by the complex coefficients, $w_k|_{k=1,2,3,..N}$.
That is,

$$y(t)=\sum_{k=1}^{N} w_k.x_k(t) \qquad (5.1)$$

FIGURE – 5.2

ARRAY PROCESSING MODEL USED IN THIS CHAPTER

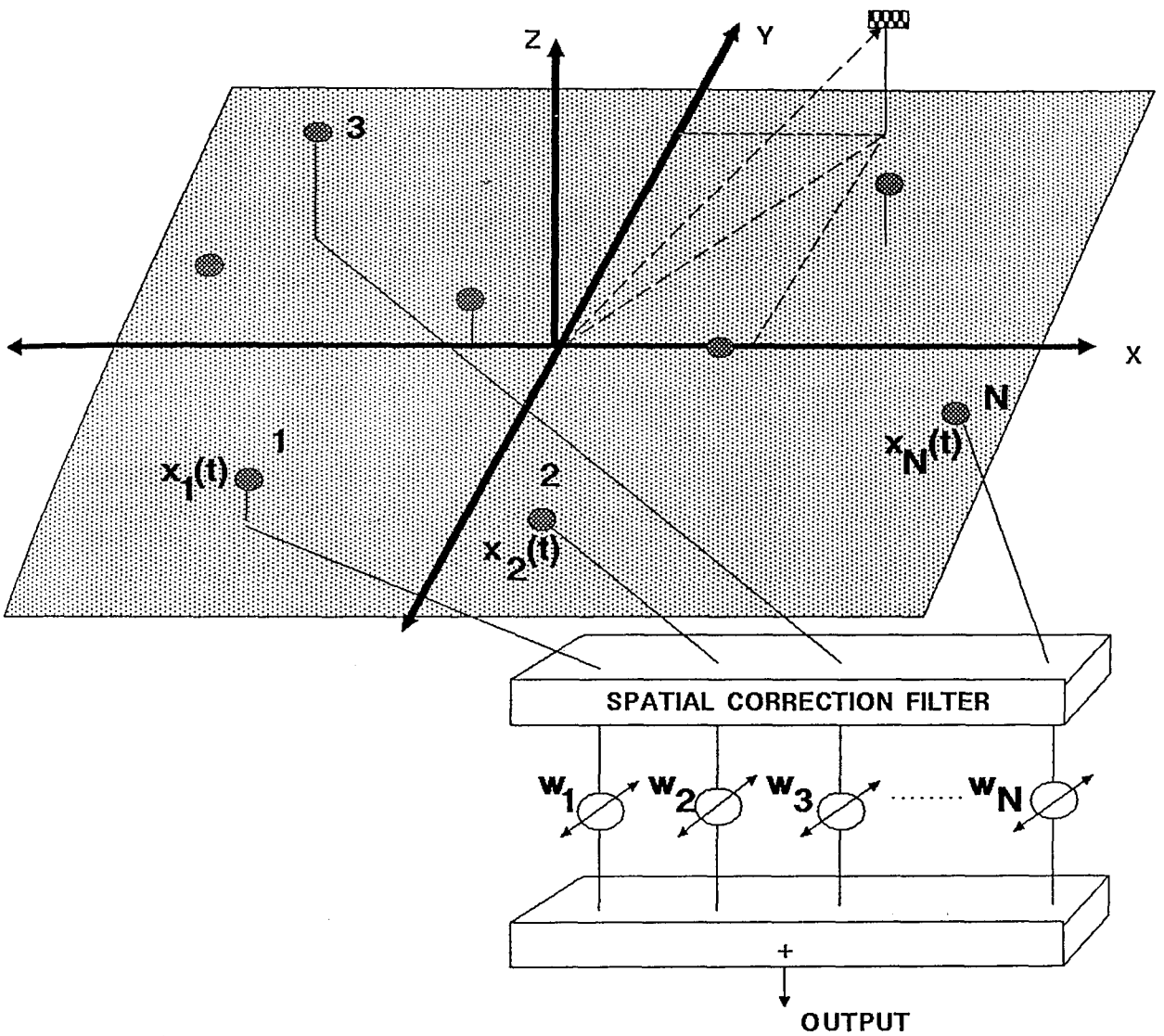

: denotes an array element

: denotes an emitting source

or in more compact form:

$$y(t)=\underline{x}(t)^H\ \underline{w} \tag{5.2}$$

where
$\underline{x}(t)=[\![x_1(t),\ x_2(t),\ldots,x_N(t)]\!]^T$
$x_i(t)$ *is given by equation* 2.26
$\underline{w}=[\![w_1,\ w_2,\ \ldots,\ w_N\ ]\!]^T$

Now the average output power from the array is given by:

$$\begin{aligned} P_{out} &= E[\ \|y(t)\|^2]=E[y(t)^H y(t)] \\ &= E[\ \underline{w}^H\ \underline{x}(t).\underline{x}(t)^H\ \underline{w}] \end{aligned}$$

i.e. $$P_{out}=\underline{w}^H \mathbf{R}_{xx}\ \underline{w} \tag{5.3}$$

If the incident signals are uncorrelated, then the output from the array can be expressed as the sum of powers of the separate sources, that is,

$$P_{out}=P_{d\text{-}out}+P_{J\text{-}out}+P_{n\text{-}out} \tag{5.4}$$

where
$P_{d\text{-}out}=$ *desired output power* $=\underline{w}^H \mathbf{R}_{dd}\underline{w}$
$P_{J\text{-}out}=$ *total jammer output power* $=w^H \mathbf{R}_{JJ}\underline{w}$
$=\sum_i P_i$ *where* $i=[1,\ldots,M]$
$P_{n\text{-}out}=$ *noise output power* $=\underline{w}^H \mathbf{R}_{nn}\underline{w}$

Equation 5.4 can also be written as follows:

$$P_{out} = \underline{w}^H \mathbf{R}_{dd}\underline{w} + \underline{w}^H \mathbf{R}_{JJ}\underline{w} + \underline{w}^H \mathbf{R}_{nn}\underline{w} \tag{5.5}$$

i.e.

$$P_{out} = P_d\cdot(\underline{w}^H \underline{S}_d)^2 + \sum_{j=1}^{M} P_j\cdot(\underline{w}^H \underline{S}_j)^2 + \sigma^2.\underline{w}^H \underline{w} \tag{5.6}$$

If the output signal to noise plus interference ratio (*SNIR*) is defined as the ratio of the wanted signal power to the total unwanted power then:

$$SNIR_{out} = \frac{\underline{w}^H \mathbf{R}_{dd} \underline{w}}{\underline{w}^H \mathbf{R}_{n+J} \underline{w}} = \frac{P_d \cdot (\underline{w}^H \underline{S}_d)^2}{\sum_{i=1}^{M} P_i \cdot (\underline{w}^H \underline{S}_i)^2 + \sigma^2 \cdot \underline{w}^H \underline{w}} \tag{5.7}$$

In the next section the useful concept of array pattern will be presented.

5.3 ARRAY PATTERN

Array pattern is defined as the output obtained from the array as a unity power emitting source is moved around in space. *Figure* 5.3 shows the magnitude of an array pattern for a linear array with all weights equal to one. It is clear from this figure that the array pattern has a number of lobes [MA-74]. The largest one is called the *main lobe*, while the remaining lobes are known as *sidelobes*. The main lobe is generally steered towards the direction of a desired source. As has been mentioned in *Chapter* 2, the direction of propagation is represented generally by a vector called the *slowness vector* and symbolized by $\underline{a}$.

Ideally, the beamformer should permit the passage of signals propagated with the slowness vector $\underline{a}_0$ and, at the same time, reject all the other existing signals.

FIGURE – 5.3

Array Pattern of a linear array of 5 isotropic uniformly distributed elements

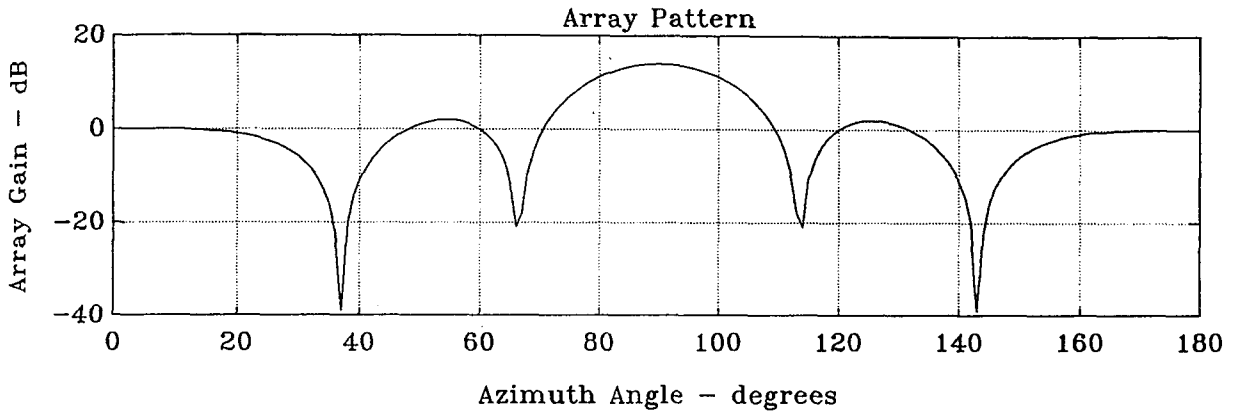

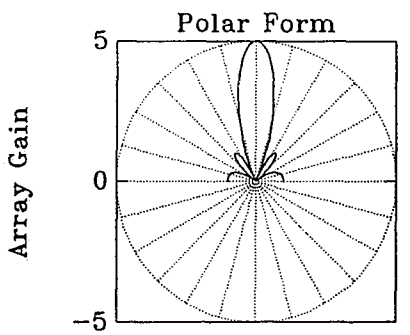

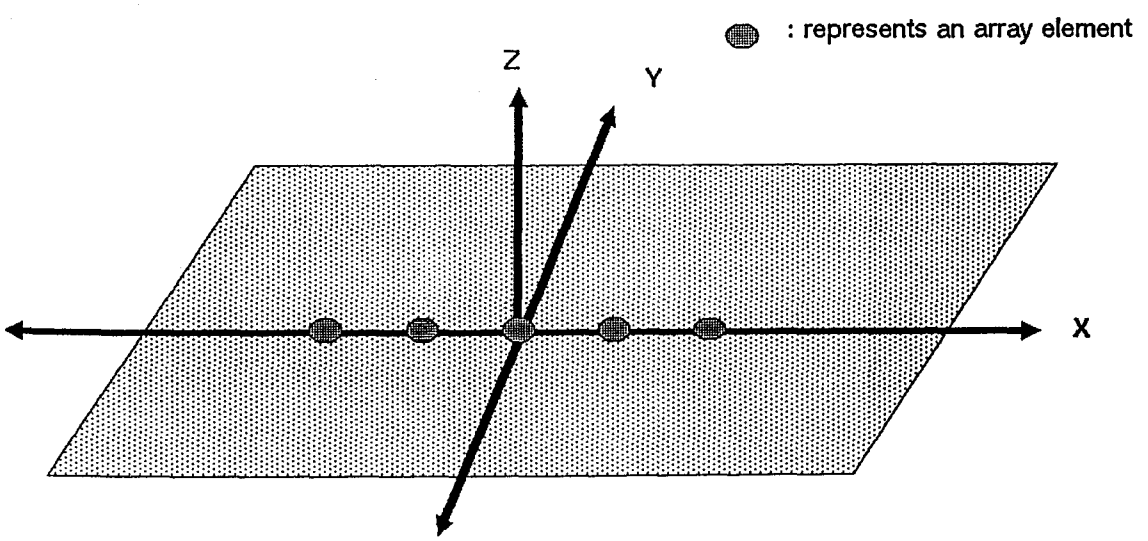

Let the main beam of the array be steered towards $\underline{a}_0$. Then the delays at each sensor of the array are given by:

$$T_k = -\underline{a}_0{}^T \underline{r}_k \quad \text{for } k=1,2,3,\ldots,N \tag{5.8}$$

where

T_k *is the delay at* k^{th} *sensor element with respect to the centre of the array,*

$\underline{r}_k$ *vector representing the location of the* k^{th} *sensor element with respect to the centre of the array,*

N *represents the number of sensors.*

Suppose the incident signal is a plane of unity power propagating in a different direction $\underline{a}$ then:

$$x_k(t)=exp[\![\ j\omega(t-\underline{a}^T\underline{r}_k\ ]\!] \tag{5.9}$$

However, the beamformer output $y(t)$ is formed by a weighted version of the received signal

$$\begin{aligned} y(t) &= \sum_{k=1}^{N} w_k.x_k(t-T_k) \qquad (5.10)\\ &= \sum_{k=1}^{N} w_k.exp[\![\ j\omega(t+\underline{a}_0{}^T\underline{r}_k-\underline{a}^T\underline{r}_k\ ]\!]\\ &= \sum_{k=1}^{N} w_k.exp[\![-j(\underline{k}-\underline{k}_0)^T\underline{r}_k]\!]\ .\ exp[\![\ j\omega\ t]\!]\\ &= g(\underline{k}-\underline{k}_0).exp[\![j\omega\ t]\!] \end{aligned}$$

$$\text{where}\quad g(\underline{k})=\sum_{k=1}^{N} w_k.exp[\![\ -j\underline{k}^T\underline{r}_k]\!]= \text{array pattern} \tag{5.11}$$

Equation 5.11 shows that the array pattern is essentially the Fourier Transform of the weighting function w_k, taking into account the position $\underline{r}_k$ of the sensors of the array.

The term $g(\underline{k}-\underline{k}_0)$ indicates that the array has steered its main lobe in a direction parallel to $\underline{a}_0=\frac{\underline{k}_0}{\omega}$, thus attenuating any plane wave travelling in direction $\underline{a}=\frac{\underline{k}}{\omega}$ different from $\underline{a}_0$. The objective of adaptive arrays located in an environment of spatially distributed emitters can be said to be the adjustment of the array pattern in such a way as to receive a desired directional signal attenuating the remaining signals as much as possible.

A more general equation for the array pattern can obtained when employing the concepts presented in *Chapter* 2, and in particular from the use of *Equation* 2.18. If this is done then, in compact form, the array pattern can be represented as follows:

$$g(\underline{k}_i)=\underline{w}^H \underline{S}_i \tag{5.12}$$

where $\underline{S}_i$ *is the vector* $\underline{S}_{l_i}$ *of Equation* 2.18.

Figure 5.4 shows the magnitude of a planar array with all the weights equal to unity.

FIGURE – 5.4

Array Pattern of a planar array of 15 (5x3) isotropic elements

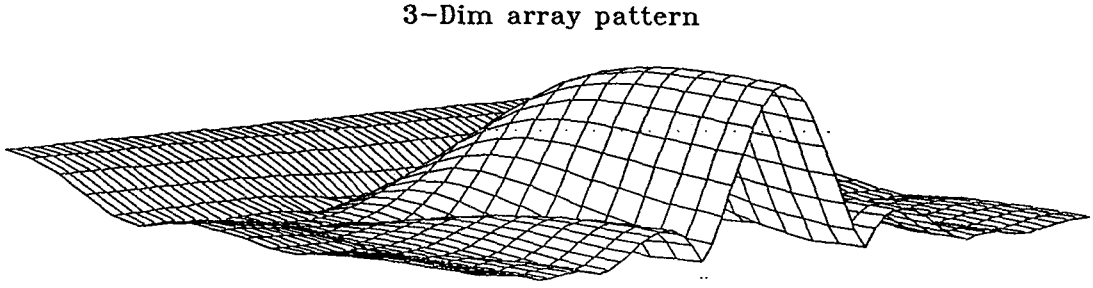

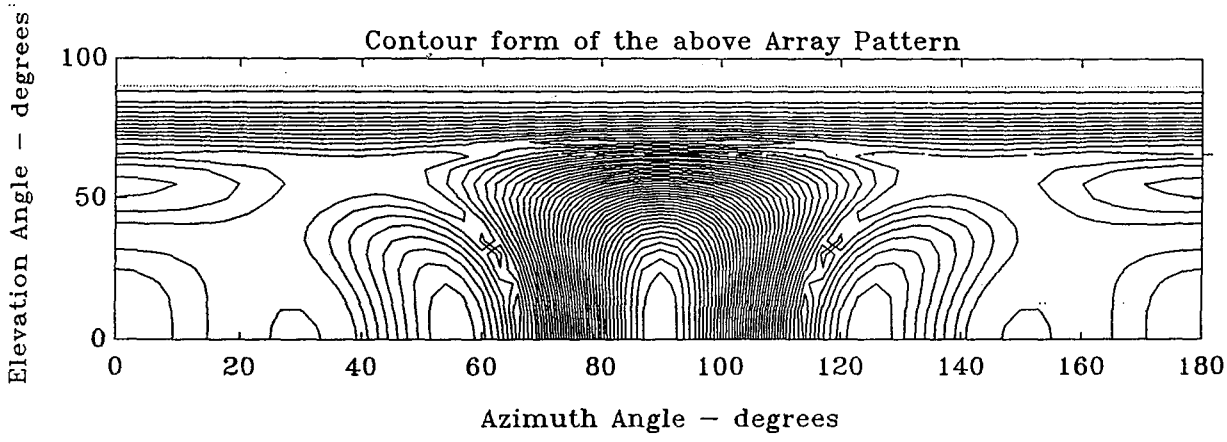

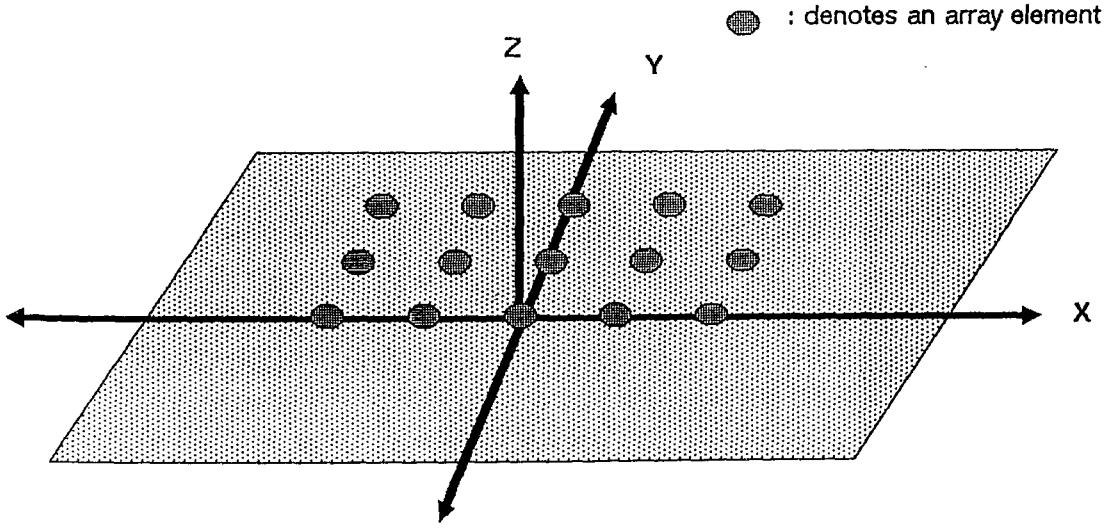

5.4 OPTIMUM SOLUTIONS AND PROBLEMS OF STEERED VECTOR ADAPTIVE ARRAYS

Without loss of generality, the assumption that the incident signals are narrowband is employed in this chapter. This assumption leads to the array model shown *Figure* 5.2 with N sensors located in a known geometry. In such a case, the task of the adaptive processor is the selection of appropriate complex weights $\underline{w}$ ($\underline{w} \in C^N$) in order to receive the desired signal as well as possible according to some performance criteria and, at the same time, to suppress any interfering source as much as possible. It is important to note here that the different performance measures converge towards the same steady state solution, which is known as Wiener-Hopf solution [HUD-81], [MON-80]. For instance, in order to obtain maximum SNIR at the output of a steered vector adaptive array the optimum steady state weights should be given by the Wiener-Hopf vector:

$$\underline{w}_{opt} = (data\ covariance\ matrix)^{-1}.(steering\ vector) \qquad (5.13)$$

where, as has been shown in previous sections, the covariance matrix is given by *Equation* 2.21 and where the steered vector adaptive arrays use as their steering vector the known SPV of the desired signal. That is

$$\underline{U}_s = q.\underline{S}_d \quad where\ q=scalar \qquad (5.14)$$

However, the major drawbacks associated with the use of *Equation* 5.13 are:

1. the power inversion of the desired signal, which results in the cancellation of the desired signal when it has high power;
2. the degraded performance of the array when pointing errors occur ;
3. The reduction of the output *SNIR* when the number of interferences increases;
4. the passage of interferences to the output of the array when (*i*) their power is compared to noise (i.e. low power) (*ii*) they have high power but are located close together in space (*iii*) the angular separation between some of them and the beam direction is small. Then an immediate consequence is the drop of the $SNIR_{out}$.

The *modified Applebaum* adaptive array [GUP-84] overcomes the first drawback and is robust in respect of the second. This improvement on performance in the modified Applebaum process is achieved by using a filter to remove the desired signal from the construction of the covariance matrix so that:

$$\underline{w}_{opt} = \mathbf{R}_{n+J}^{-1} \cdot \underline{U}_s \qquad 5.15$$

Let us call *Equation* 5.15 the "modified" Wiener-Hopf. Although *Equations* 5.13 and 5.15 appear to be completely different, this is not in fact the case. It can be shown [MON-80] that they differ only by a scalar factor and, therefore, these two weights offer identical maximum SNIR even though they have a number of different effects on the process.

However, both *Equations* 5.13 and 5.15 always allow interference to pass at the output of an array of sensors, thus contaminating the desired signal, as will be shown analytically in the next section. For this

reason, the weight-vectors provided by these equations are not appropriate for complete interference cancellation. The aim of the next section will be concentrated on highlighting the above problems by using *signal subspace* techniques instead of *conventional* techniques. The considerations of the following section result in a new algorithm which extends the signal subspace concepts to steered vector adaptive arrays.

5.5 SOLUTIONS FOR COMPLETE INTERF. CANCELLATION

Consider a N-dimensional observation space $\mathbf{H}$ of the data covariance matrix $\mathbf{R}_{xx}$ and let $\underline{S}_d, \underline{S}_1, \ldots, \underline{S}_M, \underline{w}$ be elements of this space. As was mentioned in a previous chapter, this space can be decomposed into two subspaces: the signal subspace $\mathbf{H}_s$ with $dim[\mathbf{H}_s]=M+1$ and the noise subspace $\mathbf{H}_n$ with $dim[H_n]=N$-M-1

$\mathbf{H}_s$ *is spanned by* $\underline{S}_d, \underline{S}_1, \ldots, \underline{S}_M$
or equivalently by the $M+1$ *eigenvectors of* $\mathbf{R}_{xx}$ *which correspond to its* $M+1$ *largest eigenvalues (i.e colums of* $\mathbb{E}_s$)

$\mathbf{H}_n$ *is spanned by remaining* N-M-1 *eigenvectors of* $\mathbf{R}_{xx}$ *(i.e colums of* $\mathbb{E}_n$)

It is clear (see *Figure* 5.5) that the noise subspace $\mathbf{H}_n$ is the complement of the signal subspace $\mathbf{H}_s$ i.e. $\mathbf{H}=\mathbf{H}_s \oplus \mathbf{H}_n$; where $\oplus$ means direct sum.

Thus, consider the eigen-decomposition of $\mathbf{R}_{xx}$, that is:

FIGURE – 5.5

DECOMPOSITION OF THE SUBSPACE SPANNED BY THE COLUMNS OF DATA COVARIANCE MATRIX WHEN THE DESIRED SIGNAL IS PRESENT

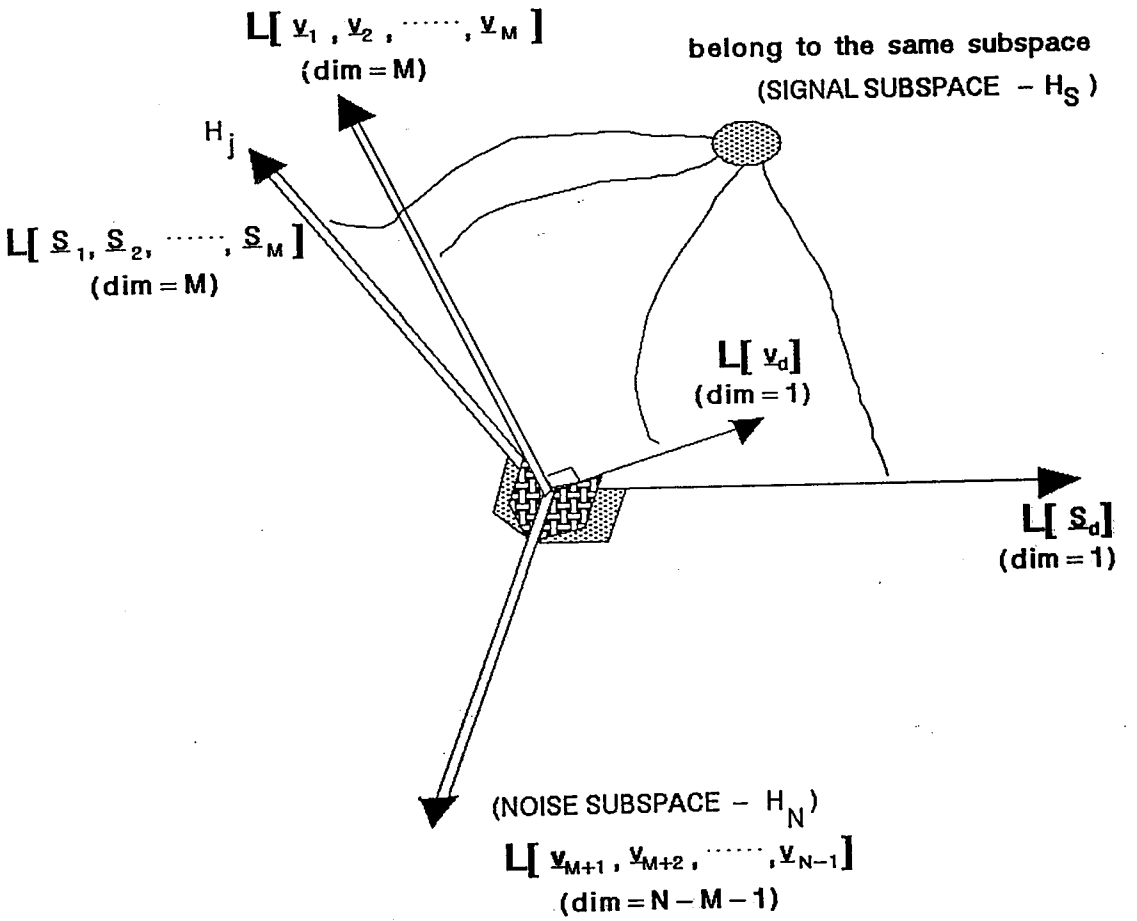

Note : L[.] means 'spanned by ...'

$$\mathbf{R}_{xx} = \left(\mathbf{E}_s \; \mathbf{E}_n \right) \cdot \left[\begin{bmatrix} \mathbf{D}_s & \mathbf{O} \\ \mathbf{O} & \mathbf{O} \end{bmatrix} + \sigma^2 . \mathbf{I} \right] . \left(\mathbf{E}_s \; \mathbf{E}_n \right)^H \qquad (5.16)$$

where $\mathbf{E}_s$ is an $N \times (M+1)$ matrix, $\mathbf{E}_n$ an $N \times (N-M-1)$ matrix, $\mathbf{I}$ an $N \times N$ matrix;

and

$$\begin{matrix} \uparrow \\ N \\ \downarrow \end{matrix} \quad \begin{matrix} \overset{\uparrow}{M+1} \\ \downarrow \end{matrix} \begin{bmatrix} \mathbf{D}_s & \mathbf{O} \\ \mathbf{O} & \mathbf{O} \end{bmatrix} \qquad (5.17)$$

$$\leftarrow M+1 \rightarrow$$

$$\leftarrow\!\!-\!\!- \quad N \quad -\!\!-\!\!\rightarrow$$

Thus, the decomposition shown in *Figure* 5.5 has been performed.

The optimum vector, as this results from *Equations* 5.13 and 5.16, is given by:

$$\underline{w}_{opt} = \mathbf{E}_s . \left(\mathbf{D}_s + \sigma^2 . \mathbf{I} \right)^{-1} . \mathbf{E}_s{}^H . \underline{U}_S + \boxed{\sigma^{-2} . \mathbf{P}_{\mathbf{E}_n} . \underline{U}_S} \qquad (5.18)$$

This can be rewritten in the following form:

$$\underline{w}_{opt} = \sum_{i=1}^{M+1} l_i . \mathbf{P}_{\underline{E}_{si}} . \underline{U}_S + \boxed{\sigma^{-2} . \mathbf{P}_{\mathbf{E}_n} . \underline{U}_S} \qquad (5.19)$$

where

l_i = *the* i^{th} *diagonal element of* $\left(\mathbf{D}_s + \sigma^2 . \mathbf{I} \right)^{-1}$

$\underline{E}_{si}$ = *the* i^{th} *column of* $\mathbf{E}_s$

$\mathbf{P}_{\underline{E}_{si}}$ = *Projection operator of the subspace spanned by* $\underline{E}_{si}$

Thus, by using last equation the optimum Wiener-Hopf solution can be

redefined as:

> *Consider the vectors which result from the projection of the steered vector on to each eigenvector of the data covariance matrix and weighted by the corresponding eigenvalue. The summation of those vectors provides the Wiener-Hopf solution.*

By using *Equation*-5.6, the output power can be expressed as:

$$P_{out} = P_d \cdot (\underline{w}_{opt}{}^H \underline{S}_d)^2 + \sum_{i=1}^{M} P_i \cdot (\underline{w}_{opt}{}^H \underline{S}_i)^2 + \sigma^2 \cdot \underline{w}_{opt}{}^H \underline{w}_{opt}$$

$$= P_{d\text{-}out} + P_{J\text{-}out} + P_{n\text{-}out} \qquad 5.20$$

where

$$P_{d\text{-}out} = P_d \cdot \left\{ \underline{U_S}^H . \mathbf{E}_s . \left(\mathbf{D}_s + \sigma^2 . \mathbf{I} \right)^{-1} . \mathbf{E}_s{}^H . \underline{S}_d \right\}^2 \qquad (5.21)$$

$$P_{J\text{-}out} = \sum_{i=1}^{M} P_i \cdot \left\{ \underline{U_S}^H . \mathbf{E}_s . \left(\mathbf{D}_s + \sigma^2 . \mathbf{I} \right)^{-1} . \mathbf{E}_s{}^H . \underline{S}_i \right\}^2 \qquad (5.22)$$

$$P_{n\text{-}out} = \sigma^2 . \underline{U_S}^H . \mathbf{E}_s . \left(\mathbf{D}_s + \sigma^2 . \mathbf{I} \right)^{-2} . \mathbf{E}_s{}^H . \underline{U_S} + \boxed{\sigma^{-2} . \underline{U_S} . \mathbf{P}_{\mathbf{E}_n} . \underline{U_S}} \qquad (5.23)$$

In the absence of any jamming signals $P_{J\text{-}out}=0$. In addition $\mathbf{D}_s$ and $\mathbf{I}$ become scalars and equal to P_d and 1 respectively. Then the output power is given by:

$$P_{out} = P_d \cdot \frac{\left[\underline{U_S}^H . \mathbf{P}_{\mathbf{E}_s} . \underline{S}_d \right]^2}{\left[P_d + \sigma^2 \right]^2} + \sigma^2 . \frac{\underline{U_S}^H \mathbf{P}_{\mathbf{E}_s} . \underline{U_S}}{\left[P_d + \sigma^2 \right]^2} \qquad (5.24)$$

where the first term in the last equation is the desired signal ($P_{d\text{-}out}$) at the output of the array, while the second term is the the output noise ($P_{n\text{-}out}$) and where

$$\underline{U}_s = q.\underline{S}_d, \quad q = scalar$$

In addition $\mathbf{E}_s$ (which in this case is a vector) and $\underline{S}_d$ belong to the same subspace (a line); which means that

$$\mathbb{P}_{\mathbf{E}_s}.\underline{S}_d = \underline{S}_d \tag{5.25}$$

Therefore

$$P_{out} = P_d.\frac{[\![\underline{U}_s{}^H.\underline{S}_d]\!]^2}{[\![P_d + \sigma^2]\!]^2} + \sigma^2.\frac{\underline{U}_s{}^H.\underline{U}_s}{[P_d + \sigma^2]^2} \tag{5.26}$$

From the last equation it is clear that desired output power is degraded with increased desired signal power P_d at the input of the array (i.e. power inversion). In addition, the output SNR becomes:

$$SNR_{out} = \frac{P_d}{\sigma^2}.(\underline{S}_d{}^H.\underline{S}_d) = SNR_{in}.\|\underline{S}_d\|^2 = \frac{P_d}{\sigma^2}.N \tag{5.27}$$

which is the maximum SNR.

However, in the presence of pointing errors, $\mathbf{E}_s$ and $\underline{S}_d$ do not belong to the same one dimensional subspace and *Equation* 5.25 is not valid; That is,

$$\mathbf{P}_{\mathbf{E}_s}.\underline{S}_d \neq \underline{S}_d \tag{5.28}$$

and *Equations*-5.26 and 5.27 are not true. In this case, the output power of the desired signal in *Equation* 5.24 decreases. This, in conjunction with the fact that all the terms which have the "delete line" in *Equations* 5.18 5.19 and 5.23 are not zero (and so they contribute more noise terms at the output of the array), may result in serious undesirable effects on the output SNR.

It is clear from *Equation* 5.22 that when the interference sources are present the contribution of the i^{th} interference to the output of the array is given by:

$$P_{i\text{-}out} = P_i \cdot \left\{ \underline{U}_S{}^H . \mathbb{E}_s . \left(\mathbb{D}_s + \sigma^2 . \mathbb{I} \right)^{-1} . \mathbb{E}_s{}^H . \underline{S}_i \right\}^2 \qquad (5.29)$$

Therefore it follows that the performance of the system will deteriorate as the number of interferences increases so that there are more terms of the form shown in *Equation* 5.29 which contribute to the output.

Let us next examine, in a similar fashion to the above discussion, the MODIFIED WIENER-HOPF equation (*Equation* 5.15).
In this case the decomposition of the observation space **H** is as shown in *Figure* 5.6 where

H_s *is spanned by* $\underline{S}_1,\ldots,\underline{S}_M$ *or equivalently by the* M eigenvectors of $\mathbf{R}_{n+J}$ *which correspond to its* M *largest eigenvalues* (*i.e. columns of* $\mathbb{E}_S$)

$\mathbf{H}_n$ *is spanned by remaining* N-M *eigenvectors of* $\mathbf{R}_{n+J}$

Thus, by decomposing $\mathbf{R}_{n+J}$, like the decomposition of *Equation* 5.16, it is implied that

FIGURE – 5.6

DECOMPOSITION OF THE SPACE SPANNED BY THE COLUMNS OF DATA COVARIANCE MATRIX WHEN THE DESIRED SIGNAL IS NOT PRESENT

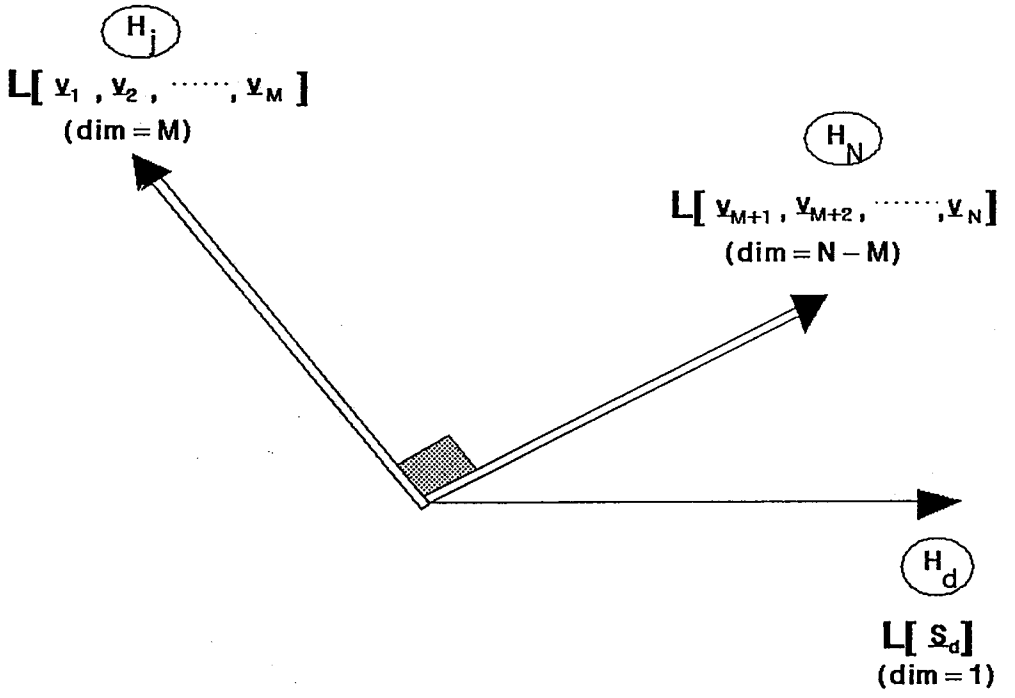

Note : $L[.]$ means 'spanned by ...'

$$\mathbf{R}_{n+J} = \left(\mathbf{E}_s \; \mathbf{E}_n \right) . \left[\begin{bmatrix} \mathbf{D}_s & \mathbf{O} \\ \mathbf{O} & \mathbf{O} \end{bmatrix} + \sigma^2 . \mathbf{I} \right] . \left(\mathbf{E}_s \; \mathbf{E}_n \right)^H \quad (5.30)$$

but in this case $\mathbf{E}_s$, $\mathbf{D}_s$ and $\mathbf{E}_n$ are different from those of *Equation* 5.16 and the dimensionalities are $N \times M$, $M \times M$ and $N \times (N\text{-}M)$, respectively, while σ is the variance of the noise the same in both cases.

The optimum weight will be given by a similar equation to that of *Equation* 5.18. That is,

$$\underline{w}_{opt} = \mathbf{E}_s . \left(\mathbf{D}_s + \sigma^2 . \mathbf{I} \right)^{-1} . \mathbf{E}_s{}^H . \underline{U}_S + \sigma^{-2} . \mathbf{P}_{\mathbf{E}_n} . \underline{U}_S \quad (5.31)$$

where now the term $\sigma^{-2} . \mathbf{P}_{\mathbf{E}_n} . \underline{U}_S \neq \underline{0}$.

Following the same analysis as with Wiener-Hopf, the output powers for the desired signal, interferences and noise will be:

$$P_{d\text{-}out} = P_d . \left\{ \underline{U}_S{}^H . \mathbf{E}_s . \left(\mathbf{D}_s + \sigma^2 . \mathbf{I} \right)^{-1} . \mathbf{E}_s{}^H . \underline{S}_d \right\}^2 \quad (5.32)$$

$$P_{J\text{-}out} = \sum_{i=1}^{M} P_i . \left\{ \underline{U}_S{}^H . \mathbf{E}_s . \left(\mathbf{D}_s + \sigma^2 . \mathbf{I} \right)^{-1} . \mathbf{E}_s{}^H . \underline{S}_i \right\}^2 \quad (5.33)$$

$$P_{n\text{-}out} = \sigma^2 . \underline{U}_S{}^H . \mathbf{E}_s . \left(\mathbf{D}_s + \sigma^2 . \mathbf{I} \right)^{-2} . \mathbf{E}_s{}^H . \underline{U}_S + \sigma^{-2} . \underline{U}_S{}^H . \mathbf{P}_{\mathbf{E}_n} . \underline{U}_S \quad (5.34)$$

And, in the absence of any interferences, the output powers are given by:

$$P_{d\text{-}out}=\frac{P_d}{\sigma^4}\cdot\left(\underline{U_s}^H\cdot\mathbf{P}_{\mathbb{E}_n}\cdot\underline{S}_d\right)^2 \tag{5.35}$$

$$P_{J\text{-}out}=0 \tag{5.36}$$

$$P_{n\text{-}out}=\sigma^{-2}\cdot\underline{U_s}\cdot\mathbf{P}_{\mathbb{E}_n}\cdot\underline{U_s} \tag{5.37}$$

However, because now $\mathbb{E}_n$ spans the whole observation space, this means that the projection operator applied to any vector belonging to that space leaves it unchanged, that is

$$\mathbf{P}_{\mathbb{E}_n}\cdot\underline{S}_d=S_d \tag{5.38}$$

$$\mathbf{P}_{\mathbb{E}_n}\cdot\underline{U_s}=\underline{U_s} \tag{5.39}$$

Therefore

$$P_{out}=P_d\cdot\left[\!\left[\frac{\underline{U_s}^H\underline{S}_d}{\sigma^2}\right]\!\right]^2+\sigma^2\cdot\frac{\|\underline{U_s}\|^2}{\sigma^4} \tag{5.40}$$

and

$$SNIR_{out}=SNR_{out}=\frac{P_d}{\sigma^2}\cdot(\underline{S}_d{}^H\cdot\underline{S}_d)=SNR_{in}\cdot\|\underline{S}_d\|^2=N.\frac{P_d}{\sigma^2} \tag{5.41}$$

It is obvious from *Equation* 5.40 that now the desired output at the output of the array is proportional to that at the input, so the power inversion problem is not present.

In addition, in this case, *Equation* 5.38 is always true, even if pointing errors occur, in contrast to *Equation* 5.25 which is not valid in the case of pointing errors and which is the cause of the reduction of the SNIR at the output of the array. Thus, the "modified" Wiener-Hopf out-performs to the "full" Wiener-Hopf.

On the basis of the above discussion it is clear that the optimum weights for maximization of SNIR always allows interferences to pass to the output of the array.

The question is how can the interference contribution be eliminated from the output of the array i.e. how can complete cancellation of interferences be achieved. An appropriate solution for complete interference cancellation which is less susceptible to pointing errors and does not suffer from power inversion problems could be provided by the following Theorem.

THEOREM 4. :

a) *The eigenvector corresponding to the maximum eigenvalue of the rank-1 matrix* $\underline{w}.\underline{w}^{\mathsf{H}}$ *where* $\underline{w}$ *is the projection of the optimum Wiener-Hopf solutions* $\mathbf{R}_{xx}^{-1}\underline{U}_S$ *or* $\mathbf{R}_{n+J}^{-1}.\underline{U}_S$ *on to the subspace spanned by the eigenvectors corresponding to the minimum eigenvalue of the matrix*

$$\mathbf{R}_{xx} - \min_{\alpha}\left\{\sum_{\substack{i=1 \\ eig_i \neq 0}}^{N} 1+|eig_i\left(\mathbf{R}_{xx} - eig_{min}(\mathbf{R}_{xx}).\mathbf{I} - \alpha.\underline{S}_d.\underline{S}_d^H\right)|\right\} .\underline{S}_d.\underline{S}_d^H \tag{5.42}$$

provides a weight-vector appropriate for complete cancellation of unknown interferences.

b) *the process maintains the output noise power equal to that at the input.*

PROOF :

By minimizing the function:

$$\min_{\alpha}\left\{\sum_{\substack{i=1 \\ eig_i \neq 0}}^{N} 1+|eig_i\left(\mathbf{R}_{xx} - eig_{min}(\mathbf{R}_{xx}).\mathbf{I} - \alpha.\underline{S}_d.\underline{S}_d^H\right)|\right\} \tag{5.43}$$

the power of the desired signal becomes known. Thus, *Equation* 5.42 is the data covariance matrix where the desired signal effects have been removed.

Let $\underline{w}_{interf.cancel}$ be the eigenvector which corresponds to the maximum eigenvalue of $\underline{w}.\underline{w}^H$. Then

$$\underline{w}_{interf.\ cancel} = \underline{eig}_{max}(\underline{w}.\underline{w}^H)$$

$$= \frac{\underline{w}}{\sqrt{\underline{w}^H.\underline{w}}}$$

$$= \frac{\mathbf{P}_{\mathbf{E}_n}.\underline{w}_{opt}}{\sqrt{\underline{w}^H_{opt}.\mathbf{P}_{\mathbf{E}_n}.\mathbf{P}_{\mathbf{E}_n}.\underline{w}_{opt}}}$$

$$= \frac{\mathbf{P}_{\mathbf{E}_n}.\underline{w}_{opt}}{\sqrt{\underline{w}^H_{opt}.\mathbf{P}_{\mathbf{E}_n}.\underline{w}_{opt}}} \qquad (5.44)$$

Consider the observation space $\mathbf{H}$ $dim[H]=N$ of the covariance matrix $\mathbf{R}_{n+J}$ which is decomposed as shown in *Figure* 5.6. Now the subspace $\mathbf{H}_j$ spanned by $\underline{S}_1,\ldots,\underline{S}_M$ is also spanned by the M eigenvectors of $\mathbf{R}_{n+J}$ corresponding to its M largest eigenvalues while the remaining N-M eigenvectors span the subspace $\mathbf{H}_j^{\perp}$.

Let $\mathbf{P}_{\mathbf{E}_n}$ be the projection operator of the subspace $\mathbf{H}_j^{\perp}$ which is spanned by $\underline{E}_{ni}$, $i=M+1,\ldots,N$ eigen-vectors of $\mathbf{R}_{n+J}$.

Then, the projection of the optimum Wiener-Hopf solution given by *Equation* 5.15 on to the noise subspace is given by:

$$\mathbf{P}_{\mathbf{E}_n}.\underline{w}_{opt} = \mathbf{P}_{\mathbf{E}_n}.\left\{\mathbf{E}_s.\left(\mathbf{D}_s+\sigma^2.\mathbf{I}\right)^{-1}.\mathbf{E}_s{}^H.\underline{U}_S + \sigma^{-2}.\mathbf{P}_{\mathbf{E}_n}.\underline{U}_S\right\}$$

$$= \frac{1}{\sigma^2}.\mathbf{P}_{\mathbf{E}_n}.\mathbf{P}_{\mathbf{E}_n}.\underline{U}_S \qquad (using\ Lemma\text{-}2)$$

$$= \frac{1}{\sigma^2}.\mathbf{P}_{\mathbf{E}_n}.\underline{U}_S \qquad (5.45)$$

Equation 5.45 in conjunction with *Equation* 5.44, and the idempotent property of projection operator $\mathbf{P}_{\mathbf{E}_n}=\mathbf{P}_{\mathbf{E}_n}.\mathbf{P}_{\mathbf{E}_n}$ (Lemma-2) gives:

$$w_{interf.\ cancel} = \frac{\mathbf{P}_{\mathbf{E}_n}.\underline{U}_S}{\sqrt{\underline{U}_S{}^H.\mathbf{P}_{\mathbf{E}_n}.\underline{U}_S}} \qquad (5.46)$$

The output jammer power of the array using as weighting vector, the vector given by *Equation* 5.46, will be:

$$P_{J\text{-}out} = \sum_{i=1}^{M} P_i.(\underline{w}^H_{interf.\ cancel}.\underline{S}_i)^2$$

$$= \sum_{i=1}^{M} P_i.\frac{1}{\underline{U}_S{}^H.\mathbf{P}_{\mathbf{E}_n}.\underline{U}_S}.(\underline{U}_S^H.\mathbf{P}_{\mathbf{E}_n}.\underline{S}_i)^2$$

However,

$$\mathbf{P}_{\mathbf{E}_n}.\underline{S}_i=\underline{0} \qquad (5.47)$$

Therefore,

$$P_{J\text{-}out}=0 \qquad (5.48)$$

This proves part(a) of the Theorem. Part(b) can be proved by using *Equation* 5.6. Then,

$$P_{n\text{-}out} = \sigma^2.\underline{w}^H_{interf\ cancel}.\underline{w}_{interf\ cancel} =$$

$$=\sigma^2.\frac{\underline{U_s}^H.\mathbf{P}_{\mathbb{E}_n}.\mathbf{P}_{\mathbb{E}_n}.\underline{U_s}}{\underline{U_s}^H.\mathbf{P}_{\mathbb{E}_n}.\underline{U_s}}=$$

$$=\sigma^2 \tag{5.49}$$

It can easily be proved (using Theorem 2.12 in [LIN-78]) that $\underline{w}_{interf.cancel}\in\mathbf{H}_j$ given by *Equation*-5.27 is the best approximation to $\underline{w}_{opt}\in\mathbf{H}$.

Now, by using Theorem 4, *Equation* 5.6 becomes:

$$P_{out} = P_d.\ \underline{S}_d{}^H.\mathbf{P}_{\mathbb{E}_n}.\underline{S}_d + \sigma^2 \tag{5.50}$$

Thus, the signal-to-noise power ratio at the array output will be:

$$SNR_{out} = \frac{P_d}{\sigma^2}.\ \underline{S}_d{}^H.\mathbf{P}_{\mathbb{E}_n}.\underline{S}_d \tag{5.51}$$

However, the angle between the $\mathbf{H}_d$ and $\mathbf{H}_j^{\perp}$ subspaces is

$$\cos\theta=\frac{\sqrt{\underline{S}_d{}^H.\mathbf{P}_{\mathbb{E}_n}.\underline{S}_d}}{\sqrt{\underline{S}_d{}^H.\underline{S}_d}} \tag{5.52}$$

Therefore, *Equation* 5.51 is equivalent to:

$$SNR_{out} = \frac{P_d}{\sigma^2}.\ (\underline{S}_d{}^H.\underline{S}_d).cos\,^2\theta \tag{5.53}$$

where θ=*angle between* H_d *and* $H_j^{\perp}$ *subspaces*

In the absence of interferences, $\mathbb{E}_n$ spans the whole observation space; which implies that $\cos\theta=1$ and the provided SNR_{out} is equivalent to modified Wiener-Hopf SNR_{out} (see *Equation* 5.41).

Equation 5.53 shows that if there is an interference very close to the desired signal direction then $\theta \rightarrow 90^{\circ}$, which implies that the output SNR deteriorates seriously. However, this undesirable property is not restricted to the proposed processor. The Wiener-Hopf processor (and all other known processes) also suffers from this restriction when interferences are located close to the desired signal direction.

It is important to point out that the minimization problem presented by *Equation* 5.42 has a global minimum which is positive (and equal to the power of the desired signal) if the desired signal is present, and zero if it is absent. This is illustrated in *Figure* 5.7 for a signal environment where the desired signal of power 0.7 is present and then for the same environment when it is absent.

FIGURE–5.7

COST FUNCTION VARIATION GIVEN BY EQUATION 5.43 FOR THE ARRAY ENVIRONMENT PROVIDED AT THE BOTTOM OF THE PAGE

(a linear array of 5 isotropic elements is used)

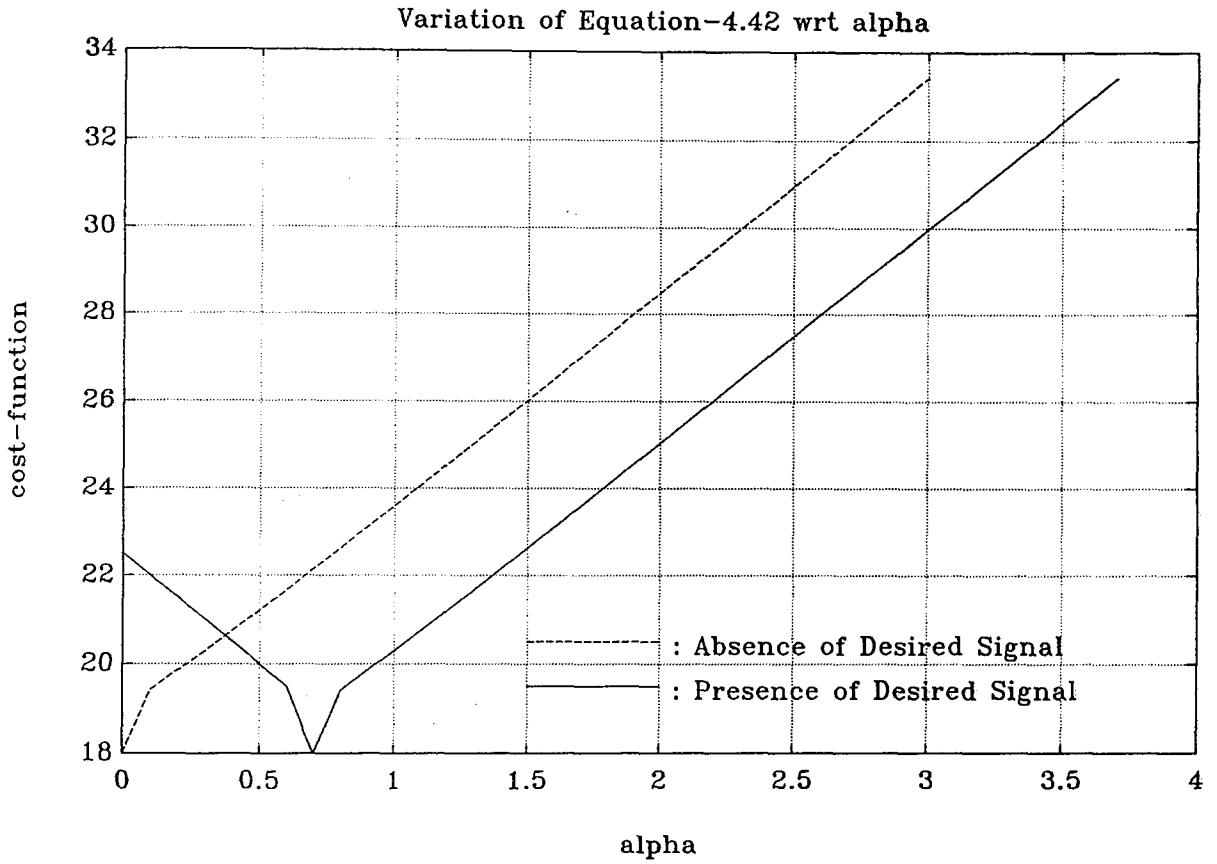

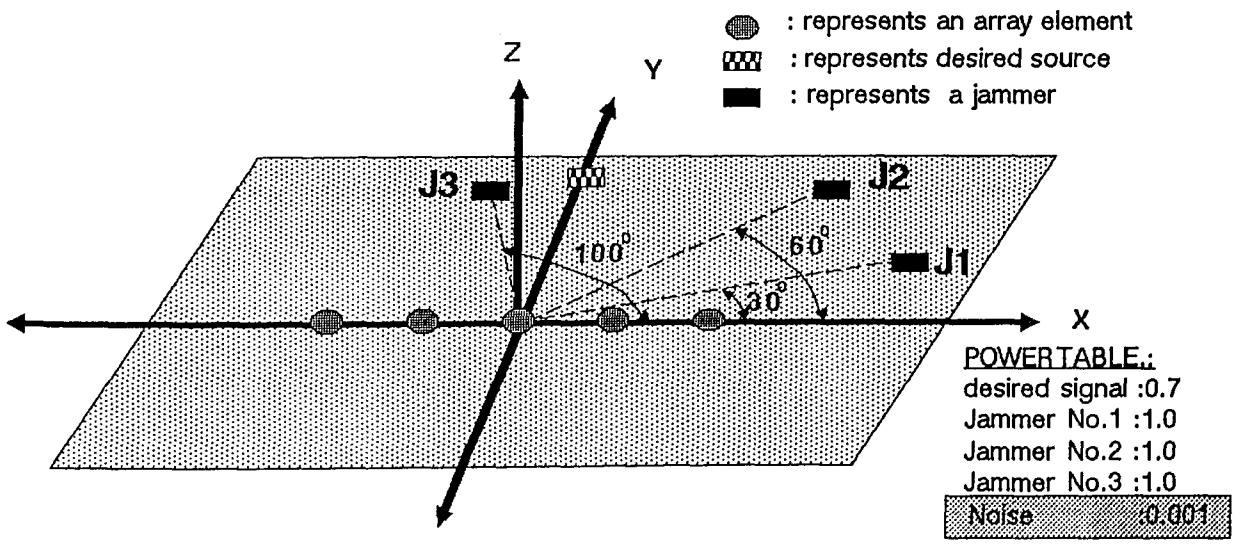

5.7 PROPOSED ALGORITHM

The proposed algorithm can be presented as a series of steps as follows:

STEP-1: Estimate the data covariance matrix

STEP-2: Find the minimum eigenvalue of this matrix

STEP-3: Estimate the following matrix:

$$\mathbf{R}_{xx} - \min_{\alpha}\left\{\sum_{\substack{i \\ eig_i \neq 0}} 1 + eig_i\left(\mathbf{R}_{xx} - eig_{min}(\mathbf{R}_{xx}).\mathbf{I} - \alpha.\underline{S}_d.\underline{S}_d^H\right)\right\}.\underline{S}_d.\underline{S}_d^H$$

STEP-4: Perform eigen-decomposition of the matrix estimated in step-3:

STEP-5: Find the projection operator of the space spanned by the eigenvectors corresponding to the minimum eigenvalue of the decomposition performed in the previous step.

STEP-6: Apply the above operator to the steering vector. This gives a new vector. Divide this vector by its magnitude. This provides the $\underline{w}_{interf.cancel}$.

STEP-7: Weight the inputs of the array with $\underline{w}_{interf.cancel}$

The minimization problem involved in *STEP-3* can be performed using any line search method technique. In the previous section (*Figure* 5.7) this was performed using simplex Nelder and Mead minimization technique [WAL-75] with accuracy equal to *epsilon* of the computer.

5.8 ASPECT-WEIGHT-VECTOR

Equation-5.46 in the previous section, provides a weight-vector appropriate for complete interference cancellation, but only when the interference sources are uncorrelated with the desired signal.

It is not difficult to see, however, that when some interferences are correlated with each other, rather than with the desired signal, then the use of *Equation* 5.46 will suppress them completely. However it does not provide deep nulls to each of the correlated interference locations. Instead, *Equation*-5.46 provides one null in a location which results from a linear combination of interference locations.

The limitations of *Equation*-5.46 can be overcome by using ASPECT. The ASPECT algorithm can provide a weight-vector which works even in a fully correlated signal environment. The reason is that ASPECT provides the necessary information with respect to interference subspace and this is independent of any correlation between sources. In addition, this vector does not suffer from *power inversion problems* or *pointing errors* therefore there is no need for filtering the desired signal effects when forming the covariance matrix. Of course the weight-vector should be orthogonal to the interference subspace $\mathbf{H}_j$ and, by looking at *Figure*-5.5, it is not difficult to find a vector which is orthogonal to both interference and noise subspace (see *Figure*-5.8).

In order to provide a weight-vector for complete interference cancellation the following step (as ***STEP-5a.2c.1***) should be added to the ASPECT algorithm.

.....

5a.2c

5a.2c.1 • *let* $\mathbf{S}=[\underline{S}_d,\mathbf{S}_{irf}]$ where $\underline{S}_d$ is the column of $\mathbf{S}$ which is closer to the steering direction.

• estimate the projection operator $\mathbf{Q}_{irf}$

• estimate the weight-vector $\underline{w}_{ASPECT}=c^{-1}.\mathbf{Q}_{irf}.\underline{S}_d$

• multiply input of the array by $\underline{w}_{ASPECT}$

• update $\mathbf{P}_{\mathbf{S}}=\mathbb{I}-\mathbf{Q}_{irf}-\underline{w}_{ASPECT}.\underline{w}^{H}_{ASPECT}$

where $c = \sqrt{\underline{S}_d{}^{H}.\mathbf{Q}_{irf}.\underline{S}_d}$

$\mathbf{Q}_{irf}$=*Projection operator to the subspace* $H_j^{\perp}$

5a.2d

FIGURE – 5.8

ASPECT WEIGHT – VECTOR

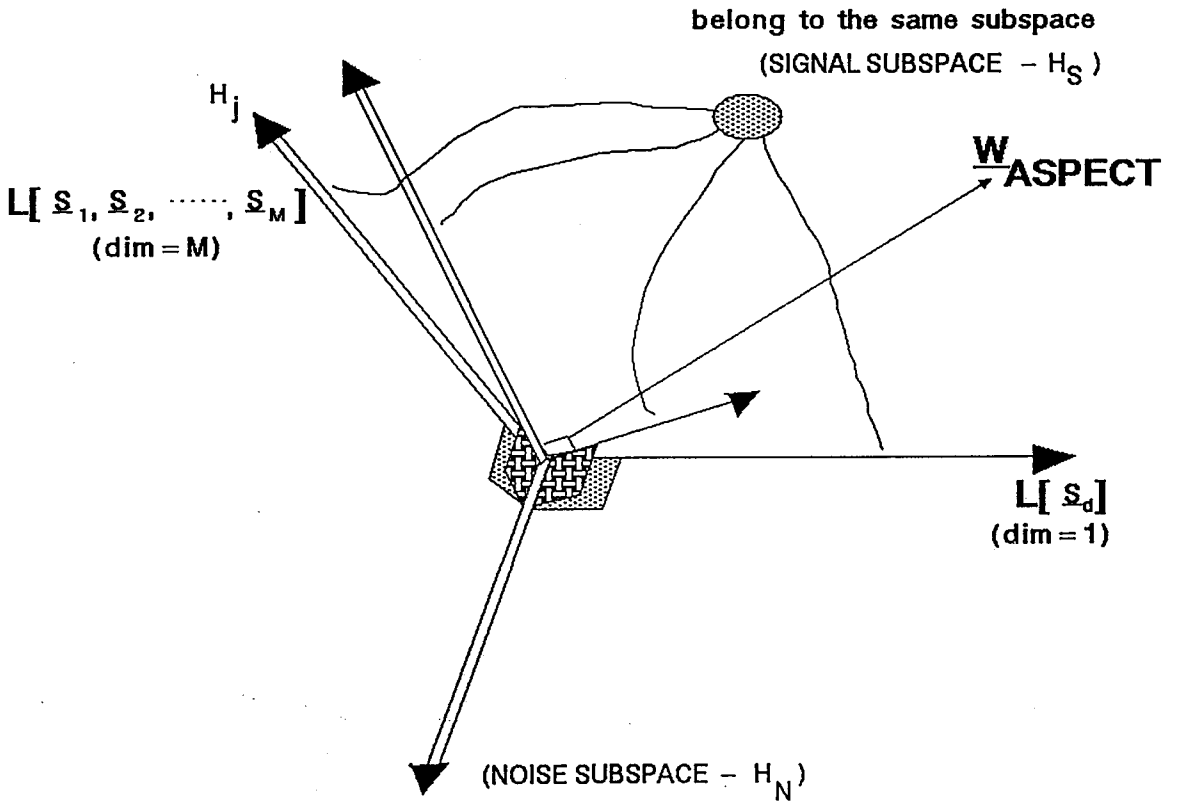

Note : $L[.]$ means 'spanned by ...'

CHAPTER 6

STEERED VECTOR ADAPTIVE ARRAY COMPUTER SIMULATIONS

6.1 COMPUTER EXPERIMENTS

In order to demonstrate the performance of the $\underline{w}_{interf.cancel}$ and $\underline{w}_{ASPECT}$ processor, a set of computer simulations was carried out using an *APRICOT XEN-i* 386/30 with 80387 co-processor, and for illustration purposes, a uniform linear array of five isotropic elements with interelement spacing of $\frac{\lambda}{2}$ was used.

The signal environment was synthesized as follows:

- the desired signal was located at 90° degrees and was set to have unity power;
- three jammers were assumed present: the first fixed at 30°, the second at 60° and the third at 100°. All three were taken to have unity power;
- thermal and isotropic noise was assumed present at each element. Two power levels namely 0.001 (−30dB) and then 0.1 (−10dB) were considered.

The performance of the $\underline{w}_{interf.cancel}$ processor was also compared with

that of the Wiener-Hopf (given by *Equation* 5.15). The results are shown in *TABLE-1* indicating that indeed the $\underline{w}_{interf.cancel}$ processor does cancel the unknown interferences completely. Thus, the array pattern which is shown in *Figure* 6.1 presents very deep nulls at the locations of the *unknown* interferences while it provides a *free way* to the desired signal. By considering that each deep null provides the location of an interference, it can be seen that these deep nulls are easily distinguishable from the rest of the nulls of the array pattern and they provide unbiased estimates of the unknown interference locations while the remaining nulls correspond to *pseudo interferences.* The same points are illustrated in *Figure* 6.2 where the noise level has been increased from -30 to -10dB.

A criterion for comparing algorithms is with respect to the output SNIR. Thus, in the above simulation studies the output SNIR is examined for two processors:

- the processor based on *Equation* 5.46,
- a Wiener-Hopf processor, based on *Equation* 5.15.

The results of the examination are shown in *Figure* 6.3 (for noise at -30dB), and in *Figure* 6.4 (for noise at -10dB) where the third interference is with variable location (0°,180°). It can be concluded from *Figures* 6.3 and 6.4 that the output SNIR of the $\underline{w}_{interf.cancel}$ processor for most of the directions, is almost identical to that of the Wiener-Hopf processor which provides the optimum SNIR.

Let next consider the more complicated situation where the first interference has been moved close to the second, that is, their directions are now assumed to be at 60° and 62° azimuth angles say. *Figure*-6.5 (for noise at -30dB), and *Figure* 6.6 (for noise at -10dB) show the results and illustrate the above points once again. However, these

TABLE-1

WIENER PROCESSOR

	LOCATION	I/P	I/P(dB)	O/P	O/P(dB)
desired	(0,90)	1	0	5.4652×10^{3}	67.376
interf-1	(0,30)	1	0	9.2907×10^{-4}	-30.320
interf-2	(0,60)	1	0	3.4203×10^{-3}	-24.659
interf-3	(0,100)	1	0	5.1982×10^{-1}	-28.414
noise	—	0.001	-30	2.3372×10^{3}	33.687
SNIR	—	0.33322	-4.7727	2.3378×10^{3}	33.688
SNR	—	10000	30	2.3383×10^{3}	33.689

EQUATION-5.46 PROCESSOR

	LOCATION	I/P	I/P(dB)	O/P	O/P(dB)
desired	(0,90)	1	0	2.3372	3.6870
interf-1	(0,30)	1	0	2.7417×10^{-32}	-315.62
interf-2	(0,60)	1	0	4.6026×10^{-32}	-313.37
interf-3	(0,100)	1	0	8.4568×10^{-32}	-310.73
noise	—	0.001	-30	1.0000×10^{-3}	-30
SNIR	—	0.33322	-4.7727	2.3372×10^{3}	33.687
SNR	—	10000	30	2.3372×10^{3}	33.687

FIGURE – 6.1

ARRAY PATTERNS for EQUATION – 5.46 and WIENER – HOPF PROCESSORS (UNCORRELATED SIGNALS with NOISE LEVEL at – 30dB)

(A linear array of 5 isotropic uniformly distributed elements is used)

directions: desired signal at 90 – degrees;
jammers at 30,60 and 100 degrees;

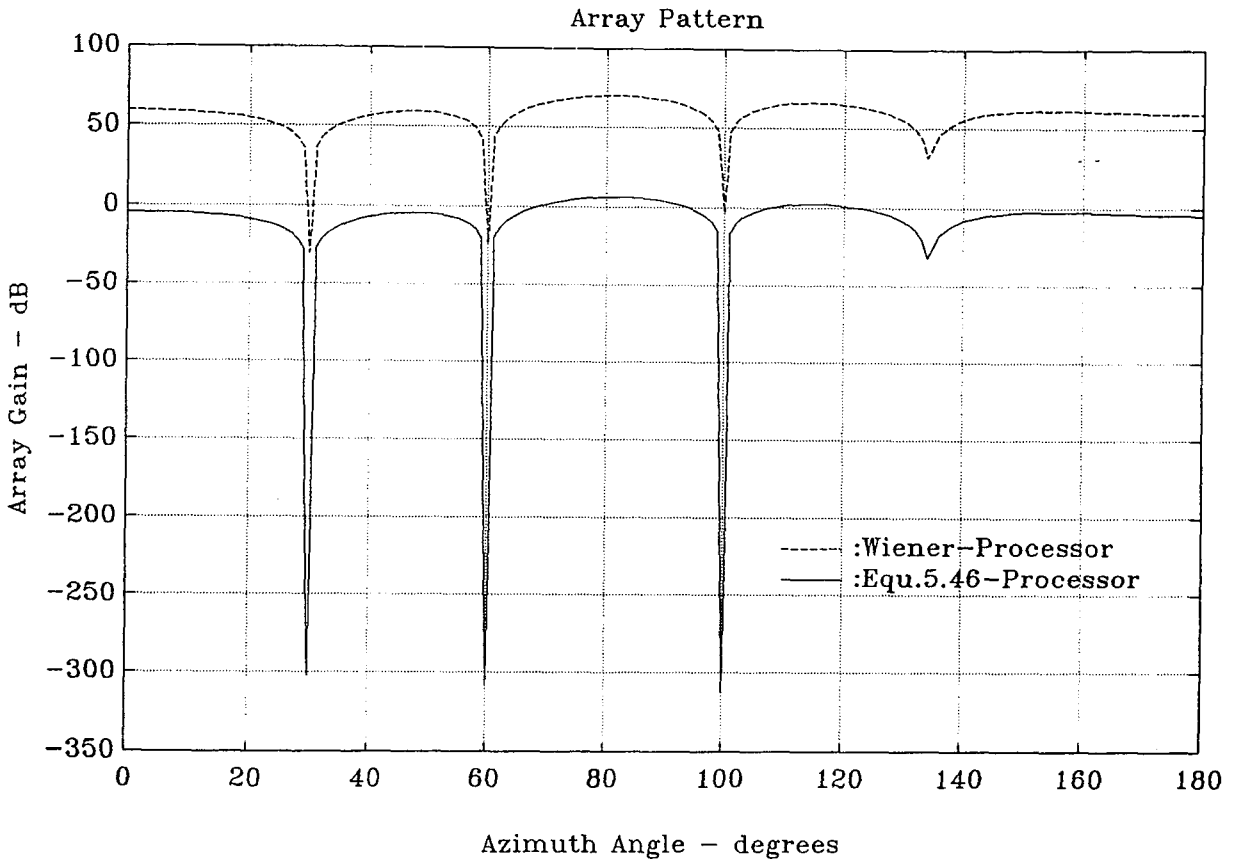

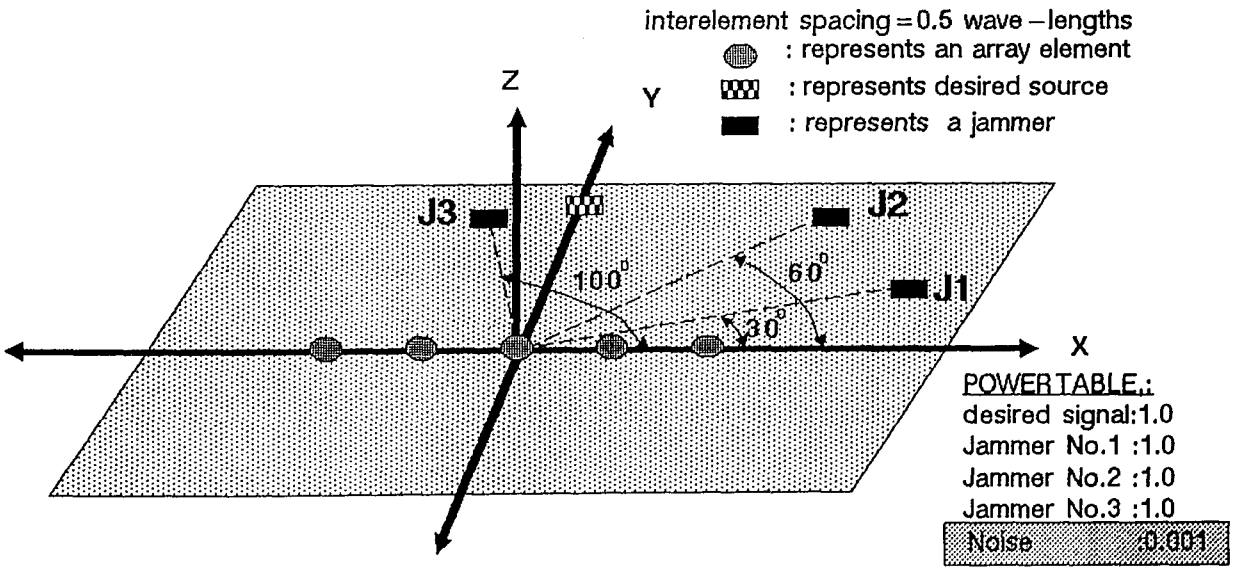

FIGURE – 6.2

ARRAY PATTERNS for EQUATION – 5.46 and WIENER – HOPF PROCESSORS (UNCORRELATED SIGNALS with NOISE LEVEL at – 10dB)

(A linear array of 5 isotropic uniformly distributed elements is used)

***directions:* desired signal at 90 – degrees;**
jammers at 30,60 and 100 degrees;

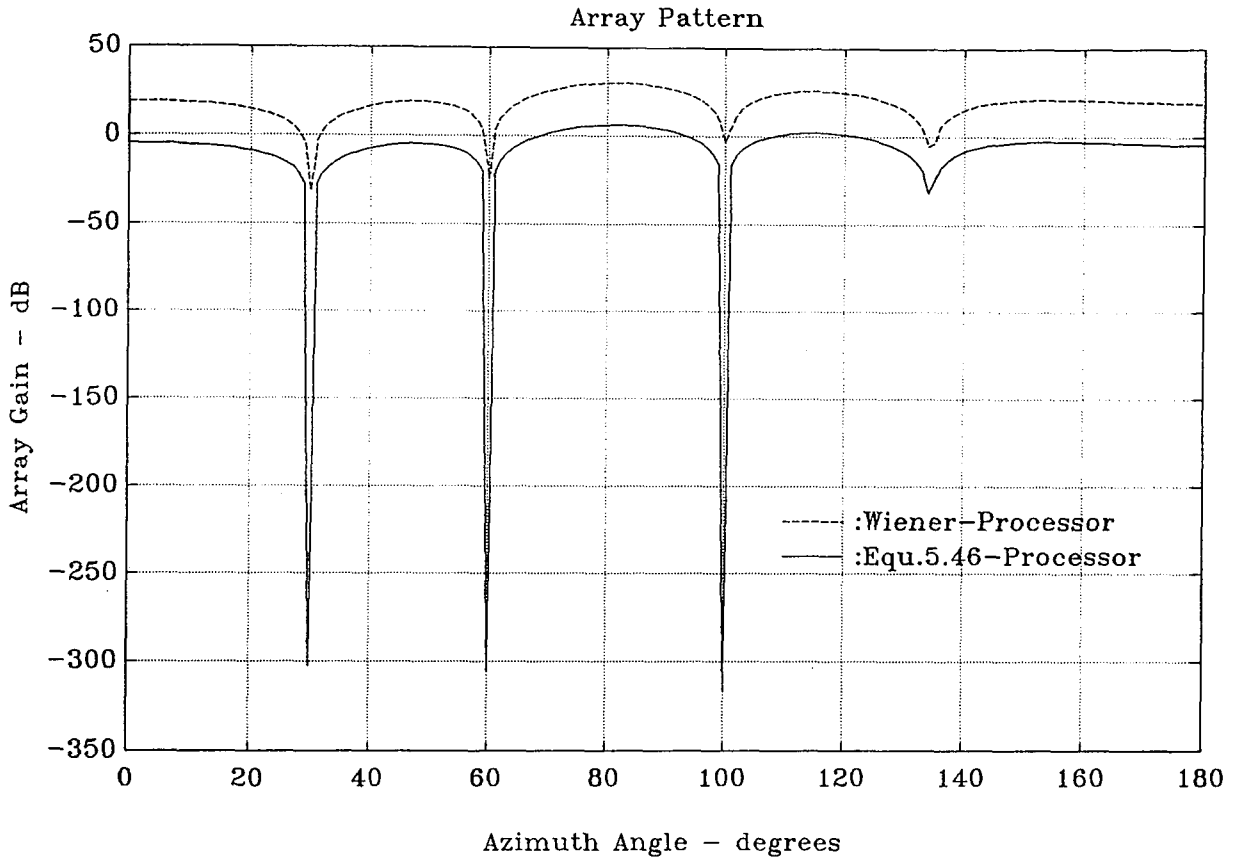

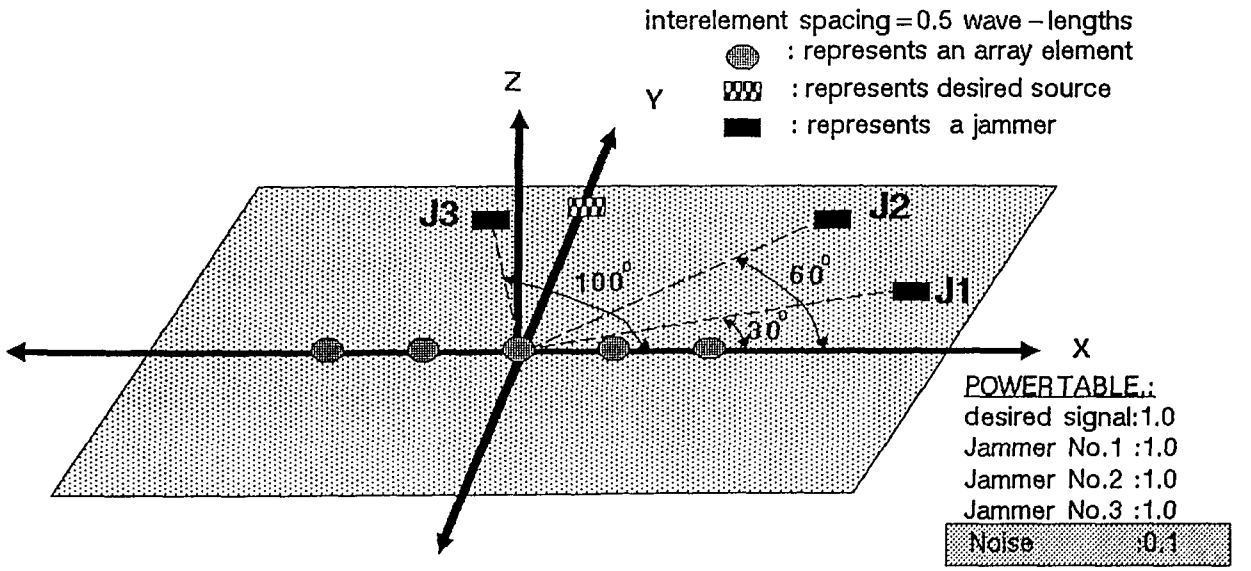

FIGURE – 6.3

OUTPUT SNIR versus AZIMUTH ANGLE FOR EQUATION – 5.46 and WIENER – HOPF PROCESSOR
when JAMMER N0.3 IS MOVED FROM 0 to 180 DEGREES
with noise level at – 30dB

(A linear array of 5 isotropic uniformly distributed elements is used)

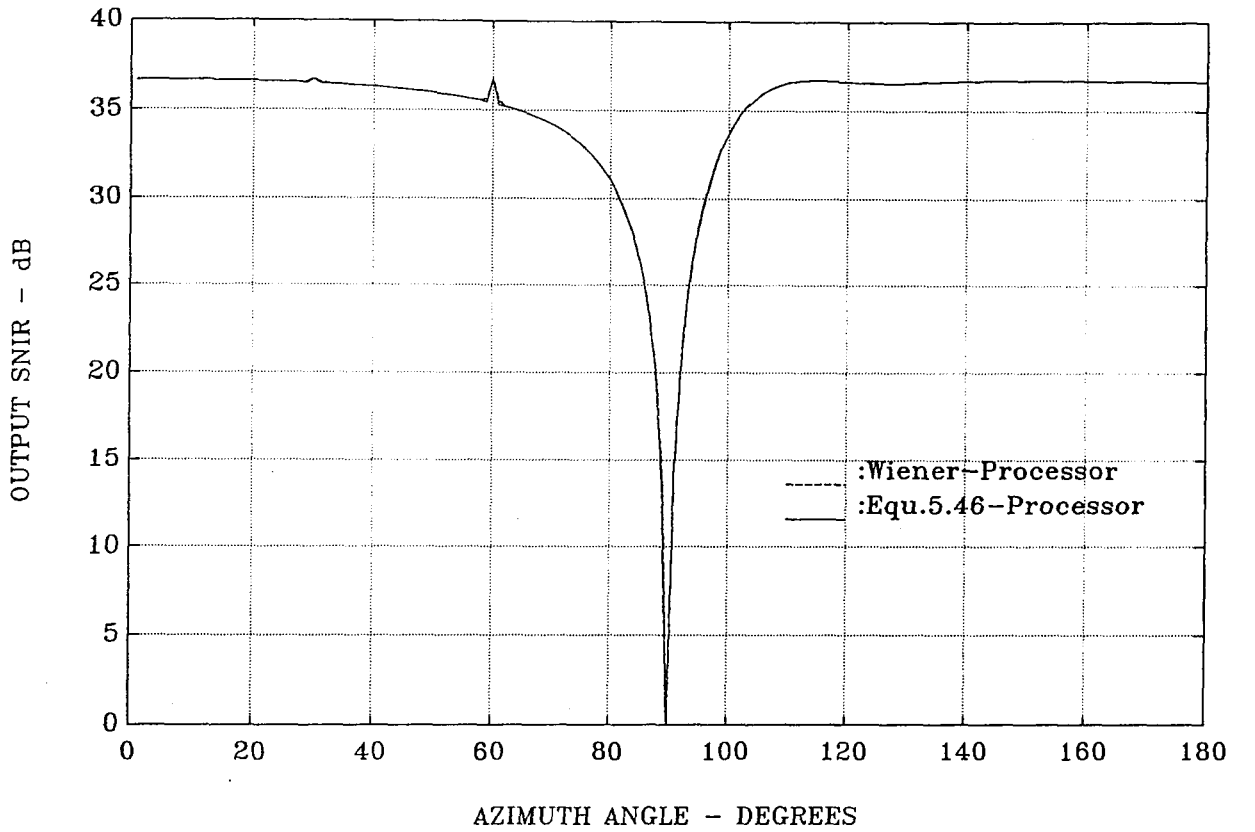

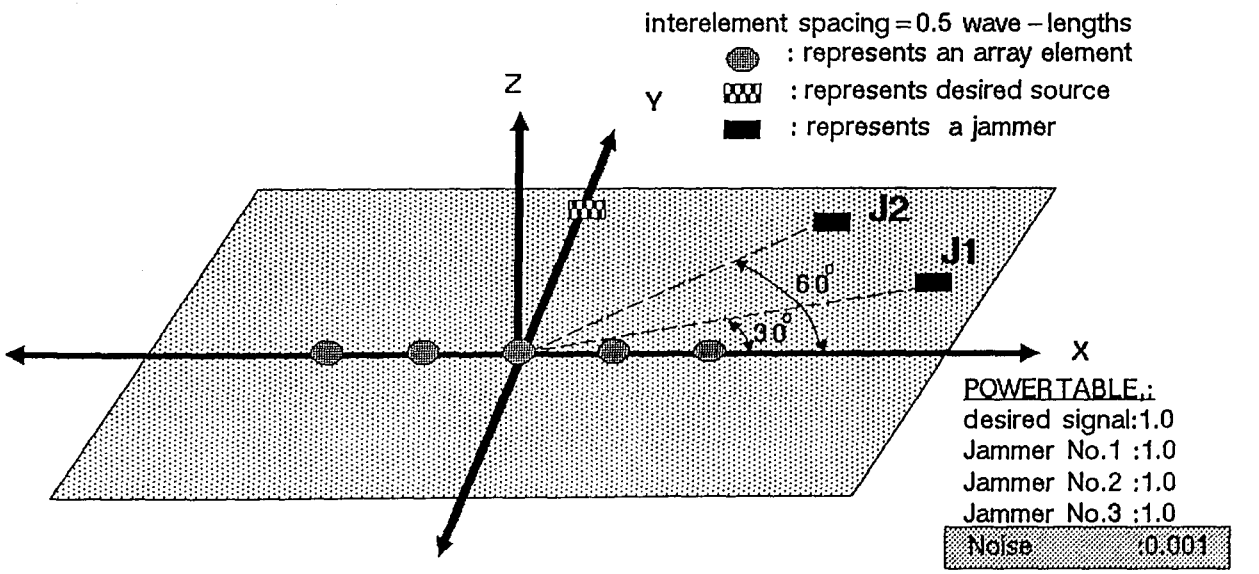

FIGURE – 6.4

OUTPUT SNIR versus AZIMUTH ANGLE FOR EQUATION – 5.46 and WIENER – HOPF PROCESSOR
when JAMMER N0.3 IS MOVED FROM 0 to 180 DEGREES
with noise level at – 10dB

(A linear array of 5 isotropic uniformly distributed elements is used)

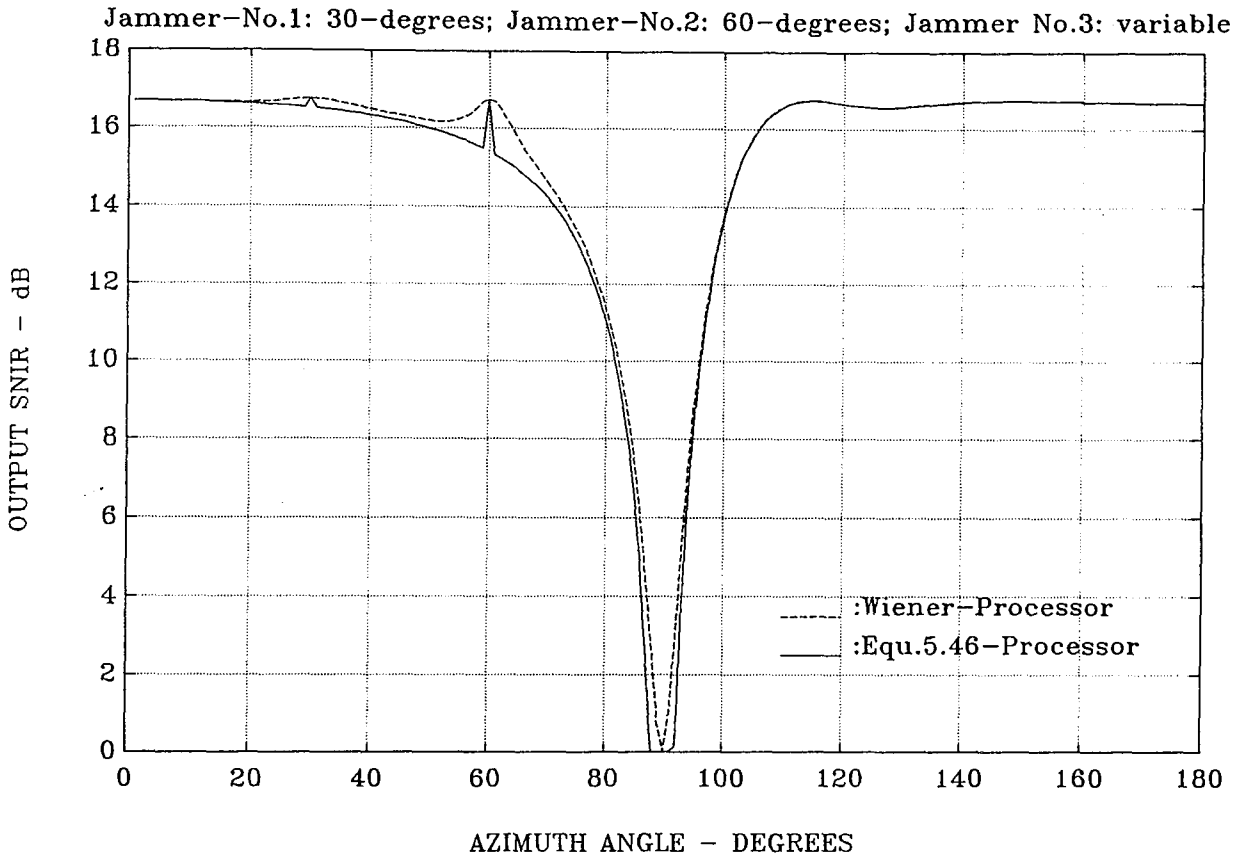

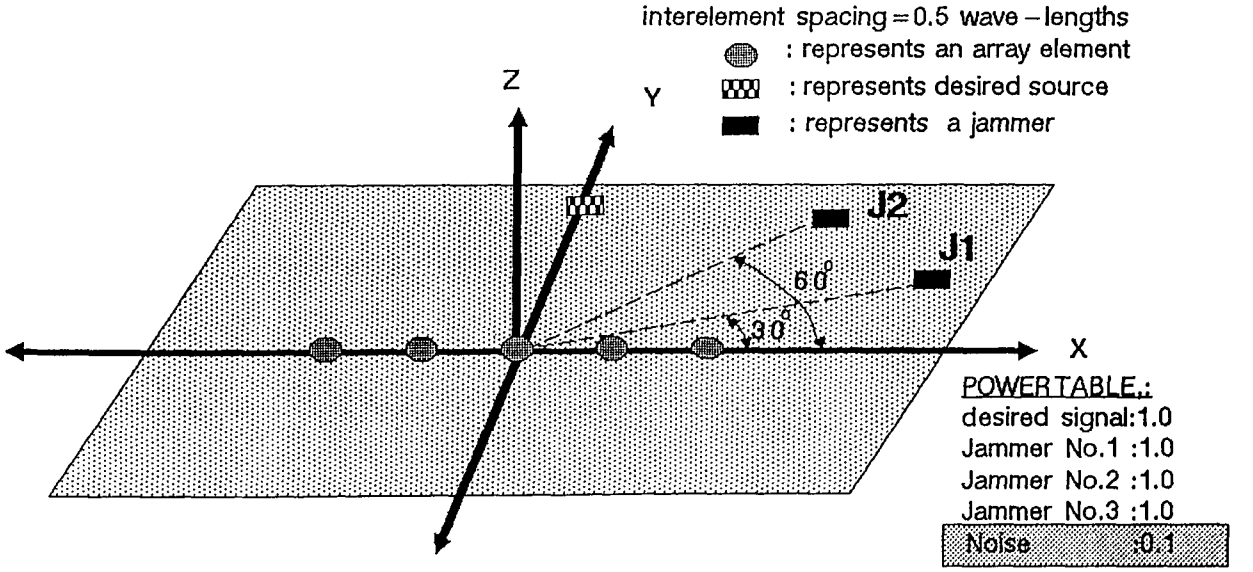

FIGURE – 6.5

ARRAY PATTERNS for EQUATION – 5.46 and WIENER – HOPF PROCESSORS (UNCORRELATED SIGNALS with NOISE LEVEL at –30dB)

(A linear array of 5 isotropic uniformly distributed elements is used)

directions: desired signal at 90 – degrees;
jammers at 60,62 and 100 degrees;

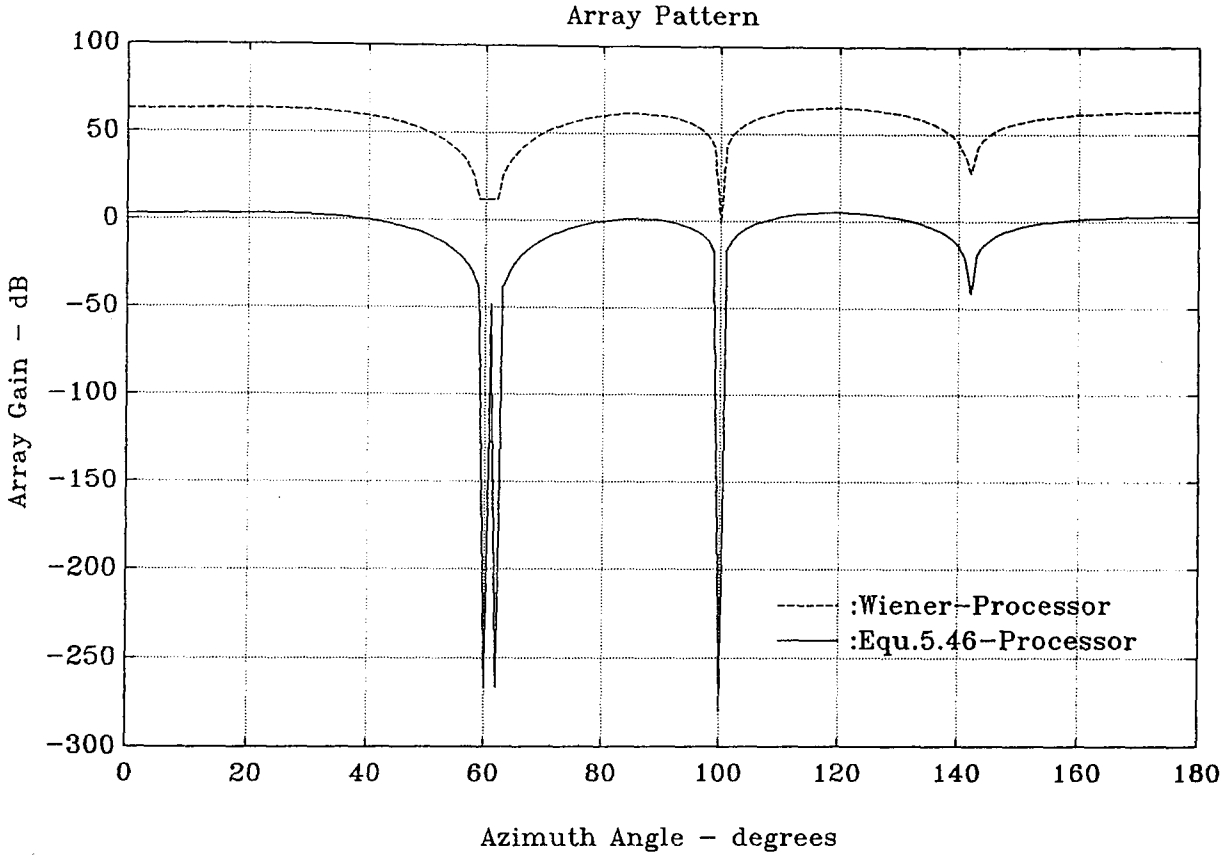

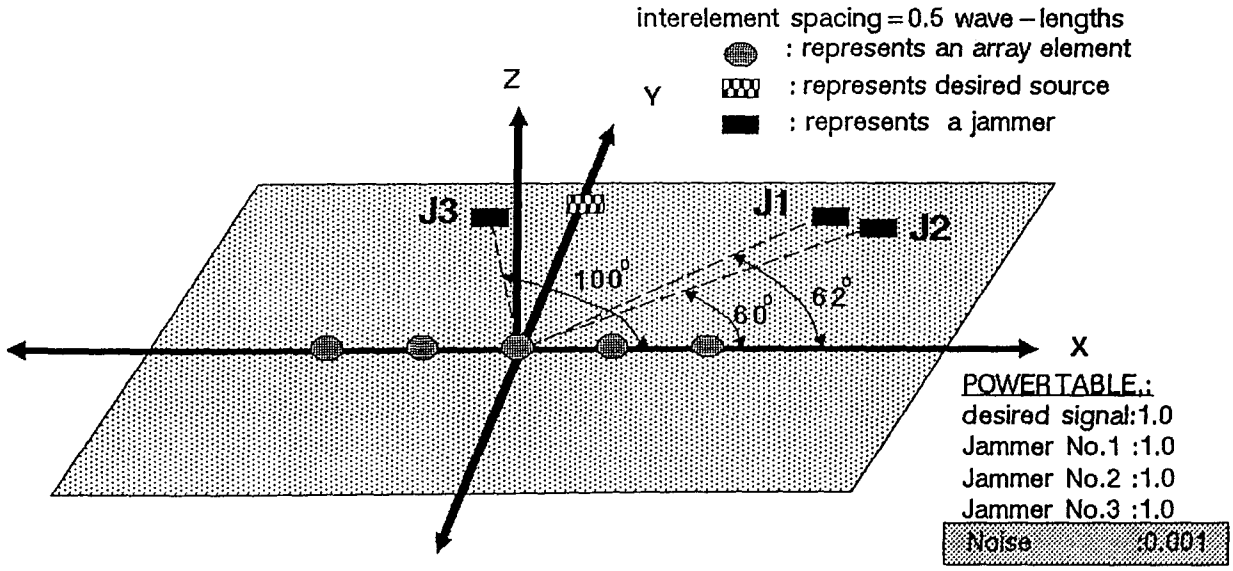

FIGURE – 6.6

ARRAY PATTERNS for EQUATION – 5.46 and WIENER – HOPF PROCESSORS (UNCORRELATED SIGNALS with NOISE LEVEL at – 10dB)

(A linear array of 5 isotropic uniformly distributed elements is used)

directions: desired signal at 90 – degrees;
jammers at 60,62 and 100 degrees;

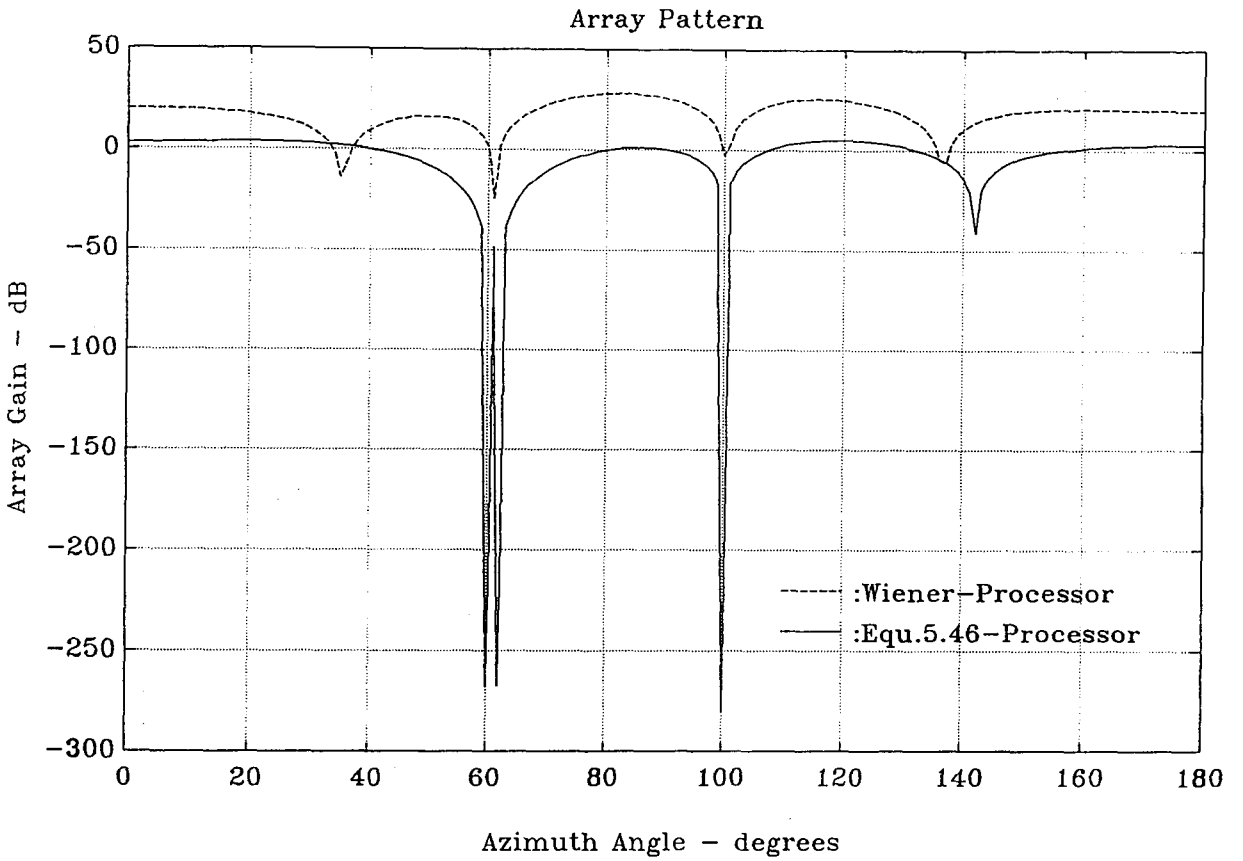

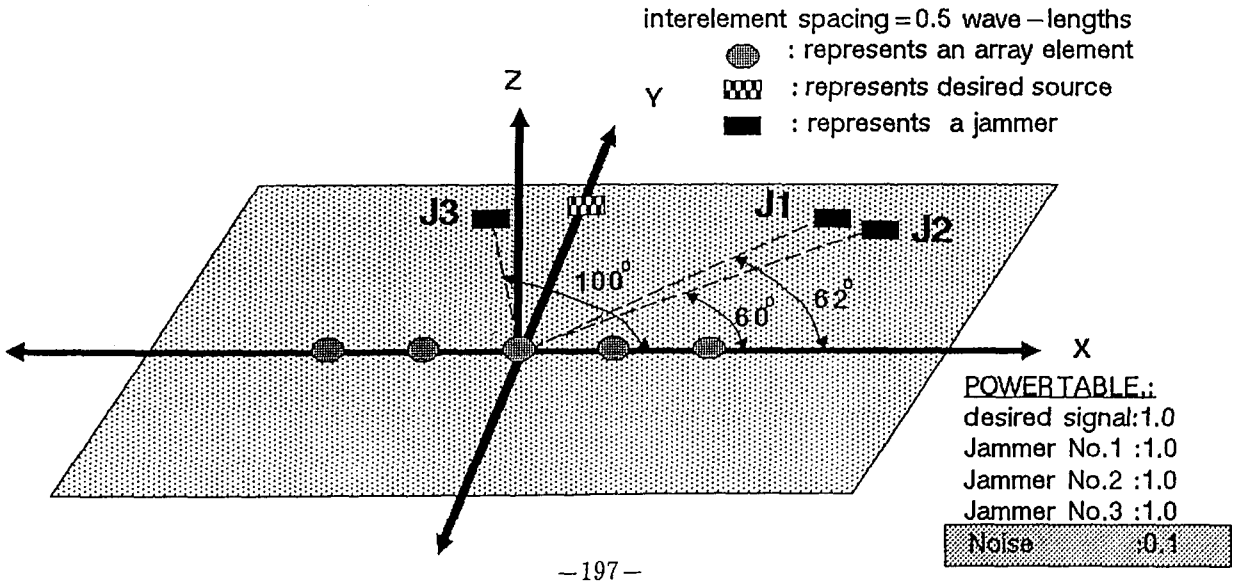

figures also show an additional interesting characteristic. That is, the resolving power of the $\underline{w}_{interf.cancel}$ processor as compared with that of the Wiener-Hopf. By using the Wiener-Hopf processor it is not possible to distinquish the two interfering sources whereas it is with the processor based on $\underline{w}_{interf.cancel}$. The corresponding results with respect to SNIR are shown in *Figures* 6.7 and 6.8

It is also of interest to compare the proposed processor with that of Citron and Kailath processor [CIT-84]. The Citron-Kailath processor also uses the ideas of high resolution techniques in order to provide the appropriate weight. However, their technique is based on subtracting signals between adjacent sensors and the transformation applied means effectively a reduction in the dimensionality of the observation space by one. *Figure* 6.9 shows that the proposed processor based on *Equation* 5.46 is significantly superior to that of Citron-Kailath with respect to:

- output SNIR and
- that a jammer has to be closer to the direction of the desired source before it leads to a deterioration in system performance.

This superiority increases as the number of present interference increases. In addition comparison has been made with respect to pointing error effects in the Wiener-Hopf ("modified" and "full" version), $\underline{w}_{interfe.cancel}$ and Citron-Kailath processor. *Figure* 6.10 and *Figure* 6.11 (for -30db and -10db noise power respectively) show that the proposed processor is more susceptible to pointing errors than the "modified" Wiener-Hopf solution, but is superior to both the Citron-Kailath and "full" Wiener-Hopf processors. It is important to note the Citron-Kailath behavior to pointing errors when the noise is -10dB; it is obviously inferior even to the "full" Wiener-Hopf

processor.

It is important to point out that in an environment where there are no interfering sources present, that is, the only source present is the desired directional signal, the Citron-Kailath processor provides zero weight vector and so there is complete signal nulling and the output SNR becomes zero. This is a disturbing asymptotic result. The proposed weight $\underline{w}_{interf.cancel}$, however, overcomes this problem and it provides a solution which is equivalent to Wiener-Hopf solution. That is, the weight vector is co-linear with the steered vector. *Figure* 6.12 presents the results for one such situation.

Next, consider the ASPECT algorithm with the modification presented in the *Section* 5.8. and examine the behaviour of the ASPECT weight processor in a situation involving uncorrelated sources. Table-2 and *Figures* 6.13 show the results. The situation is considered in which two interferences are correlated (*Figure* 6.14) and then the situation where these two interfering sources are both fully correlated with the desired signal (see *Figures* 6.15). ASPECT even in this situation provides satisfactory results. *Figure* 6.16 illustrates the behavior of Wiener processor and *Equation* 5.46 for the same environment. The superiority of ASPECT is clear by comparing the last two figures.

FIGURE – 6.7

OUTPUT SNIR versus AZIMUTH ANGLE FOR EQUATION – 5.46 and WIENER – HOPF PROCESSOR
when JAMMER No.3 IS MOVED FROM 0 to 180 DEGREES.
with noise level at – 30dB

(A linear array of 5 isotropic uniformly distributed elements is used)

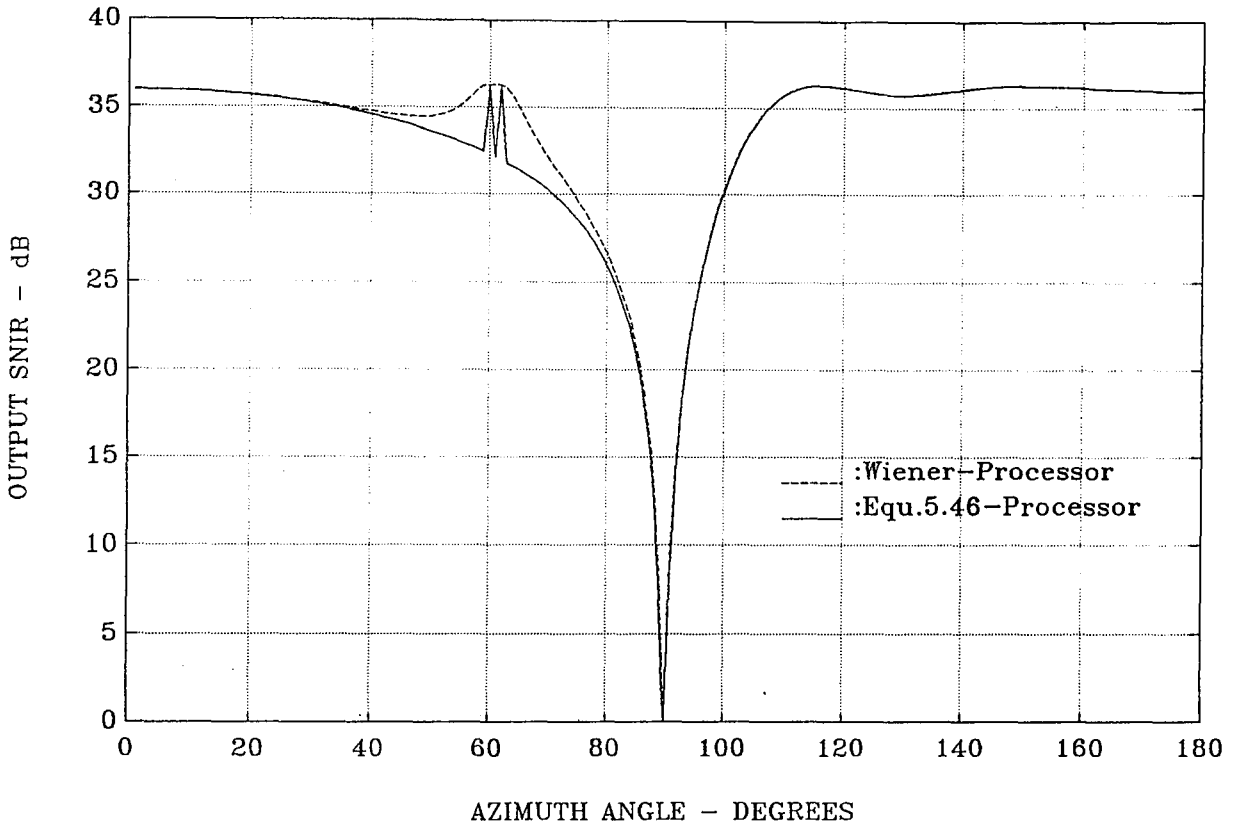

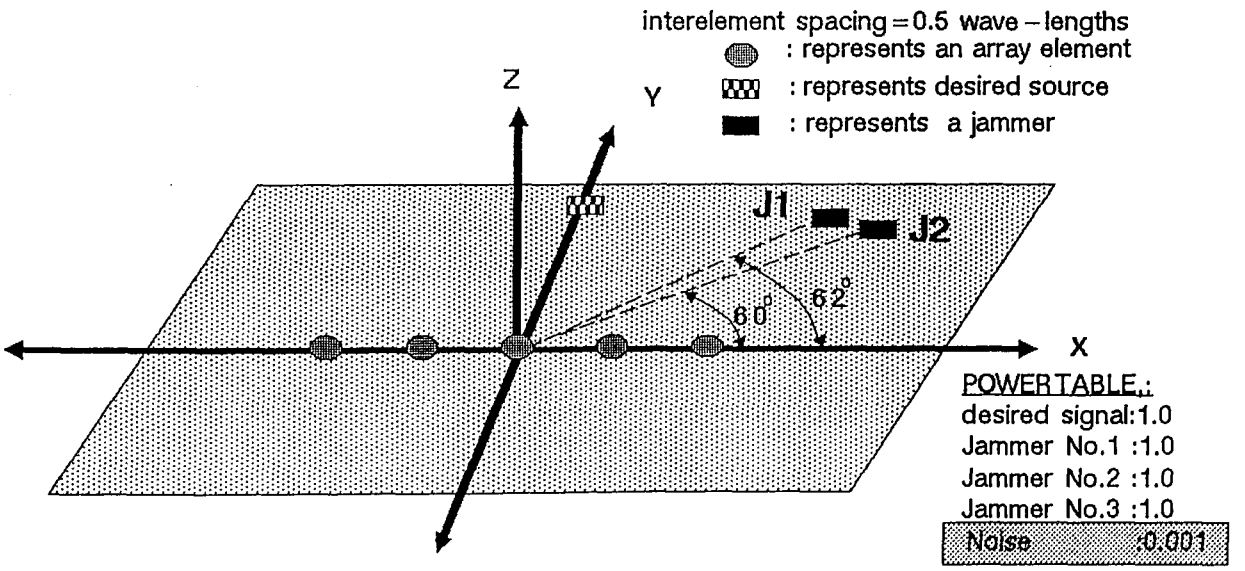

FIGURE – 6.8

OUTPUT SNIR versus AZIMUTH ANGLE FOR EQUATION – 5.46 and WIENER – HOPF PROCESSOR
when JAMMER No.3 IS MOVED FROM 0 to 180 DEGREES.
with noise level at – 10dB

(A linear array of 5 isotropic uniformly distriburted elements is used)

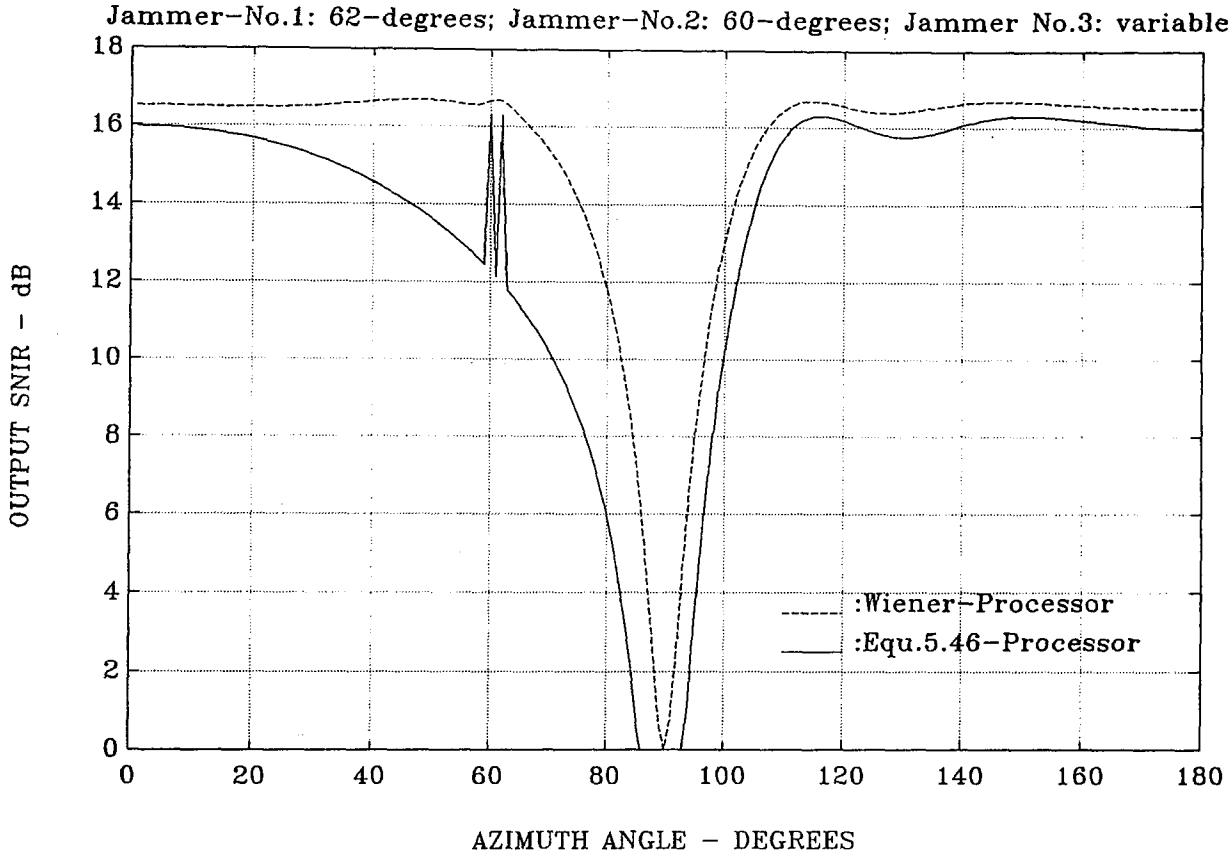

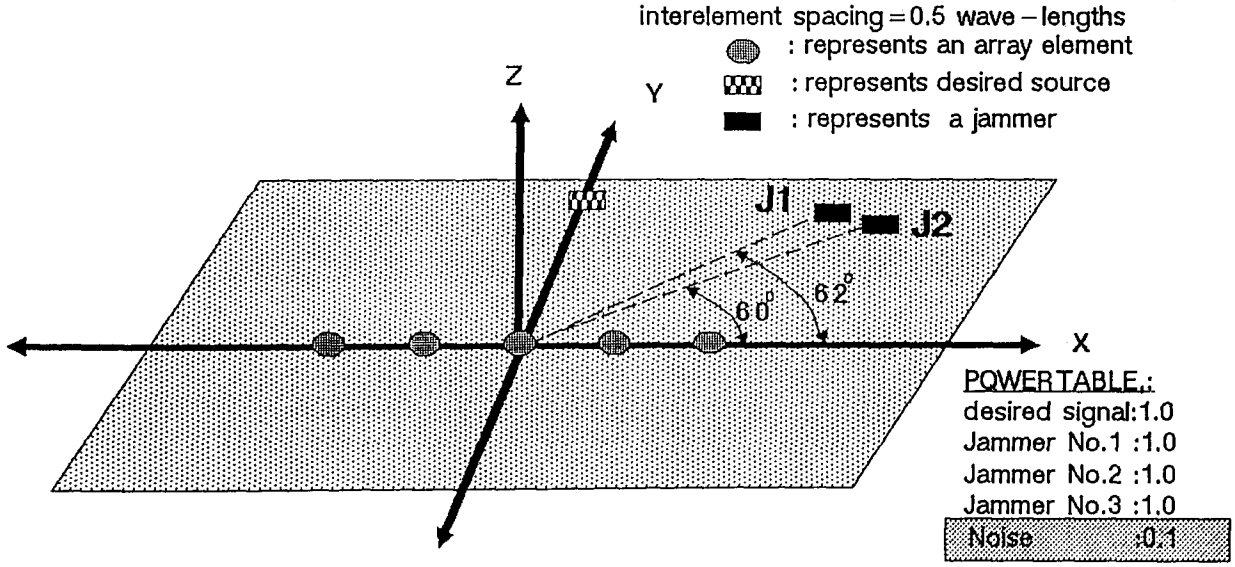

FIGURE – 6.9

OUTPUT SNIR versus AZIMUTH ANGLE FOR:
1. WIENER – HOPF PROCESSOR
2. EQUATION – 5.46 PROCESSOR and
3. CITRON – KAILATH PROCESSOR

when JAMMER No.3 IS MOVED FROM 0 to 180 DEGREES. Noise level at – 10dB.

(A linear array of 5 isotropic uniformly distributed elements is used)

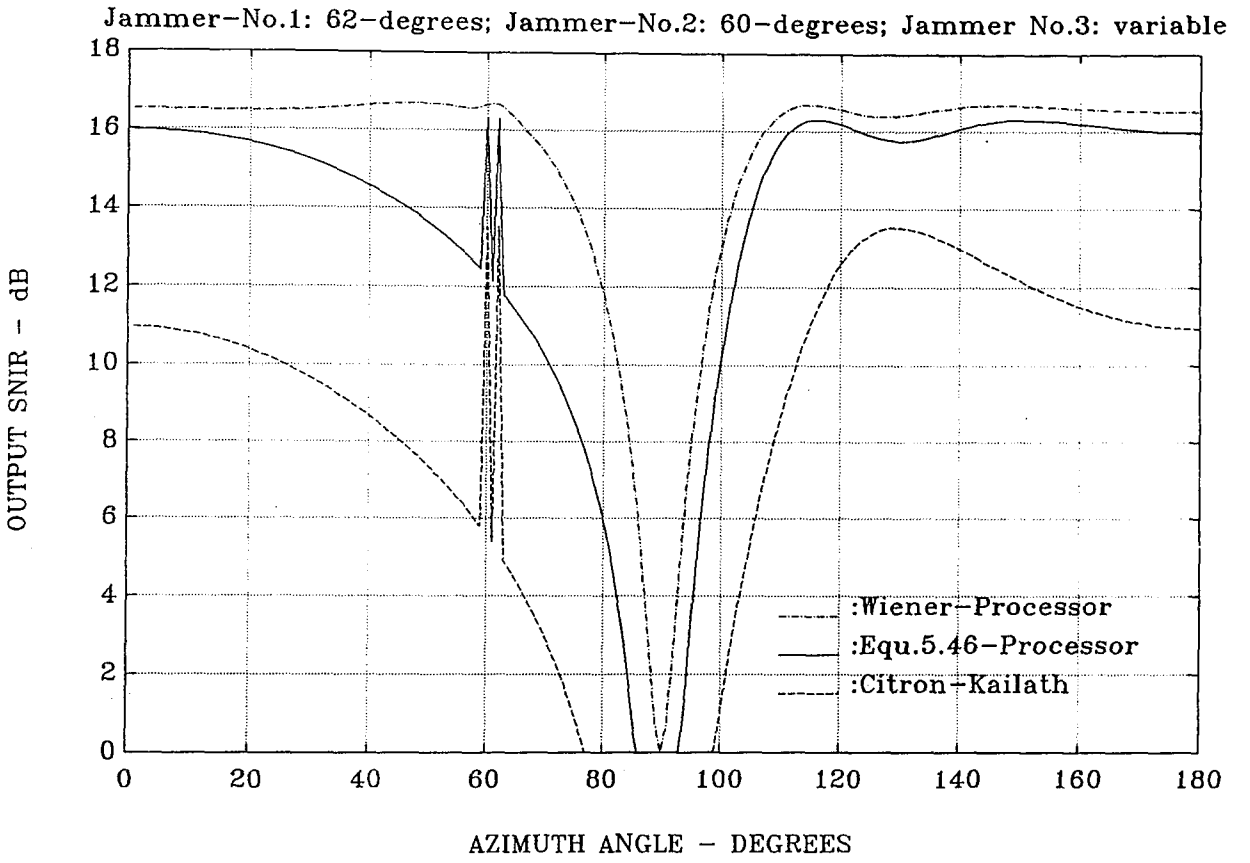

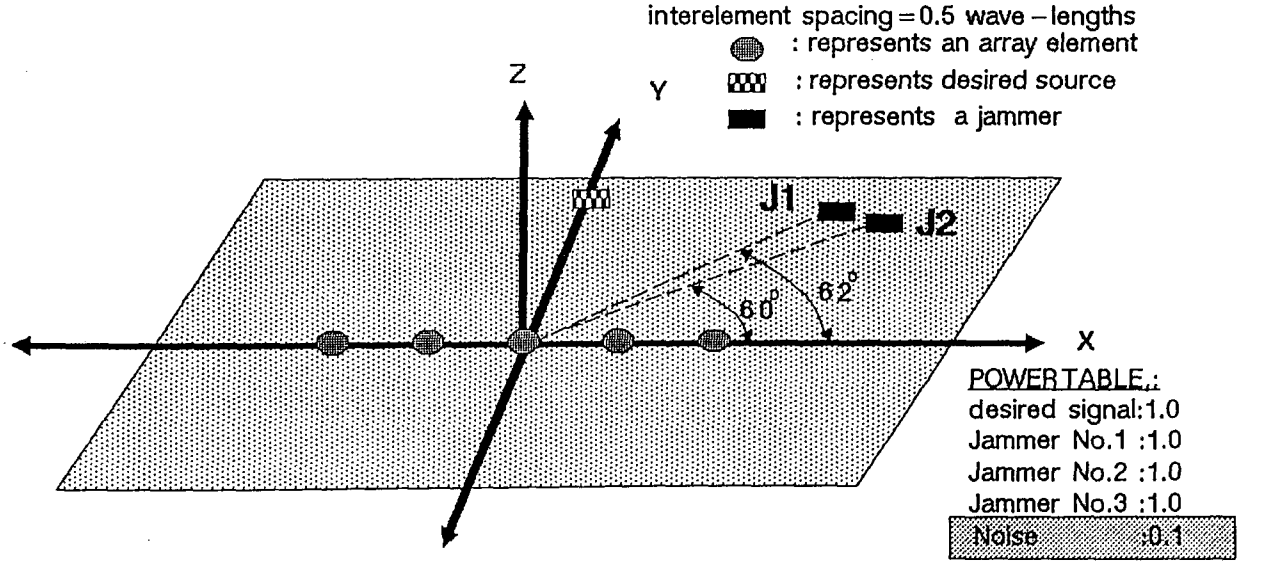

FIGURE – 6.10

OUTPUT SNIR when POINTING ERRORS OCCUR with DESIRED SIGNAL at 90 – DEGREES

FOR:
1. modified WIENER – HOPF PROCESSOR
2. EQUATION – 5.46 PROCESSOR
3. CITRON – KAILATH PROCESSOR and
4. full WIENER – HOPF PROCESSOR

(A linear array of 5 isotropic uniformly distributed elements is used)

Noise level at – 30dB.

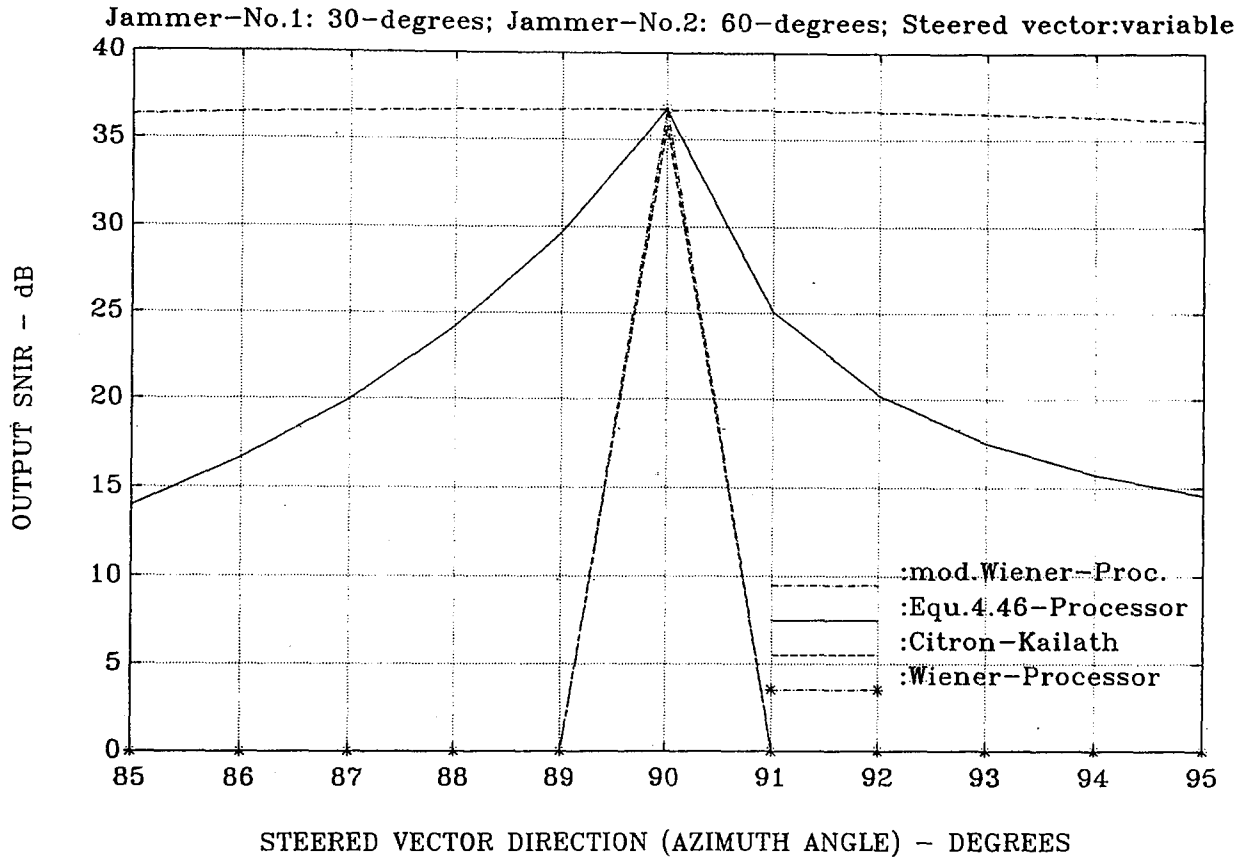

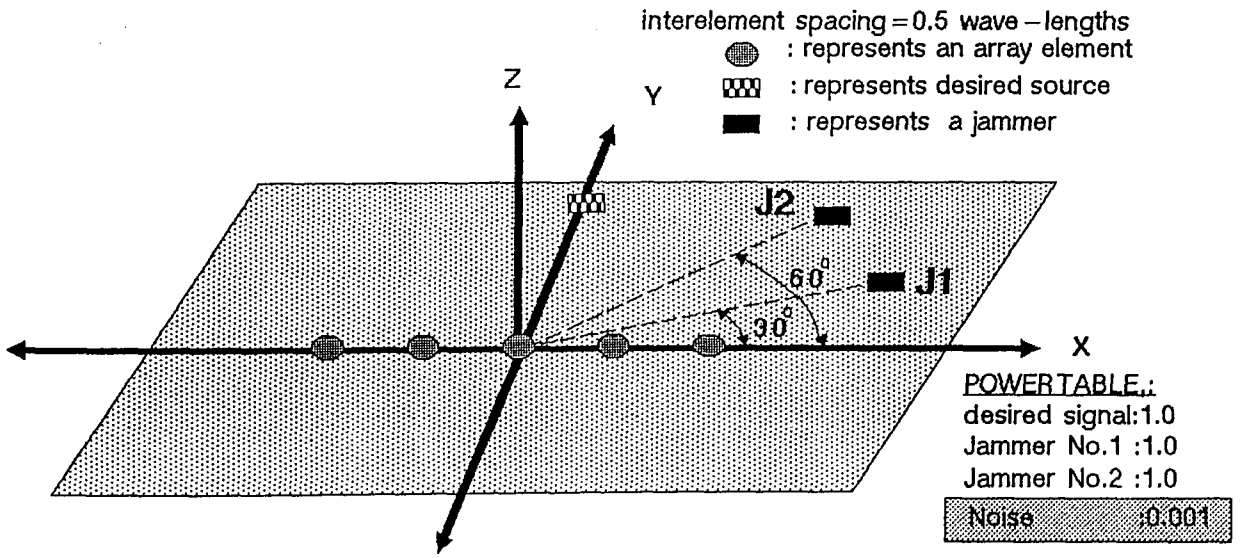

FIGURE – 6.11

OUTPUT SNIR when POINTING ERRORS OCCUR with DESIRED SIGNAL at 90 – DEGREES

FOR:
1. modified WIENER – HOPF PROCESSOR
2. EQUATION – 5.46 PROCESSOR
3. CITRON – KAILATH PROCESSOR and
4. full WIENER – HOPF PROCESSOR

(A linear array of 5 isotropic uniformly distributed elements is used)

Noise level at – 10dB.

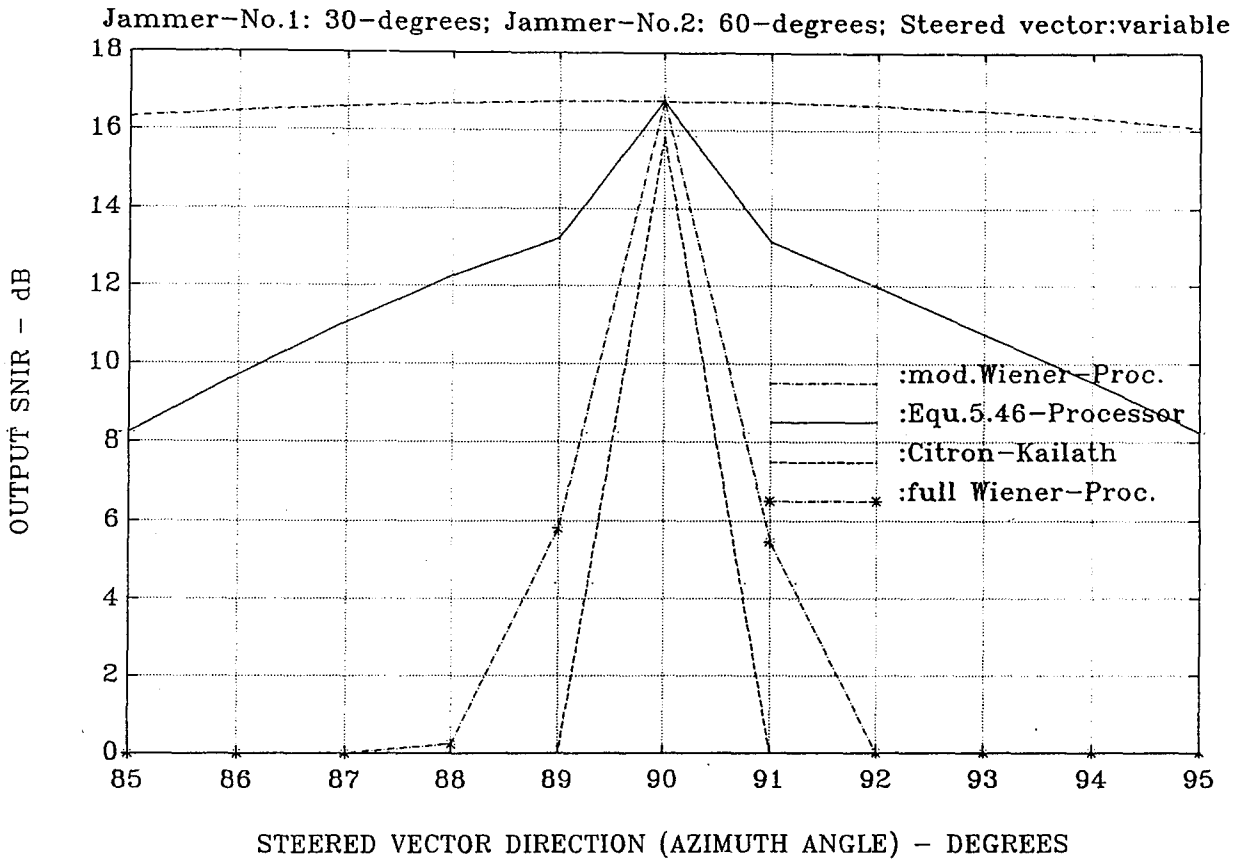

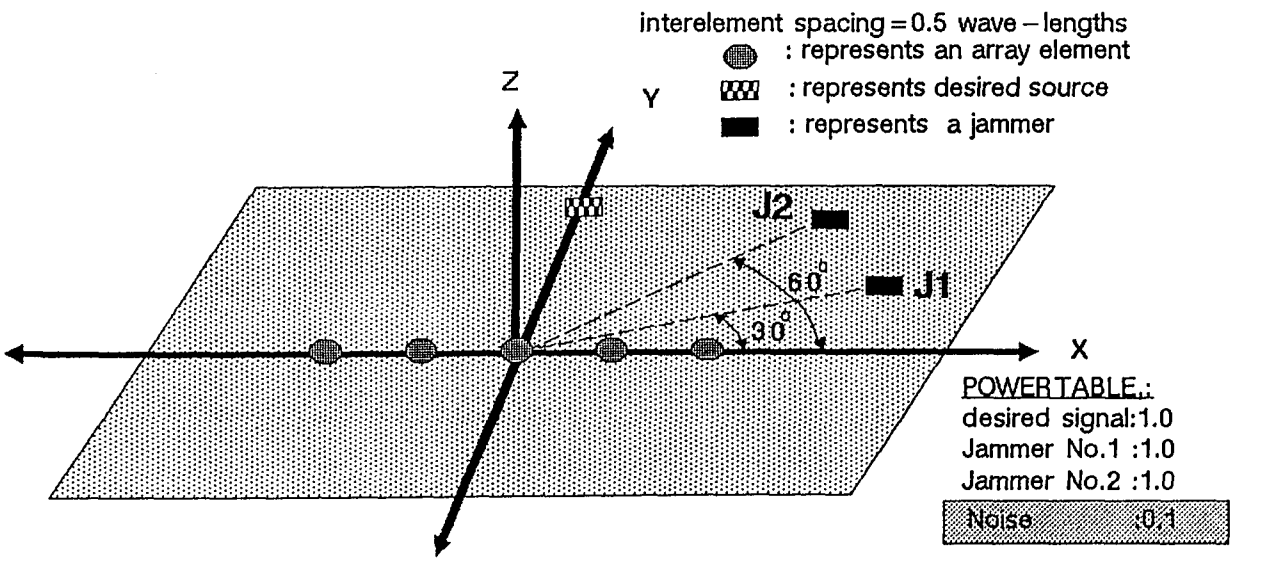

FIGURE-6.12

SIGNAL ENVIRONMENT WITH NO INTERFERENCE PRESENT

$\underline{w}_{citron\text{-}kail} = [\,0\ 0\ 0\ 0\ 0\,]^T$ $\underline{w}_{wiener} = [\,10\ 10\ 10\ 10\ 10\,]^T$

$\underline{w}_{interf.cancel} = [\,4.4721\text{x}10^{-1}\ \ 4.4721\text{x}10^{-1}\ \ 4.4721\text{x}10^{-1}\ \ 4.4721\text{x}10^{-1}\ \ 4.4721\text{x}10^{-1}\,]^T$

				WIENER PROCESSOR		EQU.5-46 PROC.	
	LOCATION	I/P	I/P(dB)	O/P	O/P(dB)	O/P	O/P(dB)
desired	(0,90)	10	0	2500	33.979	5	6.9897
noise	—	0.1	-10	50	16.99	0.1	-10
SNIR	—	10	10	50	16.99	50	16.99
SNR	—	10	10	50	16.99	50	16.99

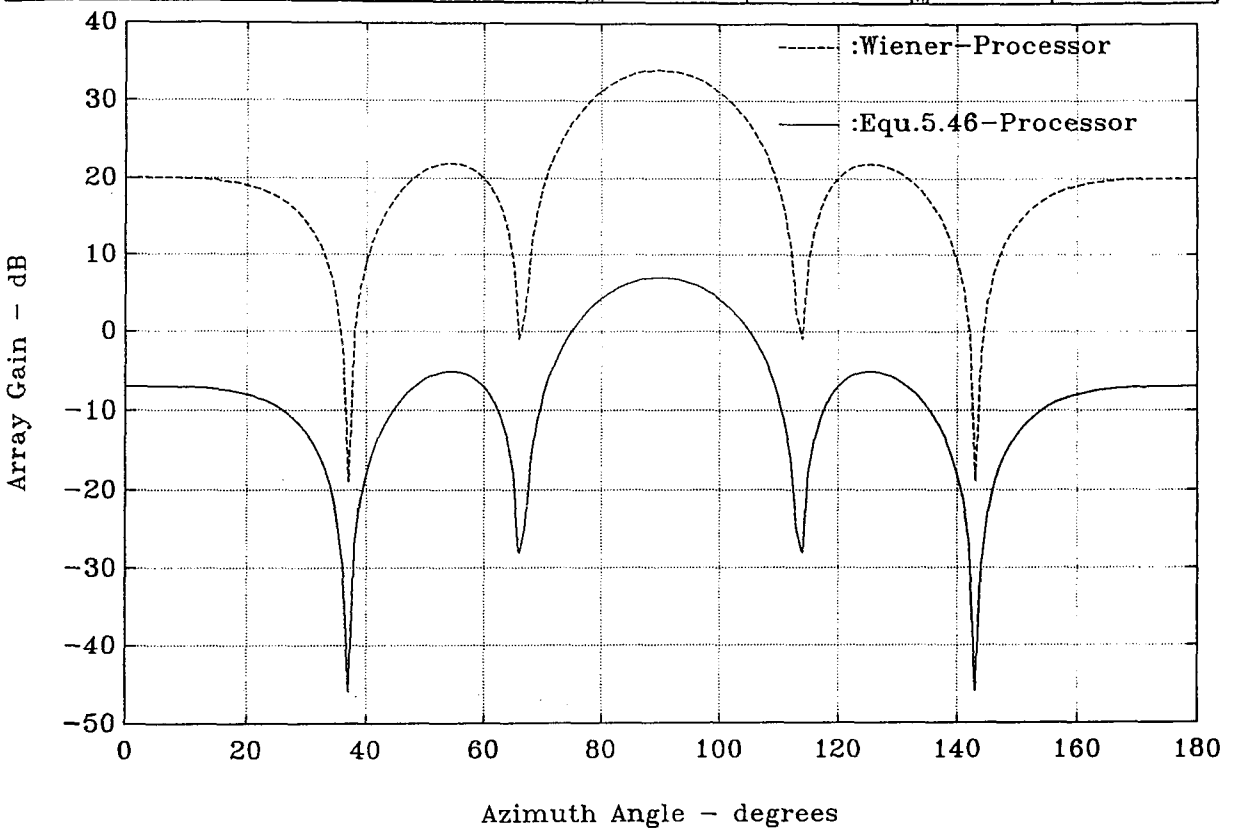

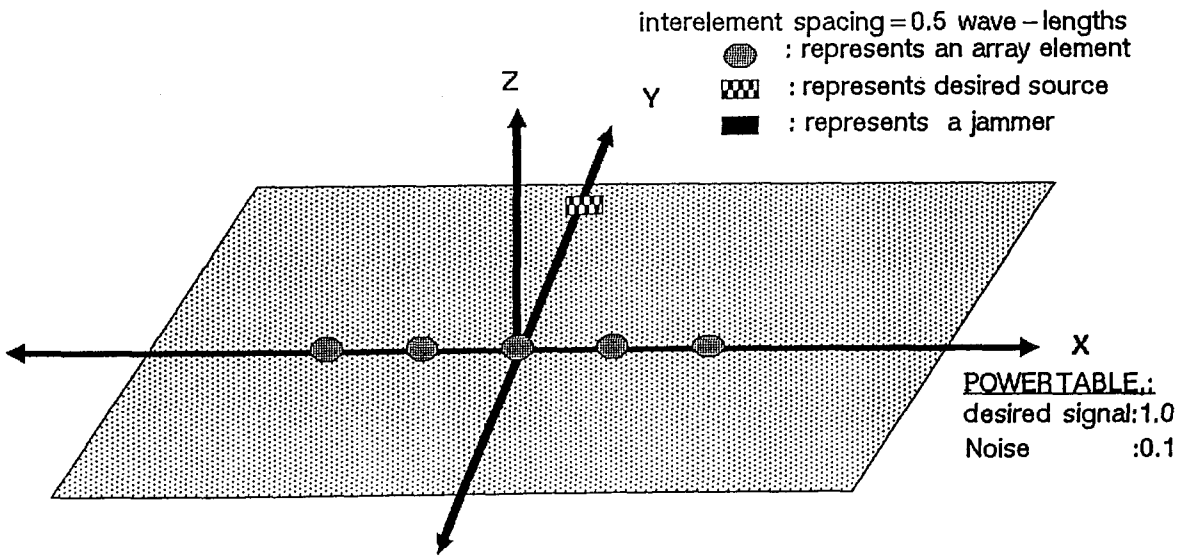

TABLE-2

ASPECT-WEIGHT PROCESSOR

	LOCATION	I/P	I/P(dB)	O/P	O/P(dB)
desired	(0,90)	1	0	6.8739	8.3720
interf-1	(0,40)	1	0	0.0000	-348.4475
interf-2	(0,50)	1	0	0.0000	-347.2566
noise	—	0.1	-10	0.1	-10
SNIR	—	0.4762	-3.2222	68.7386	18.3720
SNR	—	10	10	68.7386	18.3720

FIGURE – 6.13

ASPECT – WEIGHT – VECTOR FOR UNCORRELATED SOURCES

one desired source in the presence of two interfering sources
initial interf. directions :(0,15),(0,65),(0,165) initial pointing direction:(0,95) final interf. directions :(0,40),(0,50) final pointing direction :(0,90)

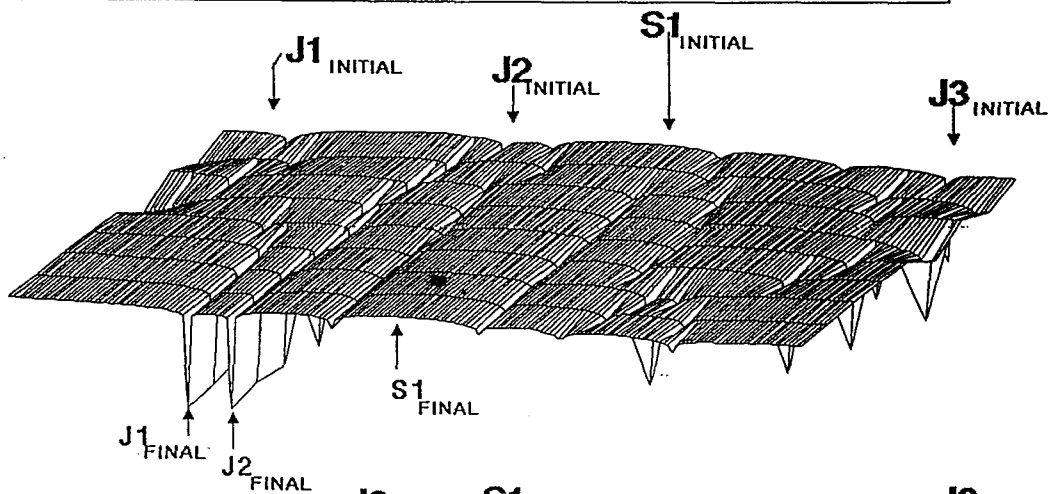

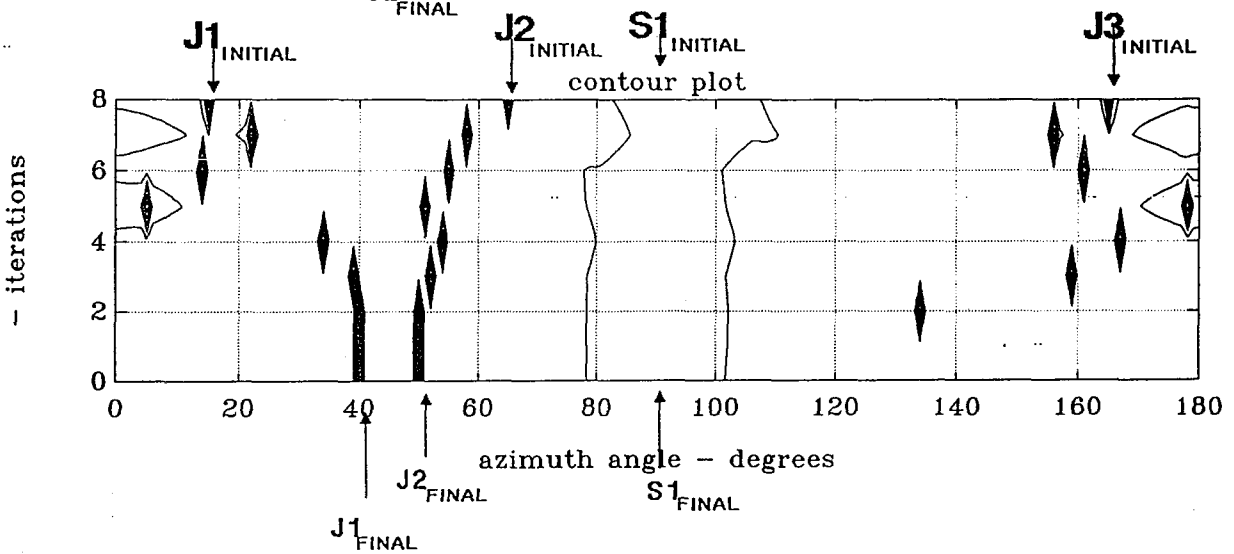

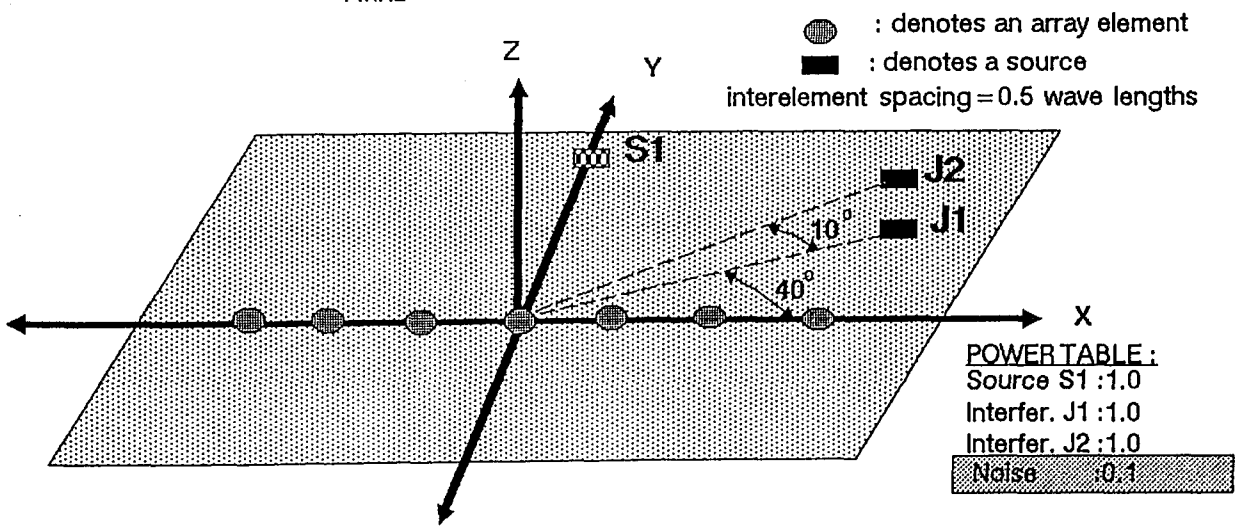

POWER TABLE :
Source S1 :1.0
Interfer. J1 :1.0
Interfer. J2 :1.0
Noise :0.1

FIGURE – 6.14

ASPECT – WEIGHT – VECTOR FOR TWO FULLY CORRELATED INTERFERING SOURCES

one desired source in the presence of two interfering sources
initial Interf. directions :(0,15),(0,65),(0,165) initial pointing direction:(0,95) final interf. directions :(0,40),(0,50) final pointing direction :(0,90)

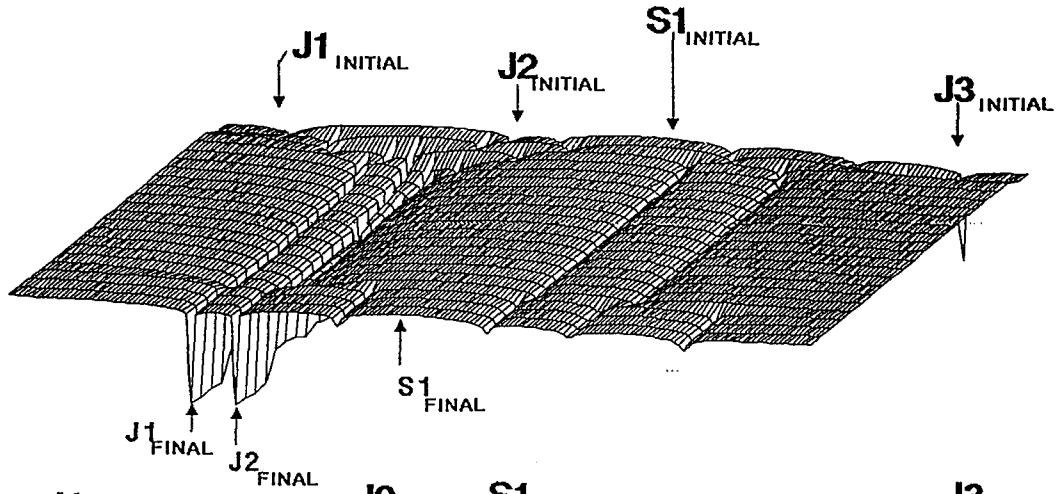

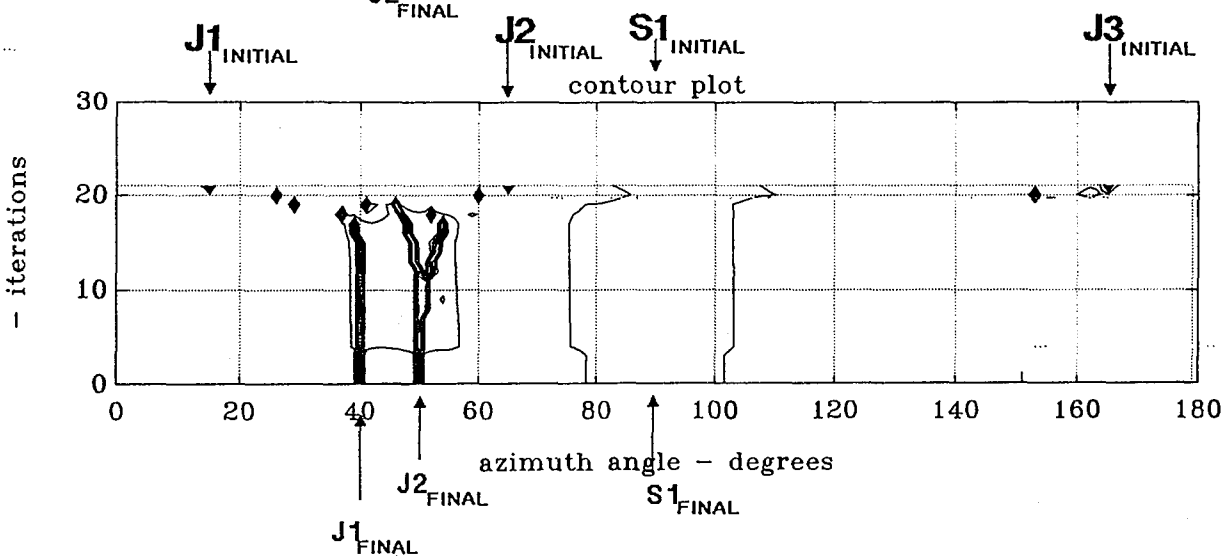

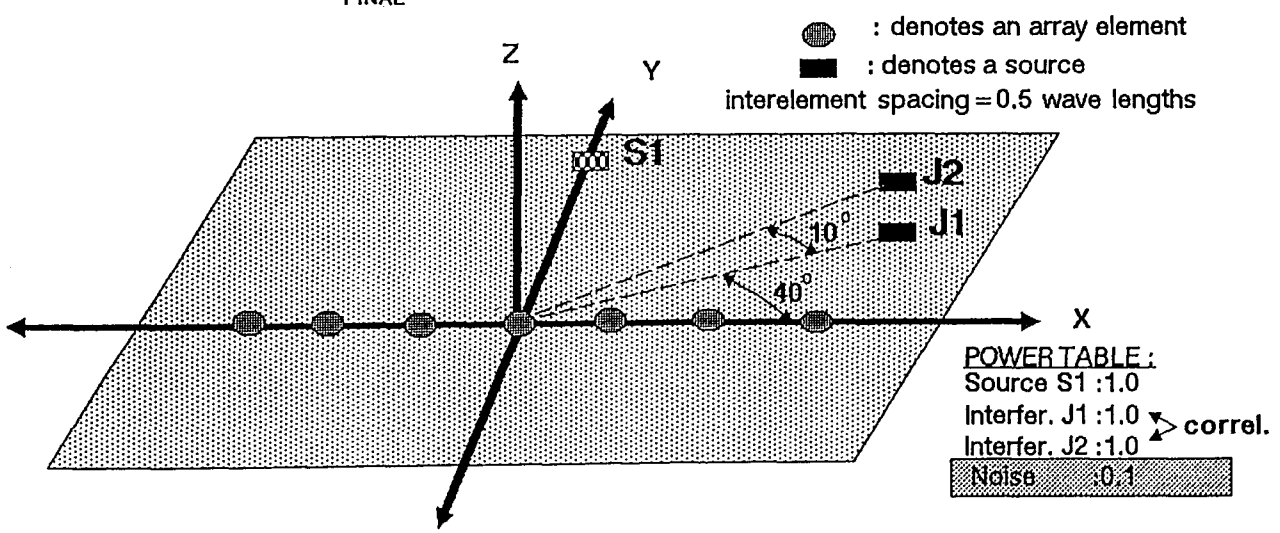

FIGURE – 6.15

ASPECT – WEIGHT – VECTOR FOR DESIRED SIGNAL FULLY CORRELATED WITH TWO INTERFERING SOURCES

one desired source in the presence of two interfering sources
initial interf. directions :(0,15),(0,65),(0,165) initial pointing direction:(0,95) final interf. directions :(0,40),(0,50) final pointing direction :(0,90)

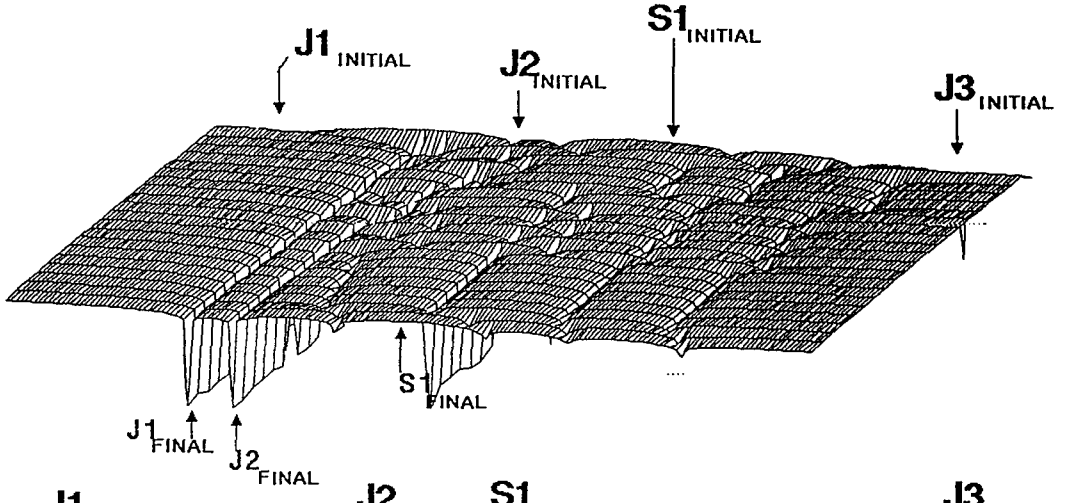

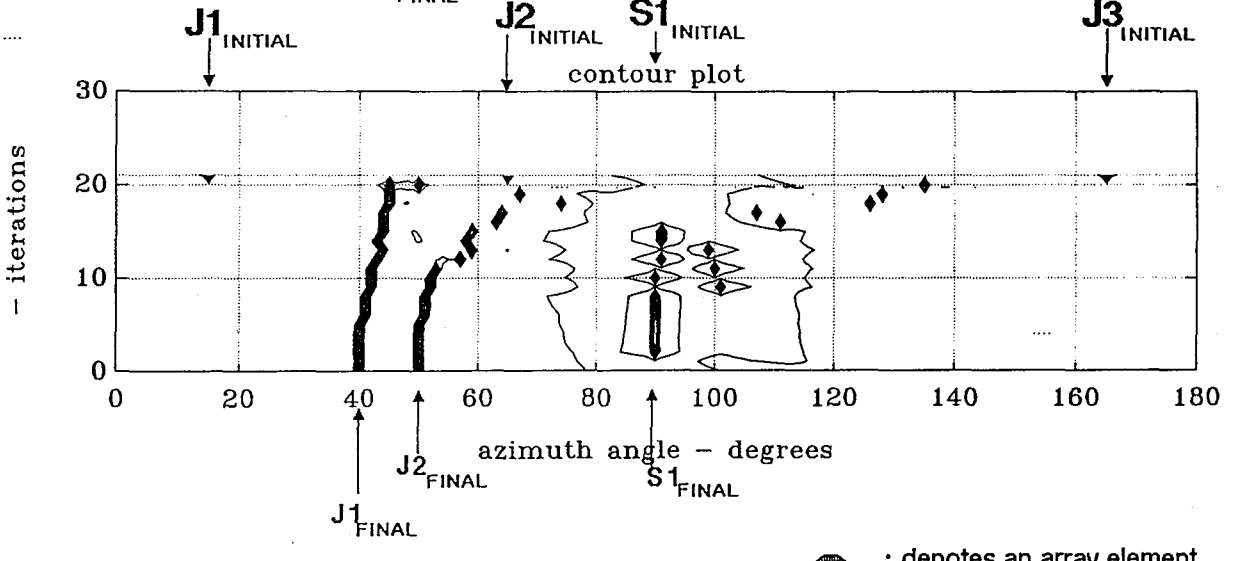

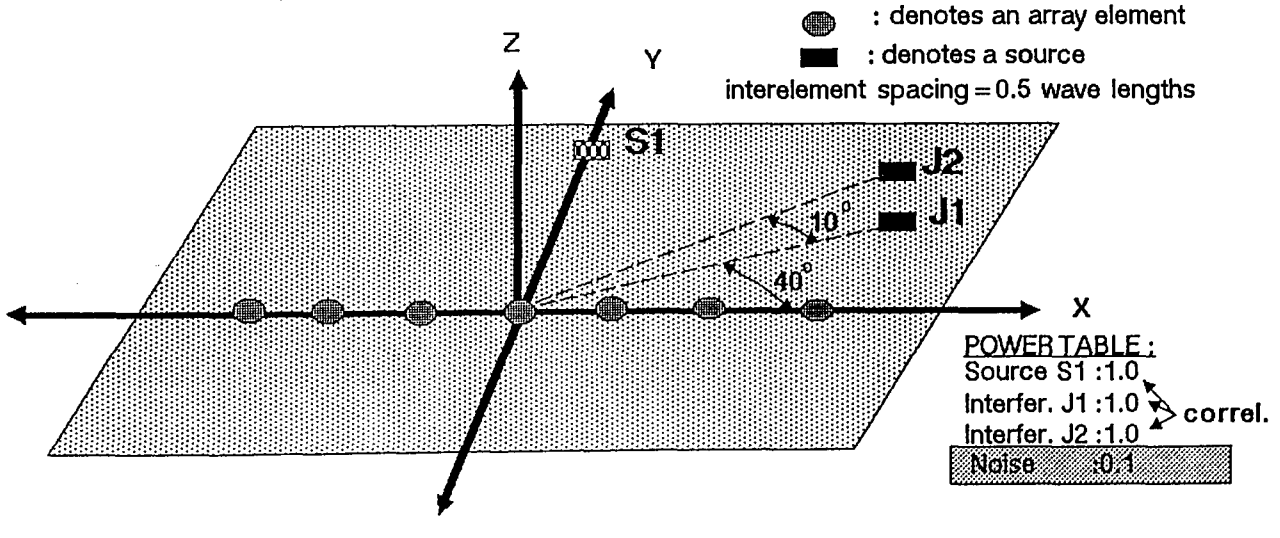

FIGURE – 6.16

WIENER PROCESSOR AND EQU. 5.46 PROCESSOR

FOR DESIRED SIGNAL FULLY CORRELATED WITH TWO INTERFERING SOURCES

one desired source in the presence of two interfering sources
initial interf. directions :(0,15),(0,65),(0,165) initial pointing direction:(0,95) final interf. directions :(0,40),(0,50) final pointing direction :(0,90)

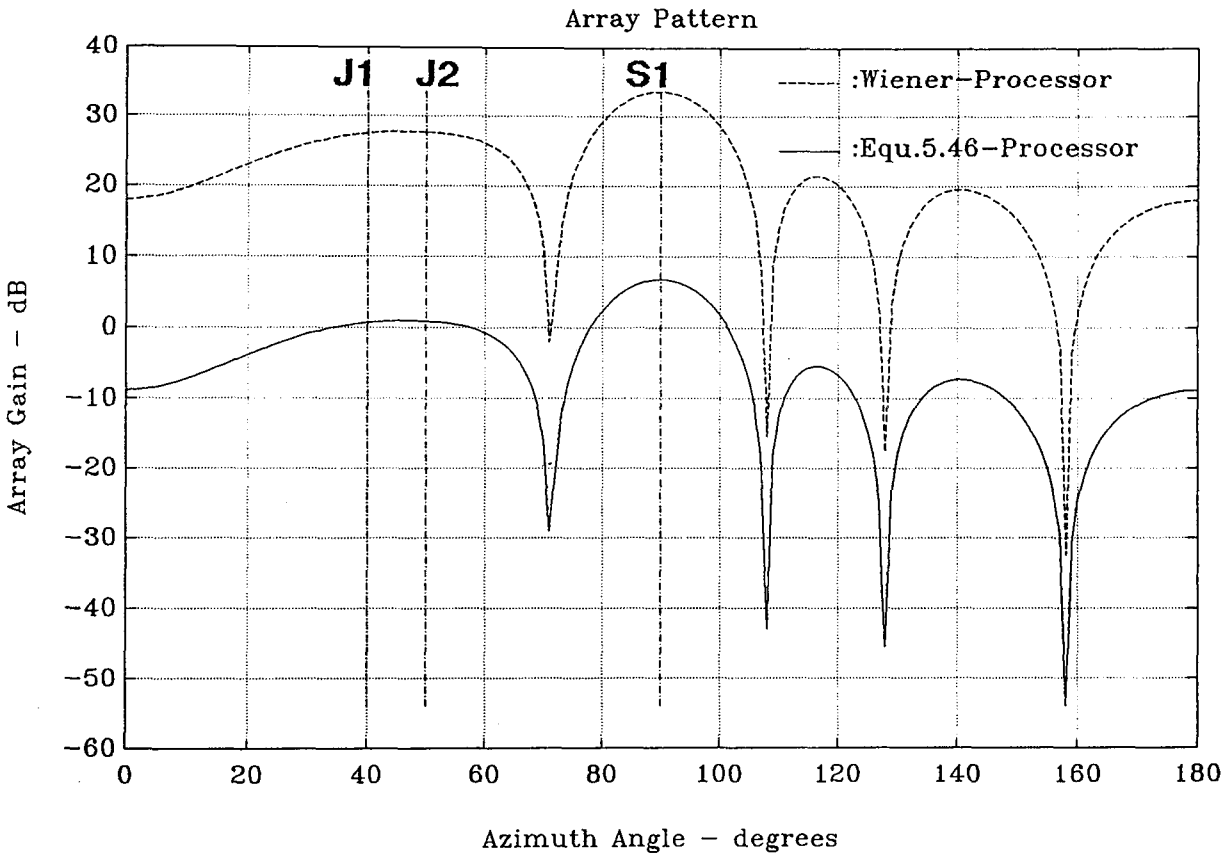

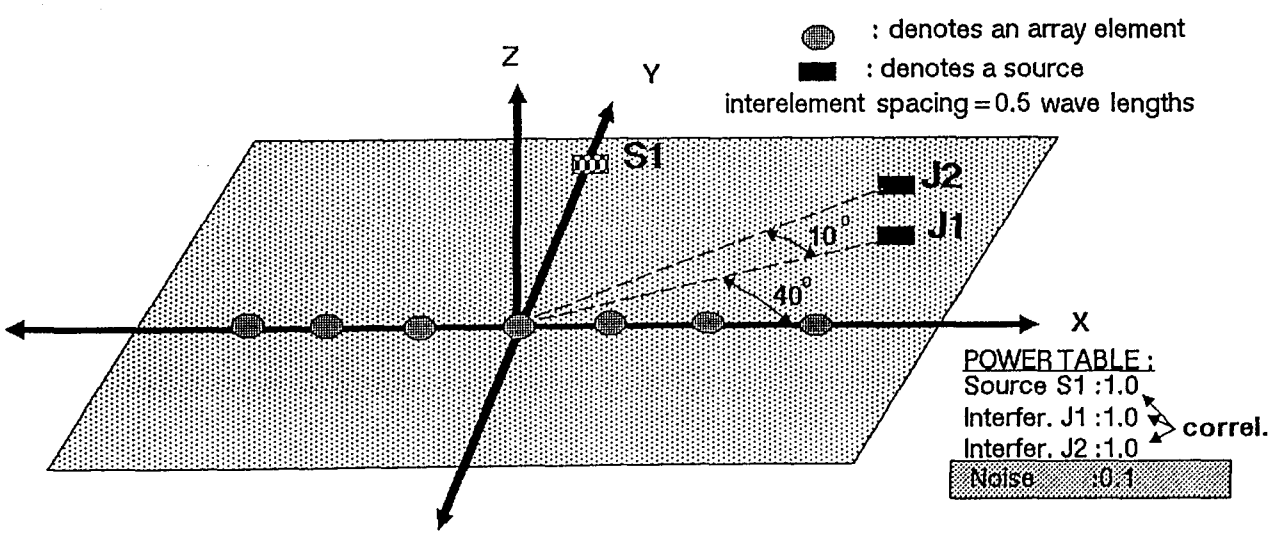

6.2 CONCLUDING REMARKS

On the basis of the above discussion, it can be seen that the proposed processor accomplishes the following tasks:

- provides complete interference cancellation with the output of the array composed from the desired signal and thermal noise;
- provides the number of interferences which exist in the array environment;
- provides unbiased estimates of the directions of the arrivals of the interferences thus, if desired, allowing the steering of the main lobe to one of these interferences which then may become the next desired signal;
- can be implemented easily as the eigendecomposition is nowadays feasible with, for example, wavefront VLSI array processors [e.g. KUN-85];
- provides reduced subsceptibility to pointing errors and noise level;
- does not suffer from power inversion problem;
- provides the best approximation of the Wiener-Hopf solutions in the complement of the subspace spanned by the interferences
- in the case of absence of interferences, instead of providing complete signal nulling, provides solution equivalent to Wiener-Hopf optimum solutions.
- The process is independent of the presence of the desired signal effects.

The above are achieved in some cases at the expense of slight reduction in SNIR.

CHAPTER 7

SUMMARY and CONCLUSIONS

7.1 SUMMARY OF CONTRIBUTIONS

Existing *Signal Subspace* algorithms which are designed to locate signals need to have a priori knowledge of the number of signals present, in order to estimate their directions of arrival. These algorithms fail if some of the incident signals are fully correlated (coherent). Also, algorithms used to estimate the number of signals fail when correlated signals are involved.

The first part of the research reported on in this thesis has been devoted to the study of new approaches for overcoming the problem just referred to. This has been done by developing a new algorithm called ASPECT which detects the number of signals and estimates their directions with the detection and estimation being carried out *in parallel*. This algorithm works for both correlated and uncorrelated situations and its operation is based mainly on mapping the array manifold on to an error surface and then searching that surface for a minimum. The new algorithm has been presented (see *Section*-3.3) in a form which is appropriate for VLSI implementation or for implementation which can be carried out using a parallel computer (for

instance DAP-ICL, that is an SIMD machine). Important points and facts relating to ASPECT have been summarized in the three Theorems contained in the *Section* 3.2. Computer simulation results (*Chapter*-4) have supported the theory and have shown the limitations of ASPECT. Summarising, it can be said that the precision of the results provided by ASPECT is altered when

- the angle separation between sources is small,
- the sources are correlated,
- the sources are of widely differing power levels,
- the observation time is small.

The problem is further complicated by the parallel existence of more than one of the above cases.

In addition, the limitations of the optimization method used for minimizing the ASPECT cost function influence the rate of convergence of ASPECT.

Finally, the concepts of signal subspace methods have been extended to beamformer problem (*Chapter*-5) in order to analyse the behavior of an array and, in addition, to present two new weight-vector processors (see Theorem-4 in *Section* 5.5 and modified ASPECT in *Section* 5.8) which are capable of receiving a desired signal in the presence of unknown interferences and, at the same time, to provide:

- complete interference cancellation (that is, effectively zero interference at the output of the array)
- information about the interference locations

offering less susceptibility to pointing errors and free of power inversion problems. It is important to point out that in the case of ASPECT the pointing errors are completely eliminated and it can handle situations where the desired signal and interferences are fully correlated. In

addition, the situation where the interferences are turning off, the proposed processors become identical to the Weiner-Hopf solution. Computer simulation results presented in *Chapter-6* highlight the above points, supporting the theory.

7.2 SUGGESTIONS FOR FURTHER RESEARCH

The research presented in this thesis can be extended by studying some of the following points:

- ASPECT performance depends on a minimization problem. Minimization using neuron-like networks is currently an active research area (e.g. [RUM-86], [RAS-87]). The integration of ASPECT with neuron-like networks for handling the source location and parameter estimation problem would be an interesting area of investigation.
- The application of signal subspace techniques and in particular ASPECT concepts to dynamic tracking in micro cell mobile communication systems might be of great research value.
- Futher work can be done in connection with the calculus of the array manifold. Work in this area might reveal more insights with respect to resolution, ambiguity and location problem.
- Techniques which take advantages of the correlation between desired source and interference (instead of cancelling the interference) may improve the system performance.
- Investigation of the effects of various norm *metrics* on ASPECT and the selection of the most optimum one is also an interesting

research topic.

- Extensions of ASPECT to the cases where the sources are inside the volume of the array is also an interesting problem.
- The development of new techniques (and propably extending the ASPECT algorithm) for handling signal environments where the number of sources is greater than the number of sensors is also important for both *source location* and *beamformer* array processing.
- Signal Subspace algorithms are mainly based on the knowledge and process of the covariance matrix. However, the triple correlation "*knows*" more about the signal environment than does the covariance matrix [LOH-84]. The use of triple correlation may provide new techniques for the source location and estimation problem.
- High-Resolution techiques cannot compete with the speed of fast algorithms (not even with a conventional DFT). The direct updates of the various steps of ASPECT when a *rank*-1 *modification* of the covariance matrix is involved, is an interesting extension of the work presented in this thesis.

REFERENCES

[AKA-74] Akaike H., "A New Look at the Statistical Model Identification", *IEEE Transactions on Autom. Control*, Vol.19, pp.716-723, 1974.

[ALL-63] Allen J.L., "The Theory of Array Antennas", *MIT, Lincoln Lab. Report* 323, 1963.

[APP-66] Applebaum S.P., "Adaptive Arrays", Special Project Report TA-66-1, *Syracuse University Research Corp.*, Syracuse, N.Y., Aug 1966. (republished as [APP-76]).

[APP-76] Applebaum S.P., "Adaptive Arrays", *IEEE Transactions on Antennas and Propagation*, vol.AP-24, No.5, pp 585-598, September 1976.

[AP2-76] Applebaum S.P., Chapman D.J. "Adaptive Arrays with Main Beam Constraints", *IEEE Transactions on Antennas and Propagation*, vol.AP-24, No.5, pp 650-662, September 1976.

[ATT-87] Attia E.H., "Efficient Computation of the MUSIC Algorithm as Applied to a Low-Angle Elevation Estimation in a Severe Multipath Environment", *International Conference Acoustic Speech and Signal Processing*, ICASSP-87, pp 41.10.1-41.10.4., 1987.

[BRE-76] Brennan L.E., Mallet J.D., "Efficient Simulation of

External Noise Incident on Arrays", *IEEE Transactions on Antennas and Propagation*, vol.AP-24, No.9, pp 740-741, September 1976.

[BIE-81] Bienvenu G., Kopp. L. "Source Power Estimation Method Associated with High Resolution Bearing Estimation", *Intern. Conf. Acoust. Speech and Signal Proc.*, ICASSP-81, pp 302-305, 1981.

[BIE-83] Bienvenu G., Kopp. L. "Eigensystem Properties of the Sample Covariance Matrix", *Intern. Conf. Acoust. Speech and Signal Proc.*, ICASSP-83, pp.332-335, 1983.

[BIE-85] Bienvenu G., Mermoz H.F., "Principles of High-Resolution Array Processing", in *VLSI and Modern Signal Processing, ch.*5, edited by Kung S.Y., Whitehouse H.J. and Kailath T., Prentice-Hall, 1985.

[BUR-75] Burg J.P., "Maximum Entropy Spectral Analysis", *PhD Thessis, Stanford University*, Stanford, USA, 1975.

[BUR-82] Burg J.P., Luenberger D.G., Wenger D.L., "Estimation of Structured Covariance Matrices", *Proceedings of the IEEE*, vol.70, No.9, pp 963-974, September 1982.

[CAD-87] Cadzow J., Kim Y., Shiue D., Sun Y., Xu G., "Resolution of Coherent Signals Using a Linear Array", *Intern. Conf. Acoust. Speech and Signal Proc.*, ICASSP-87, pp 37.4.1-37.4.4, 1987.

[CAN-80] Cantoni A., Godara L.C., "Resolving the directions of sources in a correlated field incident on an array", *Journal of Acoust. Soc. of America*, vol.67, No.4, pp.1247-1255, 1980.

[CAP-69] Capon J., "High Resolution Frequency-Wavenumber Spec-

trum Analysis", *Proceedings of IEEE*, vol.57, No.8, pp.1408-1418, Aug. 1969.

[COM-84] Compton, "On Eigenvalues, SNIR, and Element patterns in Adaptive Arrays", *IEEE Transactions on Antennas and Propagation*, vol. AP-32, No.6, pp 643-647, June 1984.

[CIT-84] Citron T.K. and Kailath T., "An improved Eigenvector Beamformer", *International Conference Acoustic Speech and Signal Processing*, ICASSP-84, 33.3.1-33.3.4.

[CLE-85] Clergeot H., Ouamri A., Tressens S., "High Resolution Spectral Methods for Spatial Discrimination of Closely Spaced Correlated Sources", *Intern. Conf. Acoust. Speech and Signal Proc.*, ICASSP-85, pp.15.3.1-4, 1985.

[DI-84] Di A., Tian L., "Matrix Decomposition and Multiple Source Location", *Intern. Conf. Acoust. Speech and Signal Proc.*, ICASSP-84, pp 33.4.1-33.4.4.

[DI-85] Di A., "Multiple Source Location - A Matrix Decomposition Approach", *IEEE Transactions on Acoustic Speech and Signal Processing.*, Vol ASSP-33, No.5, pp 1086-1091, October 1985.

[EVA-81] Evans J., Johnson J., Sun D., "High Resolution Angular Spectrum Estimation Technique for Terrain Scattering Analysis and Angle of Arrival Estimation", *Proceedings of First IEEE ASSP Workshop on Spectral Estimation*, Canada, 1981.

[FED-86] Feder M., Weinstein E., "Multipath and Multiple Source array Processing via the EM Algorithm", *Intern. Conf. Acoust. Speech and Signal Proc.*, ICASSP-86, pp.47.4.1-4, 1986.

[GAB-80] Gabriel W., "Spectral Analysis and Adaptive array Superresolution Techniques", *Proceedings of the IEEE*, vol.68, No.6, pp 654-665, June-1980.

[GAB-86] Gabriel W., "Introduction" in Special Issue on Adaptive Processing Antenna Systems, *IEEE Transactions on Antennas and Propagation*, Vol AP-34, No.3, pp 273-275, March 1986.

[GA2-86] Gabriel W., "Using Spectral Estimation Techniques in Adaptive Processing Antenna Systems", Special Issue on Adaptive Processing Antenna Systems, *IEEE Transactions on Antennas and Propagation*, Vol AP-34, No.3, pp 291-300, March 1986.

[GOL-83] Golub, G.H., Van Loan C.F., "Matrix Computations", North Oxford Academic, 1983.

[GUP-84] Gupta, I.J., "Performance of a Modified Applebaum Adaptive Array", *IEEE Transactions on Aerospace and Electronic Systems.* AES-20, pp 583-594, Sep 1984.

[HUD-81] Hudson, J.E., "Adaptive Array Principle", The Institution of Electrical Engineers - Peter Peregrinus, 1981.

[HUD-85] Hudson, J.E., "Antenna Adaptivity by Direction Finding and Null Steering", *IEE Proceedings*, vol.132, Pt. H, No.5, pp.307-311, August 1985.

[JOH-82] Johnson D.H., "Improving the Resolution of Bearing in Passive Sonar Arrays by Eigenvalue Analysis", *IEEE Transactions on Acoustic Speech and Signal Processing.*, Vol ASSP-30, No.4, pp 638-647, August 1982.

[JOH-85] Johnson D.H., "Properties of Eigenanalysis Methods for Bearing Estimation Algorithms", *Intern. Conf. Acoust.*

Speech and Signal Proc., ICASSP-85, pp 15.1.1-15.1.4, 1985.

[JOH-86] Johnson R.L., Miner G.E., "Comparison of Superresolution Algorithms for Radio Direction Finding", *IEEE Transactions on Aerospace and Electronic Systems.* AES-22, No.4, pp 432-441, July 1986.

[KAY-88] Kay S.M., "Modern Spectral Estimation Theory and Applications", Prentice-Hall, 1988.

[KRA-81] Kraus J., Carver K.,"Electromagnetics", McGraw-Hill,1981.

[KUN-85] Kung S.Y and Gal-Ezer R.J., "Eigenvalue, Singular Value and Least Squares Solvers via the Wavefront Array Processors", in *Algorithmically Specialized Computer Organizations*, L.Synder et al., Academic Press, 1983.

[LAW-56] Lawley D.N, "Tests of Significance of the Latent Roots of the Covariance and Correlation Matrices", *Biometrica*, Vol.41, pp.190-195, 1956.

[LIN-78] Linz P., "Theoretical Numerical Analysis", John-Wiley, 1978.

[LOH-84] Lohman A., Wirnitzer B., "Triple Correlations", *Proceedings of the IEEE*, vol.72, No.7, pp 889-901, July 1984.

[MA-74] Ma M.T., "Theory and Application of Antenna Arrays", John Wiley, 1974.

[MAD-87] Madan B., Parker S., "Adaptive Beam Forming in Correlated Interference Environment", *Intern. Conf. Acoust. Speech and Signal Proc.*, ICASSP-87, pp 1792-1795, 1987.

[MAR-86] Marr J.D., "A Selected Bibliography on Adaptive Antenna Arrays", *IEEE Transactions on Aerospace and Electronic Systems.* Vol AES-22, No.6, pp 781-798.

[MER-81] Mermoz H.F., "Spatial Processing Beyond Adaptive Beamforming", *Journal of Acoust. Soc. of America*, vol.70, No.1, pp.74-79, July 1981.

[MON-80] Monzinco R.A. and Miller T.W, "Introduction to Adaptive Arrays", John-Wiley, 1980.

[MRP-87] Marple S.L. Jr, "Digital Spectral Analysis with Applications", Prentice-Hall, 1987.

[NEF-81] Neff H. Jr., "Basic Electromagnetic Fields", Harper and Row, 1981.

[PAU-85] Paulraj A., Kailath T., "On Beamforming in Presence of Multipath", *Intern. Conf. Acoust. Speech and Signal Proc.*, ICASSP-85, pp.15.4.1-4, 1985.

[PIS-73] Pisarenko V.F., "The Retrieval of Harmonics from a Covariance Function", *Geophysical Journal of the Royal Astronomical Society*, Vol-33, pp.347-366, 1973.

[PRA-87] Prasad S., Williams R.T., Mahalanabis A.K., Sibul L.H., "A Transform based Covariance Differencing Approach to Bearing Estimation", *Intern. Conf. Acoust. Speech and Signal Proc.*, ICASSP-87, pp.26.10.1-4, 1987.

[PRO-95] Prony R., "Essai Experimental et Analytique, etc", *L'Ecole Polytechnique*, Paris, vol.1, No.2, pp 24-76, 1795.

[RAS-87] Rastogi R., Gupta P., Kumaresan R., "Array Signal Processing with Interconnected Neuron-like Elements", *Intern. Conf. Acoust. Speech and Signal Proc.*, ICASSP-87, pp 2328-2331, 1987.

[REE-74] Reed I.S., Mallet J.P., Brennan L.E., "Rapid Convergence Rate in Adaptive Arrays", *IEEE Transactions on Aerospace and Electronic Systems.* AES-9, No.6, pp 853-863,

Nov. 1974.

[RIS-83] Rissanen J., "A Universal Prior for the Integers and Estimation by Minimum Description Length", *Ann. of Stat.*, Vol.11, pp.417-431, 1983.

[ROY-86] Roy R., Paulraj A., Kailath T., "Direction of Arrival Estimation by Subspace Rotation Methods - ESPRIT", *Intern. Conf. Acoust. Speech and Signal Proc.*, ICASSP-86, pp.47.2.1-4, 1986.

[RUM-86] Rumelhart D.E., McClelland J.L., and the PDP Research Group, "Parallel Distributed Processing: Explorations in the Microstructure of Cognition", MIT Press, vol.1 and vol.2, 1986.

[RUH-70] Ruhe A., "An Algorithm For Numerical Determination of the Structure of a General Matrix", BIT-10,196-216, pp 196-216, 1970.

[SCH-81] Schmidt R.O., "A Signal Subspace Approach to Multiple Emitter Location and Spectral Estimation", *Ph.d Thesis*, Stanford University, U.S.A., November1981.

[SCH-86] Schmidt R.O., "Multiple Emitter Location and Signal Parameter Estimation", *IEEE Transactions on Antennas and Propagation*, Vol AP-34, No.3, pp 276-280, March 1986.

[SCN-84] Schender U., "Introduction to Numerical Methods for Parallel Computers", J.Wiley, 1984.

[SHA-85] Shan T., Wax M., Kailath T., "On Spatial Smoothing for Direction-of-Arrival Estimation of Coherent Signals", *IEEE Transactions on Acoustic Speech and Signal Processing.*, Vol ASSP-33, No.4, pp 806-811, August 1985.

[SH2-85] Shan T., Kailath T., "Adaptive Beamforming for Coherent Signals and Interference", *IEEE Transactions on Acoustic Speech and Signal Processing.*, Vol ASSP-33, No.3, pp 527-536, June 1985.

[SHH-87] Shahmirian V. Kesler S., "Bias and Resolution of Vector Space Methods in The Presence of Coherent Planewaves", *Intern. Conf. Acoust. Speech and Signal Proc.*, ICASSP-87, pp 2320-2323.

[SIB-84] Sibul L.H., Burke S.E., "Error Analysis of Eigenvector preprocessors used in Adaptive Beamforming", *Intern. Conf. Acoust. Speech and Signal Proc.*, ICASSP-84, pp 46.9.1-46.9.4, 1984.

[SU-83] Su G., "Signal Subspace Algorithms for Emitter Location and Multidimensional Spectral Estimation", *Ph.d Thesis*, Stanford University, U.S.A., October 1983.

[TUF-83] Tufts D., Kumaresan R., "Estimating the Angle of Arrival of Multiple Plane Waves", *IEEE Transactions on Aerospace and Electronic Systems*, vol. AES-19, No.1, pp 135-139, January 1983.

[WAL-75] Walsh G.R., "Methods of Optimization", J.Wiley, 1975.

[WAX-84] Wax M. and Kailath T., "Determining the Number of Signals by Information Theoretic Criteria", *Intern. Conf. Acoust. Speech and Signal Proc.*, ICASSP-84, Proceedings, San Diego, CA, USA, pp.6.3.1-6.3.4, 19-21 March 1984.

[WAX-85] Wax M., "Detection and Estimation of Superimposed Signals", *Ph.d Thesis*, Stanford University, U.S.A., March 1985.

[WIL-87] Williams R.T., Prasad S., Mahalanabis A.K., Sibul L.H,

"Localization of Coherent Sources Using a Modified Spatial Smoothing Technique", *Intern. Conf. Acoust. Speech and Signal Proc.*, ICASSP-87, pp.54.14.1-4, 1987.

[WIL-88] Williams R.T., Prasad S., Mahalanabis A.K., Sibul L.H, "An Improved Spatial Smoothing Technique for Bearing Estimation in a Multipath Environment", *IEEE Transactions on Acoustics Speech and Signal Processing*, Vol 36, No.4, pp 425-432, April 1988.

[WLK-66] Wilkinson J.H., "The Algebraic Eigenvalue Problem", Clarendon Press, Oxford, 1965.

[WID-66] Widrow B., "Adaptive Filters 1: Fundamentals", *System Theory Laboratory*, Stanford University, Rep. No. 6764-6, 1966.

[WID-67] Widrow B., Mantey P.E., Griffiths L.J. and Goode B.B., "Adaptive Systems", *Proceedings of the IEEE*, vol.55, No.12, pp.2143-2159, December 1967.

[WID-82] Widrow B., Duvall K., Gooch R., Newman W., "Signal Cancellation Phenomena in Adaptive Antennas: Causes and Cures", *IEEE Transactions on Antennas and Propagation*, Vol AP-30, No.3, pp 469-478, May 1982.

[ZHA-87] Zhao L., Krishnaiah P., Bai Z., "Remarks on Certain Criteria for Detection of Number of Signals", *IEEE Transactions on Acoustics Speech and Signal Processing*, Vol 35, No.2, pp 129-132, February 1988.

[CAD-88] Cadjow J.A., "A High Resolution Direction-of-Arrival Algorithm for Narrow-Band Coherent and Incoherent Sources", *IEEE Transactions on Acoustics Speech and Signal Processing*, Vol 36, No.7, pp 965-979, July 1988.

APPENDIX-1
FRAMEWORK OF SIGNAL SUBSPACE APPROACHES

High-Resolution in array processing is taken to be the ability to distinguish the effects of two equal power sources located close together. Although the resolving power of an array can usually be improved by increasing the aperture of the array, this is not, in general, acceptable and an alternative for a given array aperture is to use High-Resolution or Superresolution Techniques.

Signal Subspace approache to high resolution involves two main stages of processing. In the first stage a covariance matrix of the data at the sensors of the array is formed and in the second stage an eigenvector decomposition is performed.

When the number of emitters is smaller than the number of sensors, the determinant of the covariance matrix is equal to zero in the absence of non-directional sources. This is due to the fact that the presence of an emitter increases the rank of the covariance matrix by one.Thus

$$rank(\mathbf{R}_{xx}) = M \qquad (A1.1)$$

If, however, in addition to the directional sources there are also non-

directional sources present then the last equation is not quite true. The covariance matrix then is given by:

$$\mathbf{R}_{xx}=\mathbf{R}_{sig}+\sigma^2.\mathbf{I} \qquad (A1.2)$$

In that case $\mathbf{R}_{xx}$ has full rank (that is $rank(\mathbf{R}_{xx})=N$) and the following relationship is valid:

$$rank\left(\mathbf{R}_{xx}-\sigma^2.\mathbf{I}\right)=M \qquad (A1.3)$$

However, since the presence of noise affects only the diagonal terms of the $\mathbf{R}_{sig}$ covariance that means that

$$eig_i(\mathbf{R}_{xx})=eig_i(\mathbf{R}_{sig})+\sigma^2 \qquad (A1.4)$$

therefore

$$eig_{min}(\mathbf{R}_{xx})=eig_{min}(\mathbf{R}_{sig})+\sigma^2 \qquad (A1.5)$$

Now since $eig_{min}(R_{sig})=0$ with multiplicity $N-M$ that means

$$eig_{min}(\mathbf{R}_{xx})=\sigma^2 \qquad (A1.6)$$

with multiplicity $N-M$ also.

Therefore M can be determined by the eigenvalues of the covariance matrix and more specifically by the multiplicity of its minimum eigenvalue:

$$M=N-(multiplicity\ of\ min\text{-}eigenvalue) \qquad (A1.7)$$

Now let us consider that the eigendecomposition has been performed:

$$(\underline{v}_1,\lambda_1)\quad (\underline{v}_2,\lambda_2)\quad .....\quad (\underline{v}_M,\lambda_M)\quad (\underline{v}_{M+1},\lambda_{M+1})\quad ....\ (\underline{v}_N,\lambda_N) \qquad (A1.8)$$

where $(\underline{v}_i,\lambda_i)$ represents the i^{th} eigenvector and eigenvalue of $\mathbf{R}_{xx}$. Let

$$\lambda_1 \geq \lambda_2 \geq ..... \geq \lambda_M > \lambda_{M+1} = ... = \lambda_N = \sigma^2 \qquad (A1.9)$$

Then

$$\begin{aligned} &\mathbf{R}_{xx}.\underline{v}_i = \lambda_i.\underline{v}_i \\ &(\mathbf{R}_{sig} + \sigma^2\mathbf{I}).\underline{v}_i = \lambda_i.\underline{v}_i \\ &\mathbf{R}_{sig}.\underline{v}_i = (\lambda_i - \sigma^2).\underline{v}_i \end{aligned} \qquad (A1.10)$$

It is now clear from *Equation-A*1.9 in conjunction with *Equation-A*1.10 that the eigenvectors corresponding to the minimum eigenvalue of the $\mathbf{R}_{xx}$ will satisfy:

$$\begin{aligned} &\mathbf{R}_{sig}.\underline{v}_i = \underline{0} \qquad \forall i \in [M+1,...,N] \\ &i.e. \qquad \mathbf{R}_{sig}.\mathbf{V}_{noise} = \mathbf{O} \\ &where\ \mathbf{V}_{noise} = [\underline{v}_{M+1}, ..., \underline{v}_N] \end{aligned} \qquad (A1.11)$$

That means that these eigenvectors will be orthogonal to the subspace spanned by the columns of $\mathbf{R}_{sig}$, and because that subspace includes the *SPVs* corresponding to the directional sources, then, these eigenvectors will be orthogonal to them too.

Thus, for instance, by forming the functional:

$$f(\theta) = \underline{S}(\theta)^H . \mathbf{V} . \mathbf{V}^H . \underline{S}(\theta) \qquad (A1.12)$$

the well known as MuSIC algorithm is established.

Thus, for a linear array where the only parameter of interest is the azimuth angle, the above equation is evaluated for all SPV corresponding to angles from 0° to 180° and the directions where that equation becomes zero are the directions of the incident signals (see for instance *Figure*-3.1). A better reformulation of the Signal Subspace approach is to see the source locations as the intersection of the signal subspace with the set of all possible SPVs (array manifold).

APPENDIX–2
FINITE AVERAGING EFFECTS ON ASPECT

In *Chapter* 4 the performance of ASPECT algorithm was examined via computer simulations studies by using the theoretical (or known) covariance matrix. In this appendix attention is directed to the effects of finite averaging on the performance of ASPECT. In that case the covariance matrix is formed by using *Equation* 2.32 which has been presented in *Section* 2.6.

In order to do this the array model described in the *Section* 4.2 and illustrated in *Figure* 4.1*a* is used once again. Two signal environments are considered involving three incident signals where the first and the second signal constitute a trial pair. The trial pair is located in positions which provide 10° (for the first environment) and 5° (for the second environment) angle separation. Thus the directions of the signals are chosen as follows:

(15°,20°), (15°,30°), (10°,90°) - first situation

(15°,20°), (15°,25°), (10°,90°) - second situation

In both situations the trial pair is fully correlated and the observation time is considered to be 250 sample instances. The results are shown in *Figures* A2.1 and A2.2. In addition *Figures* A2.3 and A2.4 illustrate the results when the theoretical instead of sample covariance matrix is used. By comparing the above figures it can be concluded that the precision on the estimation of the angles of plane waves incident to an array of sensors is altered when the number of samples (observation time) used

to form the covariance matrix is small. This becomes more serious (see *Figure A*2.2) when the small observation time is combined with environments involving fully correlated sources which are located close together.

Appendix 5 illustrates the method used in order to simulate the sample covariance matrix, while *Appendix*-6 presents in a simplified step-form an example of the results provided by ASPECT MATLAB program for both theoretical and sampled covariance matrices.

FIGURE – A2.1 (Sources No.1 and No.2 are correlated. 250 snapshots)

	TRUE directions	INITIAL directions	directions estimated by ASPECT
source No.1	(15.0, 20.0)	(0.0, 5.0)	(14.9999, 19.9964)
source No.2	(15.0, 30.0)	(0.0, 50.0)	(14.9998, 29.9934)
source No.3	(10.0, 90.0)	(0.0, 100.0)	(10.0015, 89.9993)
source No.4	———	(0.0, 165.0)	———

cost:1.000000000000000e+000

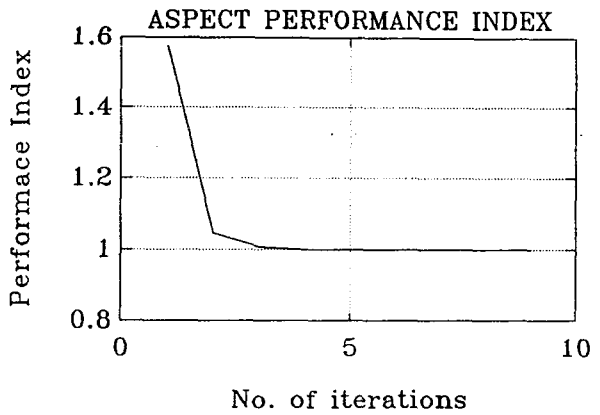

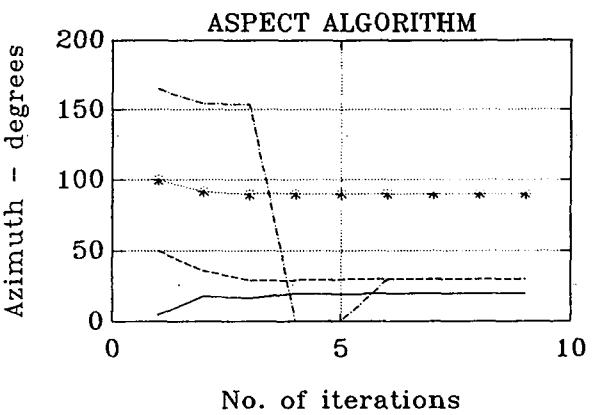

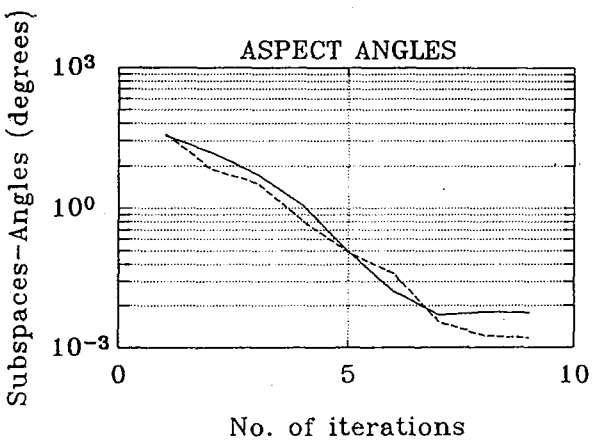

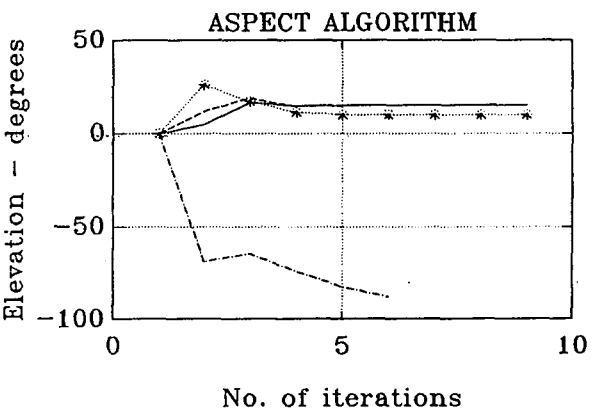

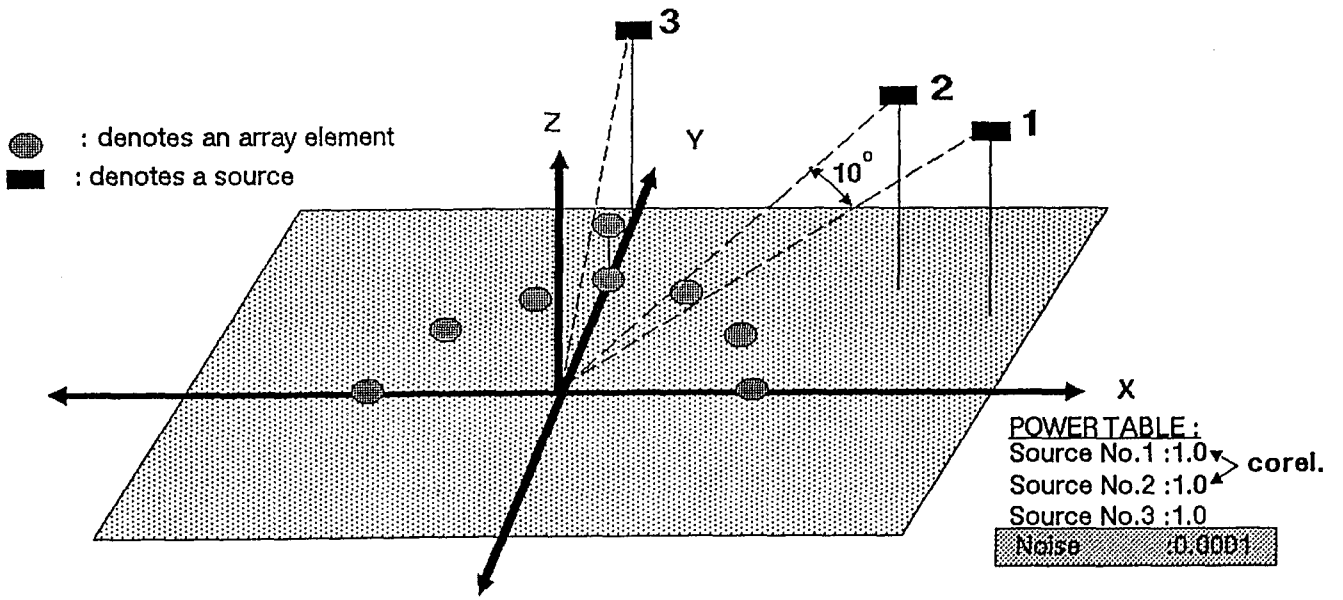

FIGURE – A2.2 (Sources No.1 and No.2 are correlated. 250 snapshots)

	TRUE directions	INITIAL directions	directions estimated by ASPECT
source No.1	(15.0, 20.0)	(0.0, 5.0)	(14.9975, 19.9783)
source No.2	(15.0, 25.0)	(0.0, 50.0)	(15.0014, 24.9842)
source No.3	(10.0, 90.0)	(0.0, 100.0)	(9.9980, 89.9998)
source No.4	———	(0.0, 165.0)	———

cost: 1.000000000000000e+000

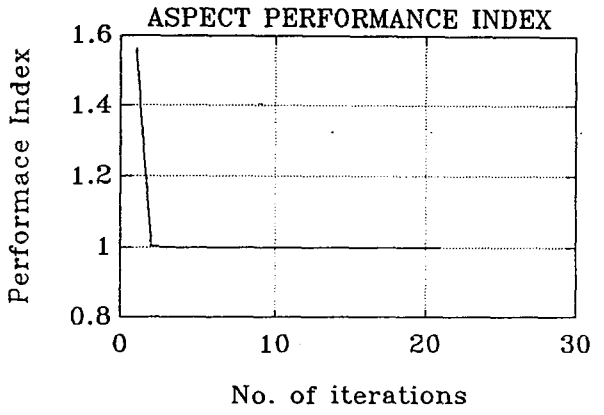

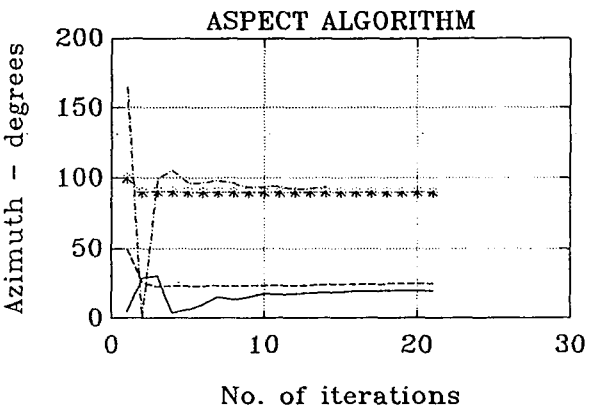

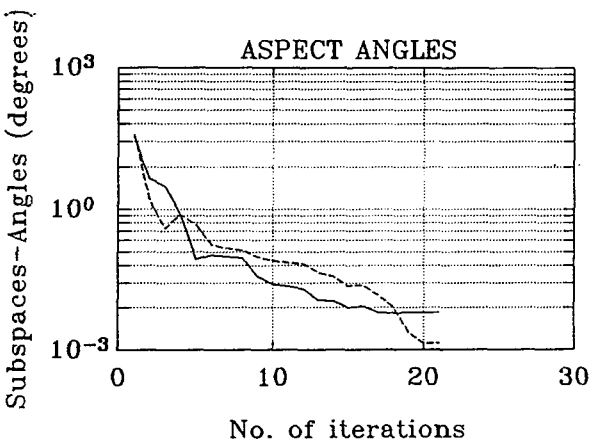

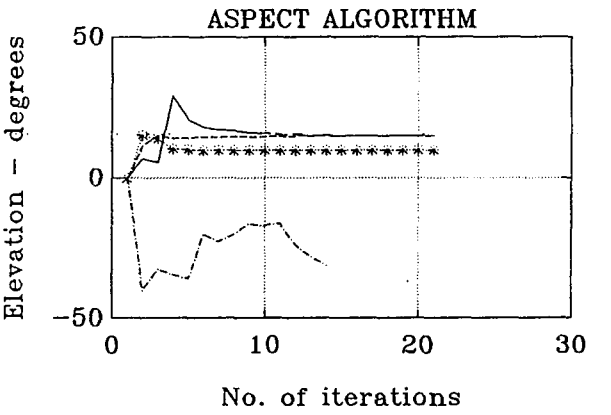

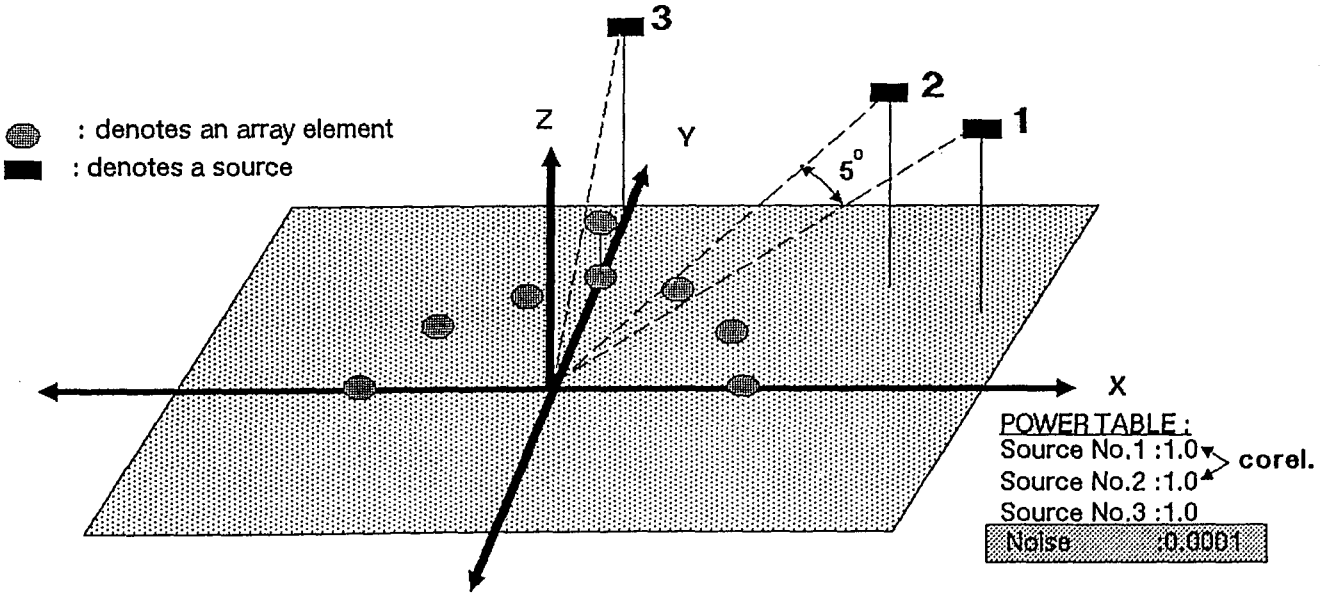

FIGURE – A2.3 (Sources No.1 and No.2 are correlated)

	TRUE directions	INITIAL directions	directions estimated by ASPECT
source No.1	(15.0, 20.0)	(0.0, 5.0)	(15.0000,20.0000)
source No.2	(15.0, 30.0)	(0.0, 50.0)	(15.0000,30.0000)
source No.3	(10.0, 90.0)	(0.0, 100.0)	(10.0000,90.0000)
source No.4	———	(0.0, 165.0)	———

cost:1.000000000000000e+000

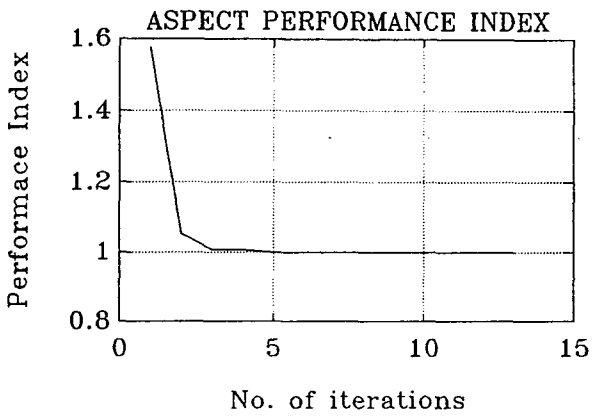

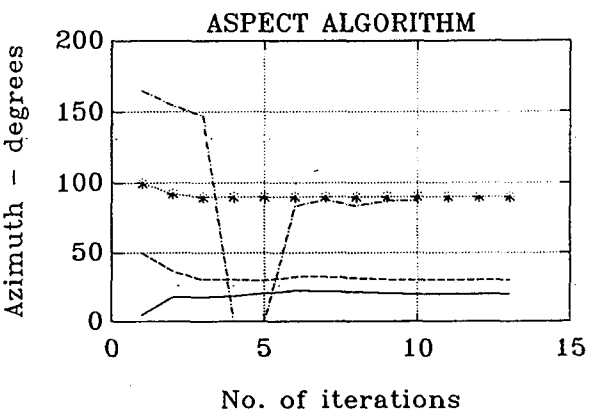

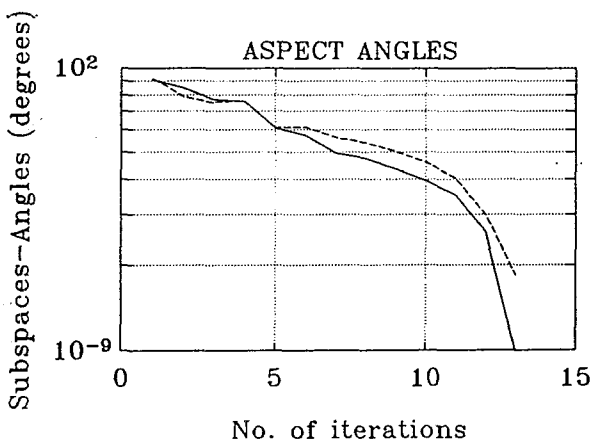

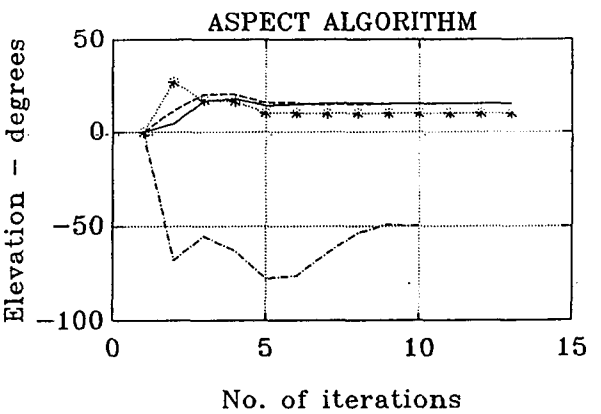

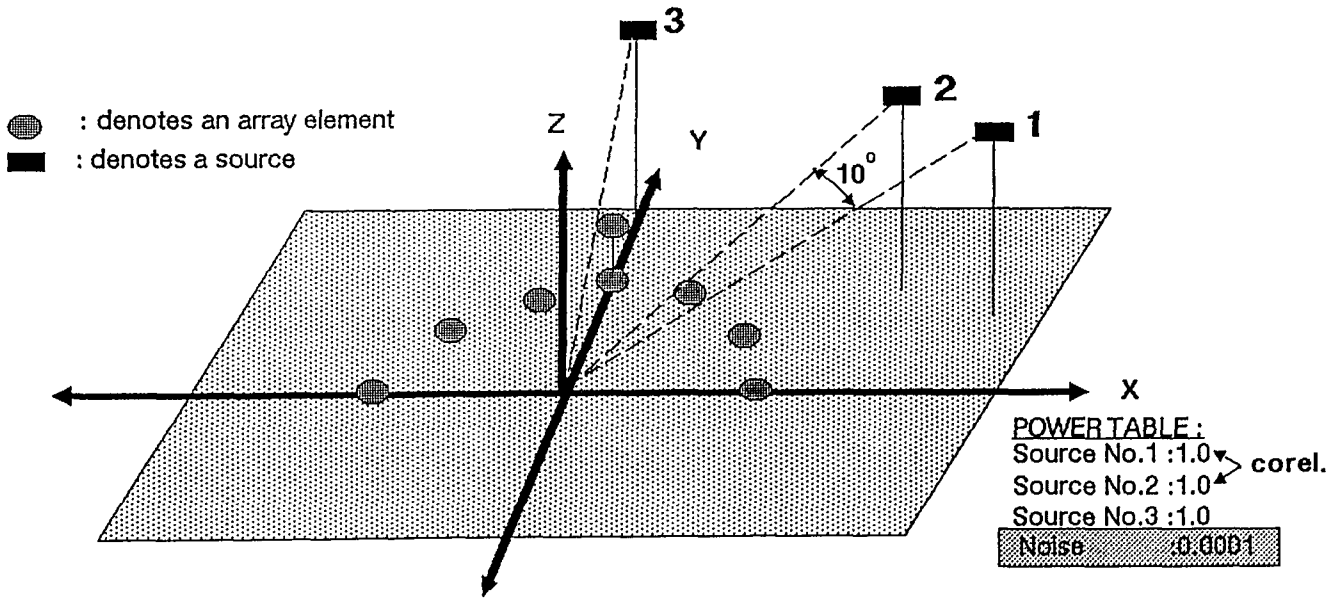

FIGURE – A2.4 (Sources No.1 and No.2 are correlated)

	TRUE directions	INITIAL directions	directions estimated by ASPECT
source No.1	(15.0, 20.0)	(0.0, 5.0)	(15.0000,20.0000)
source No.2	(15.0, 25.0)	(0.0, 50.0)	(15.0000,25.0000)
source No.3	(10.0, 90.0)	(0.0, 100.0)	(10.0000,90.0000)
source No.4	———	(0.0, 165.0)	———

cost: 1.000000000000000e + 000

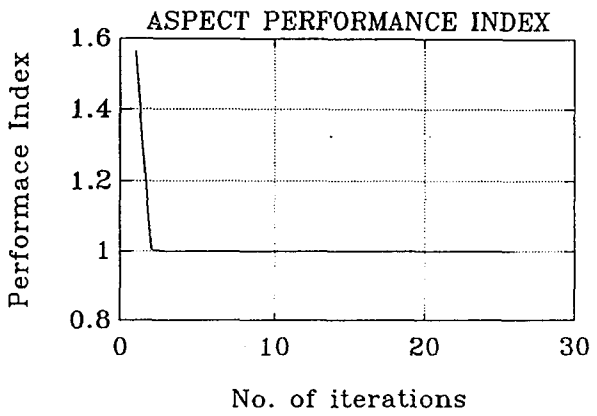

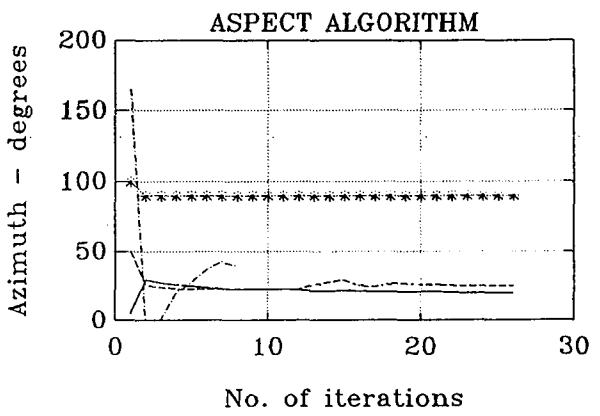

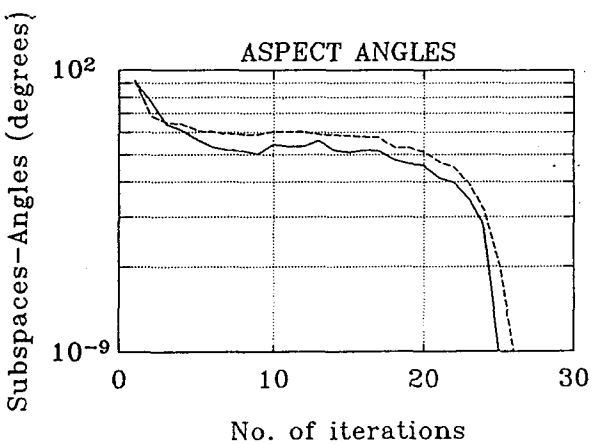

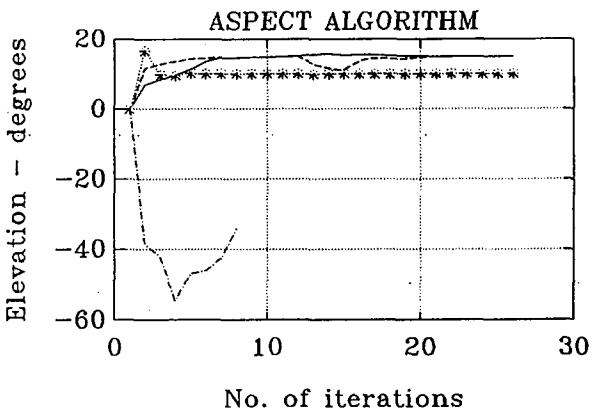

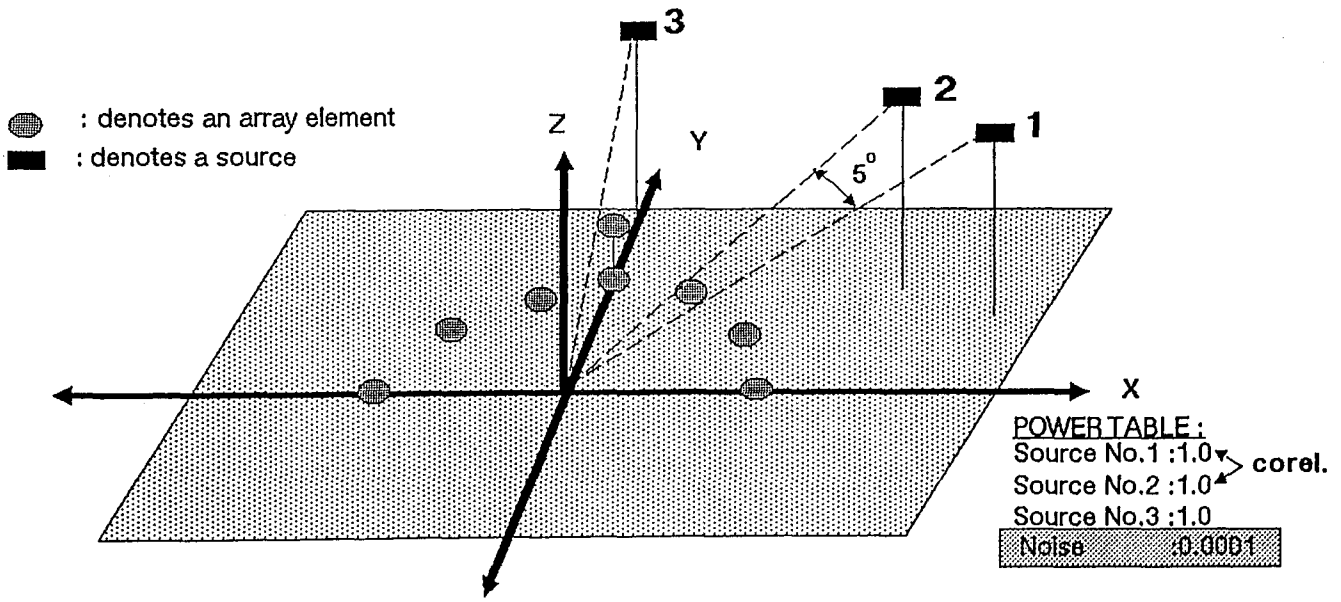

APPENDIX-3
GRADIENT and HESSIAN OF THE COST FUNCTIONS GIVEN BY EQUATION-3.41, 3.42, 3.43

This Appendix serves to give the Hessian Matrices and the gradient vectors of *Equation* 3.41, 3.42 and 3.43. These equations are repeated below as follows:

$$\xi_{41} = \text{trace}\left\{\mathbf{P_S}.\mathbf{Q_E}.\mathbf{P_S}.\mathbf{P_E}\right\} \tag{A3.1}$$

$$\xi_{42} = \prod_{k=1}^{D} \xi_k \qquad \textit{where} \qquad \xi_k = h_k^n \tag{A3.2}$$

$$h_k = sec\Theta_k = \frac{1}{\sqrt{\underline{E}_k^H.\mathbf{P_S}.\underline{E}_k}}$$

Θ_k= the angle between $\underline{E}_k$ and its projection onto the subspace spanned by the columns of **S**.

$$\xi_{43} = \text{trace}\left\{\mathbf{Q_S}.\mathbf{P_E}\right\} \tag{A3.3}$$

By considering *Equation-A*3.1, its gradient vector with respect to the

parameter p_i, that is $\nabla_{p_i}\xi_{41}$, is given by:

$$\nabla_{p_i}\xi_{41}=trace\left\{\mathbf{P}_{\mathbf{S}(p_i)}\cdot\mathbf{Q}_{\mathbf{E}}\cdot\mathbf{P}_{\mathbf{S}}\cdot\mathbf{P}_{\mathbf{E}}+\mathbf{P}_{\mathbf{S}}\cdot\mathbf{Q}_{\mathbf{E}}\cdot\mathbf{P}_{\mathbf{S}(p_i)}\cdot\mathbf{P}_{\mathbf{E}}\right\} \tag{A3.4}$$

$$where\ \ \mathbf{P}_{\mathbf{S}(p_i)}=\frac{\partial\mathbf{P}_{\mathbf{S}}}{\partial p_i}$$

By taking the first derivative of *Equation-A*3.4 with respect to a second parameter q_j then:

$$\begin{aligned}\nabla^2_{p_iq_j}\xi_{41}=trace\Big\{ & \mathbf{P}_{\mathbf{S}(p_iq_j)}\cdot\mathbf{Q}_{\mathbf{E}}\cdot\mathbf{P}_{\mathbf{S}}\cdot\mathbf{P}_{\mathbf{E}} + \\ & +\mathbf{P}_{\mathbf{S}(p_i)}\cdot\mathbf{Q}_{\mathbf{E}}\cdot\mathbf{P}_{\mathbf{S}(q_j)}\cdot\mathbf{P}_{\mathbf{E}}+ \\ & +\mathbf{P}_{\mathbf{S}(q_j)}\cdot\mathbf{Q}_{\mathbf{E}}\cdot\mathbf{P}_{\mathbf{S}(p_i)}\cdot\mathbf{P}_{\mathbf{E}}+ \\ & +\mathbf{P}_{\mathbf{S}}\cdot\mathbf{Q}_{\mathbf{E}}\cdot\mathbf{P}_{\mathbf{S}(p_iq_j)}\cdot\mathbf{P}_{\mathbf{E}}\Big\}\end{aligned} \tag{A3.5}$$

$$where\ \ \mathbf{P}_{\mathbf{S}(p_iq_j)}=\frac{\partial^2\mathbf{P}_{\mathbf{S}}}{\partial p_i\partial q_j}$$

On the other hand the elements of the gradient vector of the scalar function ξ_k in *Equation-A*3.2 with respect to the parameter p_i, that $\nabla_{p_i}\xi_k$, is given by:

$$\nabla_{p_i}\xi_k=-\ \tfrac{n}{2}\cdot\ \underline{E}_k^H\cdot\mathbf{P}_{\mathbf{S}(p_i)}\cdot\underline{E}_k\cdot h_k^{n+2} \tag{A3.6}$$

If $p=\theta$ then the last equation provides the i^{th} element of the gradient vector $\underline{\nabla}\xi_k$ while if $p=\phi$ then it provides the $(i+K)^{th}$ element of $\underline{\nabla}\xi_k$, where $i\in[\![1,\ldots,K]\!]$, $i\in\mathcal{N}^+$.

By taking the first derivative of the *Equation A*3.6 with respect to a second parameter q_j then:

$$\nabla^2_{p_i q_j}\xi_k = -\frac{n}{2}\cdot \underline{E}_k^H \cdot \mathbf{P}_{\mathbf{S}(p_i q_j)} \cdot \underline{E}_k \cdot h_k^{n+2} - \frac{n+2}{2}\cdot \underline{E}_k^H \cdot \mathbf{P}_{\mathbf{S}(p_i)} \cdot \underline{E}_k \cdot h_k^2 \cdot \nabla_{q_j}\xi_k$$

$$\Rightarrow \nabla^2_{p_i q_j}\xi_k = -\frac{n}{2}\cdot \underline{E}_k^H \cdot \mathbf{P}_{\mathbf{S}(p_i q_j)} \cdot \underline{E}_k \cdot h_k^{n+2} - \frac{n+2}{n}\cdot \frac{\nabla_{p_i}\xi_k \cdot \nabla_{q_j}\xi_k}{\xi_k} \tag{A3.7}$$

It is not difficult to prove then that the elements of the gradient vector of the cost function ξ_{42} are given by:

$$\nabla_{p_i}\xi_{42} = \sum_{k=1}^{D} \left\{ \nabla_{p_i}\xi_k \cdot \prod_{\substack{l=1 \\ l\neq k}}^{D} \xi_l \right\} = \xi_{42} \cdot \sum_{k=1}^{D} \frac{\nabla_{p_i}\xi_k}{\xi_k} \tag{A3.8}$$

while the elements of the Hessian Matrix of the cost function are given by:

$$\nabla^2_{p_i q_j}\xi_{42} = \sum_{k=1}^{D} \left\{ \nabla^2_{p_i q_j}\xi_k \cdot \prod_{\substack{l=1 \\ l\neq k}}^{D} \xi_l + \nabla_{p_i}\xi_k \cdot \sum_{\substack{s=1 \\ s\neq k}}^{D} \left(\nabla_{q_j}\xi_s \cdot \prod_{\substack{l=1 \\ l\neq j \\ l\neq k}}^{D} \xi_l \right) \right\}$$

$$= \xi_{42} \cdot \sum_{k=1}^{D} \left\{ \frac{\nabla^2_{p_i q_j}\xi_k}{\xi_k} + \frac{\nabla_{p_i}\xi_k}{\xi_k} \cdot \sum_{\substack{s=1 \\ s\neq k}}^{D} \left(\frac{\nabla_{q_j}\xi_s}{\xi_s} \right) \right\}$$

$$= \xi_{42} \cdot \sum_{k=1}^{D} \left\{ \frac{\nabla^2_{p_i q_j}\xi_k}{\xi_k} + \frac{\nabla_{p_i}\xi_k}{\xi_k} \cdot \frac{\nabla_{q_j}\xi_{42}}{\xi_{42}} - \frac{\nabla_{p_i}\xi_k}{\xi_k} \cdot \frac{\nabla_{q_j}\xi_k}{\xi_k} \right\} \tag{A3.9}$$

Finally, the elements of the gradient vector of the scalar cost function given by *Equation-A*3.3 with respect to the parameter p_i, that $\nabla_{p_i}\xi_{43}$, are given by:

$$\nabla_{p_i}\xi_{43} = -trace\left\{ \mathbf{P}_{\mathbf{S}(p_i)} \cdot \mathbf{P}_{\mathbf{E}} \right\} \tag{A3.10}$$

and by taking the first derivative of the last equation with respect to a second parameter q_j then:

$$\nabla^2_{p_i q_j}\xi_{43} = -trace\left\{\mathbf{P}_{\mathbf{S}(p_i q_j)}.\mathbf{P}_{\mathbf{E}}\right\} \qquad \text{(A3.11)}$$

Since the gradient vector of any of the three cost functions has the following form:

$$\nabla\xi = [\frac{\partial\xi}{\partial\theta_1}, \frac{\partial\xi}{\partial\theta_2}, \ldots, \frac{\partial\xi}{\partial\theta_K}, \frac{\partial\xi}{\partial\phi_1}, \frac{\partial\xi}{\partial\phi_2}, \ldots, \frac{\partial\xi}{\partial\phi_K}]^T \qquad (A3.12)$$

where ξ *is any one of* ξ_{41}, ξ_{42} *or* ξ_{43};

therefore if $p=\theta$ then *Equations* A3.4, A3.8 and A3.10 provide the i^{th} element of the gradient vector $\underline{\nabla}\xi$ while if $p=\phi$ these equations give the $(i+K)^{th}$ element of $\underline{\nabla}\xi$, where $i\in[\![1,\ldots,K]\!]$, $i\in\mathcal{N}^+$.

In addition the Hessian matrix has the following form:

$$\underline{\nabla}^2\xi = \begin{bmatrix} \frac{\partial^2\xi}{\partial\theta_1^2} & \frac{\partial^2\xi}{\partial\theta_2\partial\theta_1} & \ldots & \ldots & \ldots & \ldots & \frac{\partial^2\xi}{\partial\phi_K\partial\theta_1} \\ \frac{\partial^2\xi}{\partial\theta_1\partial\theta_2} & \frac{\partial^2\xi}{\partial\theta_2^2} & \ldots & \ldots & \ldots & \ldots & \ldots \\ \ldots & \ldots & \ldots & \ldots & \ldots & \ldots & \ldots \\ \ldots & \ldots & \ldots & \ldots & \ldots & \ldots & \ldots \\ \frac{\partial^2\xi}{\partial\theta_1\partial\theta_K} & \frac{\partial^2\xi}{\partial\theta_2\partial\theta_K} & \ldots & \ldots & \ldots & \ldots & \ldots \\ \frac{\partial^2\xi}{\partial\theta_1\partial\phi_1} & \ldots & \ldots & \ldots & \ldots & \ldots & \ldots \\ \ldots & \ldots & \ldots & \ldots & \ldots & \ldots & \ldots \\ \ldots & \ldots & \ldots & \ldots & \ldots & \ldots & \ldots \\ \frac{\partial^2\xi}{\partial\theta_1\partial\phi_K} & \frac{\partial^2\xi}{\partial\theta_2\partial\phi_K} & \ldots & \frac{\partial^2\xi}{\partial\theta_1\partial\phi_K} & \frac{\partial^2\xi}{\partial\phi_1\partial\phi_K} & \ldots & \frac{\partial^2\xi}{\partial^2\phi_K} \end{bmatrix}$$

This gives the necessary hint that *Equations-A*3.7, *A*3.9 and *A*3.11 provide the elements of Hessian Matrix $\underline{\nabla}^2\xi$ as follows:

- if $p=\theta$ and $q=\theta$ then they provide the $(i,j)^{th}$ element,
- if $p=\theta$ and $q=\phi$ then they provide the $(i,j+K)^{th}$ element, while
- if $p=\phi$ and $q=\phi$ then they provide the $(i+K,j+K)^{th}$ element

of the Hessian matrix where $i,j\in$ $i\in[\![1,...,K]\!]$, $j\in[\![1,...,i]\!]$.

N.B.:

- *for plane wave approximation* $p,q=\theta$ *or* ϕ , *for* $i=[1,..,K]$, *and* $j=[1,..,i]$.
- *for spherical wave propagation* $p,q=\theta$ *or* ϕ *or* r, *for* $i=[1,..,K]$ *and* $j=[1,..,i]$

APPENDIX-4

SOURCE POSITION VECTORS, THEIR PROJECTION OPERATORS and THEIR DERIVATIVES

In this Appendix the first and second derivatives of the Source Position Matrix and its Projection Operator with respect to a source location parameter are presented for planewave approximation and spherical wave propagation.

PLANEWAVE APPROXIMATION

The k^{th} element of a SPV for plane wave approximation is given by:

$$\underline{S}_i^{(k)} = G_k . e^U \qquad \begin{array}{l} G_k = k^{th} \text{ sensors characteristics} \\ U = -j.(\underline{k}_i - \underline{k}_0)^T . \underline{r}_k \end{array} \qquad (A4.1)$$

However, the first and second derivatives of the phase parameter U are given by:

$$U_{(p_i)} = \frac{\partial U}{\partial p_i} = -j.\underline{k}_{i(p_i)}^T . \underline{r}_k \qquad (A4.2)$$

$$U_{(p_iq_j)}=\frac{\partial^2 U}{\partial p_i \partial q_j}=\begin{cases} -j.\underline{k}_i^T{}_{(p_iq_i)}\cdot \underline{r}_k & if\ i=j \\ 0 & if\ i\neq j \end{cases} \qquad (A4.3)$$

where $\dfrac{\partial \underline{k}_i}{\partial p_i}=\underline{k}_{i(p_i)}$ and $\dfrac{\partial^2 \underline{k}_i}{\partial p_i \partial q_j}=\underline{k}_{i(p_iq_j)}$ (A4.4)

Therefore the first and second derivatives of the k^{th} element of the SPV $\underline{S}_i$ will be:

$$\frac{\partial \underline{S}_i^{(k)}}{\partial p_i}= G_{k(p_i)}.e^U + U_{(p_i)}.\underline{S}_i^{(k)} \qquad (A4.5)$$

$$\frac{\partial^2 \underline{S}_i^{(k)}}{\partial p_i \partial q_j}= G_{k(p_iq_i)}.e^U + U_{(q_i)}.G_{k(p_i)}.e^U + U_{(p_iq_i)}.\underline{S}_i^{(k)} + U_{(p_i)}.\nabla_{p_i}\underline{S}_i^{(k)} \qquad (A4.6)$$

SPHERICAL WAVE PROPAGATION

The k^{th} element of a SPV for spherical wave propagation is given by:

$$\underline{S}_i^{(k)}= \frac{G_k}{U}.e^{-j\pi(U+U_0-R_i)} \qquad G_k=k^{th}\ sensors\ characteristics$$

$$U=\sqrt{R_i^2-\frac{2.R_i.\underline{k}_i^T\cdot \underline{r}_k}{\pi}+\underline{r}_k^T.\underline{r}_k} \qquad (A4.7)$$

However, the first and second derivative of the phase parameter U are given by:

$$\frac{\partial U}{\partial p_i} = -\frac{R_i . \underline{k}_{i(p_i)}^T \cdot \underline{r}_k}{\pi U} \qquad (A4.8)$$

$$\frac{\partial U}{\partial R_i} = + \frac{R_i - \frac{1}{\pi} . \underline{k}_i^T \cdot \underline{r}_k}{U} \qquad (A4.9)$$

$$\frac{\partial^2 U}{\partial p_i \partial q_j} = \begin{cases} -\dfrac{R_i . \underline{k}_{i(p_i q_i)}^T \cdot \underline{r}_k}{\pi U} - \dfrac{U_{(p_i)} . U_{(q_i)}}{U} & \text{if } i=j \\ 0 & \text{if } i \neq j \end{cases} \qquad (A4.10)$$

$$\frac{\partial^2 U}{\partial p_i \partial R_j} = \begin{cases} \dfrac{U_{(p_i)}}{R_i} - \dfrac{U_{(p_i)} . U_{(R_i)}}{U} & \text{if } i=j \\ 0 & \text{if } i \neq j \end{cases} \qquad (A4.11)$$

$$\frac{\partial^2 U}{\partial R_j^2} = \begin{cases} \dfrac{1}{U} - \dfrac{U^2_{(R_i)}}{U} & \text{if } i=j \\ 0 & \text{if } i \neq j \end{cases} \qquad (A4.12)$$

Therefore the first and second derivatives of the k^{th} element of the SPV $\underline{S}_i$ will be:

$$\frac{\partial \underline{S}_i^{(k)}}{\partial p_i} = \frac{G_{k(p_i)}}{U} . e^{-j\pi(U+U_0-R_i)} - U_{(p_i)} \cdot \left(\frac{1}{U} + j.\pi\right) . \underline{S}_i^{(k)} \qquad (A4.13)$$

$$\frac{\partial \underline{S}_i^{(k)}}{\partial R_i} = \frac{G_{k(R_i)}}{U}.e^{-j\pi(U+U_0-R_i)} - U_{(R_i)}\cdot\left(\frac{1}{U}+j\pi\right).\underline{S}_i^{(k)} + j\pi.\underline{S}_i^{(k)} \tag{A4.14}$$

$$\frac{\partial^2 \underline{S}_i^{(k)}}{\partial p_i \partial q_i} = \frac{G_{k(p_i q_i)}}{U}.e^{-j\pi(U+U_0-R_i)} - \frac{U_{(q_i)}\cdot G_{k(p_i)}}{U^2}.e^{-j\pi(U+U_0-R_i)} -$$

$$- U_{(p_i q_i)}\cdot\left(\frac{1}{U}+j\pi\right).\underline{S}_i^{(k)} + \frac{U_{(p_i)}\cdot U_{(q_i)}}{U^2}.\underline{S}_i^{(k)}$$

$$- U_{(p_i)}\cdot\left(\frac{1}{U}+j\pi\right).\nabla_{q_i}\underline{S}_i^{(k)} \tag{A4.15}$$

PROJECTION OPERATORS

The derivatives of Projection Operator of the space spanned by the *SPVs*, for both shperical wave propagation and plane wave propagation, can be presented as follows:

$$\mathbf{P}=\mathbf{S}.(\mathbf{S}^H.\mathbf{S})^{-1}.\mathbf{S}^H \tag{A4.16}$$

$$\mathbf{Q}=\mathbf{I}-\mathbf{P} \tag{A4.17}$$

$$\mathbf{B}=(\mathbf{S}^H.\mathbf{S})^{-1}.\mathbf{S}^H \tag{A4.18}$$

Let $\mathbf{T}_{p_i}=\frac{\partial \mathbf{S}}{\partial p_i}$. That means

$$\mathbf{T}_{p_i}= [\underline{0},\ldots,\underline{0},\frac{\partial \underline{S}_i}{\partial p_i},\underline{0},\ldots,\underline{0}] \tag{A4.19}$$

that is $N\times K$ matrix with all but the i^{th} columns zeros. Then the first and second derivatives of projection operator $\mathbf{P}$ are given by

$$\mathbf{P}_{p_i}=\mathbf{M}_{p_i}+\mathbf{M}^H_{p_i} \qquad \textit{where } \mathbf{M}_{p_i}=\mathbf{Q}.\mathbf{T}_{p_i}.\mathbf{B} \qquad (A4.20)$$

and

$$\mathbf{P}_{p_iq_j}=\mathbf{M}_{p_iq_j}+\mathbf{M}^H_{p_iq_j} \quad \textit{where } \mathbf{M}_{p_iq_j}= -\mathbf{P}_{p_j}.\mathbf{T}_{p_i}.\mathbf{B}-\mathbf{M}_{p_i}.\mathbf{T}_{q_j}.\mathbf{B} + \mathbf{M}_{p_i}.\mathbf{M}^H_{q_j}-l.\mathbf{Q}.\mathbf{T}_{p_iq_j}.\mathbf{B} \qquad (A4.21)$$

$$\textit{where} \begin{cases} l=0 \ \textit{if } i\neq j \\ l=-1 \ \textit{if } i=j \end{cases}$$

APPENDIX-5
SIMULATION METHOD OF SAMPLE COVARIANCE MATRIX

In order to generate one sample-vector of an arbitrary signal-plus-noise field with covariance matrix a given $N \times N$ complex Hermitian matrix it is necessary [BRE-76]

1. to find the eigen-decomposition of that matrix. That is

$$\mathbf{R} = \mathbf{E}.\mathbf{D}.\mathbf{E}^{-1} \qquad \text{(A5.1)}$$

where $\mathbf{E}$ $N \times N$ complex matrix with columns the eigenvectors

$$\mathbf{E}^{-1} = \mathbf{E}^{H}$$

$\mathbf{D}$ a diagonal matrix (eigenvalues)

2. to generate N random variables which form the vector $\underline{z}$, each having independent gaussian quadrature components of zero mean and variance 0.5. This can be done as follows:
   a. generate two independent random variables x_{1_i} and x_{2_i} which are uniformly distributed on the interval [0,..,1];
   b. pass the first one through a filter with transfer function $\sqrt{ln}$. Then, at the output of that filter, there is a random variable of Rayleigh distribution r_i;
   c. pass the Rayleigh random variable r_i through a second filter with tranfer function $exp[\![j2\pi x_{2_i}]\!]$. This provide a gaussian random variable z_i.
   d. repeat steps 2a to 2c N times in parallel, that is for

$i \in [\![1,\ldots,N]\!]$. Then a random N-dim vector $\underline{z}$ is formed.

3. to pass the $\underline{z}$ vector through a filter with transfer function $\mathbf{E}.\mathbf{D}^{0.5}$ the result will be a sample vector $\underline{x}$. That is

$$\underline{x} = \mathbf{E}.\mathbf{D}^{0.5}.\underline{z} \qquad \text{(A5.2)}$$

This random vector $\underline{x}$ provides samples of the arbitrary complex covariance matrix $\mathbf{R}_{xx}$. A block diagram of this simulation method is shown in *Figure-A*5.1.

TEST:

$$\begin{aligned} E[\underline{x}.\underline{x}^H] &= E[\![\mathbf{E}.\ \mathbf{D}^{0.5}.\underline{z}.\underline{z}^H.\ \mathbf{D}^{0.5}.\mathbf{E}^H]\!] = \\ &= \mathbf{E}.\ \mathbf{D}^{0.5}.E[\![\underline{z}.\underline{z}^H]\!].\ \mathbf{D}^{0.5}.\mathbf{E}^H = \\ &= \mathbf{E}.\ \mathbf{D}^{0.5}.\mathbf{I}.\ \mathbf{D}^{0.5}.\mathbf{E}^H = \\ &= \mathbf{E}.\mathbf{D}.\ \mathbf{E}^H = \\ &= \mathbf{R}_{xx} \end{aligned}$$

FIGURE – A5.1

GENERATING A RANDOM VECTOR VARIABLE FOR A GIVEN COVARIANCE MATRIX

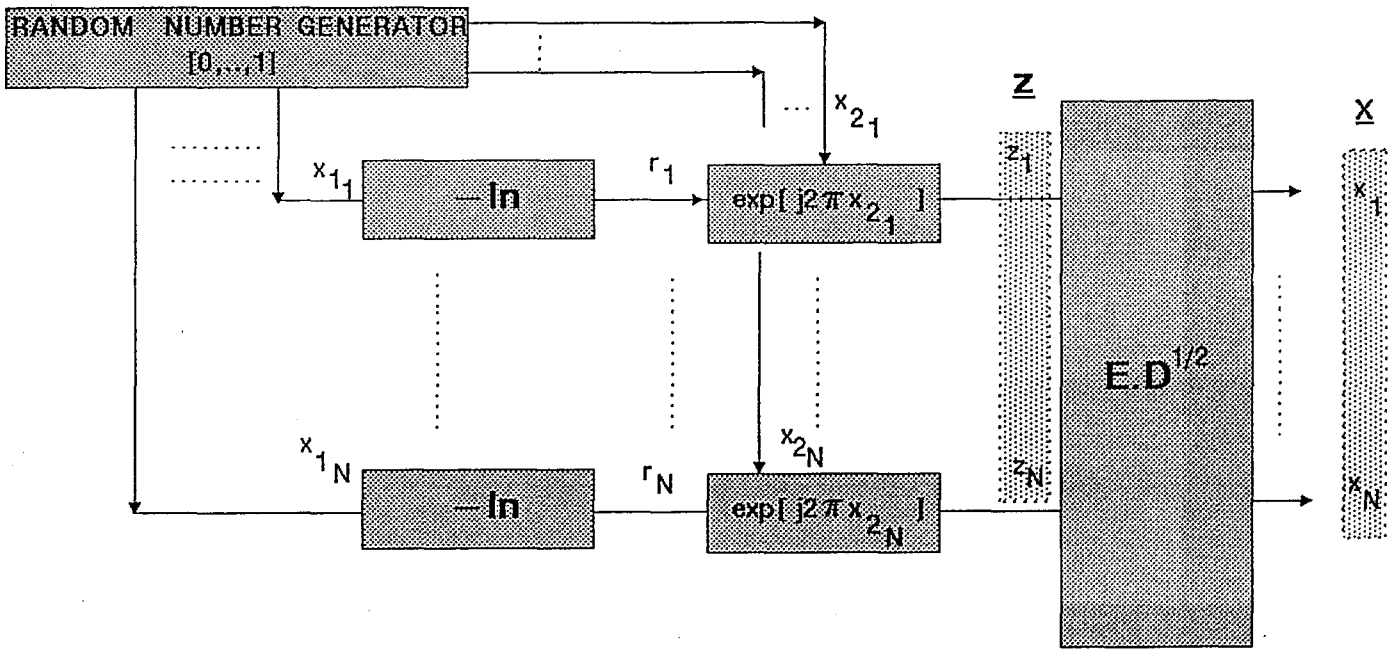

APPENDIX-6
NUMERICAL RESULTS OF AN ASPECT-EXAMPLE

POSITION OF ARRAY SENSORS

	x	y	z	..... *in half-wavelengths*
sensor No.1 :	*-1.9319*	*0.0000*	*0.0000*	$=\underline{r}_1$
sensor No.2 :	*-1.6730*	*0.9659*	*0.0000*	$=\underline{r}_2$
sensor No.3 :	*-0.9659*	*1.6730*	*0.0000*	$=\underline{r}_3$
sensor No.4 :	*0.0000*	*1.9319*	*0.0000*	$=\underline{r}_4$
sensor No.5 :	*0.9659*	*1.6730*	*0.0000*	$=\underline{r}_5$
sensor No.6 :	*1.6730*	*0.9659*	*0.0000*	$=\underline{r}_6$
sensor No.7 :	*1.9319*	*0.0000*	*0.0000*	$=\underline{r}_7$
sensor No.8 :	*0.0000*	*1.9319*	*1.0000*	$=\underline{r}_8$

LOCATIONS OF SOURCES

	elevation $\underline{\phi}$	*azimuth* $\underline{\theta}$
source No.1	*15.000*	*20.000*
source No.2	*15.000*	*30.000*
source No.3	*10.000*	*90.000*

INCIDENT SIGNALS CORRELATION MATRIX - $\mathbf{R}_{mm}$

(1.0000, 0.0000) (1.0000, 0.0000) (0.0000, 0.0000)
(1.0000, 0.0000) (1.0000, 0.0000) (0.0000, 0.0000)
(0.0000, 0.0000) (0.0000, 0.0000) (1.0000, 0.0000)

NOISE POWER - σ^2:*(0.0001, 0.0000)*

COVARIANCE MATRIX $\mathbf{R}_{xx}$

1st row: (4.8165e+000 4.8545e-017) (2.9011e+000 -2.9849e+000) (4.3311e+000 -4.3336e-001) (-1.2830e+000 3.1771e+000) (3.7226e+000 -1.5914e+000) (-3.0867e+000 2.1538e+000) (2.7942e+000 -2.1715e+000) (-2.9474e+000 1.1398e+000)

2nd row: (2.9011e+000 2.9849e+000) (4.3394e+000 4.3395e-017) (3.1601e+000 2.5038e+000) (-2.3380e+000 4.7932e-002) (4.0413e+000 1.8744e+000) (-2.2781e+000 -1.4419e+000) (4.0786e+000 1.1602e+000) (-1.4035e+000 -1.7858e+000)

3rd row: (4.3311e+000 4.3336e-001) (3.1601e+000 -2.5038e+000) (4.0503e+000 -4.6621e-017) (-1.4022e+000 2.2896e+000) (3.8577e+000 -9.8416e-001) (-2.7104e+000 1.2445e+000) (3.1882e+000 -1.5348e+000) (-2.4124e+000 3.9640e-001)

4th row: (-1.2830e+000 -3.1771e+000) (-2.3380e+000 -4.7932e-002) (-1.4022e+000 -2.2896e+000) (4.2020e+000 -4.4588e-017) (-2.3580e+000 -5.7282e-001) (3.9336e+000 2.3343e+000) (-2.6681e+000 6.5073e-001) (3.0553e+000

2.8448e+000)

5th row: *(3.7226e+000 1.5914e+000) (4.0413e+000 -1.8744e+000) (3.8577e+000 9.8416e-001) (-2.3580e+000 5.7282e-001) (4.6663e+000 -5.2204e-017) (-2.6799e+000 -9.0950e-001) (4.5491e+000 -6.9250e-001) (-1.9314e+000 -1.5644e+000)*

6th row: *(-3.0867e+000 -2.1538e+000) (-2.2781e+000 1.4419e+000) (-2.7104e+000 -1.2445e+000) (3.9336e+000 -2.3343e+000) (-2.6799e+000 9.0950e-001) (4.9922e+000 2.7105e-020) (-2.2861e+000 2.2203e+000) (4.4485e+000 9.9105e-001)*

7th row: *(2.7942e+000 2.1715e+000) (4.0786e+000 -1.1602e+000) (3.1882e+000 1.5348e+000) (-2.6681e+000 -6.5073e-001) (4.5491e+000 6.9250e-001) (-2.2861e+000 -2.2203e+000) (4.8165e+000 -4.8545e-017) (-1.3393e+000 -2.6513e+000)*

8th row: *(-2.9474e+000 -1.1398e+000) (-1.4035e+000 1.7858e+000) (-2.4124e+000 -3.9640e-001) (3.0553e+000 -2.8448e+000) (-1.9314e+000 1.5644e+000) (4.4485e+000 -9.9105e-001) (-1.3393e+000 2.6513e+000) (4.2020e+000 2.6780e-017)*

EIGENVALUES

1.0000e-004 1.0000e-004 1.0000e-004 1.0000e-004 +.0000e-004 1.0000e-004
7.7127e+000 2.8372e+001

EIGENVECTORS

1st row: *(-8.3139e-002 1.1657e-012) (-1.8391e-002 1.4306e-012) (-2.1216e-002 -1.3916e-013) (5.1488e-002 -1.6129e-012) (5.6204e-002 7.2233e-013) (8.7189e-001 3.4531e-013) (-2.7866e-001 -7.1052e-017) (3.8555e-001 -1.0787e-017)*

2nd row: *(2.4537e-001 5.1855e-001) (-1.4177e-001 -2.1336e-002) (1.6979e-001 -4.5021e-002) (-4.6575e-001 -1.0150e-001) (3.7578e-001 4.8399e-002) (-1.5774e-001 -4.9176e-002) (-2.9341e-001 8.9002e-002) (2.0756e-001 2.9036e-001)*

3rd row: *(-3.0242e-001 -3.5722e-001) (-1.1100e-001 1.6307e-001) (-5.0286e-001 -1.8032e-001) (-2.8937e-001 -3.5708e-002) (-1.2206e-001 2.9517e-001) (-2.5637e-001 -4.8897e-002) (-2.6995e-001 8.8309e-002) (3.4290e-001 5.6967e-002)*

4th row: *(1.1823e-001 -1.4194e-001) (1.6440e-001 8.6791e-003) (7.7155e-002 -3.7662e-001) (3.9154e-001 -1.0158e-001) (4.8590e-001 3.2630e-001) (-7.2449e-002 1.2464e-001) (-3.7165e-001 1.4505e-001) (-1.9031e-001 -2.6194e-001)*

5th row: *(-1.4550e-001 -3.1797e-001) (4.7368e-001 -3.2491e-001) (4.3929e-001 2.4344e-001) (1.6050e-002 -7.9651e-002) (-6.5810e-002 -9.3094e-002) (-1.7935e-001 -1.8888e-002) (-1.6743e-001 2.8356e-001) (3.0742e-001 2.0120e-001)*

6th row: *(3.1110e-001 1.5908e-001) (1.8395e-001 -3.3244e-001) (-2.1911e-001 5.1406e-002) (-2.2793e-001 -1.3495e-002) (-4.9500e-001 2.1453e-001) (1.3604e-001 1.5508e-001) (-2.6780e-001 3.0781e-001) (-3.3480e-001 -1.3642e-001)*

7th row: *(6.3771e-002 3.0783e-001) (-2.7009e-001 6.3798e-002) (-1.5788e-001 5.9839e-002) (6.5493e-001 -7.7180e-002) (-2.4249e-001 -4.3984e-002) (-1.5798e-001 3.7694e-002) (-7.9566e-002 3.6923e-001) (2.3981e-001 2.7106e-001)*

8th row: *(-2.2335e-001 -1.3313e-001) (-3.3926e-001 4.9668e-001) (4.4973e-001 4.3113e-002) (-1.5902e-001 -5.0760e-002) (-1.8314e-001 -1.0182e-001) (6.7066e-002 1.3288e-001) (-2.3964e-001 3.3691e-001) (-3.1653e-001 -3.8004e-002)*

E *matrix*

(-2.7866e-001 -7.1052e-017) (3.8555e-001 -1.0787e-017)
(-2.9341e-001 8.9002e-002) (2.0756e-001 2.9036e-001)
(-2.6995e-001 8.8309e-002) (3.4290e-001 5.6967e-002)
(-3.7165e-001 1.4505e-001) (-1.9031e-001 -2.6194e-001)
(-1.6743e-001 2.8356e-001) (3.0742e-001 2.0120e-001)
(-2.6780e-001 3.0781e-001) (-3.3480e-001 -1.3642e-001)
(-7.9566e-002 3.6923e-001) (2.3981e-001 2.7106e-001)
(-2.3964e-001 3.3691e-001) (-3.1653e-001 -3.8004e-002)

minimization of Equation 3.42

1 cost:1.57588613015542e+000 angles:3.4613e+001 3.9554e+001
0.0000e+000 5.0000e+000 (-5.4005e-002 -2.9671e-002)
0.0000e+000 5.0000e+001 (1.1560e-001 -2.9291e-002)
0.0000e+000 1.0000e+002 (-1.9534e-001 1.8979e-001)
0.0000e+000 1.6500e+002 (3.7461e-002 6.2749e-002)

```
  2    cost:1.05217380322443e+000          angles:1.6491e+001   7.6119e+000
4.4494e+000          1.7732e+001           (7.3333e-002 -3.8854e-002)
1.1359e+001          3.6362e+001           (3.6165e-002 -1.0114e-002)
2.6844e+001          9.2202e+001           (-2.4636e-001  2.7894e-001)
-6.7928e+001         1.5479e+002           (-2.0046e-002  5.3753e-002)

  3    cost:1.00773379652949e+000          angles:5.7822e+000  4.1323e+000
 1.6472e+001         1.7490e+001           (5.2409e-002 -2.1671e-002)
2.0405e+001          3.0023e+001           (2.6192e-002  2.6586e-002)
1.7239e+001          8.9834e+001           (-2.8565e-001  2.2282e-001)
-5.5228e+001         1.4729e+002           (-1.4536e-002  9.0618e-004)

  4    cost:1.00680448044605e+000          angles:4.7357e+000  4.6954e+000
1.7934e+001          1.8501e+001           (7.7658e-002 -1.2487e-002)
2.0088e+001          3.0391e+001           (1.0839e-002  1.2044e-003)
1.6623e+001          8.9998e+001           (-2.8700e-001  2.2292e-001)
-6.2749e+001         -1.7188e+002          (1.8230e-002  1.4310e-002)

  5    cost:1.00005739432137e+000          angles:4.4109e-001  4.2692e-001
1.3915e+001          2.0572e+001           (4.5583e-002  3.4677e-003)
1.5835e+001          2.9819e+001           (3.8439e-002  3.0710e-003)
1.0366e+001          9.0083e+001           (-2.9358e-001  2.0567e-001)
-7.7722e+001         -1.5294e+002          (1.7772e-003  1.2968e-003)

  6    cost:1.00003930997895e+000          angles:2.1131e-001  4.6199e-001
1.4668e+001          2.2518e+001           (6.1301e-002  8.7464e-003)
1.5787e+001          3.2053e+001           (2.3284e-002 -3.1735e-004)
1.0160e+001          9.0031e+001           (-2.9304e-001  2.0480e-001)
-7.6436e+001         8.2865e+001           (-6.6023e-004 -2.5506e-004)

  7    cost:1.00000532538827e+000          angles:4.3183e-002  1.8193e-001
1.5254e+001          2.1860e+001           (5.8127e-002  6.7096e-003)
1.4457e+001          3.2471e+001           (2.6317e-002  2.2947e-003)
1.0036e+001          8.9998e+001           (-2.9287e-001  2.0481e-001)
-6.4207e+001         8.8325e+001           (2.0429e-004 -1.8370e-004)

  8    cost:1.00000205919905e+000          angle:2.5981e-002  1.1334e-001
1.5269e+001          2.1277e+001           (5.3567e-002  5.6403e-003)
1.4744e+001          3.1726e+001           (3.0963e-002  3.2019e-003)
1.0012e+001          9.0000e+001           (-2.9285e-001  2.0479e-001)
-5.3792e+001         8.3582e+001           (2.6336e-004  1.2530e-004)

  9    cost:  1.00000042320060e+000        angle:1.0614e-002  5.1632e-002
1.5227e+001          2.0430e+001           (4.6296e-002  4.5918e-003)
1.4753e+001          3.0612e+001           (3.8164e-002  4.2192e-003)
1.0001e+001          9.0001e+001           (-2.9290e-001  2.0487e-001)
-4.9227e+001         8.6627e+001           (3.3772e-005  1.7641e-004)

  10   cost:1.00000006075084e+000          angle:3.7629e-003  1.9614e-002
1.5061e+001          2.0158e+001           (4.3463e-002  4.5589e-003)
1.4981e+001          3.0152e+001           (4.1003e-002  4.2653e-003)
1.0000e+001          9.0000e+001           (-2.9302e-001  2.0486e-001)
-4.9651e+001         8.7108e+001           (3.5194e-005  3.6929e-005)
```

11 cost:1.00000000341802e+000 angle:1.0255e-003 4.6249e-003
1.5022e+001 2.0024e+001 (4.2544e-002 4.3976e-003)
1.4982e+001 3.0051e+001 (4.1931e-002 4.4328e-003)
1.0000e+001 9.0000e+001 (-2.9303e-001 2.0489e-001)
9.9990e+003 9.9990e+003 (0.0000e+000 0.0000e+000)

12 cost:1.00000000000499e+000 angle:3.9881e-005 1.7645e-004
1.5000e+001 1.9999e+001 (4.2232e-002 4.4194e-003)
1.5000e+001 2.9999e+001 (4.2242e-002 4.4203e-003)
1.0000e+001 9.0000e+001 (-2.9305e-001 2.0488e-001)
9.9990e+003 9.9990e+003 (0.0000e+000 0.0000e+000)

13 cost:1.00000000000000e+000 angle:1.0000e-009 8.5377e-007
1.5000e+001 2.0000e+001 (4.2237e-002 4.4199e-003)
1.5000e+001 3.0000e+001 (4.2237e-002 4.4199e-003)
1.0000e+001 9.0000e+001 (-2.9305e-001 2.0488e-001)
9.9990e+003 9.9990e+003 (0.0000e+000 0.0000e+000)

FINAL RESULT
cost:1.00000000000000e+000 angle:1.0000e-009 8.5377e-007
1.5000e+001 2.0000e+001 ←SOURCE No.1
1.5000e+001 3.0000e+001 ←SOURCE No.2
1.0000+001 9.0000e+001 ←SOURCE No.3

↑ ϕ ↑ θ

.....

SAMPLE COVARIANCE MATRIX - No. of Samples = 250

1st row: *(4.8288e+000 0.0000e+000) (2.9190e+000 -2.9707e+000) (4.3436e+000 -4.2511e-001) (-1.2493e+000 3.1818e+000) (3.7280e+000 -1.5644e+000) (-3.0576e+000 2.1743e+000) (2.7943e+000 -2.1360e+000) (-2.9208e+000 1.1652e+000)*

2nd row: *(2.9190e+000 2.9707e+000) (4.3101e+000 -4.2327e-020) (3.1607e+000 2.4936e+000) (-2.3222e+000 1.1902e-001) (4.0023e+000 1.8566e+000) (-2.3002e+000 -1.3660e+000) (4.0188e+000 1.1404e+000) (-1.4396e+000 -1.7173e+000)*

3rd row: *(4.3436e+000 4.2511e-001) (3.1607e+000 -2.4936e+000) (4.0574e+000 -6.5355e-021) (-1.3681e+000 2.3151e+000) (3.8461e+000 -9.7099e-001) (-2.6916e+000 1.2857e+000) (3.1661e+000 -1.5148e+000) (-2.4009e+000 4.3931e-001)*

4th row: *(-1.2493e+000 -3.1818e+000) (-2.3222e+000 -1.1902e-001) (-1.3681e+000 -2.3151e+000) (4.1269e+000 1.2571e-019) (-2.3016e+000 -6.4050e-001) (3.8590e+000 2.2956e+000) (-2.6059e+000 5.6434e-001) (2.9923e+000 2.7881e+000)*

5th row: *(3.7280e+000 1.5644e+000) (4.0023e+000 -1.8566e+000) (3.8461e+000 9.7099e-001) (-2.3016e+000 6.4050e-001) (4.6068e+000 -1.6463e-020) (-2.6612e+000 -8.1513e-001) (4.4665e+000 -6.8311e-001) (-1.9329e+000 -1.4700e+000)*

6th row: *(-3.0576e+000 -2.1743e+000) (-2.3002e+000 1.3660e+000) (-2.6916e+000 -1.2857e+000) (3.8590e+000 -2.2956e+000) (-2.6612e+000 8.1513e-001) (4.8984e+000 -1.5668e-020) (-2.2712e+000 2.1043e+000) (4.3568e+000 9.6761e-001)*

7th row: *(2.7943e+000 2.1360e+000) (4.0188e+000 -1.1404e+000) (3.1661e+000 1.5148e+000) (-2.6059e+000 -5.6434e-001) (4.4665e+000 6.8311e-001) (-2.2712e+000 -2.1043e+000) (4.7058e+000 1.3662e-019) (-1.3503e+000 -2.5367e+000)*

8th row: *(-2.9208e+000 -1.1652e+000) (-1.4396e+000 1.7173e+000) (-2.4009e+000 -4.3931e-001) (2.9923e+000 -2.7881e+000) (-1.9329e+000 1.4700e+000) (4.3568e+000 -9.6761e-001) (-1.3503e+000 2.5367e+000) (4.1069e+000*

1.9558e-020)

EIGENVALUES

9.4718e-005 9.7093e-005 9.8938e-005 1.0158e-004 1.0505e-004 1.0689e-004 7.5547e+000 2.8086e+001

EIGENVECTORS

1st row: *(2.0793e-001 3.4103e-012) (5.9083e-001 3.0033e-012) (-4.3704e-002 -2.2333e-012) (5.9285e-002 5.8492e-013) (-5.1670e-001 2.3977e-013) (3.3008e-001 6.4600e-013) (-2.7280e-001 -4.9537e-018) (3.8976e-001 -2.4904e-017)*

2nd row: *(-5.3310e-001 -3.2847e-001) (-6.3026e-002 -8.4990e-002) (3.4832e-001 -2.1863e-001) (-2.5700e-001 -3.4453e-001) (-9.0785e-002 -6.2763e-002) (-9.1424e-002 2.9718e-002) (-2.9024e-001 9.3416e-002) (2.1201e-001 2.8897e-001)*

3rd row: *(-5.0928e-002 2.4689e-001) (-5.3528e-001 -2.0139e-001) (7.4949e-002 3.8493e-001) (4.4406e-001 6.0596e-002) (-1.6817e-001 -7.4535e-002) (2.8715e-002 1.3637e-001) (-2.6464e-001 8.9154e-002) (3.4698e-001 5.5620e-002)*

4th row: *(1.7452e-001 5.2658e-002) (2.9431e-002 -1.9498e-001) (1.9014e-001 2.3774e-001) (-4.4191e-001 3.2947e-002) (2.9134e-001 -2.6545e-001) (3.0647e-001 3.5431e-001) (-3.7456e-001 1.4105e-001) (-1.8464e-001 -2.6411e-001)*

5th row: *(3.2895e-001 -1.2261e-001) (6.7948e-002 2.1532e-001) (1.7168e-001 1.8380e-001) (-2.1924e-001 3.8743e-001) (1.6604e-001 1.4399e-001) (-5.0728e-001 -1.2365e-001) (-1.6275e-001 2.8658e-001) (3.0992e-001 1.9686e-001)*

6th row: *(-4.0824e-002 -3.1008e-001) (-1.3449e-001 2.0788e-001) (-5.1538e-001 5.6108e-002) (-1.4669e-002 -3.4415e-002) (-3.8780e-001 -6.5886e-004) (-2.4120e-001 2.5504e-001) (-2.7280e-001 3.0568e-001) (-3.3068e-001 -1.4108e-001)*

7th row: *(1.2335e-001 -1.4078e-001) (-1.6032e-002 3.3232e-002) (-4.5389e-001 -1.6095e-001) (1.7919e-001 -2.2697e-001) (5.1249e-001 -8.0827e-002) (3.1368e-001 -8.2734e-002) (-7.5887e-002 3.7331e-001) (2.4098e-001 2.6541e-001)*

8th row: *(-2.1453e-001 4.0717e-001) (4.0013e-001 -3.1067e-003) (1.3377e-001 2.5753e-002) (3.3862e-001 -1.2900e-001) (1.1186e-001 -2.2645e-001) (-2.8170e-001 -2.4997e-001) (-2.4444e-001 3.3629e-001) (-3.1284e-001 -4.3130e-002)*

E ***matrix***

(-2.7280e-001 -4.9537e-018) (3.8976e-001 -2.4904e-017)
(-2.9024e-001 9.3416e-002) (2.1201e-001 2.8897e-001)
(-2.6464e-001 8.9154e-002) (3.4698e-001 5.5620e-002)
(-3.7456e-001 1.4105e-001) (-1.8464e-001 -2.6411e-001)
(-1.6275e-001 2.8658e-001) (3.0992e-001 1.9686e-001)
(-2.7280e-001 3.0568e-001) (-3.3068e-001 -1.4108e-001)
(-7.5887e-002 3.7331e-001) (2.4098e-001 2.6541e-001)
(-2.4444e-001 3.3629e-001) (-3.1284e-001 -4.3130e-002)

minimization of Equation 3.42

1 cost:1.57531307068895e+000 angle:3.4865e+001 3.9316e+001
0.0000e+000 5.0000e+000 (-5.1135e-002 -3.1193e-002)
0.0000e+000 5.0000e+001 (1.1585e-001 -2.6924e-002)
0.0000e+000 1.0000e+002 (-1.9463e-001 1.9090e-001)
0.0000e+000 1.6500e+002 (3.7250e-002 6.2095e-002)

2 cost:1.04574106559480e+000 angle:1.5531e+001 7.0216e+000
4.7101e+000 1.8064e+001 (7.9500e-002 -3.9348e-002)
1.1602e+001 3.5938e+001 (3.2368e-002 -6.8600e-003)
2.6256e+001 9.1922e+001 (-2.5149e-001 2.7689e-001)
-6.9226e+001 1.5459e+002 (-1.7624e-002 5.3211e-002)

```
  3    cost:1.00642814777630e+000          angle:5.4558e+000  3.5002e+000
1.6312e+001          1.6823e+001           (6.0756e-002 -1.8094e-002)
1.8814e+001          2.9894e+001           (3.0876e-002  1.8210e-002)
1.7231e+001          8.9736e+001           (-2.8835e-001  2.2656e-001)
-6.4480e+001         1.5379e+002           (-9.7853e-003  1.6821e-002)

  4    cost:1.00024640319875e+000          angle:1.1581e+000  5.2558e-001
1.4705e+001          1.9875e+001           (5.0547e-002 -6.9185e-004)
1.4524e+001          2.9331e+001           (3.8137e-002  3.3668e-003)
1.1391e+001          9.0211e+001           (-2.9385e-001  2.0798e-001)
-7.4240e+001         -1.5512e+002          (6.3671e-003  4.3138e-003)

  5    cost:1.00000414640989e+000          angle:1.1883e-001  1.1447e-001
1.4988e+001          1.9385e+001           (4.0747e-002  3.6089e-003)
1.4859e+001          2.9570e+001           (4.8047e-002  7.8469e-003)
1.0134e+001          8.9966e+001           (-2.9283e-001  2.0511e-001)
-8.2512e+001         -1.4960e+002          (3.3485e-004  1.9313e-004)

  6    cost:1.00000029675989e+000          angle:1.6438e-002  4.0966e-002
1.5087e+001          2.0041e+001           (4.5036e-002  5.4932e-003)
1.4912e+001          2.9993e+001           (4.4389e-002  5.7707e-003)
1.0033e+001          8.9997e+001           (-2.9271e-001  2.0482e-001)
-8.8034e+001         2.9895e+001           (-6.8203e-006  1.0878e-004)

  7    cost:1.00000000613061e+000          angle:5.1731e-003  3.6730e-003
1.4999e+001          2.0018e+001           (4.4881e-002  5.5995e-003)
1.5000e+001          3.0006e+001           (4.4651e-002  5.6961e-003)
1.0004e+001          8.9999e+001           (-2.9269e-001  2.0478e-001)
9.9990e+003          9.9990e+003           (0.0000e+000 0.0000e+000)

  8    cost:1.00000000581389e+000          angle:5.8840e-003  1.8842e-003
1.5000e+001          1.9994e+001           (4.4727e-002  5.5781e-003)
1.4999e+001          2.9991e+001           (4.4820e-002  5.7136e-003)
1.0003e+001          8.9999e+001           (-2.9269e-001  2.0478e-001)
9.9990e+003          9.9990e+003           (0.0000e+000  0.0000e+000)

  9    cost:1.00000000543223e+000          angle:5.7408e-003  1.6460e-003
1.5000e+001          1.9996e+001           (4.4742e-002  5.5875e-003)
1.5000e+001          2.9993e+001           (4.4809e-002  5.7027e-003)
1.0001e+001          8.9999e+001           (-2.9269e-001  2.0478e-001)
9.9990e+003          9.9990e+003           (0.0000e+000  0.0000e+000)


FINAL RESULT
 cost:1.00000000543223e+000                angle:5.7408e-003  1.6460e-003
1.5000e+001          1.9996e+001           ←SOURCE No.1
1.5000e+001          2.9993e+001           ←SOURCE No.2
1.0001e+001          8.9999e+001           ←SOURCE No.3
     ↑                    ↑
     φ                    θ
```

N.B.: 9.999e+003 means that this direction has been eliminated as pseudo direction